Variabilité et devenir des apports sédimentaires par les fleuves côtiers: cas du système Têt - Littoral roussillonnais dans le golfe du Lion

François Bourrin

UNIVERSITÉ VIA DOMITIA PERPIGNAN

THÈSE DE DOCTORAT SPECIALITÉ OCÉANOLOGIE

VARIABILITÉ ET DEVENIR DES APPORTS SÉDIMENTAIRES PAR LES FLEUVES CÔTIERS : CAS DU SYSTÈME TÊT - LITTORAL ROUSSILLONNAIS DANS LE GOLFE DU LION

Thèse soutenue à l'Université de Perpignan le 5 Octobre 2007

par **François BOURRIN**

sous la direction de Xavier DURRIEU DE MADRON

Pour obtenir le grade de docteur de l'Université de Perpignan

Discipline Océanologie

Jury composé de

Robert LAFITE	Pr. Univ. Rouen	Rapporteur
Sabine CHARMASSON	DR IRSN	Rapporteur
Carl AMOS	Pr. Univ. Southampton	Examinateur
Olivier RADAKOVITCH	McF Univ. Aix-en-Provence	Examinateur
Aldo SOTTOLICHIO	McF Univ. Bordeaux	Examinateur
Xavier DURRIEU DE MADRON	CR CNRS, HDR	Directeur de thèse
Nabila MAZOUNI	CR Cépralmar	Invitée

Remerciements

Je vais profiter de ces quelques lignes au début de ce manuscrit pour faire un historique de mes années passées dans la recherche dont une bonne partie au CEFREM à l'Université de Perpignan et bien sur afin de remercier toutes les personnes avec qui j'ai pu collaborer de près ou de loin. J'ai commencé mes premiers pas dans la recherche au sein de l'équipe METHYS au Département de Géologie et d'Océanographie de l'Université de Bordeaux. Sous la direction d'Aldo Sottolichio, je me suis familiarisé avec les ADCP dans l'estuaire de la Gironde afin de mesurer des structures hydrodynamiques particulières. Celles-ci n'étant pas présentes lors de la campagne de mesure, (d'ailleurs moi non plus car je me suis cassé la jambe après un vulgaire accident de foot…), l'objet de mon stage de DEA a dû être modifié. C'est là qu'est intervenu Xavier Durrieu de Madron qui m'a documenté sur la conversion du signal acoustique des ADCP en vue d'en extraire un signal de turbidité. A la suite de ce stage de DEA fructueux, je suis venu faire un tour à Perpignan où j'ai rencontré Xavier qui m'a alors proposé un contrat d'ingénieur pour installer entre autre une bouée météo-marine. Après une première année de conception et de mise en place instrumentale avec l'aide précieuse de Jacques Carbonne et Gilles Saragoni (des bricoleurs hors pairs), on m'a proposé de faire une thèse de doctorat. Voilà comment j'en suis arrivé après quatre années de travail de terrain, au CEFREM à Perpignan, mais aussi dans d'autres laboratoires français et étrangers, à effectuer cette thèse de doctorat. Et c'est déjà le temps de soutenir, de faire quelques pots de départ et quelques sorties dans les bars et de partir…peut-être pour mieux revenir dans ce beau pays qu'est le pays catalan. Un vieux proverbe gavatx dit que la catalogne sans le vent (Tramontane) et ses habitants (les catalans) ça serait le paradis. Ce n'est pas tout à fait vrai... En tout cas, à part la science du terrain, ce pays se prête aux nombreuses escapades sportives que j'ai faites mais aussi qu'il me reste à faire avec mes compères du labo et autres lascars. Voilà le temps des remerciements. Je remercie donc tous mes collègues du CEFREM : Serge, Xavier pour l'encadrement, Gilles pour les activités subaquatiques, Patrick pour les bonnes sorties de VTT, Vincent, Franck, Javier, Philippe pour les sorties au Tio Pepe et à la rhumerie parmi tant d'autres…, Nicole pour les concours gâteau, Jérôme de Bordeaux pour les parties de flipper sur les campagnes embarquées et le squash, Dominique pour les parties de tennis, Jacques pour sa disponibilité, Jérôme, Anna, Wolfgang, Gérard, Rosy, Egon, Annie, Bénédicte et Maud. Je remercie aussi Elias pour sa bonne humeur, mes potes de l'EPHE, Céline de Banyuls pour les sorties SYSCOLAG, Caroline du BDSI. Je tiens à remercier mes parents, et de gros bisous à Vanessa ma muse qui m'a soutenu dans les moments difficiles.

Table des matières

1 INTRODUCTION

La zone côtière est l'espace de transition entre la mer et la terre. La proximité de la mer, et ses interactions avec la terre modèlent les entités naturelles physiques et biologiques du littoral, ainsi que les activités socio-économiques qui lui sont liées. La délimitation de la zone côtière varie suivant que l'on s'intéresse aux écosystèmes ou aux activités économiques et humaines à proximité. Généralement la zone côtière est limitée à terre à une bande de 15 kilomètres minimum incorporant l'arrière-pays et rattachée à un bassin hydrographique bien défini. En mer, la zone côtière correspond à la limite des eaux territoriales, soit 12 miles nautiques. Cette limite est un peu floue si l'on considère les échanges de matières organique ou inorganique, à ses interfaces : le bassin versant, l'atmosphère et le large (**Figure 1-1**). D'un point de vue environnemental et géologique, cette limite peut être étendue à la limite d'influence des apports continentaux en mer ; autrement dit, la zone côtière s'étend depuis les sources de matière (bassin versant) jusqu'aux puits (marge continentale et bassin profond).

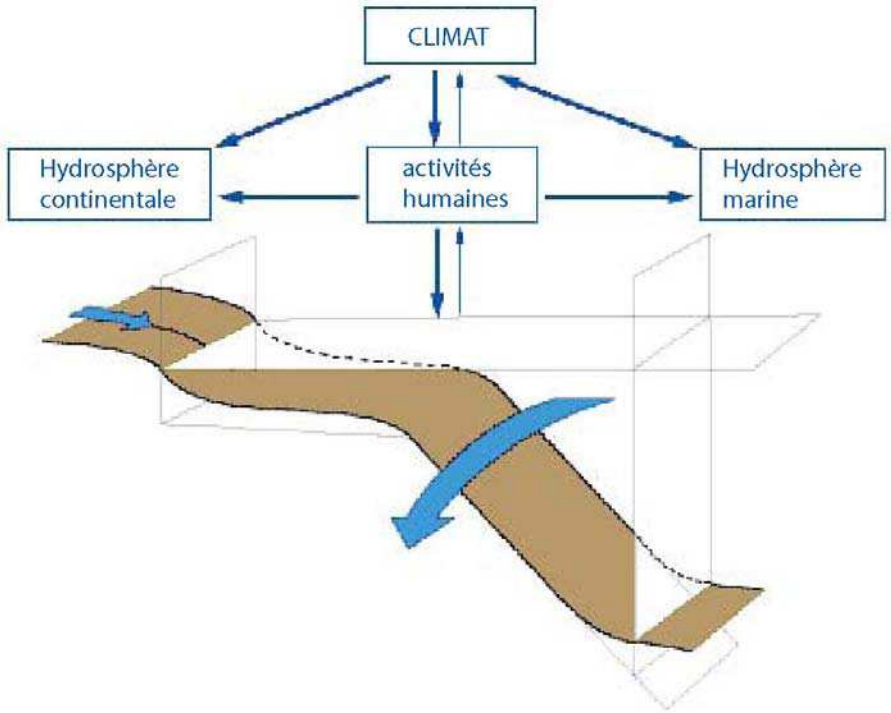

Figure 1-1 : La zone côtière et ses interfaces, influencées par le climat et les activités humaines.

Les échanges qui règnent aux interfaces de la zone côtière sont directement influencés par le climat (**Figure 1-1**). Dans cette zone fragile, la pression grandissante des activités humaines et le changement climatique agissent donc dans une certaine mesure sur les échanges à ses interfaces. Le traceur qui va nous permettre de suivre ces échanges, leur variabilité et par là, celle du climat est l'ensemble {eau + particule}.

Une des interfaces importantes de la zone côtière, qui fait l'objet de notre étude, est la zone des embouchures des fleuves, lieu de transit et de dépôt des apports organiques et inorganiques, qu'ils soient d'origine naturelle ou anthropique. Les embouchures des fleuves forment des environnements deltaïques façonnés par 3 forçages différents : le fleuve (apports sédimentaires), la houle et la marée. Selon l'importance relative de ces 3 forçages, on peut distinguer 4 formes principales de deltas (**Figure 1-2**) : le type estuarien avec plusieurs formes, influencé par la marée ; le type allongé dominé par le fleuve ; le type lobé influencé à la fois par le fleuve et la houle ; et le type cuspidé dominé par la houle (**Coleman and Wright, 1975**).

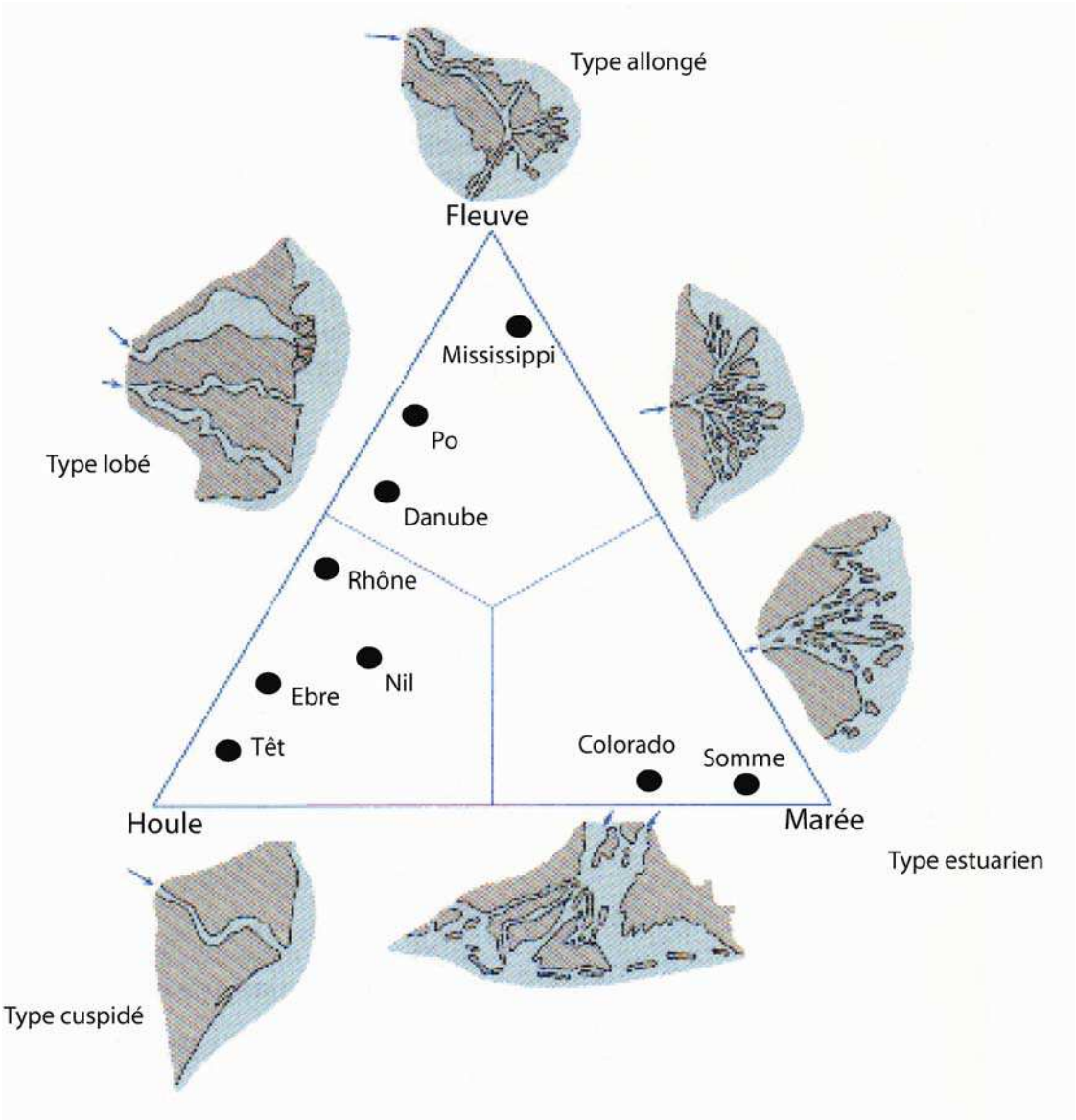

Figure 1-2 : Les différents types d'environnements deltaïques suivant la dominance des vagues, du fleuve ou de la marée (redessiné d'après Galloway, 1975).

Chaque delta se prolonge en mer dans sa partie sous-marine vers 20-30 m de profondeur par le **prodelta : zone de stockage temporaire du matériel fin d'origine continentale**. Dans les zones où la marée domine, le prodelta correspond au « bouchon vaseux » ou zone de turbidité maximale qui se déplace dans l'estuaire suivant l'importance de la marée et du fleuve. Dans les zones sans marée, le prodelta occupe une position fixe autour de 30 m de profondeur à la limite d'action des fortes houles de tempête et des courants extrêmes. Suivant l'importance des apports fluviatiles et de l'hydrodynamisme, le prodelta peut être directement connecté à la vasière qui occupe une position variable sur le plateau (**Figure 1-3**). Si les apports sédimentaires sont suffisamment importants, la vasière occupe une position côtière et le prodelta est confondu avec la vasière (**Figure 1-3 A**). Si au contraire l'hydrodynamique domine, la vasière occupe une position plus centrale sur le plateau et le prodelta occupe alors une position isolée de la vasière (**Figure 1-3 B à D**). Les prodeltas sont présents devant n'importe quelle embouchure que ce soit devant les estuaires de grande taille avec de forts apports ou les graus des lagunes et les fleuves côtiers caractérisés par de faibles apports terrigènes.

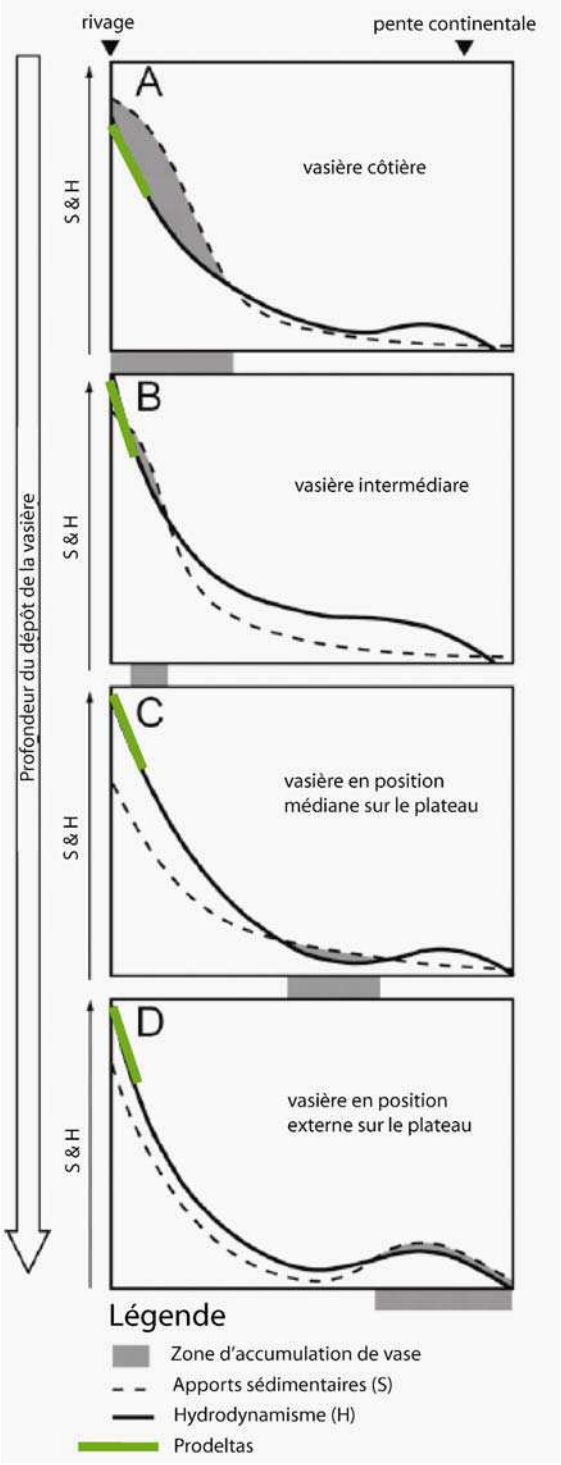

Figure 1-3 : Modèle conceptuel expliquant la position du dépôt de vase par rapport au prodelta sur les marges continentales, dépendant de la balance entre les apports sédimentaires (S) et l'hydrodynamisme (H) (d'après McCave, 1972 et repris par Cattaneo et al., 2007).

Les prodeltas concentrent les sédiments fins mais aussi les contaminants d'origine anthropique qui leur sont associés. Ils constituent à la fois un piège de matière pour le bassin versant et une source de matière pour la vasière et le bassin profond. La dynamique des échanges des **prodeltas** avec les autres **unités fonctionnelles de la zone côtière** que sont le **littoral**, la **vasière**, et le **domaine du large** (**Figure 1-1**), joue donc un rôle prépondérant dans la qualité de cette zone. La connaissance fine de ces interactions est importante pour la gestion durable de cet environnement. En l'absence de marée, la dynamique des environnements prodeltaïques est contrôlée par les vagues, les courants et les apports sédimentaires, plus particulièrement lors des évènements hydro-climatiques extrêmes. Une étude à la fois haute-fréquence et sur le long terme, des mécanismes hydro-sédimentaires régissant cet environnement est donc nécessaire en vue d'une compréhension globale de la zone côtière.

1.1 Contexte général

L'objectif affiché de ce travail de thèse est l'étude de la variabilité et du devenir des apports sédimentaires fins par les fleuves côtiers, et l'étude des interactions intervenant entre les prodeltas et les autres unités fonctionnelles de la zone côtière dans une mer sans marée.

La zone d'étude retenue est le système Têt – littoral roussillonnais localisé dans le golfe du Lion au NO de la Méditerranée. Ce système composé du fleuve Têt et de son prodelta est situé à la sortie du golfe du Lion, zone sous l'influence des apports du Rhône et de tous les fleuves côtiers situés plus au Nord le long de la côte du Languedoc-Roussillon, ainsi que par la circulation générale du golfe du Lion (**Figure 1-4**). Dans une mer sans marée, ce système est soumis à l'influence des évènements hydro-climatiques extrêmes. On distingue (1) les crues et tempêtes durant les hivers énergétiques et humides, et (2) la propagation d'eaux côtières très denses engendrées par les vents continentaux durant les hivers froids et secs. Ces vents sont à l'origine de la formation des plongées d'eaux denses sur le plateau et de leur écoulement le long de la pente continentale. Ces évènements hydro-climatiques peuvent se produire sur des périodes très courtes (un jour voire quelques heures pour les crues et tempêtes) mais parfois sur des périodes plus longues (quelques semaines à quelques mois pour les eaux denses). Afin de mesurer l'influence de ces évènements, il est donc nécessaire d'installer un réseau d'instruments de mesure qui permette de suivre les apports sédimentaires

par les fleuves et la dynamique sédimentaire côtière à la fois à haute fréquence et sur le long-terme. Ce type de réseau instrumenté est difficile à installer au niveau d'une grande embouchure comme le Rhône du fait de ses crues dévastatrices et de l'activité du chalutage, mais réalisable devant un petit fleuve côtier comme la Têt. Les résultats obtenus sur ce système pourront ensuite être extrapolé aux autres fleuves côtiers méditerranéens.

Figure 1-4 : Image satellite MERIS du golfe du Lion prise le 8 décembre 2003 (Agence Spatiale Européenne, Frascati, Italie).

Ce travail de recherche a pu bénéficier des travaux de thèse précédemment réalisés sur ce système. Le fleuve Têt a été étudié d'un point de vue géochimique dans le cadre de la thèse de **Garcia-Estevez (2005)**. Le transport des sédiments non cohésifs le long du littoral du Languedoc-Roussillon a été étudié par **Durand (1999)** et **Certain (2002)**. Le transport des sédiments fins a été étudié dans l'ensemble du golfe du Lion par **Monaco (1971)** et **Aloïsi (1986)**. La variabilité des échanges entre le plateau du golfe du Lion et le large a été étudiée par **Guarracino (2004).** L'apport et le devenir des contaminants métalliques par les fleuves

au golfe du Lion ont été étudiés par **Roussiez (2006)**. L'impact des tempêtes et de l'activité du chalutage sur le plateau a enfin été comparé dans le golfe du Lion par **Ferré (2004)**. Il manquait alors une étude sur la dynamique sédimentaire des prodeltas afin de compléter les connaissances sur l'ensemble de la zone côtière du golfe du Lion.

1.2 Problématique et méthodologie

Dans ce contexte, l'étude des mécanismes hydro-sédimentaires du prodelta de la Têt et de ses échanges avec les autres unités de la zone côtière, nécessite un suivi à la fois haute fréquence et sur le long terme, afin de répondre notamment aux questions suivantes :

- Comment identifier et délimiter les prodeltas dans la zone côtière méditerranéenne ?
- Quels sont les forçages principaux influençant la dynamique des prodeltas ?
- Comment agissent ces unités fonctionnelles par rapport au reste de la zone côtière ? Agissent-elles comme des zones puits ou sources de matière ? Quels sont les échanges avec les autres unités que sont le bassin versant, le littoral, la marge et le bassin profond ?
- Quelles est la variabilité des prodeltas en termes de dynamique sédimentaire à l'échelle évènementielle, saisonnière voire interannuelle ?
- Enfin, est-ce que les prodeltas enregistrent un signal sédimentaire à plus ou moins long terme ? Peut-on évaluer leur vulnérabilité en termes de changement climatique dans la zone côtière ? Doivent-ils être pris en compte dans la gestion intégrée du littoral ?

Nous tenterons de répondre à ces questions au cours de cette étude qui s'organise en cinq parties dont cette introduction générale (**Première Partie**) :

Dans la **Deuxième Partie**, nous définirons les caractéristiques et le fonctionnement des hydro-systèmes côtiers du golfe du Lion. Après un état de l'art sur les caractéristiques du golfe du Lion et de ses différentes unités sédimentaires fonctionnelles, celles des différents fleuves du golfe du Lion et des prodeltas associés (**Partie 2.1**), nous détaillerons le site étudié (**Partie 2.2**).

Dans la **Troisième Partie** seront présentées la stratégie générale employée et la plateforme d'observation à la base de cette étude (**Partie 3.1**). Nous détaillerons les mesures et les analyses effectuées dans la **Partie 3.2**.

Dans la **Quatrième Partie**, nous exposerons les résultats et valorisations des expériences menées autour de cette plateforme expérimentale. Dans la **Partie 4.1**, une compilation des données disponibles sur les fleuves (apports solides et liquides) et les prodeltas associés (taux d'accumulation) du Languedoc-Roussillon sera faite. Les bilans liquides et solides seront établis grâce à l'ensemble des données recueillies auprès des divers organismes (la Banque Hydro, http://www.hydro.eaufrance.fr/) ; et la Compagnie Nationale du Rhône (CNR, http://www.cnr.tm.fr/fr/index.htm) ainsi que les données issues de notre étude pour la Têt. Un premier bilan des taux d'accumulation sur les prodeltas du Languedoc-Roussillon sera réalisé à l'aide du ^{210}Pb sur des carottages effectués sur les prodeltas de la Têt et de l'Aude. Dans les **Parties 4.2** et **4.3**, nous aborderons l'impact des évènements hydro-climatiques extrêmes (crues et tempêtes) sur le système Têt–Littoral roussillonnais, et sa connexion avec le large, notamment avec la sortie du golfe du Lion et les canyons du Cap de Creus et du Lacaze-Duthiers. Cette étude haute-fréquence a été réalisée durant l'hiver 2003-2004 grâce au déploiement d'instruments autonomes de mesure dans la zone côtière : courantomètres, OBS, altimètres, ADCP avec capteur de vagues, et sur la pente continentale : courantomètres, OBS, CTD. Plusieurs évènements de crues et tempêtes ont ainsi pu être mesurés. Une comparaison entre deux tempêtes dont l'une est associée à une crue sera faite dans la **Partie 4.2**. La connexion de la zone côtière avec la pente continentale lors d'un épisode de crue/tempête touchant le littoral roussillonnais sera abordée dans la **Partie 4.3**. Dans la **Partie 4.4,** des mesures de la dynamique sédimentaire effectuées sur une année en 2004-2005 sur le prodelta de la Têt permettront d'aborder la variabilité saisonnière de la circulation hivernale et une comparaison des processus durant les hivers 2003-2004 et 2004-2005. Enfin, dans la **Partie 4.5**, on s'intéressera à l'enregistrement sédimentaire du prodelta de la Têt. Les mesures des taux de sédimentation à l'échelle séculaire (^{210}Pb) et les datations au ^{14}C permettront d'atteindre la variabilité séculaire et millénaire de l'enregistrement sédimentaire du prodelta, afin d'évaluer la valeur du signal sédimentaire pour les littoraux faiblement alimentés.

Enfin, dans la **Cinquième Partie**, on effectuera une synthèse des résultats obtenus durant cette étude afin de répondre aux questions que l'on se posait en introduction. Une généralisation des résultats obtenus sur le prodelta de la Têt à l'ensemble des fleuves côtiers du golfe du Lion sera également faite. Enfin, une synthèse générale sera tirée et des perspectives seront émises en guise de conclusions à cette étude.

1.3 Intérêt pour la communauté scientifique

Ce travail de recherche s'inscrit naturellement dans le cadre de la **Zone Atelier (ZA) ORME (Observatoire Régional de l'Environnement Méditerranéen)** du CNRS (http://medias.obs-mip.fr/orme/). Cette ZA a pour but la mise en place d'un observatoire sur le long terme et à haute fréquence de la zone côtière du golfe du Lion dans un continuum Terre-Mer et dans le cadre d'un programme pluridisciplinaire. A terme, cette ZA constituera un des points d'un réseau méditerranéen, européen et international.

Ce travail de recherche s'est également appuyé sur deux programmes scientifiques de soutien : le programme **SYStèmes CÔtiers et LAGunaires (SYSCOLAG)** financé par la région Languedoc-Roussillon (http://www.ifremer.fr/syscolag/) et le programme européen **EUROpean STRATA FORMation (EUROSTRATAFORM)** (http://www.soc.soton.ac.uk/CHD/EUROSTRATAFORM/). Le programme SYSCOLAG est une collaboration de travaux de thèse (dont celui-ci) et de laboratoires de recherche dans différents domaines allant de la socio-économie, la géographie physique, à la biologie-géologie, et convergeant tous vers la gestion intégrée du littoral du Languedoc-Roussillon. Les principaux résultats de ce programme sont la réalisation d'une base de données pluridisciplinaire, utilisable par les décideurs et actionnaires locaux (http://syscolag.teledetection.fr/), ainsi qu'une publication commune dans une revue scientifique (**Partie 4.1**). Ce programme a également permis de donner une approche plus globale et appliquée à ce travail de recherche qui n'en reste pas moins fondamental. Le programme EUROSTRATAFORM a pour but d'étudier la formation de strates sédimentaires sur les marges continentales et le transfert du matériel particulaire depuis les sources (fleuves) jusqu'aux puits (bassin profond). Ce programme a également permis une collaboration accrue avec plusieurs laboratoires internationaux de pointe dont l' « Instituto de Ciencias del Mar » (CMIMA-CSIC) de Barcelone (Espagne), le « National Oceanographic Centre » (NOC) de Southampton (UK) et le « Bedford Institute of Oceanography » à Halifax (Canada). Ces collaborations ont fait l'objet de séjours de travail dans ces différents laboratoires ainsi que plusieurs publications (**Parties 4.3** et **4.4**, et **Annexe 2**).

Ce travail de recherche a permis la rédaction de plusieurs articles scientifiques dont 5 forment des chapitres de ce manuscrit (**Parties 4.1, 4.2, 4.3, 4.4,** et **4.5**). Quatre des cinq articles présentés dans ce manuscrit font partie de revues spéciales des programmes

EUROSTRATAFORM et SYSCOLAG. Ce travail de recherche a également été présenté dans plusieurs congrès nationaux et internationaux.

Enfin, ce travail de recherche a été mené conjointement avec l'étude, la mise en place et la maintenance d'une station autonome de mesure sur la Têt et son prodelta : la **Plateforme d'Observation de l'Environnement Méditerranéen du Littoral Languedoc-Roussillon (POEM-L2R)**. En effet, j'ai participé en tant qu'ingénieur d'étude pendant l'année précédant mon travail de thèse à la conception et à la mise en place de cette plateforme expérimentale. Les résultats de terrain autour de cette station ont permis d'alimenter plusieurs autres travaux de recherche qui ont fait l'objet de thèses, dont : (1) la calibration du modèle Symphonie en vue d'une spatialisation et d'une budgétisation sédimentaire à l'échelle du Golfe du Lion (**Ulses, 2005**), (2) la calibration d'un modèle de dynamique sédimentaire côtière (**Denamiel, 2006**), et (3) l'analyse des relations du niveau marin et des aquifères côtiers (**Aunay, 2007**). Cette station a également servi de base pour une étude hydrodynamique en vue de l'installation d'un émissaire de rejet des eaux usées des STEP de la ville de Perpignan (**Safege-Cetiis, 2006**).

2 CADRE RÉGIONAL : CARACTÉRISTIQUES ET FONCTIONNEMENT DES HYDRO-SYSTÈMES CÔTIERS MÉDITERRANÉENS

2.1 Les systèmes {fleuves côtiers – prodeltas} dans le golfe du Lion

2.1.1 Le golfe du Lion : une marge continentale à construction deltaïque

2.1.1.1 Généralités

Le golfe du Lion est une marge continentale à construction deltaïque. Il forme un plateau relativement large, incisé par de nombreux canyons sous-marins. Il est soumis à la fois aux apports saisonniers du Rhône, ainsi qu'à ceux de toute une série de fleuves côtiers à caractère torrentiel. Les apports grossiers de ces fleuves alimentent le littoral sableux à proximité des embouchures, alors que les apports fins sont transportés au grès des vagues et des courants sur toute la plateforme et au-delà, vers le bassin profond. Depuis la stabilité du haut niveau marin actuel vers 6000 ans BP environ (**Aloïsi et al., 1978**), ces apports se sont répartis sur toute la plateforme depuis l'embouchure du Rhône où la vasière holocène fait plus de 40 m d'épaisseur jusque sur le plateau roussillonnais au SO où ces dépôts ne font plus que quelques mètres d'épaisseur (**Labaune, 2005**).

Les cartes morpho-sédimentaires des fonds du golfe du Lion présentées dans cette étude sont issues d'une compilation faite pour le site ORME (http://medias.obs-mip.fr/orme/) (**Monaco and Aloïsi, 2000**) à partir de documents cartographiques établis dans le cadre de thèses (**Aloïsi, 1986; Got, 1973; Monaco, 1971**) et de cartes publiées (**Aloïsi et al., 1973; BRGM, 1996**). J'ai intégré ces différentes cartes dans un SIG afin de faciliter l'utilisation de ces données et en vue de les intégrer de manière dynamique dans le site internet ORME.

La répartition de cette vasière holocène montre bien la prépondérance des apports du Rhône par rapport aux fleuves côtiers du pourtour du Languedoc-Roussillon, et le transport général d'est en ouest sur le plateau (**Figure 2-1**). Des dépôts locaux, comme au sud de l'embouchure de l'Aude, montrent également le comblement de dépressions formées avant la dernière transgression marine ainsi que des dépôts associés à des embouchures fluviatiles temporaires (**Monaco, 1971**).

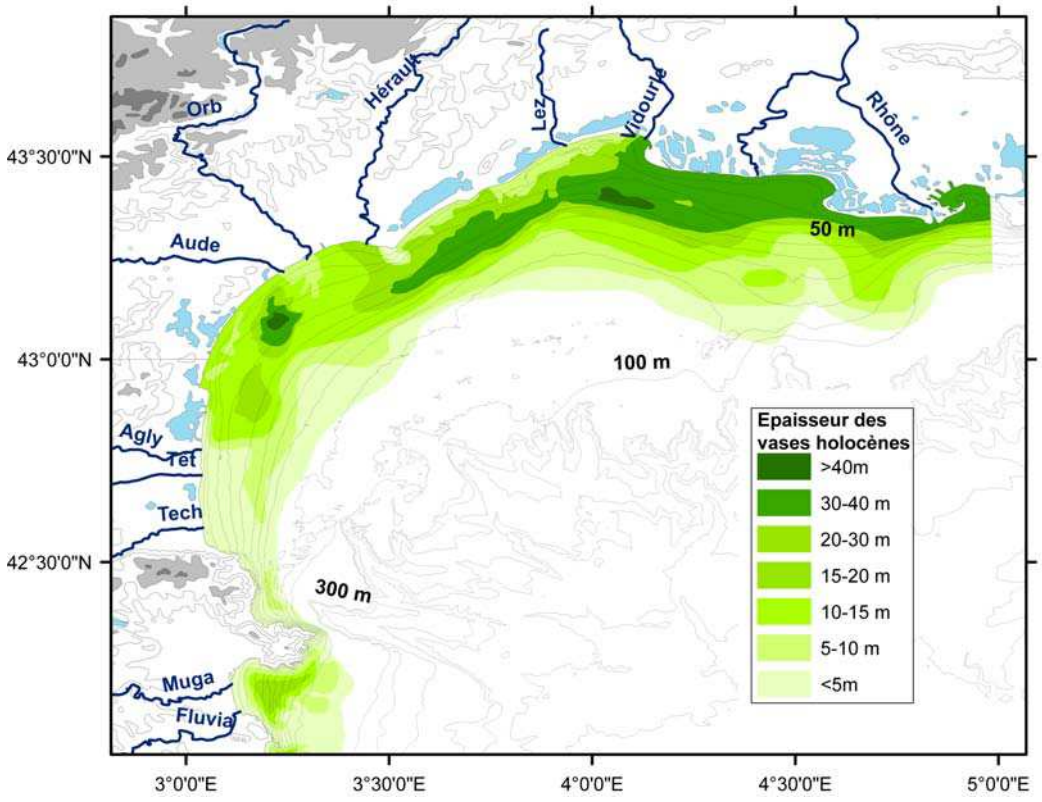

Figure 2-1 : Carte morpho-bathymétrique du golfe du Lion montrant la répartition des épaisseurs de la vasière holocène (Monaco and Aloïsi, 2000).

2.1.1.2 Caractéristiques morpho-bathymétriques et sédimentaires

Les différentes unités sédimentaires du golfe du Lion : les sables littoraux, la vasière circa-littorale (silts et vases) et le domaine du large comprenant notamment des sables hétérogènes (**Figure 2-2**), forment autant d'unités fonctionnelles distinctes interagissant entre elles.

Le littoral sableux est alimenté par les différents fleuves. Ce matériel est mobilisé lors des épisodes de tempête et déplacé suivant la dérive littorale. Il existe plusieurs cellules avec des directions de dérive différentes le long du littoral du golfe du Lion qui dépendent de l'angle d'incidence des vagues principales par rapport à la côte. Les cellules et directions principales de ces dérives littorales sont bien connues et ont été établies par méthodes bathymétrique (**Certain, 2002; Durand, 1999**) ou traçages radioactifs (**Anguenot and Monaco, 1967; Courtois and Monaco, 1969**).

La vasière apparaît à partir de 30 m de profondeur à la limite d'action des vagues de tempête et des forts courants. Elle est directement connectée au delta/prodelta en face du grand Rhône

mais détachée des embouchures et prodeltas des autres fleuves du golfe du Lion. Sa limite externe se situe aux alentours de 90 m de profondeur.

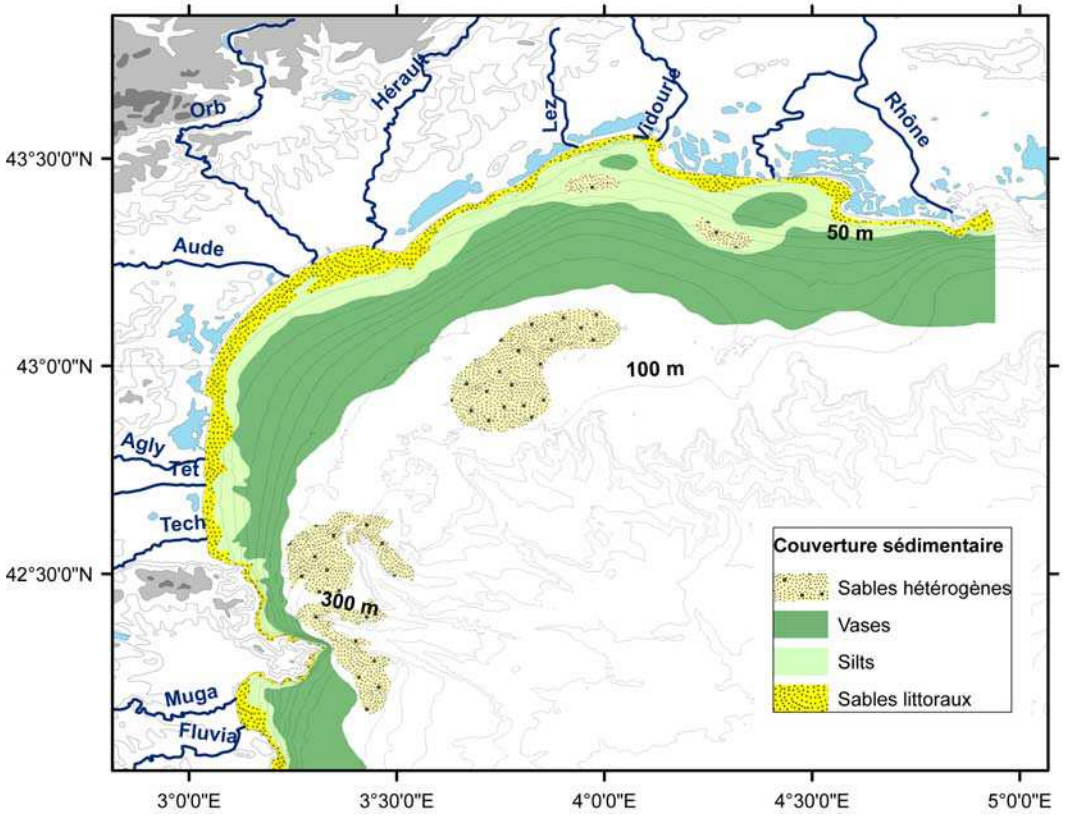

Figure 2-2 : Carte morpho-bathymétrique et sédimentaire du golfe du Lion montrant la répartition des dépôts de surface (Monaco and Aloïsi, 2000).

Le domaine du large est composé de formations hétérogènes de sables et de vases, localisées entre l'isobathe 90 m et la rupture de pente vers 200 m de profondeur. Des formations de sables hétérogènes se situent au milieu du domaine du large ainsi qu'en tête des canyons du Cap de Creus et du Lacaze-Duthiers.

2.1.1.3 Circulations induites par le vent et thermo-haline

Les unités sédimentaires et fonctionnelles du golfe du Lion sont soumises à différents forçages. Dans une mer sans marée, la circulation sur le plateau est induite principalement par le vent. Les vents principaux sont le Mistral de secteur nord et la Tramontane de secteur nord-ouest, vents continentaux à l'origine de tourbillons méso-échelle anticyclonique et cyclonique dans les parties est et ouest du golfe du Lion respectivement (**Estournel et al., 2003**). En période hivernale, conditions non stratifiées, ces vents favorisent la dispersion des panaches

fluviaux et le refroidissement des eaux de surface à l'origine des plongées d'eau dense (**Figure 2-3a**). Les vents marins de SE sont à l'origine des tempêtes et des crues sur le littoral. Ils induisent la formation d'un courant côtier transportant les panaches fluviaux le long du littoral depuis le NE jusqu'au SO (**Figure 2-3b**), lieu d'exportation préférentiel du matériel du plateau vers la sortie du golfe du Lion (**Ulses, 2005**). Le plateau est bordé par un courant de pente (**courant Liguro-Provançal**) dont les instabilités (méandres) favorisent les échanges côte-large, en particulier au niveau des canyons sous-marins (**Figure 2-3c**).

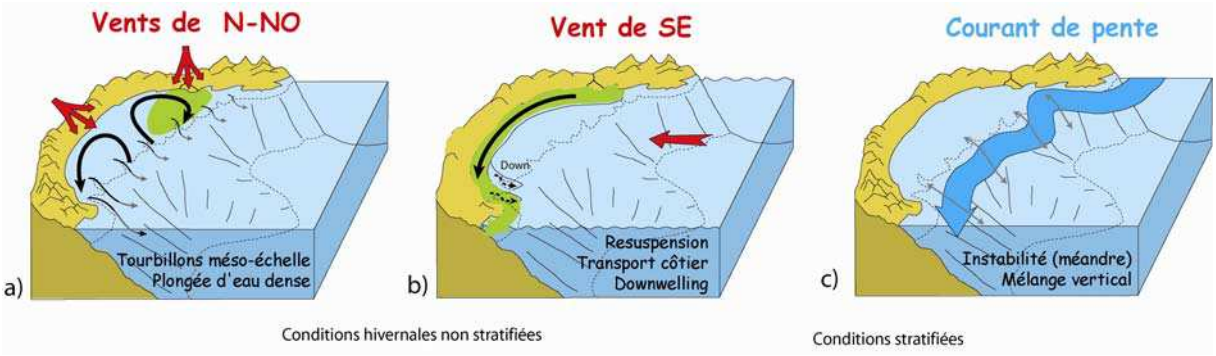

Figure 2-3 : Schémas montrant les principaux mécanismes d'échange côte-large dans le golfe du Lion sous l'influence des vents continentaux (a), sous l'influence des vents marins de SE (b), et du courant de pente (ou thermo-halin) (c).

2.1.1.4 Un climat particulier vecteur d'évènements extrêmes

Le climat méditerranéen est un climat particulier à l'origine d'évènements hydro-climatiques extrêmes. Les étés très chauds et secs alternent avec des périodes automnales et hivernales parfois très pluvieuses à l'origine des crues dévastatrices sur le littoral du golfe du Lion. Les vents marins de secteur E à SE sont également à l'origine des tempêtes qui touchent le littoral. Des années chaudes et humides alternent avec des années froides et sèches. Durant ces années caractérisées par de faibles apports fluviaux, les forts vents continentaux refroidissent les masses d'eaux côtières et du plateau. Celles-ci deviennent ainsi plus denses et se propagent sur le plateau jusqu'aux canyons où ces courants de gravité s'intensifient avec la pente et érodent les fonds marins (**Canals et al., 2006**). Cependant, ces années sont des années exceptionnelles où les processus hydrodynamiques ont un fort impact sur les fonds marins. Les années normales moins énergétiques semblent avoir moins d'impact sur la dynamique hydro-sédimentaire du golfe du Lion.

2.1.2 Influence du Rhône et des fleuves côtiers

2.1.2.1 Des régimes hydrologiques contrastés

Le Rhône est actuellement un des plus gros fleuves en termes d'apports liquide et solide à la Mer Méditerranée avec le Po en Italie, et dans une moindre mesure l'Ebre en Espagne ; en effet le Nil a un très faible débit voire nul depuis la construction de l'énorme barrage d'Assouan à partir de 1960 (**Tableau 2-1**).

Fleuves	Débit liquide (m^3/s)			Charge solide (X 10^6 m^3/an)	Période étudiée
	Minimum	Maximum	Moyenne		
Rhône	234 [(1)]	11000 [(2)]	1700 [(1)]	8 [(3)]	1920-2004
Po	275 (4)	11580 (4)	1480 [(4)]	10.4 [(5)]	1919-1996
Ebre	136	712	426 [(6)*]	0.1 [(6)*]	1960-1999
Nil	/	/	951 [(7)*]	~0*	1871-1999

Tableau 2-1 : Comparaison des caractéristiques du Rhône avec quelques uns des plus gros fleuves de Méditerranée [(1) CNR, 2006 ; (2) Balland et al., 2004 ; (3) Antonelli, 2002 ; (4) Po River Basin Authority, 2005 ; (5) Hovius, 1998 ; (6) Carles Ibañez, 1996 ; (7) Vörösmarty et al., 1996 ; * après la construction de barrages].

Le Rhône a un caractère saisonnier marqué avec de forts débits durant les crues automnales et hivernales, ainsi que pendant la fonte des neiges au printemps, et des débits faibles durant l'été. Le caractère saisonnier du Rhône reste bien moins marqué que pour les fleuves côtiers du golfe du Lion dont le fonctionnement ressemble à celui des oueds nord-africains avec des débits faibles voire nuls en été (cas de l'Agly, **Serrat., 1999**) et de forts débits lors de crues-éclairs (cas de la Têt, **Serrat et al., 2001**). L'essentiel du matériel sédimentaire de ces fleuves côtiers est de ce fait apporté pendant les crues.

2.1.2.2 Régimes de crues et périodes de retour

Le Rhône possède le plus large bassin versant de la zone côtière du golfe du Lion (95500 km² à Beaucaire) s'étalant sur une grande partie du territoire français. De ce fait il est soumis à différents régimes de crue suivant l'origine des précipitations. On distinguera 3 types principaux selon **Pardé, 1925** :

- Le **type océanique** lorsque les précipitations d'origine atlantique parviennent sur le haut du bassin versant engendrant des crues avec des débits relativement faibles (4000 à 5000 m^3/s) ; ces crues interviennent principalement en hiver.
- Le **type cévenol** lorsque les entrées maritimes provoquent de fortes précipitations en aval du bassin engendrant des débits importants (jusqu'à 9000 m^3/s) ; ces crues interviennent essentiellement à l'automne et au printemps.
- Enfin, le **type généralisé** lorsque l'ensemble du bassin versant est affecté par des précipitations d'origine diverse, avec des débits > 9000 m^3/s comme le cas de la crue de décembre 2003 (débit estimé à 12000-13000 m^3/s et corrigé à 11000 m^3/s dans le rapport **Balland et al., 2004**).

Fleuves	Nature des bassins versant (avant la plaine)	Superficie (km^2)	Longueur (km)	Pente moyenne (‰)	Altitude de la source (m)
Tech	Roches cristallines et métamorphiques	726	82	30	2400
Têt	Roches cristallines et métamorphiques	1300	114	17	2450
Agly	Calcaires et marnes	1040	80	8.8	1230
Aude	Calcaires, marnes et molasses	4830	150	13	2180
Orb	Calcaires, marnes et molasses	1437	115	7.4	850
Hérault	Calcaires, marnes et molasses	2550	135	10.7	1560
Lez	Calcaires, marnes et argiles	1235	24	4	100
Vidourle	Calcaires, argiles et marnes	1335	85	6	520
Rhône	Variée	95500	812	4	3600

Tableau 2-2 : Caractères géomorphologiques des bassins-versants des fleuves du golfe du Lion. Sources DDAF des Pyrénées Orientales et DIREN du Languedoc-Roussillon.

Contrairement au Rhône, les fleuves côtiers du golfe du Lion sont caractérisés par un bassin versant moins large et beaucoup plus pentu, qui peut être rapproché au type **bassin côtier montagneux** défini par **Milliman et Syvitski, 1992** (**Tableau 2-2**). Ces fleuves côtiers ont des bassins versants qui sont en formes « d'amphithéâtre » tourné vers la mer. Ils sont le réceptacle des eaux de pluie arrivant principalement par les entrées maritimes de la Méditerranée. Leur débit d'étiage est très faible et subissent des crues brèves très fortes du type cévenol durant la période automnale au printemps.

Ainsi, au niveau du golfe du Lion et plus particulièrement au niveau de ces fleuves côtiers on ne s'intéressera par la suite qu'à seulement 2 types de crues :

- Le **type cévenol** qui affecte des zones restreintes à certains bassins versants sous l'effet des entrées maritimes. Ces crues peuvent provoquer des dégâts dévastateurs dans les bassins versant concernés (cas de la crue de novembre 1999 sur l'Agly : **Gaume et al., 1999** ; cas de la crue de septembre 2002 sur le Lez : **Delrieu et al., 2002**). Ces crues peuvent également être appelées **crues-éclairs** au « **flash-flood** », mais on trouve également le terme de « **oceanic flood** » selon **Wheatcroft (2000)**, à ne pas confondre avec le type océanique du Rhône. Le terme « oceanic flood » correspond aux crues-éclairs des fleuves côtiers qui ont un impact direct et rapide sur l'hydrologie de la zone côtière par les apports en eaux douces et solides. Ce type de crue isolée aux bassins côtiers roussillonnais sera étudié dans la **Partie 4.3**.
- Le **type généralisé ou méditerranéen étendu** lorsque tous les fleuves côtiers (depuis le Tech jusqu'au Vidourle) ainsi que le Rhône sont simultanément affectés par des crues en réponse à des entrées maritimes. Ce dernier cas sera étudié dans les **Parties 4.2** et **4.5** (crue de décembre 2003 dans le golfe du Lion).

Les caractéristiques hydrologiques des fleuves côtiers du golfe du Lion et du Rhône seront abordées dans la **partie 4.1** et les périodes de retour de crue sont récapitulées dans le **Tableau 2-3**.

Fleuves	Période de mesure	Station de référence	Débits instantanées en m^3/s, période de retour T en années				
			T2	T5	T10	T20	T50
Tech	1976-2007	Elne	550	940	1200	1500	1800
Têt	1970-2007	Perpignan	310	560	720	880	1100
Agly	1967-2004	Estagel	400	710	920	1100	1400
Aude	1965-2006	Moussan	630	1000	1300	1500	1800
Orb	1966-2006	Béziers	620	1000	1300	1500	1900
Hérault	1952-2004	Agde	780	1100	1300	1500	1800
Lez	1975-2006	Montferrier	100	200	260	310	390
Vidourle	1969-2006	Marsillargues	440	690	850	1000	1200
Rhône	1920-2002	Beaucaire	5800	7200	8200	9100	10000

Tableau 2-3 : Période de retour des crues des fleuves du golfe du Lion et débits instantanées associés. Données consultables sur la banque Hydro.

2.1.2.3 Le fleuve Têt : un exemple de fleuve côtier du Languedoc-Roussillon

La Têt est un fleuve côtier à caractère torrentiel situé sur le littoral roussillonnais à la sortie du golfe du Lion. Son bassin versant est divisé en deux parties : une partie montagneuse de sa source (2450 m) à l'entrée de la plaine où se situe le lac de Vinça (250 m), soit une pente moyenne de 37 ‰, caractérisée par des formations cristallines et métamorphiques ; et une partie plate en arrivant dans la plaine roussillonnaise (pente moyenne de 4 ‰). La plaine est caractérisée par des formations plus meubles d'âge Pliocène et Holocène, facilement érodables notamment par les crues (**Figure 2-4**). La Têt y emprunte un chemin plus ou moins rectiligne qui a été stabilisé par l'homme depuis la fin du XVIIe s. jusqu'à aujourd'hui (**Desailly, 1990**), avant de se jeter dans la mer à proximité de Canet-en-Roussillon.

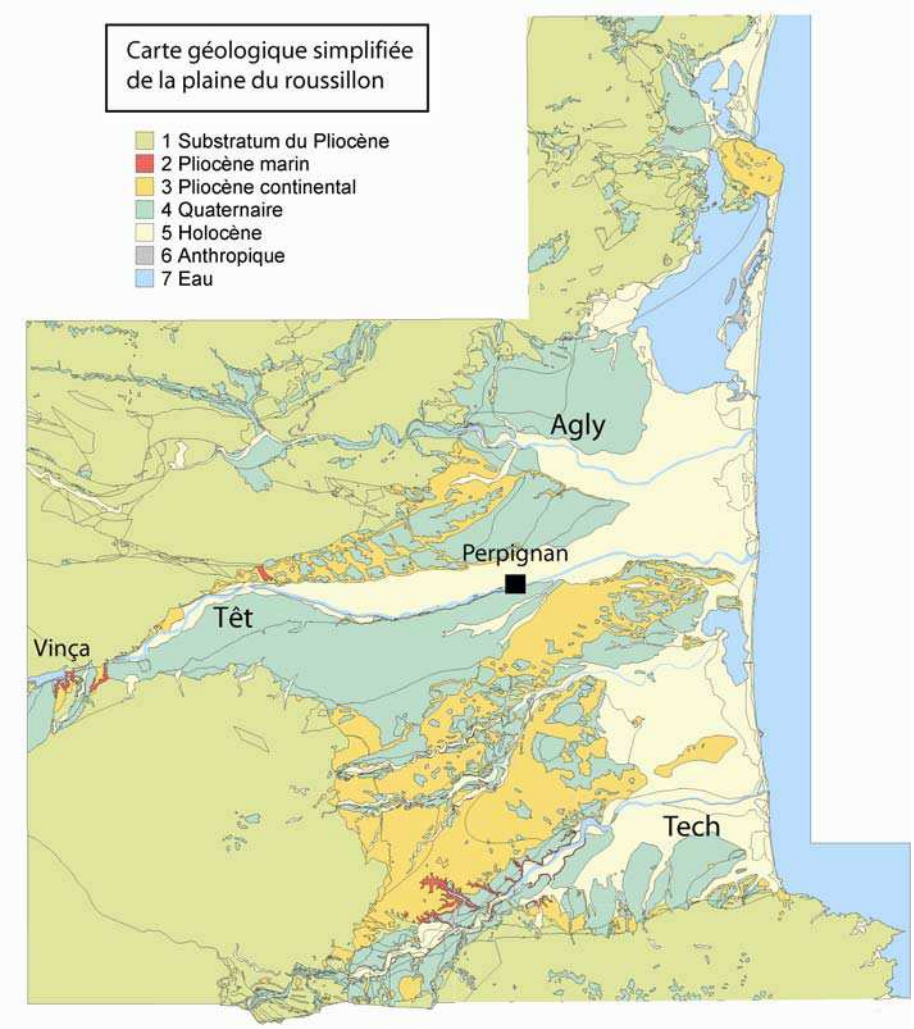

Figure 2-4 : Carte géologique simplifiée de la plaine du Roussillon. BRGM. Aunay (2007).

Le lac de Vinça situé à 55 km de l'embouchure est un lac de barrage construit en 1978 et servant à écrêter les crues de grande ampleur et ainsi protéger les villes situées en contrebas dont celle de Perpignan. De nombreuses crues dévastatrices de la Têt sont mentionnées dans la littérature (**Desailly, 1990**) depuis 1876, et le barrage de Vinça semble jouer son rôle après 1978 (**Figure 2-5**). En effet, les débits maximum enregistrés à Perpignan avant 1978 montrent de nombreuses crues dévastatrices qui ont détruit à plusieurs reprises les ponts de la ville. La crue de 1940, aussi appelée « **l'aiguât** » est une des crues les plus importantes de mémoire d'homme avec un débit maximum supérieur à 3500 m^3/s soit plus de 2 fois le débit moyen du Rhône. Depuis la création du barrage, les débits maximaux enregistrés à Perpignan sont bien inférieurs à 1000 m^3/s et ne crée plus de dégâts importants en aval. Cependant, en écrêtant les crues, le barrage semble aussi retenir une partie difficilement évaluable de la charge

sédimentaire en suspension (**Garcia-Estevez, 2005**) et ainsi contribuer à l'appauvrissement du stock sableux sur le littoral et à l'érosion côtière.

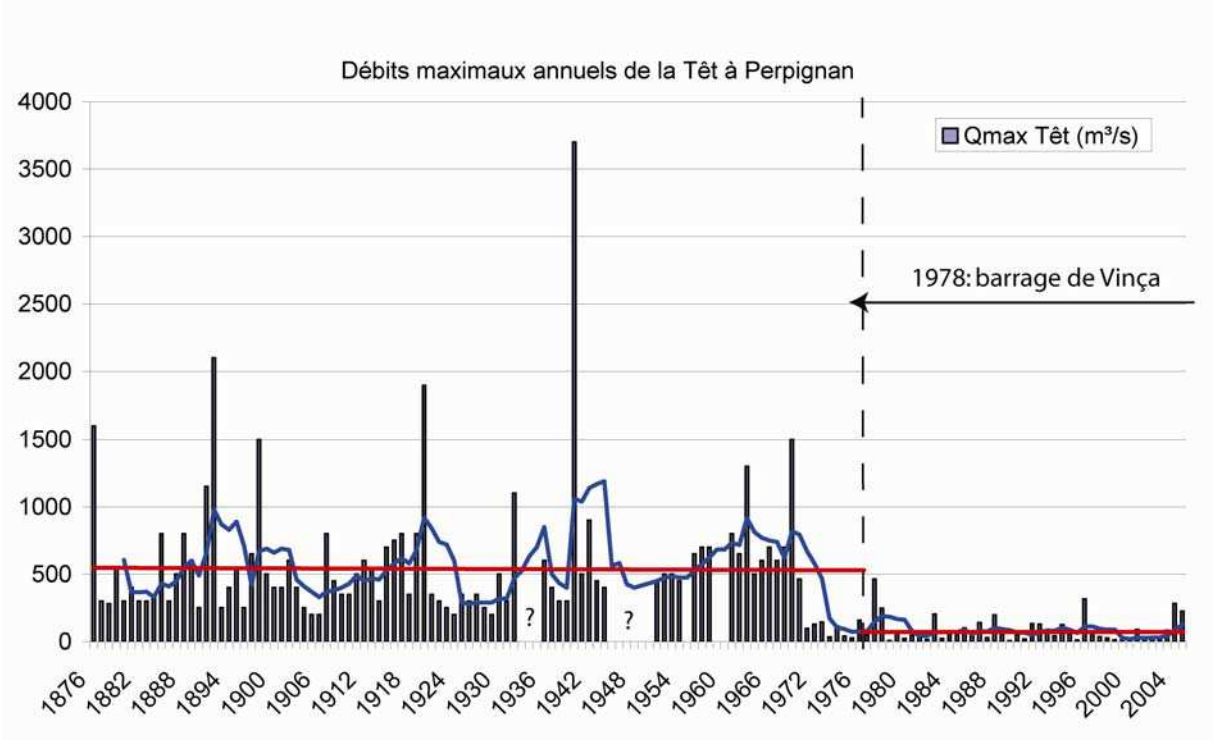

Figure 2-5 : Débits maximaux annuels de la Têt à Perpignan. D'après Delorme (1980), pour les données 1876-1970 et données issues de la banque Hydro de 1970 à 2004. Deux plateaux (droites rouges) sont identifiés correspondant à la moyenne des débits maximaux avant et après la construction du barrage de Vinça.

2.1.3 Des formations côtières particulières : les prodeltas

2.1.3.1 Définition des prodeltas

Beaucoup de termes sont cités dans la littérature pour définir les prodeltas, et beaucoup de confusion existe dans la traduction des termes anglo-saxons se rapportant aux prodeltas (« deltaic fronts », « subaqueous delta »…). On retiendra la définition suivante : le prodelta correspond à la prolongation sous-marine du delta. Il se forme généralement vers 30 m de profondeur en dessous de la limite d'action des vagues (**Diaz et al., 1996**). Il est formé essentiellement de sédiments cohésifs qui concentrent les contaminants organiques ainsi que les métaux (**Roussiez, 2006**). Suivant la taille du système et l'influence des apports solides du fleuve, le prodelta peut être soit localisé en continuité du delta (cas du Rhône, **Figure 2-6 a**),

soit isolé dans le cas des fleuves côtiers (cas de la Têt, **Figure 2-6 b**). Le Rhône forme un delta bien développé qui se prolonge jusqu'à des profondeurs importantes (~60 m). Son prodelta est continu avec le delta et se confond avec la vasière médiane. Dans le cas des fleuves côtiers, le delta n'est pas très développé et généralement limité à de faibles profondeurs dans la zone côtière. Le prodelta n'est pas en continuité entre le delta et la vasière, et il forme une tache isolée vers 30 m de profondeur entre le delta et la vasière médiane.

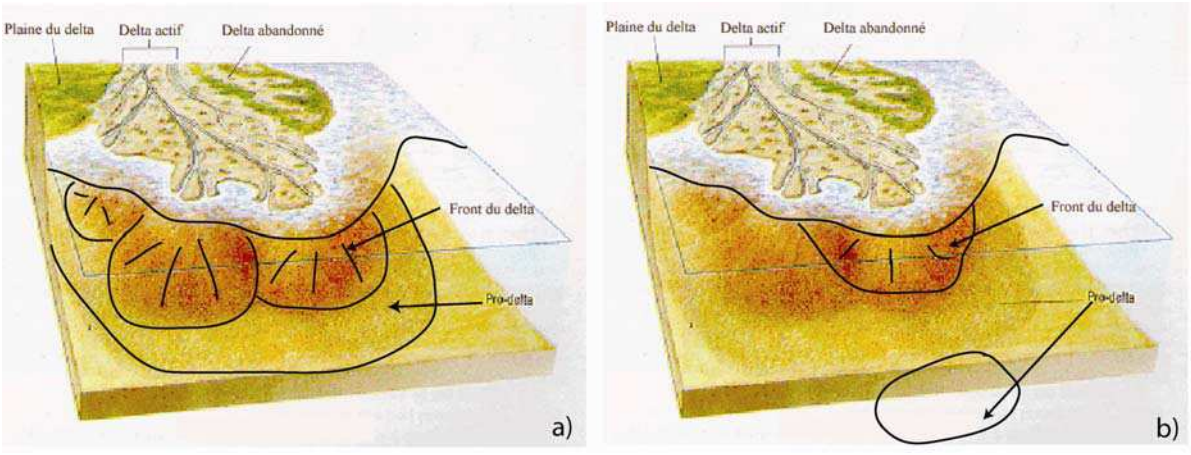

Figure 2-6 : Schéma d'un delta bien développé et de son prodelta. (type Rhône, a) et d'un delta et prodelta reliés à un petit fleuve côtier (type Têt, b)

2.1.3.2 Mise en place et localisation

Les prodeltas sont présents devant n'importe quelle embouchure, que se soit en face des fleuves, ou des graus des lagunes. Ils se forment dès qu'il y a débouché en mer de suspensions solides qui se déposent sous l'effet de la gravité et de la floculation lorsque l'énergie du milieu diminue (**Pauc, 2005**). Ils sont l'expression des évènements hydro-climatiques à l'interface Terre-Mer. En effet, leur persistance et leur accroissement est fonction de la balance entre les apports sédimentaires et les phénomènes de resuspension/advection. Ils se développent donc en fonction de l'intensité et du nombre de crue, et sont érodés durant les tempêtes et par les courants côtiers intenses.

Dans le golfe du Lion, ils sont localisés en face du Rhône, ainsi qu'en face des fleuves côtiers (**Figure 2-7**). Leur cartographie précise a été établie à partir des concentrations en argiles gonflantes telles que les smectites (**Aloïsi and Monaco, 1975**), et des concentrations en

métaux (**Roussiez et al., 2005**) dans les sédiments de surface. Le prodelta du Rhône est bien développé et est défléchi vers l'ouest montrant l'influence du transport d'est en ouest dans la zone. Le prodelta du Vidourle est situé dans le golfe d'Aigues-Mortes et son extension se fait entre son débouché naturel et un grau de vidange emprunté durant les crues (**Aloïsi et al., 1975**). Les prodeltas de l'Aude, Orb et Hérault semblent se confondre en un seul édifice centré au droit du débouché de l'Aude. Des prodeltas reliques (ou actifs ?) sont également localisés au débouché de l'étang de Thau et en face du secteur Port-La-Nouvelle - Gruissan. Les prodeltas de la Têt et du Tech forment quant à eux, des tâches isolées sur le littoral roussillonnais encerclés par des rochers littoraux affleurant (**Monaco, 1975**).

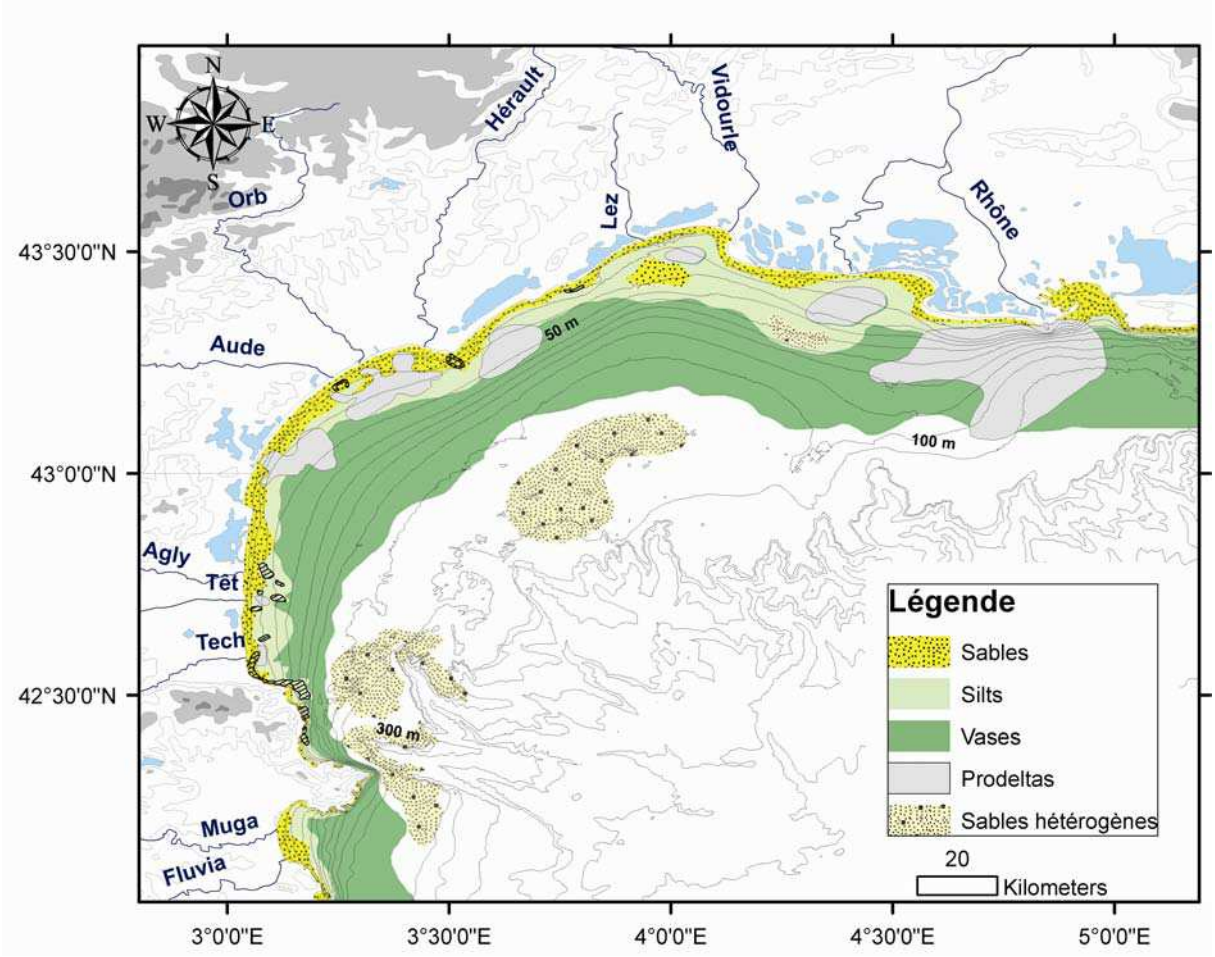

Figure 2-7 : Carte morpho-sédimentaire du golfe du Lion montrant la répartition des différentes unités sédimentaires fonctionnelles dont les prodeltas qui sont l'expression des mécanismes hydro-climatiques côtiers.

2.1.3.3 Vulnérabilité et évolution

On a vu précédemment que les prodeltas, unités fonctionnelles de la zone côtière, concentre les sédiments fins ainsi que les contaminants associés. Si ces unités sont dynamiques, elles jouent alors un rôle important dans la qualité des eaux littorales en jouant à la fois le rôle de pièges et de sources de matière. Les prodeltas doivent donc être pris en compte dans la gestion intégrée de la zone côtière, particulièrement lors de l'implantation des émissaires de rejet des eaux usées ou de fermes piscicoles. Par ailleurs, ces unités sont dépendantes des apports solides par les fleuves et du remaniement par les mécanismes hydrodynamiques. Comment ces zones vont-elles évoluer en réponse à une modification du nombre ou de l'intensité des apports et/ou des mécanismes hydrodynamiques liés au changement climatique ? Comment ces zones vont-elles évoluer en réponse à une pression anthropique de plus en plus grandissante dans la zone côtière ?

2.2 Présentation du site d'étude

2.2.1 Le prodelta de la Têt

Le plateau continental roussillonnais situé au SO du golfe du Lion, est marqué par une pente faible (4 ‰) au nord de la zone en face de l'embouchure de l'Agly. Ce plateau se rétrécie ensuite vers le sud avec une pente forte (20 ‰) en face du canyon du Cap de Creus (**Figure 2-8**). Le plateau roussillonnais présente un littoral sableux au nord et rocheux au sud du Tech. Ce littoral sableux laisse progressivement la place à une zone silteuse à partir de 15-20 m de profondeur, puis à une zone vaseuse à partir de 40-50 m de profondeur. Cette vasière est ensuite interrompue au large à partir de l'isobathe 90 m avec une zone hétérogène formée de sables et vases laissant affleurer des sédiments plus anciens. Le domaine du large s'étend jusqu'à la rupture de pente du plateau où sont situés les canyons sous-marins, qui font la transition entre la marge et le bassin profond.

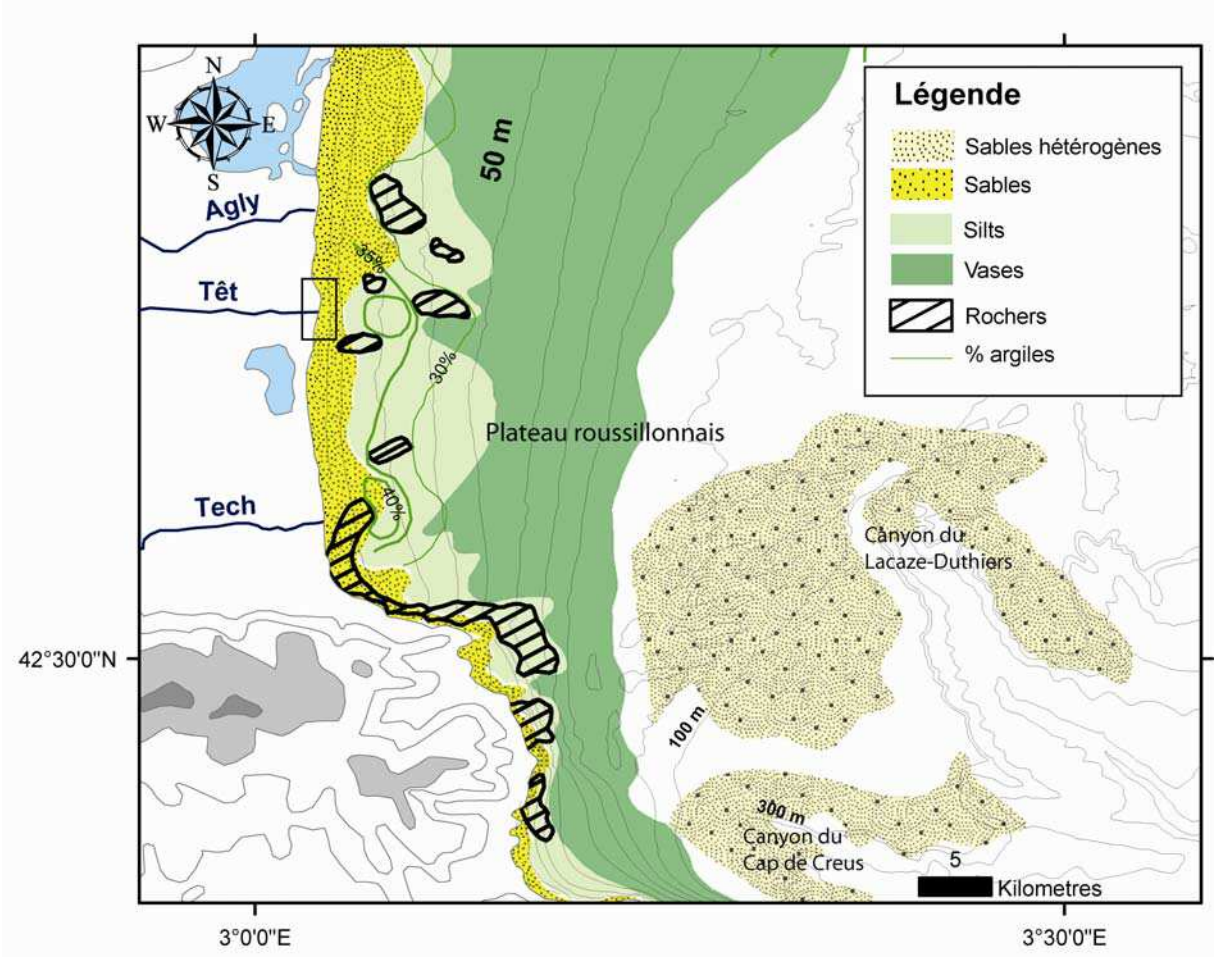

Figure 2-8 : Carte morpho-bathymétrique et sédimentaire du plateau continental roussillonnais (Monaco, 1975; Monaco and Aloïsi, 2000). Le pourcentage en argiles gonflantes dans les sédiments de surface est indiqué par les isolignes vertes. Le rectangle noir au niveau de l'embouchure de la Têt délimite la couverture bathymétrique représentée sur la Figure 2-9.

Située au sud de la zone côtière du Languedoc-Roussillon, l'embouchure de la Têt présente une flèche sableuse rattachée à sa bordure sud qui indique le sens de la dérive littorale dirigée vers le nord (**Figure 2-9**). Cette flèche sableuse est épisodiquement interrompue en cas de forte crue de la Têt et son tracé terminal est alors rectiligne (tracé en rouge, **Figure 2-9**). Dans la partie sous-marine, le delta actuel se situe légèrement au nord de l'embouchure de la Têt entre 0 et 10 m de profondeur. Un delta relique, témoin de crues anciennes et rattaché à un bras de delta abandonné, est situé plus au nord de la zone près du port de Sainte Marie.

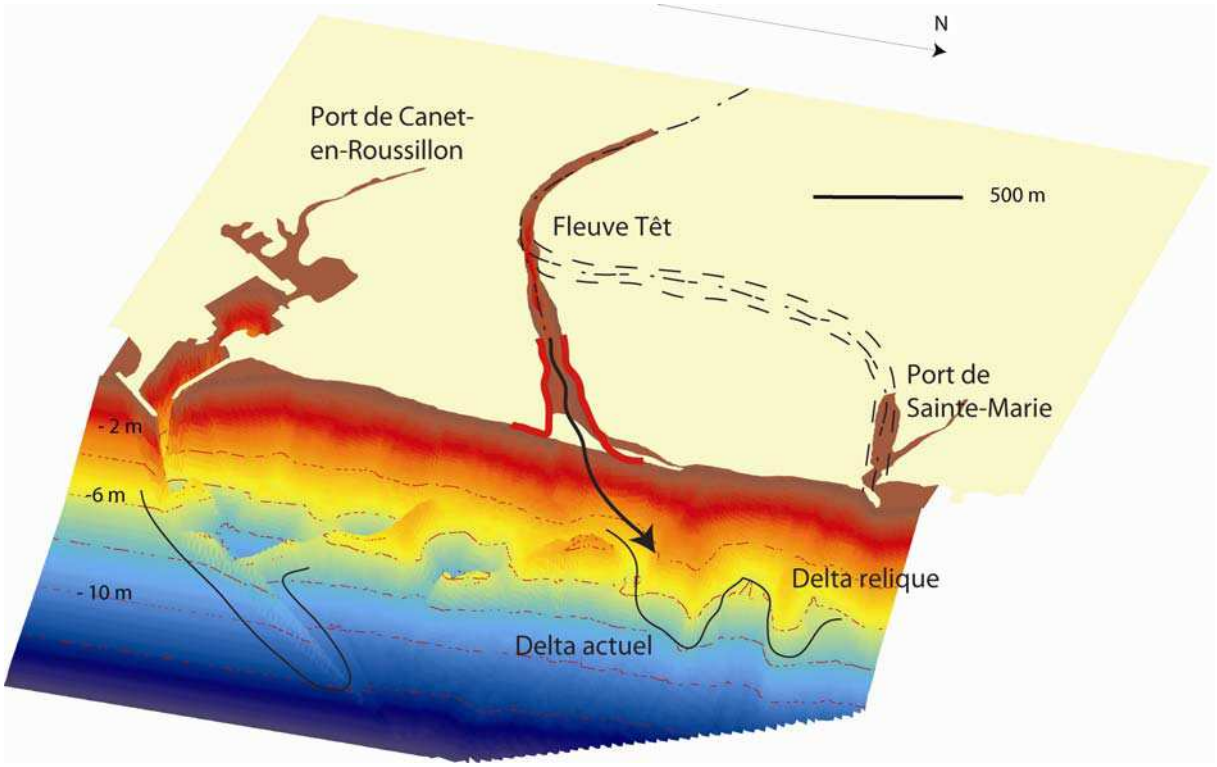

Figure 2-9 : Carte morpho-bathymétrique de l'embouchure de la Têt réalisée à partir de données bathymétriques du 18 avril 2004. La localisation de cette bathymétrie fine réalisée en avril 2004 est indiquée sur la Figure 2-8.

Le prodelta de la Têt a été caractérisé à partir de la concentration en argiles dans les dépôts superficiels de la zone côtière roussillonnaise (**Monaco, 1975**). Cette zone montre une augmentation notable de la concentration en montmorillonite (> 40%) au droit de l'embouchure du fleuve Têt centrée autour de l'isobathe 30 m et dont la superficie fait environ 12 km² (**Figure 2-8**). Cette zone de dépôt préférentiel de matériel fin se situe légèrement au sud suivant la circulation côtière résiduelle qui est principalement dirigée vers le sud, opposée au sens de la dérive littorale. Ce prodelta forme une tâche isolée entre l'embouchure et son delta sableux (0-10m), et la vasière médiane plus au large (> 50 m). Des affleurements ou rochers littoraux encadrent également le prodelta de la Têt et semblent avoir un effet directeur sur la position de cette zone.

2.2.2 Les forçages

Le littoral roussillonnais est soumis aux apports torrentiels de la Têt dont l'essentiel du flux liquide et solide est apporté durant des épisodes de « crues-éclairs » (**Serrat et al., 2001**). Les périodes de retour et débits associés des crues de la Têt ont été indiquées précédemment dans

le **Tableau 2-3**. Les vents dominants sont les vents des secteurs NO (Tramontane) et d'E-SE (Marin). La Tramontane souffle environ 80% du temps mesuré, avec une plus grande proportion des vents soufflant entre 10 et 20 m/s (**Figure 2-10**). Ce vent continental intense est responsable du mélange des eaux et de l'affaiblissement de la stratification en été, et du refroidissement intense par évaporation des eaux en hiver. Les vents marins sont moins fréquents (~20 % du temps mesuré) et sont responsables des brises marines et des entrées maritimes à l'origine des crues cévenoles.

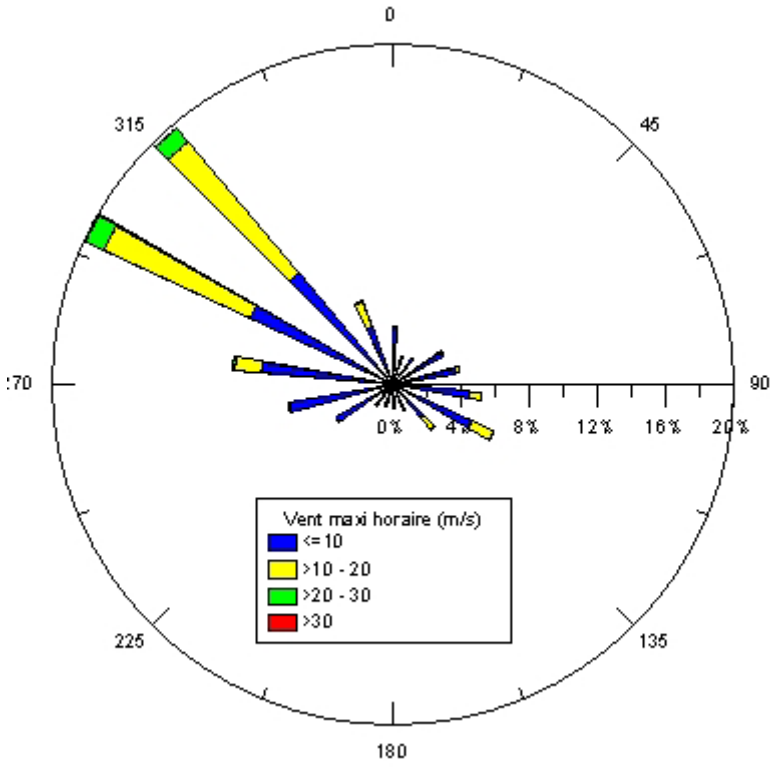

Figure 2-10 : Histogramme angulaire de la direction des vents maxi horaires mesurés au niveau du prodelta de la Têt entre 2003 et 2005.

La colonne d'eau est bien mélangée en hiver de fin octobre à fin mai. La stratification des eaux commencent au mois de juin par un réchauffement des eaux de surface (**Figure 2-11**). La thermocline s'enfonce jusqu'à ~30 m de profondeur à partir du mois de juillet jusqu'à octobre. On observe parfois des périodes de refroidissement intense des eaux de surface et une rupture de cette stratification en été dû à d'intenses coups de vent. Cette évolution de la stratification thermique de la zone côtière du prodelta de la Têt a été observée de janvier à novembre 2004 (**Figure 2-11**), mais peut varier d'une année sur l'autre en fonction de la fréquence des vents continentaux par rapport aux vents marins.

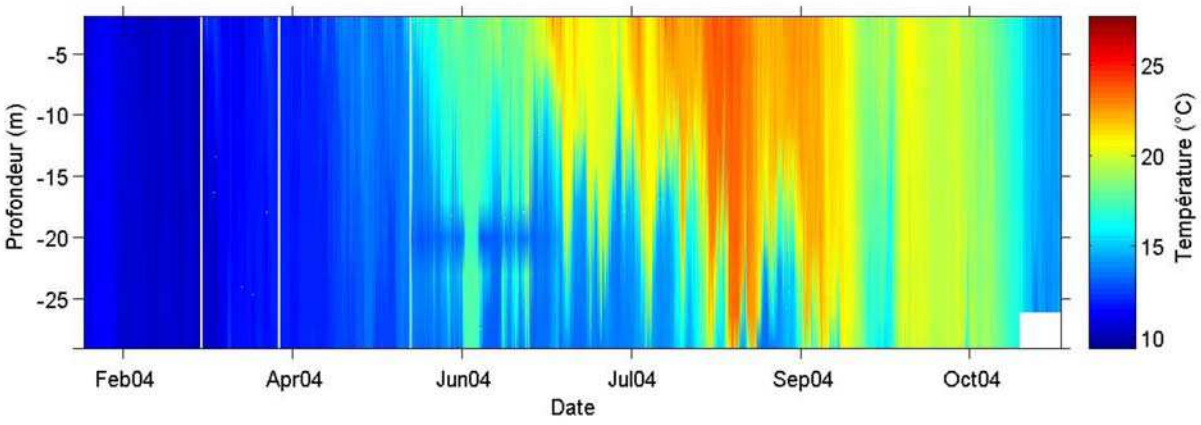

Figure 2-11 : Graphique couleur de la température de la colonne d'eau mesurée sur le prodelta de la Têt en 2004 (données issues de Safege-Cetiis, 2006).

Concernant les courants dans la zone côtière du prodelta de la Têt (**Figure 2-12**), ils sont principalement orientés le long du littoral et les lignes bathymétriques. Si on regarde les courants de fond (**Figure 2-12**, à gauche), ils sont principalement dirigés vers le S (~80 % du temps mesuré) avec la plupart des vitesses du courant comprises entre 0.1 et 0.2 m/s. Quelques inversions du courant dirigé vers le nord sont également observées (~20 % du temps). Les courants de surface (**Figure 2-12**, à droite) sont principalement dirigés vers le sud. Les inversions du courant de surface vers le nord sont très rares ; les vitesses du courant de surface sont pour la plupart > 0.3 m/s.

Enfin, dans une mer sans marée, le forçage le plus important, en domaine côtier, est la houle générée par les dépressions au large qui provoque la resuspension des sédiments côtiers lorsqu'elle déferle sur le littoral. Les vents continentaux, la Tramontane de secteur NO s'engouffrant entre les Pyrénées et le Massif Central, et le Mistral de secteur N soufflant entre le Massif Central et les Alpes, ont pour origine la différence de pression entre l'anticyclone du nord de l'Europe et le minimum dépressionnaire centré sur le golfe de Gênes. Cette dépression peut engendrer des vagues de secteur NE assez faibles (hauteur significative, Hs, rarement supérieure à 1 m, et période des pics, Tp, comprise entre 3 et 5 s, **Figure 2-13**) qui restent relativement rares (~10 % du temps mesuré). Par contre, des vagues longues et puissantes sont générées par les dépressions centrées au sud de la Corse, sur la Sardaigne et la Sicile.

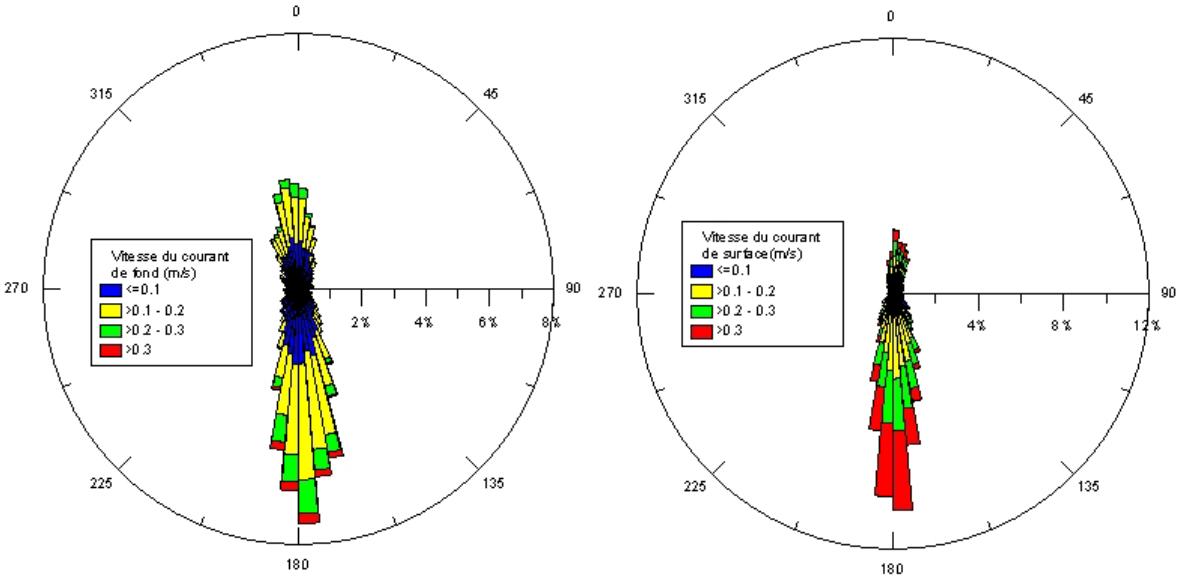

Figure 2-12 : Histogrammes angulaires de la direction et intensité des courants au fond (28 m de profondeur, à gauche) et en surface (à droite) mesurés sur le prodelta de la Têt entre 2003 et 2005.

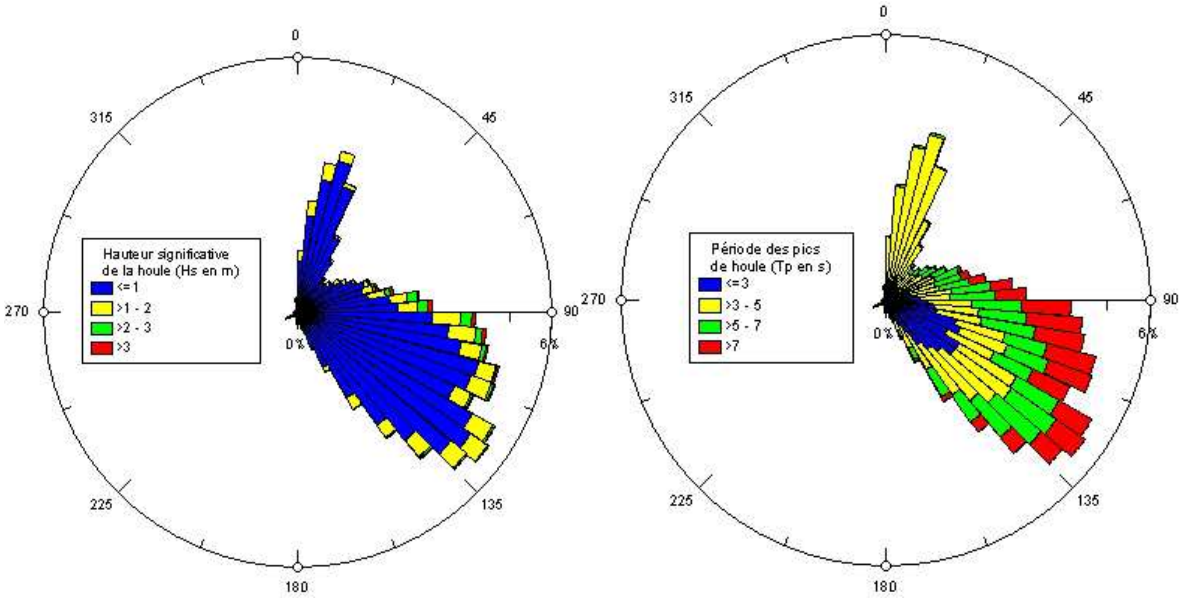

Figure 2-13 : Histogrammes angulaires de la hauteur significative des vagues (Hs à gauche) et de la période des pics des vagues (Tp à droite) mesurés sur le prodelta de la Têt entre 2003 et 2005.

Ces dépressions sont associées à de forts vents marins qui se chargent d'humidité au contact de la mer Méditerranée et sont responsables des évènements cévenols affectant la côte du golfe du Lion. Ces vagues sont de secteur E à SE caractérisées par des Hs > 1 m et des Tp > 7 s et sont les plus fréquentes (> 50% des vagues mesurées). Les plus fortes vagues générées sont de secteur E (Hs > 3 m et Tp > 7s) avec quelques rares évènements extrêmes (Hs > 7 m

et Tp> 10 s). Les périodes de retour de ces évènements extrêmes ont été évalués à partir de l'ajustement de la loi de Gumbel sur les valeurs annuelles extrêmes mesurées sur le prodelta de la Têt (2003-2005) et des valeurs extrêmes issues du modèle VagMed (1996-2000) de Météo France (**Figure 2-14**).

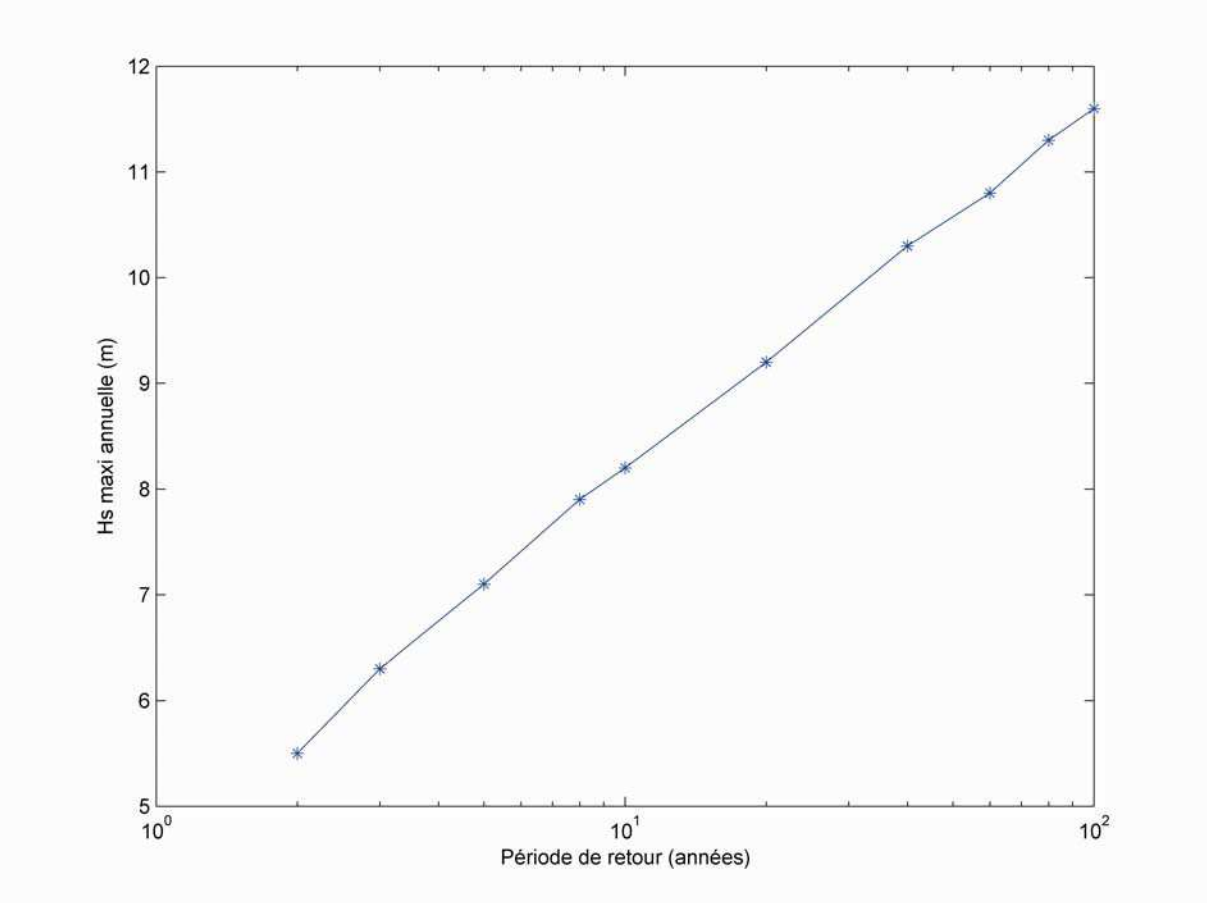

Figure 2-14 : Périodes de retour de la hauteur significative maximale annuelle des vagues selon un ajustement des mesures à loi de Gumbel.

Les périodes de retour estimées sur le prodelta de la Têt sont légèrement inférieures à celles estimées à partir des mesures de la bouée de Port-Vendres (2002-2005), qui sont elles-mêmes plus faibles que les estimations faites à partir des mesures de la bouée de Sète (1988-2001) (**Guizien, soumis**). En effet, les vagues mesurées sur le prodelta de la Têt montrent des valeurs légèrement supérieures aux deux autres stations de mesure, puisque le site de la Têt est orienté N-S et reçoit directement les vagues les plus fortes de secteur E-SE.

2.3 Conclusions

Dans le **chapitre 2**, nous avons défini les caractéristiques et le fonctionnement du golfe du Lion dans son ensemble. Nous avons ensuite caractérisé les différents hydro-systèmes côtiers du golfe du Lion. Le Rhône et son prodelta ont largement été étudiés au cours de précédentes études (**Antonelli, 2002 ; Maillet et al. 2006**). Par contre peu d'études ont été menées sur les autres fleuves côtiers du golfe du Lion. Dans ce cadre, notre étude porte sur le fleuve Têt et son prodelta dont nous avons défini les caractéristiques et les forçages agissant sur ce système.

Afin de mesurer et caractériser les mécanismes hydro-sédimentaires essentiels agissant sur le prodelta de la Têt, une stratégie d'étude particulière a été entreprise et sera détaillée dans le **chapitre 3**. Après avoir défini la stratégie générale et les campagnes de mesure associées, nous détaillerons les mesures et analyses effectuées au cours de notre étude.

3 MATÉRIEL ET MÉTHODES : LA PLATEFORME D'OBSERVATION DE L'ENVIRONNEMENT MÉDITERRANÉEN – LITTORAL LANGUEDOC-ROUSSILLON (POEM-L2R)

3.1 Stratégie générale : une approche multi-échelle

3.1.1 Un système de mesure adapté : la plateforme POEM-L2R

La Têt est un fleuve côtier torrentiel soumis aux évènements hydro-climatiques brusques et intenses du climat méditerranéen. La fréquence et la brièveté de ces évènements nécessite un dispositif instrumental et de mesure adapté. Nous avons donc mis en place la **plateforme POEM-L2R** afin de suivre à la fois les apports sédimentaires discontinus du fleuve Têt, ainsi que l'impact et le devenir de ces apports dans la zone littorale. Cette plateforme est composée d'une station fluviale automatisée, proche de l'embouchure, et d'une bouée météo-marine sur le prodelta de la Têt (**Figure 3-1**).

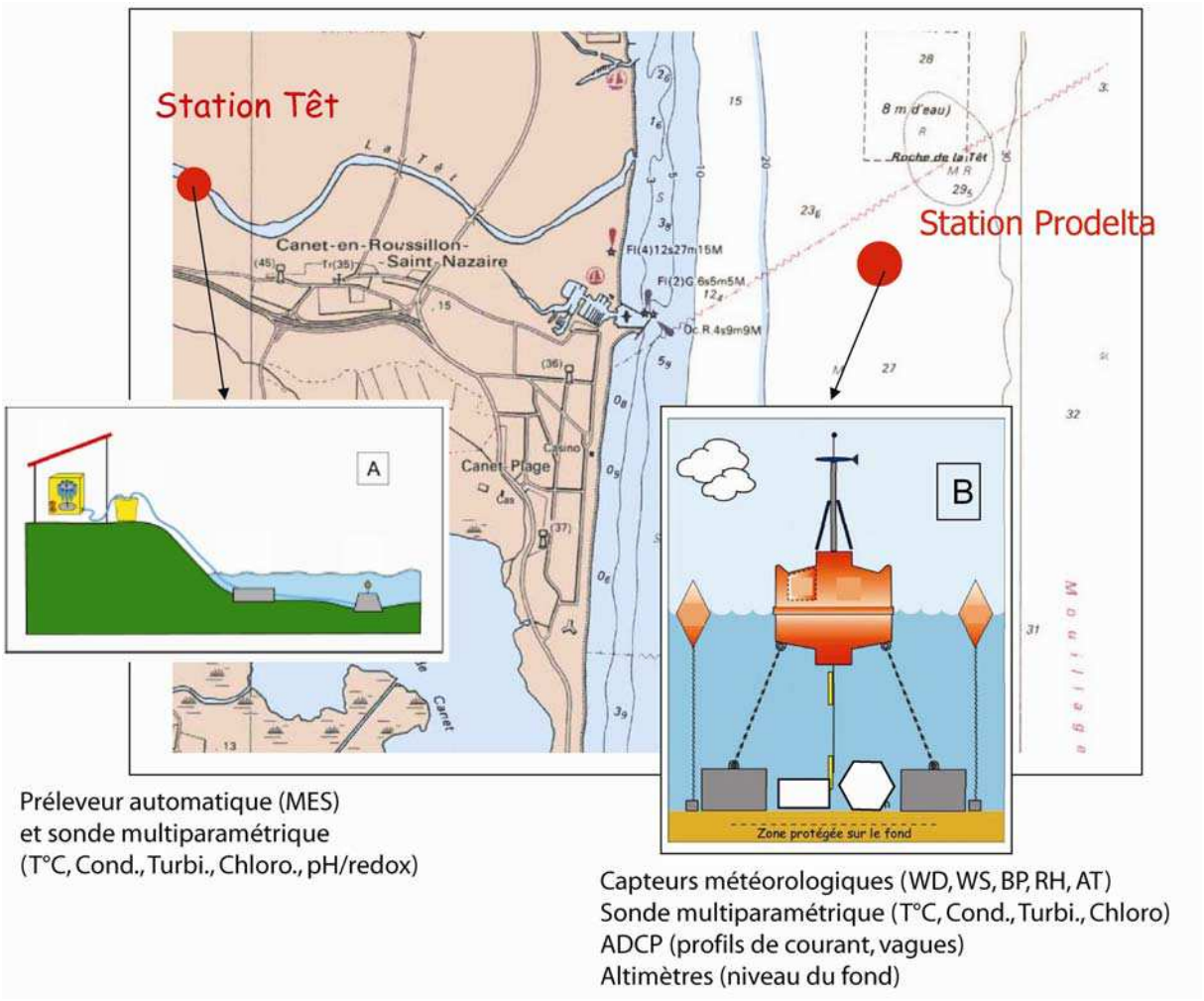

Figure 3-1 : Localisation du dispositif expérimental de la plateforme POEM à proximité de l'embouchure du fleuve Têt et sur le prodelta : A) la station Têt se situe à environ 3 km de l'embouchure sur la berge de

la Têt (42°42.830'N, 02°59.615), et B) la bouée (station Prodelta) est situé sur un fond de 28 m à environ 1.5 nm de la côte légèrement au sud de l'embouchure (42°42.250'N, 03°04.000'E).

La station fluviatile est composée d'un préleveur automatique permettant d'effectuer un échantillonnage journalier en période normale et un échantillonnage haute-fréquence en période de crue afin de mesurer les concentrations en matières en suspension, ainsi que d'une sonde multiparamétrique mesurant les paramètres température, conductivité, turbidité, chlorophylle, pH/redox (**Figure 3-1 A**). La station côtière est composée d'une suite de capteurs météorologiques (direction WD et intensité WS du vent, pression barométrique BP, humidité relative RH, température de l'air AT), d'une sonde multiparamétrique de sub-surface (température, conductivité, turbidité et teneur en chlorophylle) et de plusieurs instruments de fond : un ADCP mesurant à la fois les profils de courant et les paramètres des vagues à haute-fréquence et des altimètres mesurant les variations du niveau du sédiment (**Figure 3-1 B**).

L'ensemble du dispositif instrumental des stations fluviatile et littorale sera détaillée par la suite. Cette plateforme permet d'effectuer des mesures à haute fréquence des évènements de crues et de tempêtes, ainsi que des suivis sur le long terme afin d'évaluer la variabilité saisonnière et interannuelle des apports fluviatiles et de la dynamique sédimentaire. Les paramètres mesurés par les sondes des stations fluviatile et côtière ainsi que les données météorologiques de la station côtière sont transmises en direct par GSM au laboratoire. Les données sont validées et stockées et devront à termes être intégrées dans un serveur web dynamique.

La plateforme POEM s'insère dans une thématique plus large au sein du laboratoire concernant le transport particulaire aux interfaces de la zone côtière (**Figure 3-2**) à l'extrémité SO du golfe du Lion, la sortie du système. Cette plateforme permanente comprend en plus des stations fluviatile et littorale, un piège à particules atmosphériques situé sur les hauteurs du Cap Béar à la frontière franco-espagnole vers 150 m de hauteur, et une ligne de mouillage située en tête du canyon du Lacaze-Duthiers, permanentes depuis 13 années. Cette plateforme sert de base logistique et permet de définir le contexte « historique » à des expériences ponctuelles réalisées en parallèle.

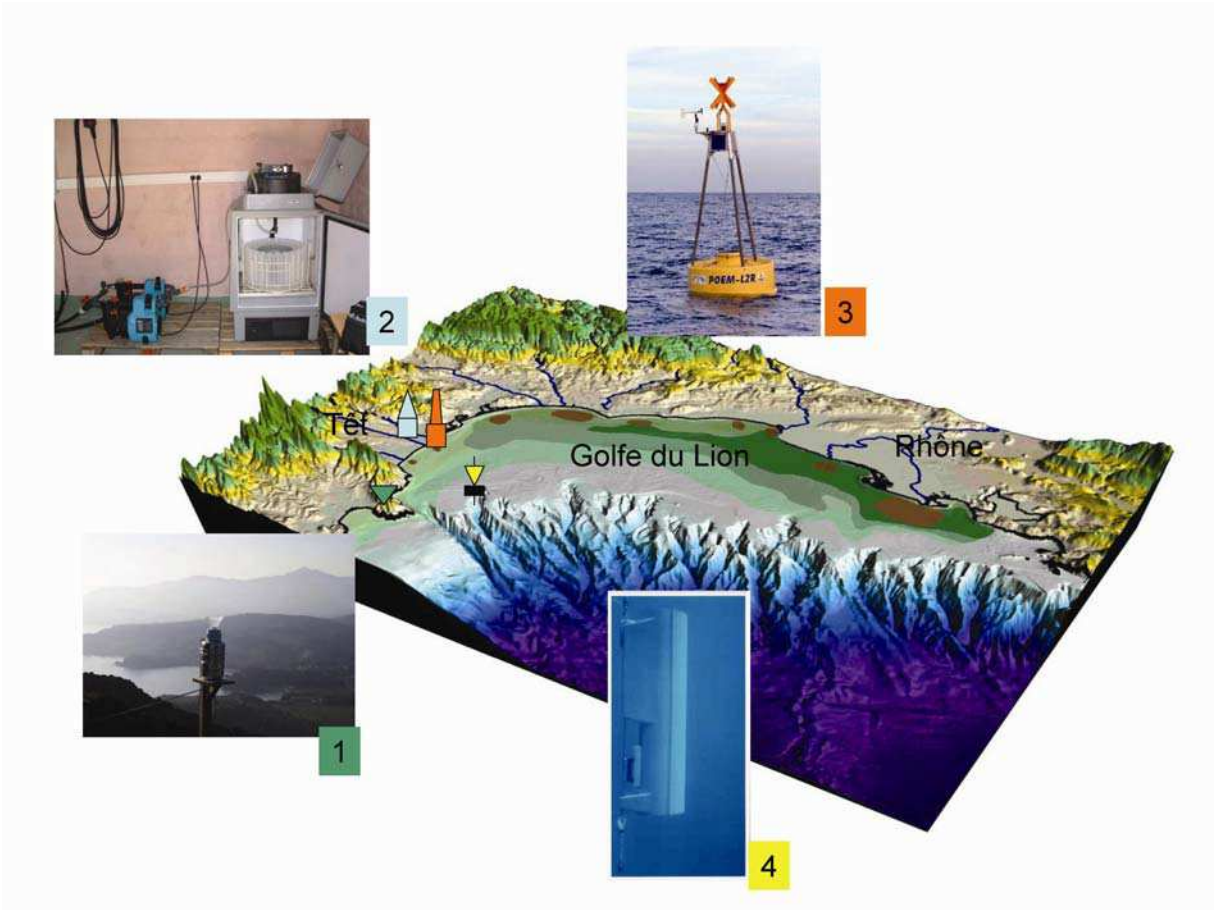

Figure 3-2 : La plateforme POEM dans son ensemble. Elle comprend 1) un piège à particule atmosphérique (interface Atmosphère-Mer), 2) la station sur le fleuve (interface Terre-Mer), 3) la bouée météo-marine (interface Mer-Sédiment) et une ligne de mouillage comprenant un piège à particules au large (interface Côte-Large).

3.1.2 Les campagnes instrumentées autour de la plateforme POEM

Plusieurs expériences se sont déroulées autour de la station permanente POEM au cours de notre étude (2003-2005, **Figure 3-3**). Celles-ci ont vu le déploiement d'un grand nombre de mouillages additionnels ayant pour but de caractériser la dynamique sédimentaire sur le prodelta de la Têt et sa relation avec le reste du plateau. Entre octobre 2003 et mai 2004, la campagne EUROSTRATAFORM s'est déroulée à la fois sur le prodelta de la Têt ainsi qu'en tête de plusieurs canyons du golfe du Lion. Les campagnes SOTON et EMISSAIRE se sont déroulées sur le delta et le prodelta de la Têt au cours du mois d'avril 2004. Enfin, la campagne US-EUROSTRATAFORM s'est déroulée entre octobre 2004 et octobre 2005 à la fois sur le prodelta de la Têt et dans la zone SO du golfe du Lion.

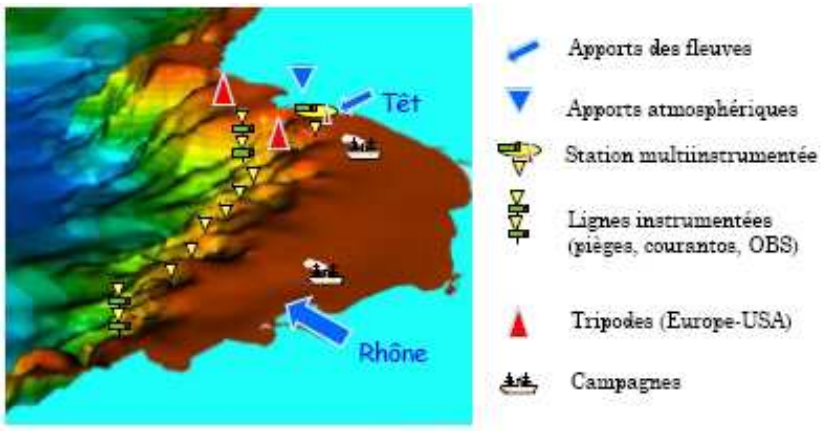

Figure 3-3 : Schéma de la répartition des différentes campagnes de mesure autour de la plateforme permanente POEM.

3.1.2.1 EUROSTRATAFORM

La campagne EUROSTRATAFORM s'est déroulée à partir d'octobre 2003 jusqu'à mai 2004 en collaboration avec l'« Instituto de Ciencias del Mar » (CMIMA-CSIC) de Barcelone (Espagne). Deux tripodes instrumentés ont été déployés sur le prodelta de la Têt en novembre 2003-janvier 2004 et février-mars 2004 en plus de l'instrumentation permanente de la plateforme POEM (**Figure 3-4**).

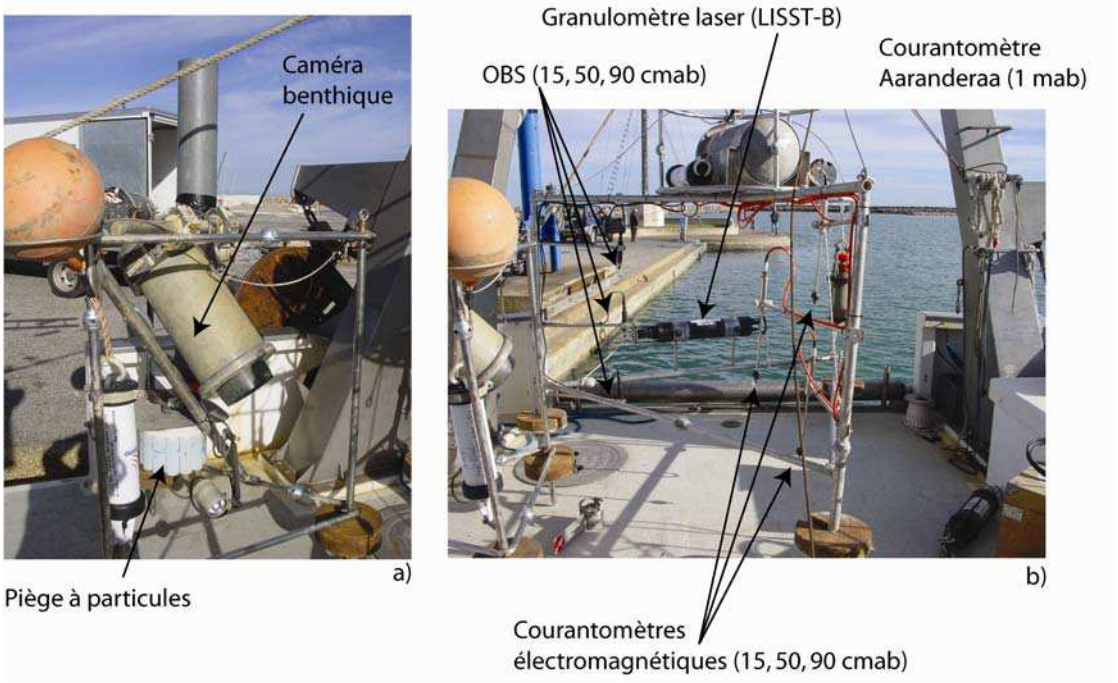

Figure 3-4 : Tripodes instrumentés déployés sur le prodelta de la Têt durant l'hiver 2003-2004 : a) Caméra benthique et piège à particules, et b) courantomètres, OBS et granulomètre laser.

Ces tripodes ont été déployés durant l'hiver 2003-2004 afin de caractériser la dynamique sédimentaire du prodelta de la Têt, et plus particulièrement l'impact des évènements hydro-climatiques extrêmes (crues et tempêtes) sur la dynamique de la zone côtière du fleuve Têt (**Partie 4.2**).

Figure 3-5 : Ligne de mouillage instrumentée type avant déploiement en tête de canyon au cours de l'expérience EUROSTRATAFORM.

Parallèlement, des lignes de mouillage instrumentées ont été déployées en tête de 7 canyons du golfe du Lion depuis le canyon du Planier jusqu'au Cap de Creus afin de caractériser le transport du matériel en suspension entre le plateau et le bassin profond (**Figure 3-3, Palanques et al. 2006**).

3.1.2.2 SOTON et EMISSAIRE

La campagne SOTON s'est déroulée au mois d'avril 2004 sur le delta et le prodelta de la Têt en collaboration avec le National Oceanographic Centre de Southampton (UK). Cette campagne s'est déroulée entre l'embouchure de la Têt et la zone de déferlement des vagues (0-10 m de profondeur), afin de caractériser le comportement des sédiments grossiers par rapport à celui des sédiments fins lors d'un évènement de tempête associé à une crue (**Partie 4.3**). La campagne EMISSAIRE s'est également déroulée au mois d'avril 2004 en collaboration avec la Communauté d'Agglomération de la ville de Perpignan (**Safege-Cetiis, 2006**) dans le cadre d'une étude de faisabilité de construction d'un émissaire marin de rejet des eaux usées.

3.1.2.3 US-EUROSTRATAFORM

La campagne US-EUROSTRATAFORM s'est déroulée à partir d'octobre 2004 jusqu'à octobre 2005. Ce programme est la suite du programme EUROSTRATAFORM en collaboration avec plusieurs équipes nord-américaines notamment le « Bedford Institute of

Oceanography » d'Halifax (Canada). Plusieurs tripodes instrumentés ont été déployé sous la bouée POEM afin d'étudier la variabilité saisonnière de la dynamique sédimentaire au niveau du prodelta de la Têt (**Partie 4.4**). D'autres tripodes ont été déployés en bordure du plateau afin d'étudier les échanges plateau-bassin profond dans les canyons du SO du golfe du Lion (**Ogston et al. soumis ; Puig et al. soumis**).

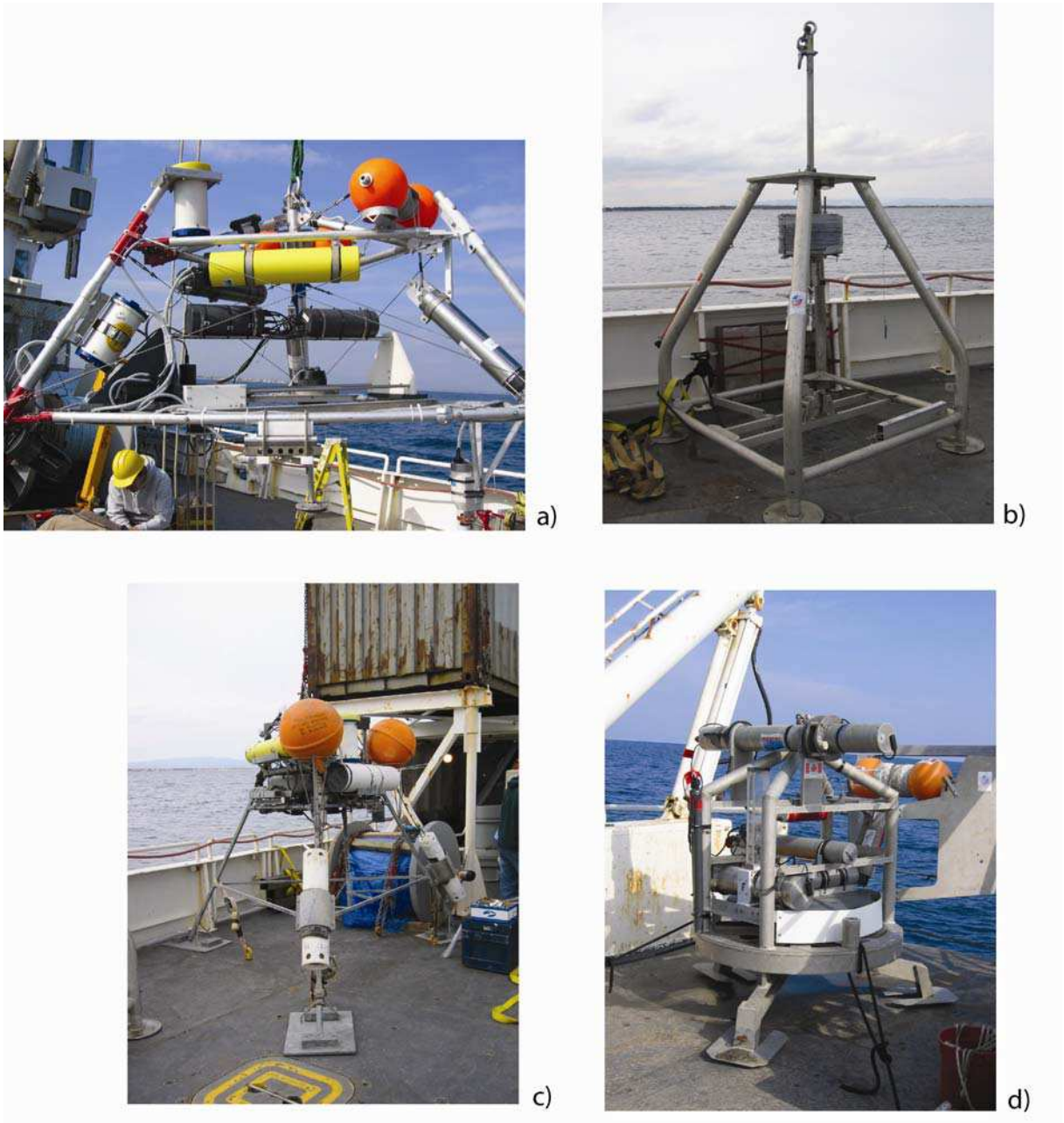

Figure 3-6 : Tripodes instrumentés déployés près de la bouée POEM lors de la campagne US-EUROSTRATAFORM qui s'est déroulée d'octobre 2004 à octobre 2005. a) Tripode ADCP déployé par Ogston, Université de Washington, b) Carottier lent du Bedford Institute of Oceanography (BIO), c) Tripode multi-instrumenté de l'Université de Washington et d) Tripode INSEECT du BIO.

3.2 Mesures et analyses

3.2.1 Les apports fluviaux

3.2.1.1 A l'échelle du golfe du Lion

Afin de quantifier à la fois les apports liquides et solides des fleuves côtiers du golfe du Lion, les données ont été récupérées auprès des diverses bases de données existantes. Les débits horaires des fleuves ont été récupérés via le logiciel **HYDRO II** développé par CEGELEC DR Lyon pour le Bureau des données sur l'eau du Ministère de l'Environnement, sur la période étudiée 2003-2005. Les débits journaliers des fleuves du golfe du Lion (Rhône, Vidourle, Lez, Hérault, Orb, Aude, Têt e Tech) ont été récupérés en ligne sur la Banque Hydro (**Banque Hydro, 2007**) et sur la banque de la Compagnie Nationale du Rhône (**Compagnie Nationale du Rhône, 2006**) depuis que les données existent (~80 ans pour le Rhône et ~30 ans pour les autres) afin de faire des statistiques.

Concernant les données de charge solide, les fleuves Rhône, Hérault et Têt ont été échantillonnés de manière précise dans le cadre du programme **ORME** et les données sont accessibles via la base de données ORME (**ORME, 2007**). Pour les autres fleuves, des études ponctuelles ont été menées (Agly ; **Serrat, 1999**) et quelques données ponctuelles sont accessibles à partir de la banque de données du réseau Rhône-Méditerranée-Corse (**Agence de l'Eau Rhône-Méditerranée et Corse, 2007**).

Toutes ses données (débit instantané en m^3/s / charge solide en suspension en mg/L) ont permis d'établir des courbes de calibration débit / charge solide en suspension pour tous les fleuves du golfe du Lion (**Partie 4.1**).

3.2.1.2 A l'échelle du fleuve Têt

Au niveau du fleuve Têt, nous avons mis en place une stratégie d'échantillonnage particulière afin de répondre à la problématique de mesure des épisodes de crue-éclairs. En effet, l'essentiel du flux annuel liquide et solide de la Têt se produit en seulement quelques jours (**Serrat et al., 2001**). Les crues sont très brèves (quelques heures) et les moyens d'échantillonnage classiques permettent difficilement d'échantillonner durant le pic de crue. Il

est donc important d'échantillonner les crues de la Têt à haute fréquence si on veut quantifier correctement le flux solide à son exutoire.

Figure 3-7 : Détails de la station fleuve installée sur les berges de la Têt à environ 3 km de l'embouchure : a) support de la sonde multiparamétrique à gauche et flotteur déclencheur du mode crue à droite, b) détail des capteurs de la sonde multiparamétrique avec racleurs sur les capteurs optiques, c) préleveur automatique réfrigéré installé dans un abri sur berge et d) rampe de filtration en laboratoire des échantillons prélevés sur le fleuve.

Un système de prélèvement automatique couplé à une sonde autonome multiparamétrique a été installé à 3 km sur les berges du fleuve Têt à partir de juillet 2004 (**Figure 3-7**). Le préleveur automatique permet d'effectuer, à l'aide d'une pompe électrique, un prélèvement journalier (mode normal) d'environ 1 litre au milieu du fleuve grâce à une dérive maintenant la tête d'aspiration à 80 cm sous la surface de l'eau. Un flotteur situé près de la sonde (**Figure 3-7 a)** permet de basculer en mode crue lorsque le niveau de l'eau atteint un seuil de 10 cm au-dessus de son niveau normal.

Le préleveur effectue alors un échantillonnage horaire. Le préleveur est relié à un modem GSM qui permet de signaler le mode crue à l'opérateur afin de récupérer les échantillons. Le dispositif contient 24 godets permettant de tenir 24 jours en mode normal ou 24 heures en

mode crue. Les échantillons sont ensuite filtrés au laboratoire sur filtres GF/F 0.4 µm afin de mesurer la charge solide (**Figure 3-7 d)**. Les filtres peuvent également permettre de faire des analyses complémentaires (granulométrie, nitrates, silice, métaux, isotopes…) sur les matières en suspension.

Une sonde multiparamétrique YSI 6600 EDS équipée de capteurs de pression, température, conductivité, pH/redox et de capteurs optiques de chlorophylle et de turbidité, équipés de ballais autonettoyants, complètent le dispositif instrumental de la station. Les capteurs de la sonde sont calibrés et vérifiés régulièrement à l'aide de solutions étalons. Cette sonde permet d'effectuer des mesures haute-fréquence (15 min) qui sont stockées temporairement dans un data logger (6200 DAS, YSI) dans l'abri sur berge. Les données sont ensuite envoyées toutes les 6 heures au laboratoire via une transmission GSM.

3.2.2 La bouée météo-marine sur le prodelta de la Têt

Afin de suivre le devenir en mer des apports de la Têt, une station marine a été développée. Nous avons donc mis en place à partir d'octobre 2003 une bouée météo-marine au niveau du prodelta de la Têt. Cette bouée est encrée sur 28 m de fond grâce à un dispositif d'ancrage adapté qui ne créent pas de resuspension au fond. En effet, la bouée est fixée au fond par des ancrages vissés dans le sédiment reliés à des chaînes tendues par des flotteurs de subsurface (**Figure 3-8**). Cette bouée crée ainsi une zone abritée au fond qui permet le déploiement sécurisé d'instruments benthiques. Le corps de la bouée possède une structure aérienne où sont disposés une série de capteurs météorologiques. Une sonde hydrologique et un caisson collecteur de données sont installés dans le corps de la bouée. Cette station a servi également de cadre logistique pour le déploiement ponctuel de nombreux tripodes instrumentés lors de campagnes internationales.

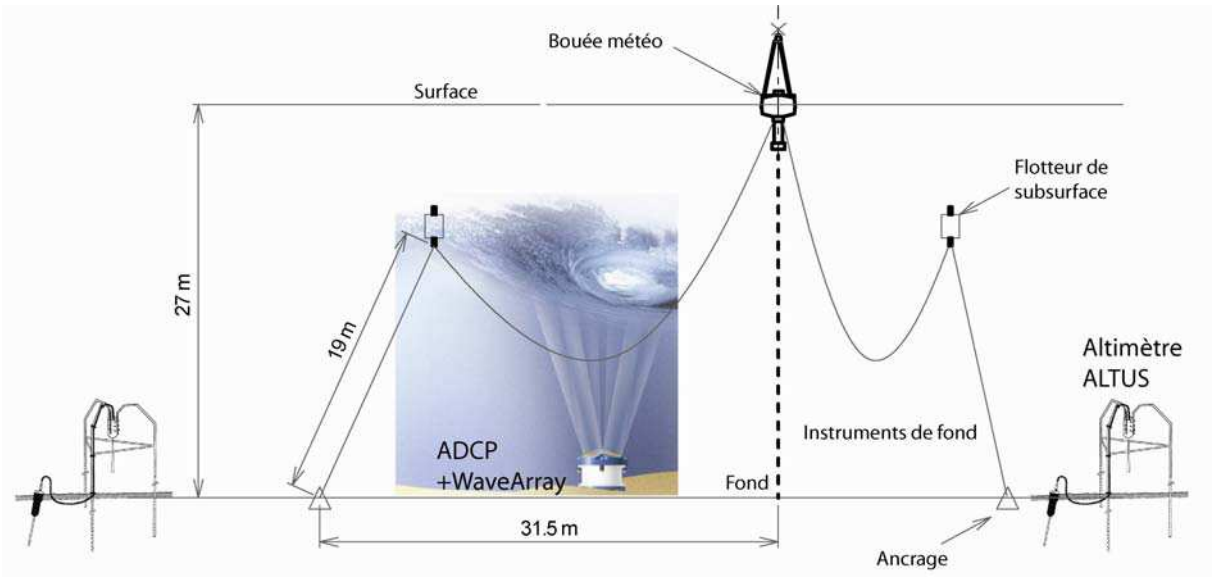

Figure 3-8 : Schéma de la bouée météo-marine instrumentée localisées au niveau du prodelta de la Têt. Localisation des instruments de fond dans la zone abritée par la bouée : ADCP et altimètres.

3.2.2.1 Les données météorologiques

Une série de capteurs météorologiques marinisés (**RM Young Compagny**) a été installée sur la bouée à 6 m de hauteur localisée sur le prodelta de la Têt (**Figure 3-1**). Elle comprend des capteurs de la direction (WD) et de l'intensité (WS) du vent, de l'humidité relative (RH) et de la température (AT) de l'air ainsi que d'un baromètre (BP) (**Figure 3-9**).

Ces capteurs sont reliés à un data logger (6200 DAS, YSI) installé dans un caisson étanche situé dans le corps de la bouée. Ce data logger est alimenté par des panneaux solaires et relié à un système de transmission GSM à distance. Une station PC installée au laboratoire permet d'interroger le dispositif bouée toutes les 6 heures afin de récupérer les données à distance. Le logiciel **Ecowatch DCP** est utilisé afin d'interroger, récupérer et stocker les données des stations fleuve et prodelta pendant des plages horaires différentes.

Les données haute fréquence de la station météorologique (Météo France) de Torreilles (code 61212001) située à proximité de la bouée permet de comparer les données et de compléter nos données en cas de panne de la bouée POEM.

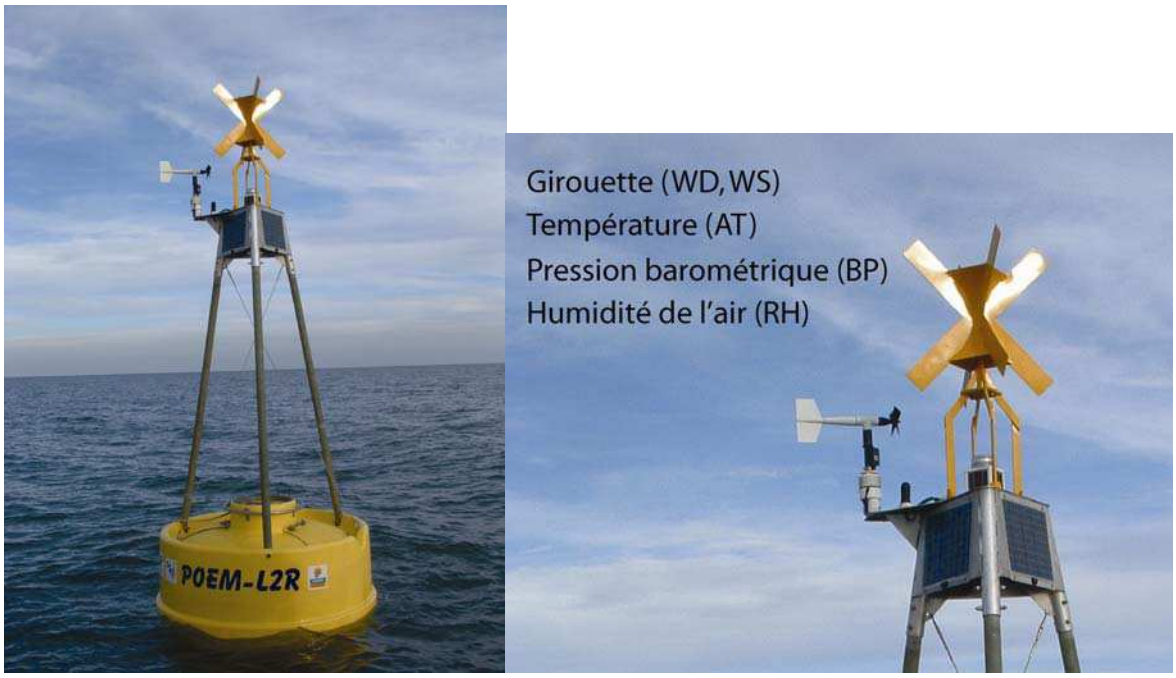

Figure 3-9 : Suite de capteurs météorologiques installée à 6 m sur le sommet de la bouée à gauche : détail de la girouette et anémomètre marinisé, sondes de température et humidité relative, sonde de pression barométrique à droite.

3.2.2.2 Les données hydrodynamiques

3.2.2.2.1 Les vagues

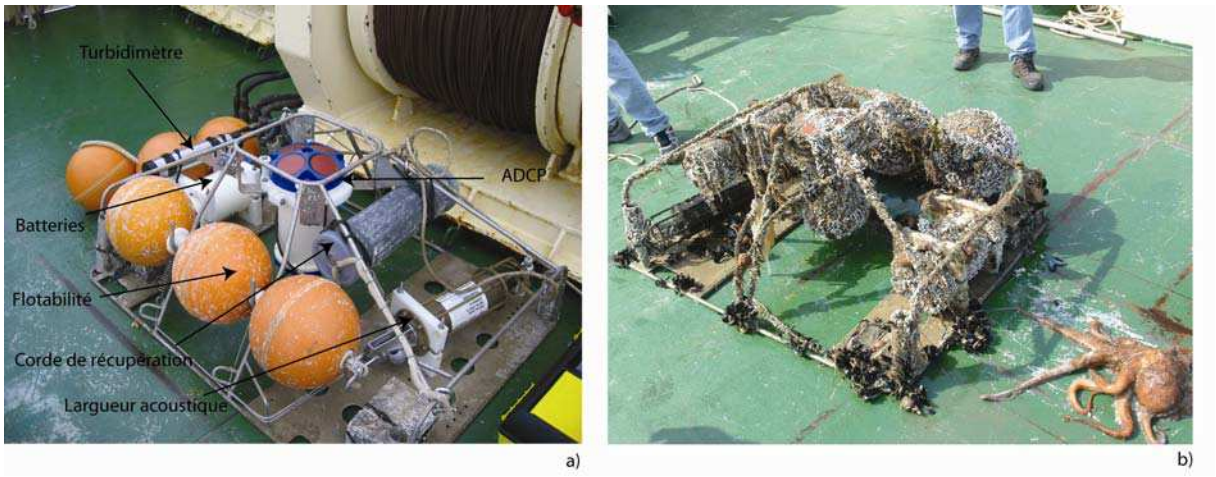

Figure 3-10 : Cage anti-chalutage de protection et de déploiement de l'ADCP avant a) et après b) déploiement d'une durée d'environ 6 mois dans la zone côtière du fleuve Têt.

Les paramètres des vagues sont mesurés grâce à un ADCP 600 kHz (RD Instruments) équipé d'un capteur de vagues. L'ADCP est installé dans une cage anti-chalutage développée avec

TECHNICAP (**Figure 3-10**). La cage est déployée sur le fond à 28 m sur le prodelta de la Têt. Les mesures des vagues sont effectuées pendant des périodes de 20 minutes toutes les 3 heures à une fréquence de 2 Hz (2400 mesures toutes les 3 heures). L'ADCP combine trois types de mesures afin de calculer les paramètres des vagues, dont les principaux sont la hauteur significative et la hauteur maximale, la période et la direction des pics de vagues. Les mesures de pression haute fréquence, de déplacement de la surface libre et des vitesses orbitales des vagues permettent d'obtenir des mesures cohérentes et de mesurer des vagues simultanées provenant de directions différentes (**RD Instruments, 2001**). Les données sont traitées avec une série de logiciels fournies par le constructeur. Le logiciel **WavesMon** permet d'extraire les données binaires du fichier de sortie de l'ADCP. Ce logiciel permet également de traiter les données de vagues en définissant les fréquences de coupure du signal de vagues et les cellules de mesure des vitesses orbitales. Le logiciel **WavesView** permet ensuite de visualiser les données et de les exporter en format ascii. Les données sont ensuite validées par élimination des valeurs jugées non réalistes selon les recommandations du constructeur et selon **Butel et al. (2002)**.

3.2.2.2.2 Le courant

Le courant est mesuré avec le même instrument que pour les mesures des vagues. L'ADCP 600 kHz déployé sur le fond permet également de mesurer le courant dans des cellules de mesure de 1 m à partir de 2 m au dessus du fond jusqu'à 2 m sous la surface. L'ADCP utilise la technique Doppler afin de mesurer les vitesses des particules en suspension dans la colonne d'eau en faisant l'hypothèse que les particules en suspension se déplacent à la même vitesse que l'eau (**RD Instruments, 1996**). Les mesures sont effectuées entre les mesures des vagues sur des périodes de 3 heures à la fréquence de 1.5 Hz (16384 mesures sur 10800 secondes). L'erreur sur la mesure est définie par la déviation standard sur les mesures et est égale à 0.42 cm/s. Le logiciel **PlanADCP** est utilisé pour planifier le déploiement en fonction du nombre de batteries, et des caractéristiques de mesures des vagues (période et fréquence des mesures) ainsi que du courant (hauteur des cellules de mesure et nombre de cellules dans la colonne d'eau). L'ADCP utilisé avec 3 packs de batteries (dont 2 dans un conteneur extérieur, **Figure 3-10**) permet une autonomie supérieure à 5 mois en enregistrant les vagues pendant 20 minutes toutes les 3 heures et le courant entre les périodes de mesure des vagues. Les données sont ensuite pré-visualisées avec le logiciel **WinADCP** et exportées sous format ascii pour

post-traitement. Le post-traitement est effectué sous **MatLab** pour valider et les visualiser les données.

3.2.2.2.3 L'hydrologie

Une sonde multiparamétrique identique à celle utilisée sur le fleuve (YSI 6600 EDS) est installée en sub-surface (1 m sous la surface) sur la bouée instrumentée du prodelta de la Têt (**Figure 3-11**). Elle comprend des capteurs optiques de turbidité et de chlorophylle ainsi qu'un capteur de température et conductivité. Les capteurs sont calibrés avec des solutions standard fournies par le constructeur (**YSI**). Alors que le capteur de conductivité du fleuve est calibré avec une solution standard à 1.407 mS/cm, celui installé en mer est calibré avec une solution standard à 12.78 mS/cm. Cette sonde est reliée au collecteur de données (6200 DAS, YSI) installée dans la bouée qui gère également les instruments météorologiques. Le pas d'échantillonnage des données est de 15 minutes. Le collecteur de données alimente un modem GSM 5 minutes toutes les 6 heures afin de transmettre les données par connexion GSM à la station relais en laboratoire. Cette plage horaire de connexion GSM permet également de modifier les paramètres d'échantillonnage ou de régler un problème quelconque directement depuis le laboratoire.

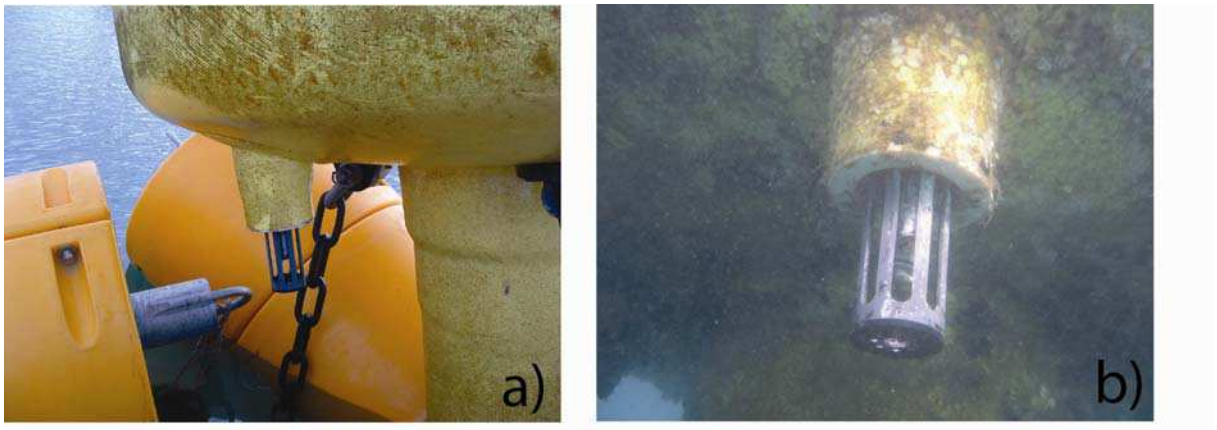

Figure 3-11 : Détails de la base de la bouée instrumentée du prodelta de la Têt : a) bouée hors de l'eau laissant apparaître l'ouverture pour la sonde, et b) la sonde multiparamétrique sur site.

3.2.3 La concentration des matières en suspension (MES)

Plusieurs approches ont été utilisées afin de mesurer les concentrations de matières en suspension : des méthodes de mesures classiques par prélèvement et filtration, aux méthodes optiques et acoustiques.

Les prélèvements d'eau effectués par le préleveur automatique sur le fleuve, ont été filtrés au laboratoire sur des filtres GF/F. La différence de poids avant et après filtration et séchage, rapportée au volume filtré donne la concentration en matières en suspension.

Des mesures in-situ en un point ont été effectuées grâce aux sondes multiparamétriques **YSI** à la fois sur le fleuve et sous la bouée. Les capteurs de turbidité (YSI 6136) mesurent la différence entre la quantité de lumière émise (830-890 nm) et la quantité captée ; source et détecteur étant positionnés à 90°. Une calibration empirique avec les données issues du préleveur sur le fleuve a été utilisée pour convertir le signal mesuré en NTU en mg/L (**Figure 3-12**). Les concentrations mesurées en mer sont très faibles par rapport à celles mesurées sur le fleuve (maximum 40 mg/L contre 1-2 g/L sur le fleuve). La même calibration a été utilisée pour la sonde positionnée en mer.

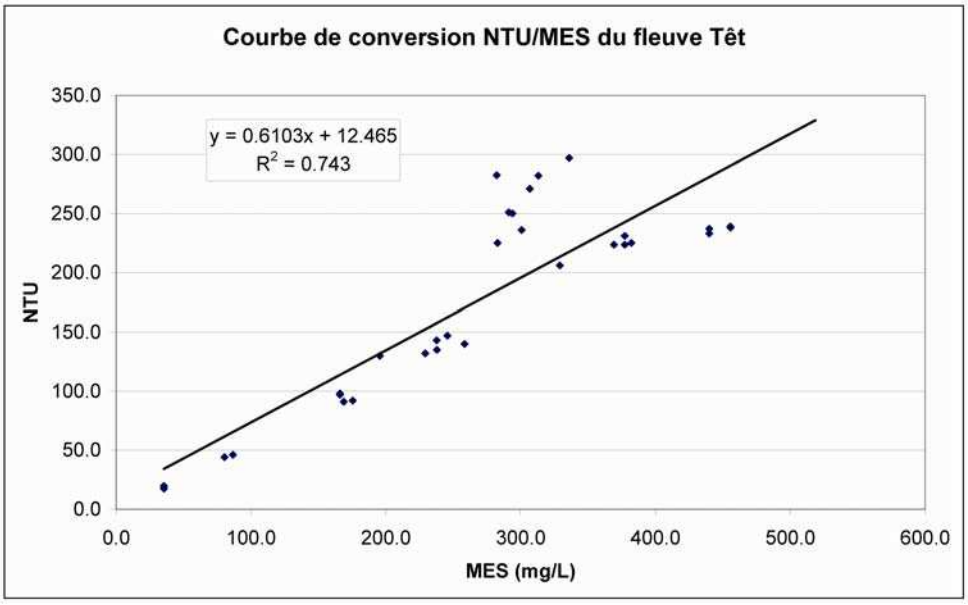

Figure 3-12 : Courbe de calibration entre les mesures de la sonde (NTU) et les concentrations de matière en suspension effectuées par filtration (mg/L).

Les intensités de rétrodiffusion acoustique mesurées par l'**ADCP** nous ont également servi à estimer les concentrations en matières en suspension. L'intérêt de cette technique est de

mesurer les concentrations en même temps que la vitesse du courant dans toute la colonne d'eau à partir d'un seul instrument. En effet, l'intensité du l'écho acoustique (EI) dépend de l'absorption du son dans l'eau, de la répartition du signal acoustique, de la puissance du signal transmis (SL) ainsi que du coefficient de rétrodiffusion acoustique. Une équation simplifiée de l'intensité de l'écho donne :

EI = SL + SV +constant -20 log (R) - 2 α R (**RD Instruments, 1996**)

avec : EI l'intensité de l'écho (dB)
SL l'intensité de la source (dB)
SV l'intensité de rétrodiffusion acoustique (dB)
α le coefficient d'absorption (dB/m)
R la distance entre le transducteur et la cellule de mesure.

Thorne and Campbell (1992) et **Hay (1991)** ont décrit de manière plus précise la relation entre l'intensité de rétrodiffusion acoustique et la concentration en MES dans la colonne d'eau :

$$M(R) = (K < P_{rms} > r)^2 \frac{< a_s > \rho_s}{< f >^2} e^{4r(\alpha_w + \alpha_s)}$$

avec : M (R) = la concentration massique par unité de volume à la distance R
K = une constante pour le système acoustique
P_{rms} = la pression rétrodiffusé
a_s = le diamètre des particules en suspension
ρ_s = densité des particules
f = fonction de la forme des particules
r = radius of suspended particles
α_w = coefficient d'atténuation par l'eau
α_s = coefficient d'atténuation par le sédiment
<> = integration over the whole water column

Cette équation peut être simplifiée afin d'obtenir une équation de la concentration massique en fonction de constantes seulement dépendantes des caractéristiques du site qui peuvent être calibrées à partir de mesures in-situ :

$$\mathrm{Log}_{10}\mathrm{M_r} = \frac{\{dB + 2r(\alpha_w + \alpha_s) - K_s\}}{S}$$

où : S = coefficient de rétrodiffusion relatif

K_s = constante dépendante du site et de l'instrument

dB = intensité de rétrodiffusion relative mesurée et corrigée des effets de répartition du son dans l'eau.

Dans cette équation, les 4 inconnues sont les coefficients K_s, S, α_w et α_s. La calibration de ces coefficients a été réalisée grâce au logiciel **Sediview** (**DRL Software Ltd, 2003**). Les paramètres nécessaires sont le profil de température et de salinité dans la colonne d'eau, la taille moyenne et la densité des particules dans la colonne d'eau, et les concentrations des MES mesurées.

3.2.4 L'altimétrie – mesure du niveau du fond sédimentaire

Des altimètres acoustiques **ALTUS** 2 MHz (**NKE**) ont été utilisés sur le fond du prodelta de la Têt à 28 m de profondeur afin de mesurer les variations du niveau des sédiments en fonction des aléas climatiques. L'altimètre **ALTUS** consiste en un transducteur acoustique servant à la fois de source et de réception d'un faisceau acoustique 2 MHz, de 3.6° de largeur, ainsi que d'un boitier étanche contenant les batteries et un capteur de pression. Il permet de mesurer les grandeurs physiques : distance transducteur-cible (altitude), niveau maximum du signal reçu par le transducteur (Echo max) et la profondeur (**NKE Electronics, 2006**). L'altimètre est conçu pour mesurer ces grandeurs physiques suivant 6 voies : 1 voie pour la profondeur, 1 voie pour l'écho max et 4 voie pour l'altitude. En théorie, les 4 voies altitude permettraient de mesurer la distance entre le transducteur et des surfaces avec des densités différentes (couche de crème de vase, surface consolidée…) (**Jestin et al., 1998**). En pratique, il a été nécessaire de faire des tests en laboratoire afin de calibrer le gain acoustique de l'altimètre afin qu'il soit maximum. De plus, les valeurs seuils de chaque voie ont été optimisées en laboratoire dans un canal avec du sédiment représentatif du site de déploiement afin de détecter des niveaux de consistance différentes. Les altimètres sont gérés par un logiciel fourni par le constructeur (**WINMEMO**) qui permet de décharger les données, planifier les déploiements, calibrer les altimètres et exporter les données. Les données sont ensuite post-traitées avec le logiciel **MATLAB** afin de filtrer et valider les données.

Les caractéristiques techniques des altimètres **ALTUS** données par le constructeur sont récapitulées dans le tableau suivant :

Type de capteur	**Gamme de profondeur (m) / Elévation min - max (mm)**	**Précision (cm)**	**Résolution (cm)**	**Ouverture**	**Amplitude du signal reçu**
Voie Profondeur : Piézo-résistif	0-20 m	+/- 6	0.8		
Voie Altitude : Transducteur acoustique	200-700 mm	+/- 2	0.41	3.6° à -3dB	
	200-2000 mm	+/- 5	0.41		
Voie Echo Max					0 à 100%

Tableau 3-1 : Données constructeur des altimètres ALTUS.

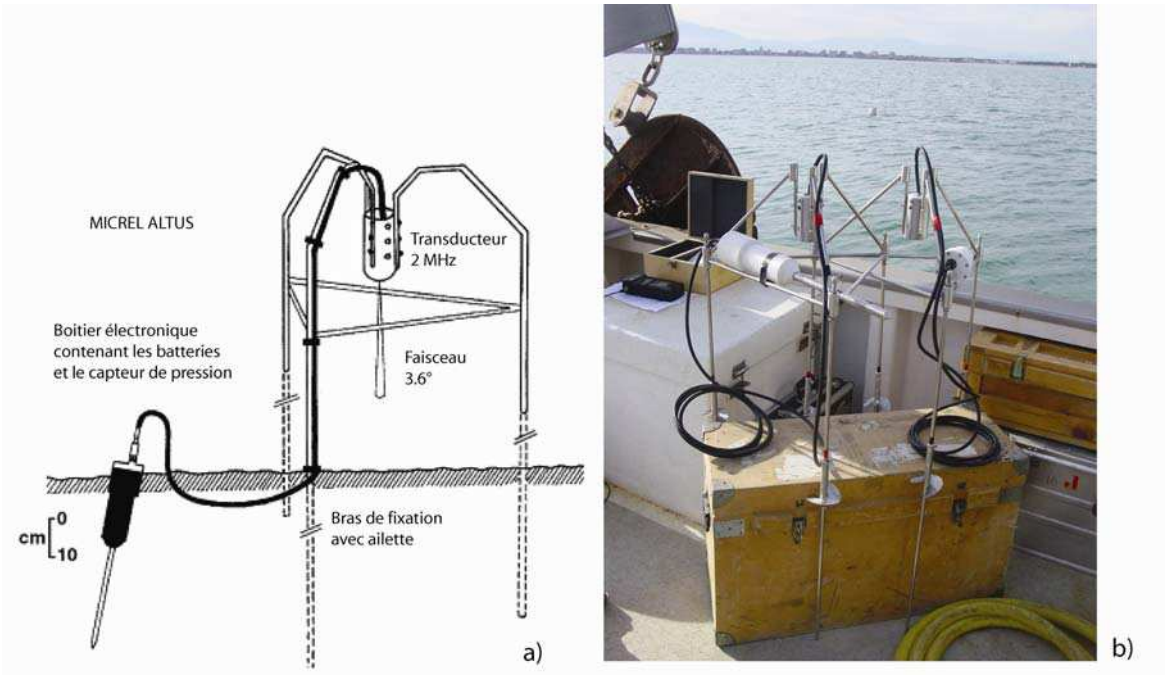

Figure 3-13 : Détail des altimètres ALTUS composés d'un boîtier électronique et d'un tripode avec le transducteur. a) schéma et b) photos de 2 ALTUS.

L'autonomie énergétique est donnée pour 4 ans en enregistrement à 15 minutes, alors que l'autonomie de mémoire ne permet qu'un déploiement d'environ 3 mois. Nous avons utilisé

plusieurs altimètres, tous n'avaient pas la même capacité de mémoire. Un ne pouvait être déployé qu'un mois alors que les autres environ 3 mois avec un enregistrement toutes les 15 minutes. Cependant, nous avons optimisé cette autonomie en ne sélectionnant que 3 voies de mesures (profondeur, Echo Max et 1 seule pour l'altitude) et en choisissant un enregistrement toutes les 20 minutes, afin d'avoir une autonomie supérieure.

3.2.5 Sédimentologie et géochimie

3.2.5.1 Prélèvements

Des carottages in-situ par plongée ont été réalisés de manière mensuelle sur le prodelta de la Têt à 28 m de profondeur à l'aide de tubes Perspex de 4 cm de diamètre et 20 cm de longueur entre octobre 2003 et octobre 2005. Un autre carottage utilisant la même technique mais avec un tube de 8 cm de diamètre et de 1 m de longueur a aussi été réalisé de manière ponctuelle (mai 2005). Les carottes de sédiments ont été échantillonnées tout les cm, le premier cm étant séparé en 2 sous-échantillons de 0.5 cm. Les échantillons ont ensuite été congelés puis lyophilisés.

3.2.5.2 Analyses granulométriques

Des analyses granulométriques ont été menées sur chaque échantillon avec un granulomètre laser Malvern Mastersizer 2000 équipé d'une unité de dispersion au laboratoire de Banyuls sur Mer (**Figure 3-14**). Cet instrument permet de mesurer la taille des particules sédimentaires entre 0.01 et 3000 μm en utilisant la diffraction d'un faisceau laser par les particules sur des anneaux de détection concentriques (théorie de Mie). Un faisceau infrarouge permet de mesurer les tailles des petites particules alors qu'un faisceau dans les plus grandes longueurs d'onde permet de mesurer les tailles des grosses particules. Un spectre de taille des particules ainsi que des paramètres granulométriques standard (D_{50}) ont ainsi été obtenus pour chaque centimètre.

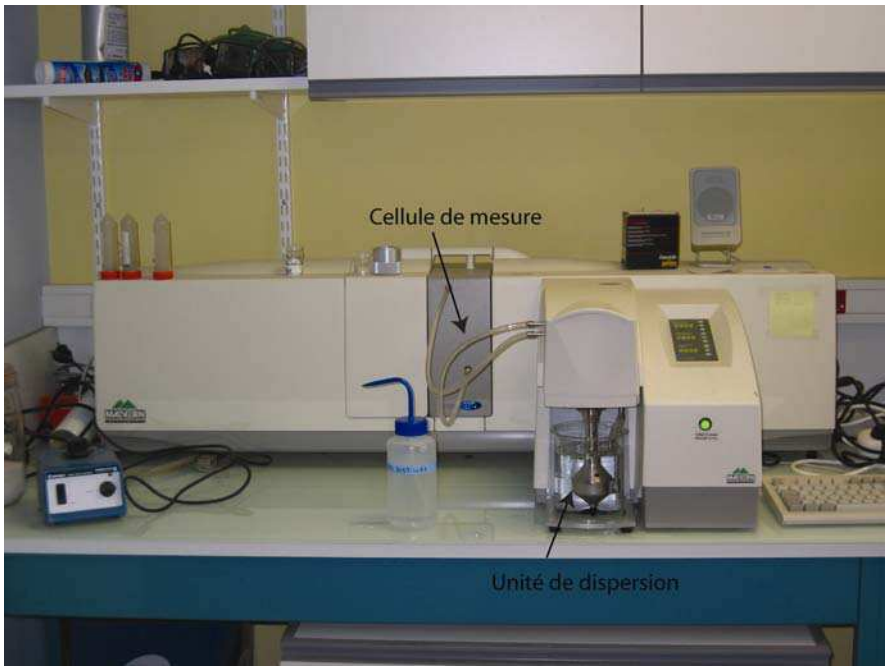

Figure 3-14 : Granulomètre laser Malvern Mastersizer 2000 équipé d'une unité de dispersion. Laboratoire de Banyuls sur mer.

3.2.5.3 L'activité du Plomb-210

Des mesures de la radioactivité du ^{210}Pb ont été réalisées au sein du laboratoire du CEFREM sur les échantillons de sédiments collectés par carottage afin d'estimer les taux de sédimentation séculaire sur le prodelta de la Têt. Les sédiments ont d'abord été lyophilisés et broyés puis ont subis plusieurs attaques acides (**Radakovitch, 1995**). Les procédures de déposition et de comptage sur chaîne alpha sont détaillées dans **Radakovitch (1995)**. La chaine de mesure est représentée sur la **Figure 3-15**.

Le ^{210}Pb est un radionucléide naturel possédant une période de demi-vie ($T_{1/2}$) de 22.3 ans descendant plus spécifiquement du Radon-222 ($T_{1/2}$=3.8 jours), qui provient lui-même du Radium-226 ($T_{1/2}$=1620 ans) qui s'échappe continuellement de la croute terrestre. Une fois dans l'atmosphère le ^{222}Rn se désintègre en ^{210}Pb qui retombe sous forme de précipitations. Dans le milieu marin, le ^{210}Pb provient ainsi des apports atmosphériques (^{210}Pb en excès ou $^{210}Pb_{xs}$), du ^{210}Pb d'origine atmosphérique ($^{210}Pb_{xs}$ également) qui transite avec les sédiments continentaux par les cours d'eau et le ^{210}Pb résultant de la décroissance radioactive in situ du ^{226}Ra qui s'échappe en permanence des sédiments que l'on appelle ^{210}Pb supporté. Le ^{210}Pb

s'adsorbe préférentiellement aux sédiments fins avec lesquels il forme un complexe stable, aux grés des phénomènes de resuspension et de redéposition.

Figure 3-15 : Chaîne de mesure (déposition et comptage) du Plomb-210 au sein du laboratoire du CEFREM.

L'activité du ^{210}Pb total (**A totale**) que l'on mesure dans les sédiments est donc la somme de l'activité du ^{210}Pb en excès (**A en excès**) qui arrive dans la colonne d'eau soit par voie atmosphérique, soit par les cours d'eau, et de l'activité du ^{210}Pb issu de la décroissance in situ du ^{226}Ra dans les sédiments (**A supportée**). Lorsque les sédiments s'accumulent avec le temps, les particules {sédiment - ^{210}Pb} enfouies sont isolées de la surface et le ^{210}Pb en excès décroît jusqu'à disparaître totalement au bout de 5 à 7 demi-vies (100-150 ans). Le sédiment ne contient alors que le ^{210}Pb supporté et la distribution de ^{210}Pb total dans le sédiment montre une décroissance logarithmique depuis des valeurs fortes de ^{210}Pb total en surface jusqu'à des valeurs constantes de ^{210}Pb supporté au fond.

3.3 Suivi de terrain

Un récapitulatif du suivi de terrain dont les résultats seront présentés en suivant est indiqué sur la **Figure 3-16**.

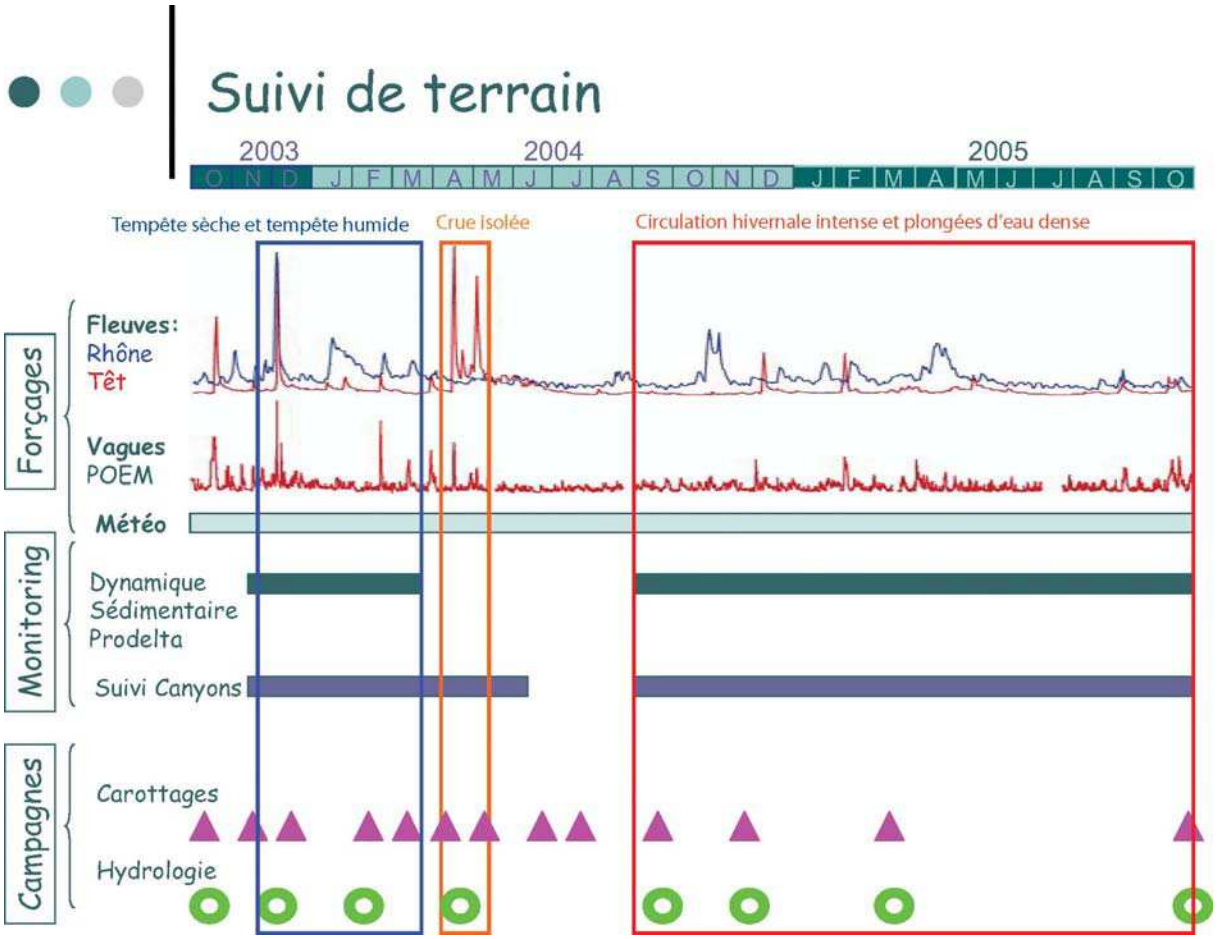

Figure 3-16 : Schéma récapitulatif du suivi de terrain d'octobre 2003 à octobre 2005.

3.4 Conclusions

Dans la **partie 3**, nous avons défini la stratégie générale adoptée lors de notre étude sur le système fleuve Têt-littoral roussillonnais. La plateforme POEM a ainsi été pensée, étudiée, réalisée et mise en place afin de caractériser la variabilité des apports liquides et solides du fleuve Têt à l'embouchure et le devenir en mer des sédiments apportés (**Partie 3.1**). Cette station en phase d'automatisation totale a été mise en place au cours de cette étude. Elle s'insère sur le long terme dans le cadre de l'**Observatoire Régional de l'Environnement Méditerranéen (ORME)**, Zone Atelier labellisée par le CNRS, Département Environnement et Développement Durable et du futur observatoire du littoral, en termes de surveillance et de mesure des changements anthropiques et/ou climatiques. Cette station permanente est la base de notre étude, elle a également permis le déploiement de nombreux autres instruments dans le cadre de collaborations nationales et internationales ayant apporté un savoir-faire et une

expérience notables. Les nombreuses séries de mesures récoltées ont été traitées et validées en vue de leur exploitation. A côté de ces mesures physiques, de nombreux échantillons de sédiments ont été récoltés et analysés par diverses méthodes (**Partie 3.2**).

Dans la **Partie 4**, nous nous attacherons à caractériser la variabilité des apports liquides et solides de tous les fleuves côtiers du golfe du Lion à partir des données existantes (banques de données et études variées) et sur la base de nos propres mesures. Des courbes de calibration débit/charge solide seront ainsi établies, et pourront servir de référence dans le cadre des estimations et des bilans de flux liquide et solide au golfe du Lion. Une étude préliminaire sur les quantités de matériel sédimentaire stocké dans les prodeltas du golfe du Lion par rapport aux quantités apportées par les fleuves sera également établie (**Partie 4.1**). Nous nous intéresserons à l'impact des évènements hydro-climatiques extrêmes sur la dynamique sédimentaire de la zone prodeltaïque du fleuve Têt. Nous aborderons dans la **Partie 4.2** l'impact hydro-sédimentaire des évènements de crues et tempêtes extrêmes associés dans un continuum Terre-Mer, généralisés à l'ensemble du golfe du Lion. Et dans la **Partie 4.3**, nous aborderons l'impact d'un évènement de crue et tempête isolé sur le prodelta de la Têt, et la relation côte-large des processus hydro-sédimentaires.

4 RÉSULTATS : EXPÉRIENCES MENÉES AUTOUR DE LA PLATEFORME INSTRUMENTÉE

CONTRIBUTION A L'ÉTUDE DES FLEUVES CÔTIERS ET PRODELTAS ASSOCIÉS DANS LES APPORTS SÉDIMENTAIRES AU GOLFE DU LION (PARTIE 4.1)

IMPACT DES ÉVENEMENTS MÉTÉO-CLIMATIQUES EXTRÊMES SUR LA DYNAMIQUE SÉDIMENTAIRE DU PRODELTA DE LA TÊT (PARTIES 4.2, 4.3, 4.4)

ENREGISTREMENT SÉDIMENTAIRE DU PRODELTA DE LA TÊT (PARTIE 4.5)

Dans le **chapitre 3**, nous avons défini la stratégie générale adoptée lors de notre étude sur le système fleuve Têt-littoral roussillonnais. La plateforme POEM a ainsi été pensée, étudiée, réalisée et mise en place afin de caractériser la variabilité des apports liquides et solides du fleuve Têt à l'embouchure et le devenir en mer des sédiments apportés. Cette station en cours d'automatisation totale a été mise en place au cours de cette étude. Elle s'insère sur le long terme dans le cadre de l'Observatoire du Littoral Méditerranéen en termes de surveillance et de mesure des changements anthropiques et/ou climatiques. Cette station permanente est la base de notre étude, elle a également permis le déploiement de nombreux autres instruments dans le cadre de collaborations nationales et internationales ayant apporté un savoir-faire et une expérience notables. Les nombreuses séries de mesures récoltées ont été traitées et validées en vue de leur exploitation. A côté de ces mesures physiques, de nombreux échantillons de sédiments ont été récoltés et analysés par diverses méthodes.

Dans le **chapitre 4.1**, nous nous attacherons à caractériser la variabilité des apports liquides et solides de tous les fleuves côtiers du golfe du Lion à partir des données existantes (banques de données et études variées) et sur la base de nos propres mesures. Des courbes de calibration débit/charge solide seront ainsi établies, et pourront servir de référence dans le cadre des estimations et des bilans de flux liquide et solide au golfe du Lion. Une étude préliminaire sur les quantités de matériel sédimentaire stocké dans les prodeltas du golfe du Lion par rapport aux quantités apportées par les fleuves sera également établie.

4.1 Contribution à l'étude des fleuves côtiers et prodeltas associés dans les apports sédimentaires au Golfe du Lion

Contribution to the study of coastal rivers and associated prodeltas to sediment supply in Gulf of Lions (NW Mediterranean Sea)

François Bourrin* Redaction, Rating curves, Data acquisition
Xavier Durrieu de Madron, Manuscript revision
Wolfgang Ludwig Rating curves, Manuscript revision

CEntre de Formation et de Recherche sur l'Environnement Marin
CNRS UMR 5110-Université de Perpignan
52, Avenue Paul Alduy, 66860 Perpignan Cedex. France

Soumis le 26/05/2006
Accepté le 15/09/2006

VIE ET MILIEU - LIFE AND ENVIRONMENT, 2006, 56 (4) : 307-314
Volume spécial du programme SYSCOLAG
Systèmes Côtiers et Lagunaires

Abstract

Sedimentation in the Gulf of Lions, north-western Mediterranean Sea, is influenced mainly by the Rhône River, one of the largest in the Mediterranean, and by several small torrential rivers along the Languedoc-Roussillon coast. These coastal rivers are characterized by strong inter-annual variability of their liquid and suspended solid discharge. These rivers are generally associated in the inner-shelf area to a distinct deposit, commonly named prodelta, of sedimentary material and associated pollutants. Sediment supplies from all coastal rivers of the gulf are estimated over the last 30 years, from an updated data set of their liquid discharge and correspondent suspended sediment concentration. Maximum mass accumulation rates derived from ^{210}Pb dating method on sediment cores were estimated on the Têt and Aude prodeltas, which collect the inputs from the Têt River and the central rivers of the Gulf of Lions respectively. Secular sedimentation rates ranged from 0.07 to 0.12 cm/yr. The comparison of the annual sediment mass buried in these prodeltas with respect to the average suspended solid river discharges, suggests that 20% (~12 x 10^6 kg/yr) and 45% (~182 x 10^6 kg/yr) of the continental material introduced in the coastal area is trapped in the Têt and Aude prodeltas respectively.

Keywords

NW Mediterranean Sea, Gulf of Lions, inner-shelf, prodeltas, coastal rivers, hydrodynamics, sediment supply

4.1.1 Introduction

On continental margins, in front of each river as well as lagoon mouths appears a preferential area of sediment accumulation under the wave storm base (**Aloïsi and Monaco, 1975; Monaco, 1971; Monaco, 1987; Pauc, 2005**). These deposition areas, commonly named prodeltas, are the subaqueaous extension of aerial deltas in the inner-shelf around 30 m water depth. They are composed of fine-grained sediments and concentrate organic material, as well as pollutants, pathogens and heavy metals of human origin (**Roussiez et al., 2005**). Prodeltas play an important role in the land-to-sea transfer of particulate matter, as secondary sources of

particulate matter to the shelf. Thus, their evolution must be relevant for the management of coastal zones because they are good indicators of the quality of littoral environments.

In the Gulf of Lions, a river dominated continental shelf incised by canyons, sediment supplies are largely influenced by inputs from the Rhône River at the northeast, and by several mountainous coastal rivers with a torrential regime along the Languedoc-Roussillon coast (**Figure 4-1**). The dispersal of riverborn sediments, mostly discharged during extreme flood events, is constrained in the littoral zone by the wind-driven coastal circulation, and form several prodeltas in the inner-shelf of the Gulf of Lions (**Aloïsi and Monaco, 1975**). The remaining part of suspended sediments not trapped in prodeltas, as well as sediments resuspended during storm events are advected cyclonically along the shelf (**Guillén et al., 2006; Ulses, 2005**).

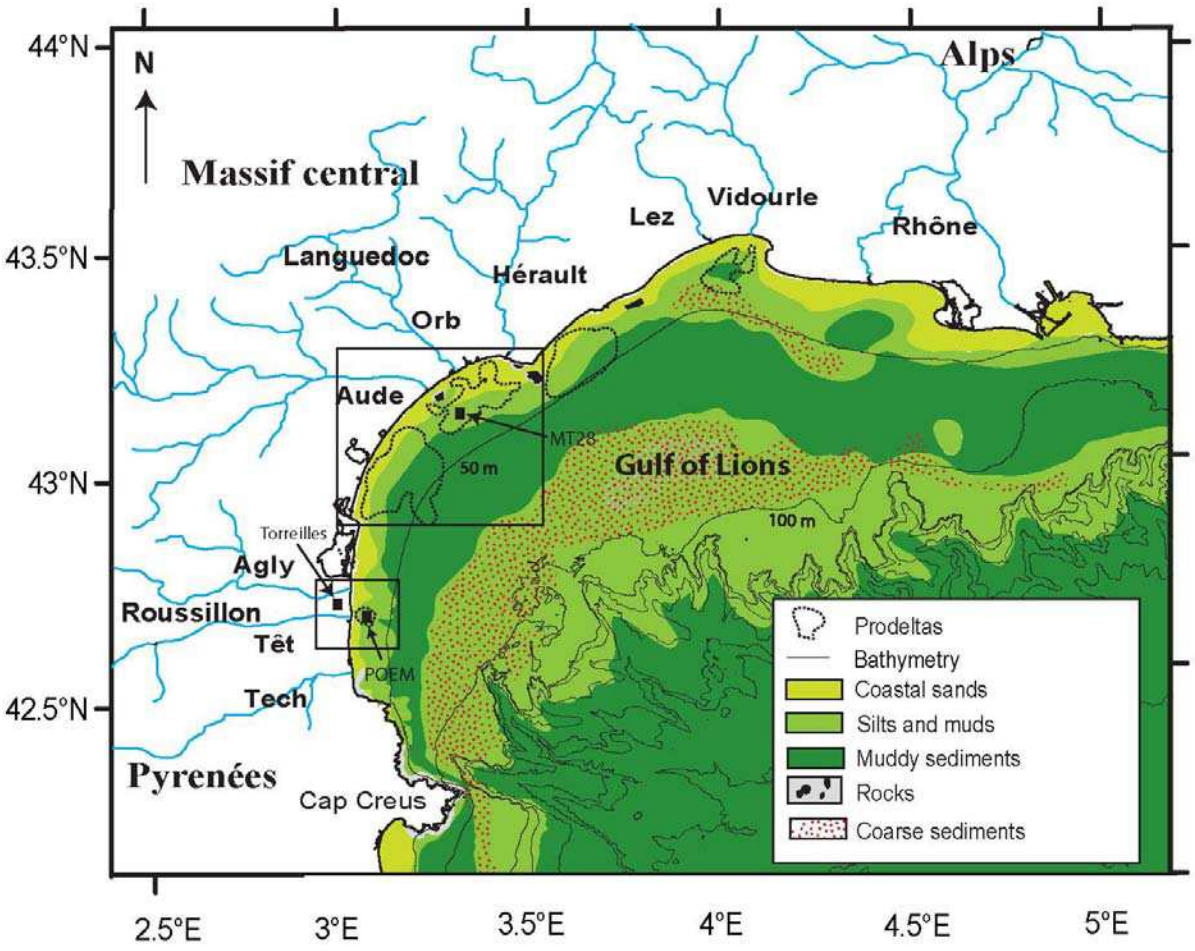

Figure 4-1 : Sedimentary map of the Gulf of Lions (modified from Aloïsi et al., 1973). The black boxes represent zoom on Aude and Têt prodeltas study areas. Black squares represent the coring sites MT28 and POEM as well as the weather station of Torreilles. Doted lines represent prodeltas defined by high content of smectite.

Sedimentation on the Rhône prodelta has been investigated intensively (**Miralles et al., 2005; Radakovitch et al., 1999**). It has been shown that the Rhône prodelta is an important sink for sediment and particle-reactive elements and pollutants: a large amount of sediment which enters the coastal area is retained in the prodelta; the remaining part is resuspended by waves and advected seaward by currents (**Lansard, 2004**). Occasionally, complete seasonal sedimentary sequences can be preserved in the prodelta area, revealing high variability of the sedimentary inputs throughout a year (**Beaudouin et al., 2005**). In contrast, the function of coastal rivers and their prodeltas along the Languedoc-Roussillon coast is poorly understood, particularly their capacity to trap riverborn sediments and associated pollutants. This study addresses several key questions regarding such systems: How much sediment are inputs by the small coastal rivers of the Languedoc-Roussillon? What are the sedimentological characteristics of the main prodeltas (Aude and Têt)? What are the sediment budgets on these prodeltas?

4.1.2 Materials and methods

4.1.2.1 Long-term river discharge time-series

The liquid discharge of the different rivers of the Gulf of Lions was compared using data from the French national data bank (HYDRO) for the last 30 years for the rivers of the Languedoc-Roussillon area (Tech, Têt, Agly, Aude, Orb, Hérault, Lez and Vidourle).

Their fluvial regime was compared with that of the Rhône River, estimated from the "Compagnie Nationale du Rhône" (CNR) databank. Solid suspended fluxes for each river were estimated by using rating curves linking coupled data of instantaneous river discharge and corresponding suspended sediment concentration (**Table 4-1**). Rating curves for the Agly, and Hérault rivers were taken from published works. Equations were determined from these data, with relatively good correlation coefficients. The significance of the Fisher test for linear relations, and the large number of measurements to estimate non-linear relations, allow the use of these rating curves to approximate the annual export of total solids in suspension from all the rivers to the Gulf of Lions.

Rivers	*Rating curve*	*References*
Tech	C=1.2485Qi+6.0628 (r^2=0.61, n=250, p<0.0001)	RMC data bank
Têt	logC=0.3866logQi²-0.0846logQi+1.011 (r^2=0.60, n=1805)	Serrat et al. (2001) + RMC data bank and POEM station measurements
Agly	$Qs=13.27Q_{dm}^{1.434}$ for Q_{dm}>50 m^3/s and $Qs=0.541Q_{dm}^{1.1829}$ for Q_{dm}<50 m^3/s (r^2=0.81, n=195)	Serrat (1999)
Aude	logC=0.1666logQi²-0.0872logQi+1.42041 (r^2=0.30, n=80)	RMC data bank+ unpublished data
Orb	C=0.0018Qi²-0.0228Qi+13.92 (r^2=0.50, n=242)	RMC data bank + unpublished data
Hérault	logC=1.9247logQi²-4.3949logQi+2.7407 (r^2=0.70, n=38)	ORME data bank (Ludwig, 2003)
Lez	C=1.9177Qi+8.0411 (r^2=0.41, n=241, p<0.0001)	RMC data bank
Vidourle	logC=0.2443logQi²+0.1827logQi+0.6983 (r^2=0.57, n=27)	RMC data bank
Rhône	logC=1.5006logQi²-8.1858logQi+12.416 (r^2=0.75, n=521)	Pont (1997) + RMC data bank

Table 4-1 : Rating curves between instantaneous river discharge (Q_i [m^3 s^{-1}]) or mean daily river discharge (Q_{dm} [m^3 s^{-1}]) and the concentration of suspended solids (C [mg L^{-1}]) or mean daily suspended solid discharge (Q_s [t day^{-1}]), obtained from a compilation of data extracted from various references and the data from this study. Determination coefficient (r^2), the number of measurements (n) and p-values associated to the Fisher test (confidence interval=0.95) for linear relations are also shown.

We grouped the different rivers by their geographical location from the south to the north of the gulf, and by hydrological regimes: the western rivers along the Roussillon coast (Tech, Têt, Agly) have catchment areas in the Pyrénées; the central rivers along the Languedoc coast (Aude, Orb, Hérault) have catchment areas between the Pyrénées and the Massif Central; and the northern rivers (Lez and Vidourle) have catchment areas between the Massif Central and the Alps.

4.1.2.2 Sedimentological and radiochemical analysis

Two 20 cm long sediment cores were collected at 28 m water depth with 4 cm of diameter perspex tube on the Têt and Aude prodelta. The Têt prodelta core was sampled by scuba divers in July 28, 2004 at the POEM station. The Aude prodelta core was subsampled in a box-core sampled in October 20, 2002 at MT28 site at 43°12'13"N / 03°16'48"E (**Figure 4-1**). Subsamples of these cores at 1 cm intervals were used for grain size and radiochemical analyses. A Malvern-Mastersizer 2000 was used for the granulometric analysis.

The radionuclide ^{210}Pb ($T_{1/2}$ = 22.3 years) was used to estimate secular sedimentation rates and quantify sediment budget on prodeltas (**Sommerfield and Nittrouer, 1999**). ^{210}Pb activities were determined by counting the alpha emission of the granddaughter radionuclide ^{210}Po extracted from sediment samples by complete acid digestion, according to the procedure described in **Radakovitch (1995)**. Activities of ^{210}Po measured and corrected are assumed to be equal to the activity of ^{210}Pb. Excess ^{210}Pb ($^{210}Pb_{xs}$) activity was determined by subtracting a mean value of supported ^{210}Pb from the total activity. The supported ^{210}Pb activity was determined at the base of the down-core profile of ^{210}Pb data. Mean mass-accumulation rates (R in g cm^{-2} yr^{-1}) were calculated using the Constant Rate of Supply (CRS) model (**Goldberg, 1963**):

$$R = \frac{\lambda S}{A_{exces}} \text{ with } S = \int_z^Z \rho A_{exces} dz$$

where S is the cumulative concentration of $^{210}Pb_{xs}$ (Bq m^{-2}) in a sedimentary layer of thickness z, and A_{exces} is the $^{210}Pb_{xs}$ activity (Bq kg^{-1}). This method takes into account down-core variations of sediment density, and constant supply of ^{210}Pb through time is assumed. Mean sediment accumulation rates (cm yr^{-1}) were determined by normalizing the sediment profile to the density measured for each sediment sample.

4.1.2.3 Mapping of prodeltas

Smectite, a specific clay contained in fine sediments, was used to delimit the prodeltas expanse. Smectite content > 20% and > 40 % were respectively used to delimit the Aude and Têt prodeltas. Maps of smectite content in surficial sediment of the Têt prodelta (**Monaco, 1975**) and the Aude prodelta (**Aloïsi and Monaco, 1975**) were integrated and referenced geographically in GIS software.

4.1.2.4 Hydrodynamics

Currents were measured with an Acoustic Doppler Profiler (ADCP 600 kHz, RD Instruments) through the whole water column at 28 m water depth at the station named POEM ("Plateforme d'Observation de l'Environnement Méditerranéen") located on the Têt prodelta

at 42°42'12"N / 03° 04'00"E (**Figure 4-1**). Depth-averaged hourly measurements were used to produce current direction statistics on the Têt prodelta

Wind direction was measured over the 2003-2005 period, at the weather station of Torreilles (Meteo France code 66212001) located at 42°45'22"N / 02°58'47"E 10 km northwestward from the POEM station (**Figure 4-1**). Hourly data were used to produce direction statistics of the dominant winds on the Têt prodelta.

4.1.3 Results

4.1.3.1 The different regimes of the Gulf of Lions Rivers

Mean annual discharges of the Rhône River, averaged over the 1977-2004 period, give estimates of 5.58×10^{10} m^3/yr of water (compared to 5.39×10^{10} m^3/yr from Antonelli et al. (2004) over the period 1961-1996), and 10.14×10^6 t/yr of fine-grained sediment (compared to 7.4×10^6 t/yr from **Pont et al. (2002)** over the period 1961-1996). The Rhône River discharge exceeds the mean annual discharge of freshwater and suspended sediment by all the coastal rivers by two orders of magnitude (**Table 4-2 top**).

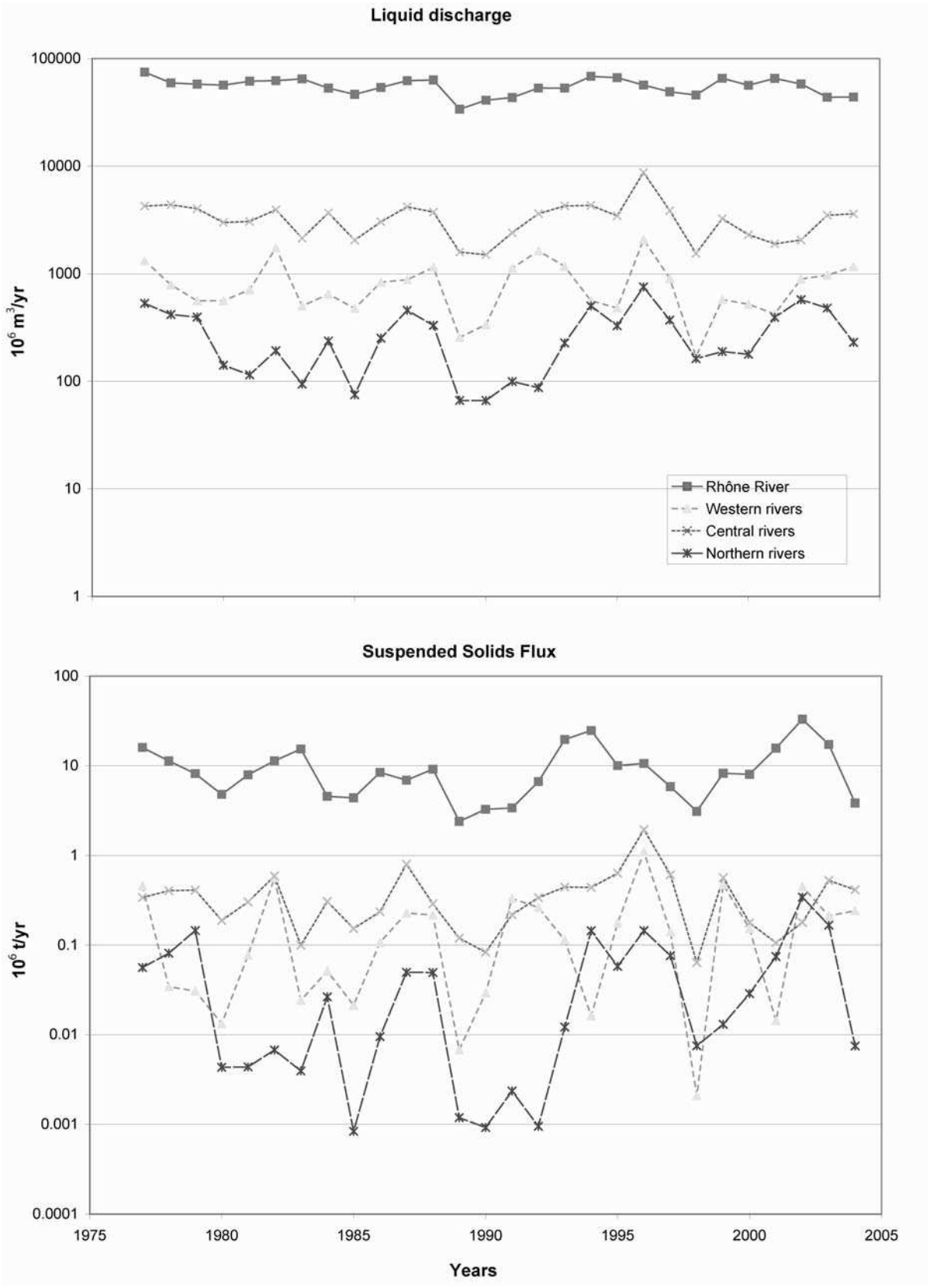

Figure 4-2 : Top, Variability of the annual liquid discharge and, bottom, variability of the annual suspended solid discharge of the rivers of the Gulf of Lions from 1977 to 2004. The western rivers include the Tech, Têt and Agly rivers. The central rivers include the Aude, Orb and Hérault rivers. The northern rivers include the Lez and Vidourle rivers.

Looking at the inter-annual variability of the mean annual water discharge, Rhône River discharge varies by a factor of 3, while the discharge of the coastal rivers vary by a factor up to 10 (**Figure 4-2 top**). This inter-annual variability is even higher if the mean annual suspended solid discharge is considered. The mean annual suspended solid flux of the Rhône River varies by a factor of 50, whilst the suspended solid flux of the northern rivers varies by a factor of 300, and up to 500 for the western rivers (**Figure 2 bottom**). Such variability both in the liquid and the suspended solid discharge of the coastal rivers comes from the fact that these rivers are characterized by extreme flash-flood events during which the major part of the total annual amount of suspended sediment is introduced to the coastal area. For example, about 78 % of the solid flux of the Têt River over the period 1978-1999 occurred in only 50 days (**Serrat et al., 2001**).

Rivers	*Average,(min-max) daily water discharge (m^3/s)*	*Average annual water discharge ($10^6 m^3/yr$)*	*Mean annual suspended solid flux ($10^6 t/yr$)*
Tech	9.55 (<1 - 625)	301.47	0.032± 0.006
Têt	10.82 (<1 - 471)	341.54	0.061± 0.018
Agly	6.13 (<1 - 1020)	193.44	0.098± 0.030
Aude	37.95 (<1 - 1300)	1197.61	0.194± 0.157
Orb	26.67 (1.05 - 1430)	841.64	0.110± 0.044
Hérault	40.61 (<1 - 1320)	1281.58	0.088± 0.028
Lez	2.17 (<1 - 239)	68.65	0.003± 0.001
Vidourle	6.83 (<1 - 783)	215.44	0.051± 0.016
Rhône	1768.59 (322 - 10861)	55812.43	10.147± 3.360

Source	*Estimated sediment supply (kg/yr)*	*Prodelta mass accumulation rate (kg/yr)*
Aude River	194×10^6	182.2×10^6
Orb River	110×10^6	
Hérault River	88×10^6	
Têt River	61×10^6	11.9×10^6

Table 4-2 : Top, Statistics of the water and suspended sediment discharges of the rivers of the Gulf of Lions over the 1977-2004 period. Uncertainties on the solid discharge estimates were calculated from (Fergusson, 1987). The average annual water discharge of the coastal rivers is 4441 x 106 m^3/yr and represents 8 % of the average annual water discharge of the Rhône. The average annual suspended solid discharge of the coastal rivers is 0.637 x 10^6 t/yr and represents about 6.3 % of the average annual suspended solid discharge of the Rhône River. Bottom, Comparison of suspended sediment supply from some rivers and accumulation rates in the associated prodelta.

4.1.3.2 Trapping of continental inputs to prodeltas

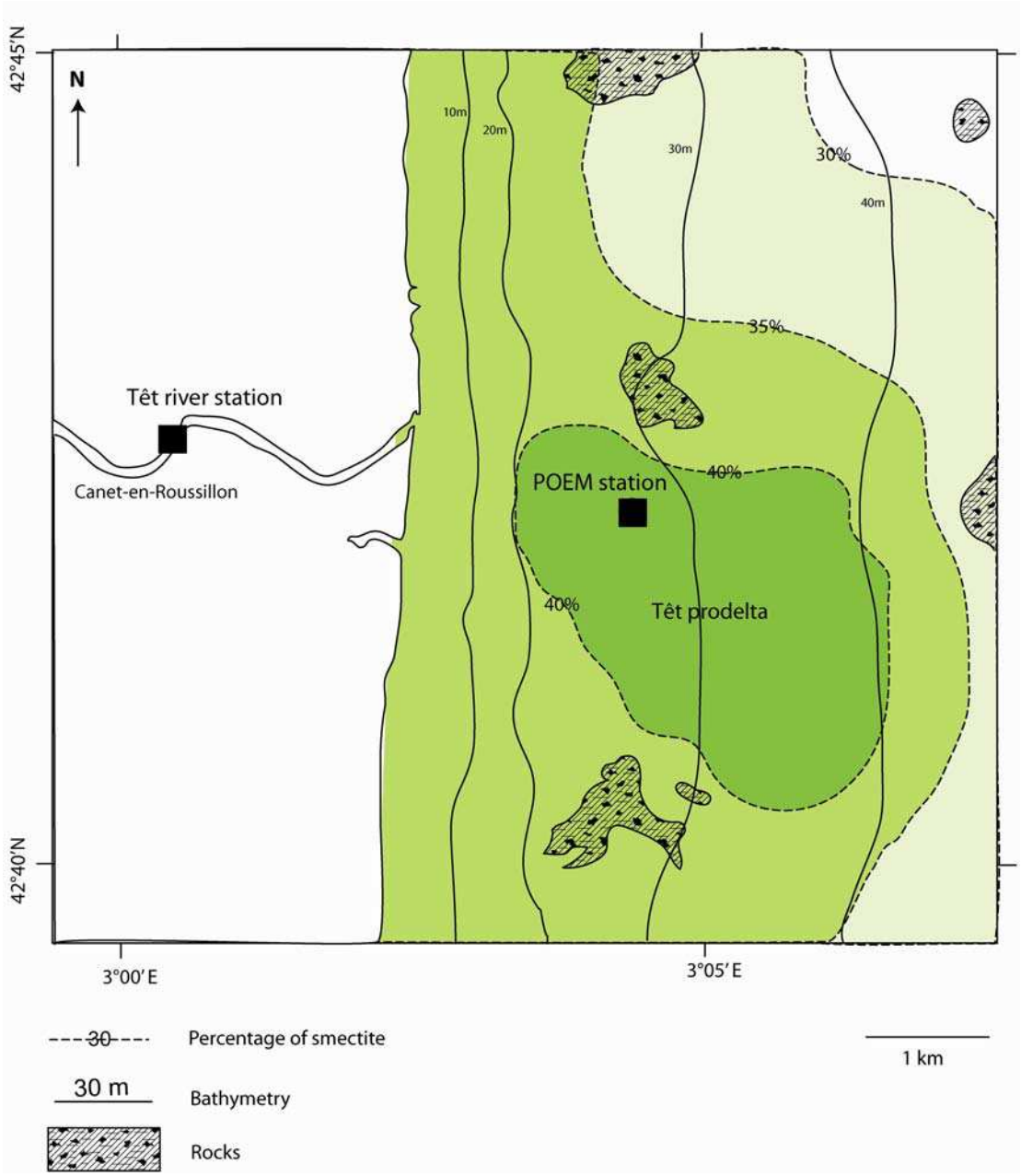

Figure 4-3 : Detailed sedimentary map of the Têt prodelta (adapted from Carte géologique de Perpignan 1/50000e, 1989). The Têt prodelta is delimited by smectite content > 40 % Monaco et Aloïsi, 1975. The black squares represent the locations of the Têt station and the coring site on the prodelta (POEM station).

The surface of the prodeltas of the Têt and the Aude rivers are well defined in the inner-shelf by accumulation of specific clay species issued from the drainage of their catchments. The Têt prodelta is defined by high content of smectite (> 40 %), and its surface estimated to 11.9 km² is located slightly southward from the river mouth (**Figure 4-3**). In the case of the Aude, the

prodelta area (smectite content > 20 %) was evaluated to 121.5 km² (**Figure 4-4**). The surface of the Aude prodelta is larger than the Têt prodelta because it concentrates the inputs of the Aude, Orb and Hérault rivers.

The sedimentary logs and down-core profile of grain-size parameters and $^{210}Pb_{xs}$ activity of the cores sampled on the Aude and the Têt prodelta are shown on the Figure 6 and represent their sedimentary record in a secular time-scale. The top layer of both sediment cores was overlaid by a thin layer (~1 cm) of fluid mud composed of aggregates enriched in organic matter. Under this layer, the top 10 cm of both cores are composed of fine sands characterized by a constant level of $^{210}Pb_{xs}$ activity (20 - 25 Bq/kg for the Têt prodelta, and 30 - 35 Bq/kg for the Aude prodelta). Below this layer, an intermediate layer formed of silts is observed where $^{210}Pb_{xs}$ activity decreases down supported ^{210}Pb activity is reached at around 14 cm depth for the Têt prodelta (**Figure 4-5a**), and below 20 cm depth for the Aude prodelta (**Figure 4-5b**); the supported ^{210}Pb activity corresponding to the remnant ^{210}Pb activity in the sediment.

The level at which the supported ^{210}Pb activity is reached defines the modern (secular age) sedimentary signal of the prodelta. In both cores, the bottom layer is composed of fine silts and clays and is characterized by low values of $^{210}Pb_{xs}$ activity (~0 Bq/kg). We thus observe coarsening-up modern sedimentary sequence both in the case of the Têt and Aude prodeltas. Sedimentation rates estimated from down-core profiles of $^{210}Pb_{xs}$ activity for the Aude and Têt prodeltas give respective values of 0.12 and 0.07 cm/yr (respective mass accumulation rates of 0.15 and 0.10 g cm^{-2} yr^{-1}).

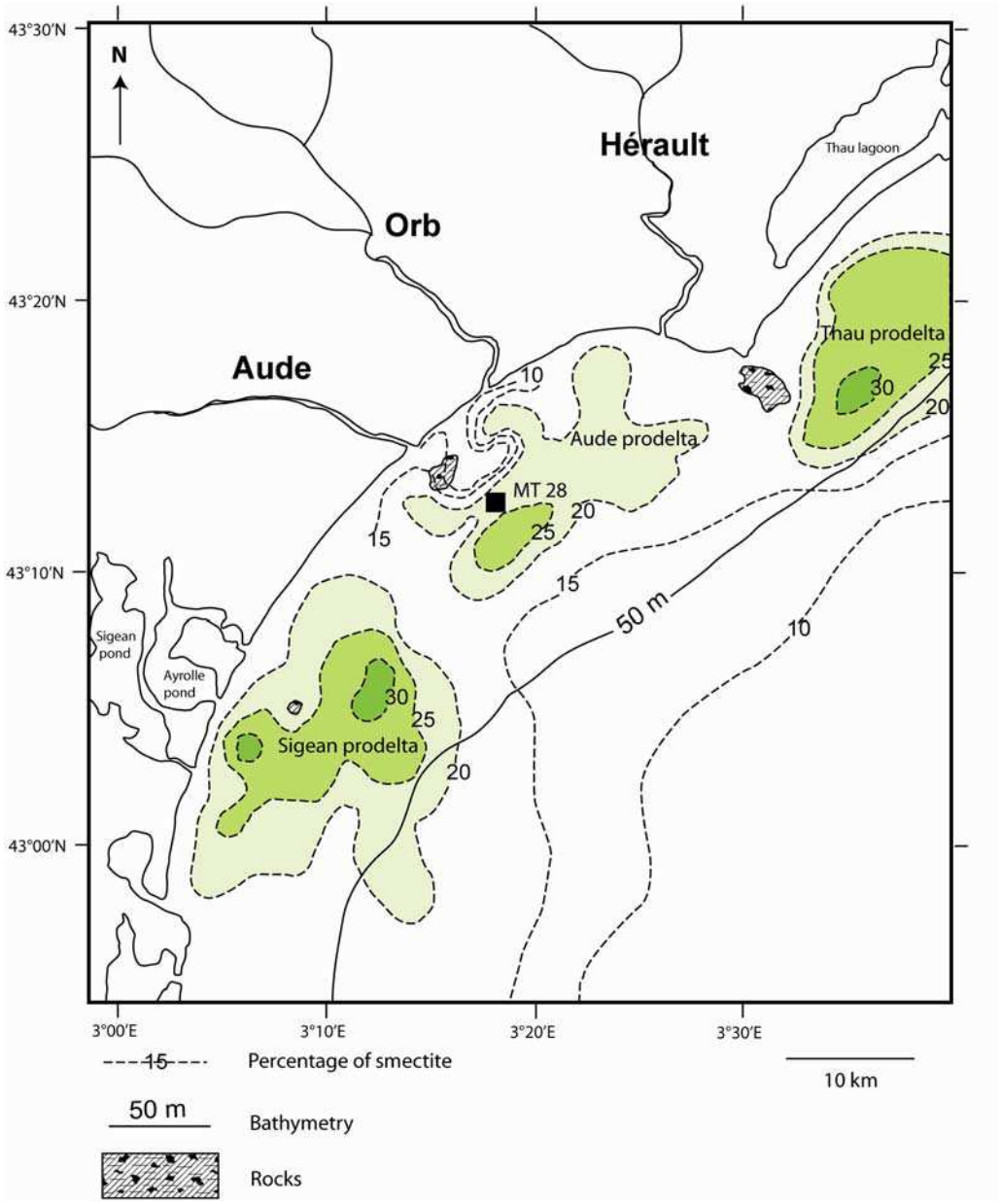

Figure 4-4 : Detailed sedimentary map of the Aude prodelta redrawn from (Aloïsi and Monaco, 1975). The Aude prodelta, common to the Aude, Orb and Hérault rivers, is delimited by smectite content > 20 %. The black square represents the location of the core MT 28. Nearby prodeltas are linked with the ponds of Sigean and Ayrolle in the south and with the Thau lagoon in the north.

4.1.4 Discussion

4.1.4.1 Today sedimentation in prodeltas in the Gulf of Lions

Down-core profiles of grain-size parameters and $^{210}Pb_{xs}$ activity on the Têt and the Aude prodeltas reveal evidence of low but recent sedimentation (**Figure 4-5**). First, the fluffy layer

observed at the top of the two cores is considered as a freshly deposited material as evidenced by the texture of the material composed of aggregates. Its formation could be due to the flocculation of riverborn suspended material located in the benthic nepheloid layer as observed on the continental shelf in the Gulf of Lions (**Aloïsi et al., 1979; Durrieu de Madron and Panouse, 1996**), or it could correspond to a relict flood layer deposited during high river discharge.

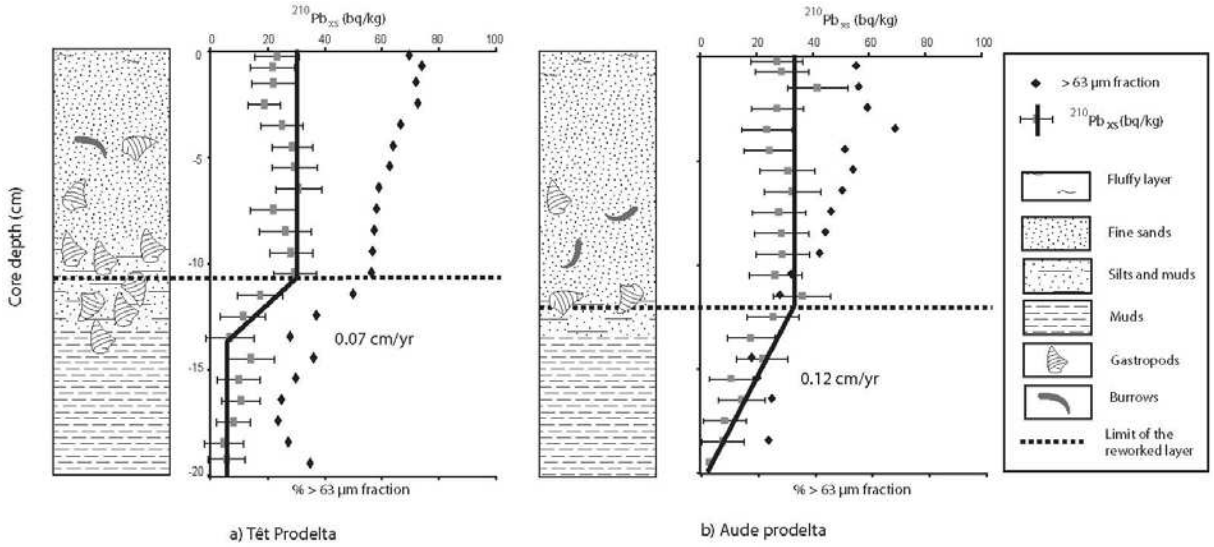

Figure 4-5°: Sedimentary logs of cores sampled on the Têt and the Aude prodeltas and down-core profiles of grain-size parameters (% of particles >63 µm) and $^{210}Pb_{xs}$ activity. Sedimentation rates in cm/yr are also shown. The limit of the reworked layer, with homogeneous $^{210}Pb_{xs}$ activities, corresponds to the sediment thickness that could be reworked by bottom currents.

Indeed, the residence time of flood layer is highly dependent up on near-bed current conditions, and is estimated to be less than 2 months on the Têt inner-shelf in relation with the recurrence of strong bottom currents induced during storm events (**Courp and Monaco, 1990**). Then constant $^{210}Pb_{xs}$ activities are observed in the top 10 cm sediment layer of both cores. The homogeneity of these values indicates that this layer has certainly been reworked by physical processes during storm events and/or bioturbation. Altimetric data on the Têt prodelta shows that erosion and deposition sequences of several centimeters during severe storm events promote the reworking of the top sediment layer (**Guillén et al., 2006; see chapter 4.2**). Grain-size parameters and constant values of $^{210}Pb_{xs}$ activity in the top 10 cm seem to indicate low sedimentation in these prodeltas, and ^{210}Pb geochronology could then give more information concerning their capacity to trap sediment.

4.1.4.2 Preliminary sediment budgets in prodeltas

Fine-grained sediment supplies amount to 61 x 10^6 kg/yr for the Têt River and 402 x 10^6 kg/yr for the group composed of the Aude, Orb and Hérault rivers (**Table 4-2 bottom**). The annual sediment trapping rate T (kg/yr) in prodelta was determined following the relation T = S x m where S is the surface of the prodelta (km²) and m the maximum mass-accumulation rate (g cm^{-2} yr^{-1}) in the prodelta. With the assumption that ^{210}Pb mass-accumulation rates throughout the area of the Têt prodelta are homogeneous, its trapping rate is estimated to about 11.9 x 10^6 kg/yr. This rate represents ~20% of the sediment flux introduced by the Têt River. In the case of the Aude prodelta, we estimated that around 45% (182.2 x 10^6 kg/yr) of the sediment inputs by local rivers is trapped. Limitations of this estimate include (1) error in the river discharge estimate, (2) error in the calculation of sedimentation rates (based on linear regression) and (3) error based on the integration of mass-accumulation rates over the area of the prodelta. The percentage of sediment trapped in the prodelta of the Têt River is in the range of other prodelta associated with mountainous flood-prone river. Estimations of ^{210}Pb maximum mass-accumulation rates and shelf accumulation rates on the Eel river margin give the same value of ~20% retained in the prodelta (**Sommerfield and Nittrouer, 1999**). The comparison of the amount of sediment trapped in the prodelta of the Rhône River compared to the suspended solid inputs is more difficult because the expanse of the Rhône prodelta is not well delimited. But according to various sources (**Beaudouin et al., 2005; Durrieu de Madron et al., 2000; Lansard, 2004; Radakovitch et al., 1999**), we could estimate that more than 50% of the fine-grained sediment introduced by the Rhône River is trapped in its prodelta. One reason could be that the frequent deposition of pluri-centimeters flood layers on the Rhône prodelta which could prevent the underlying layers from erosion by near-bed currents (**Wheatcroft and Drake, 2003**).

Prodeltas trap only a part of the total suspended sediment inputs by the rivers in the inner-shelf. The other part is advected further. In the case of the Têt prodelta, a rose diagram of the current direction throughout the year confirms the pathway of the river plume toward the south and the potential area of deposition of continental material (**Figure 4-6**).

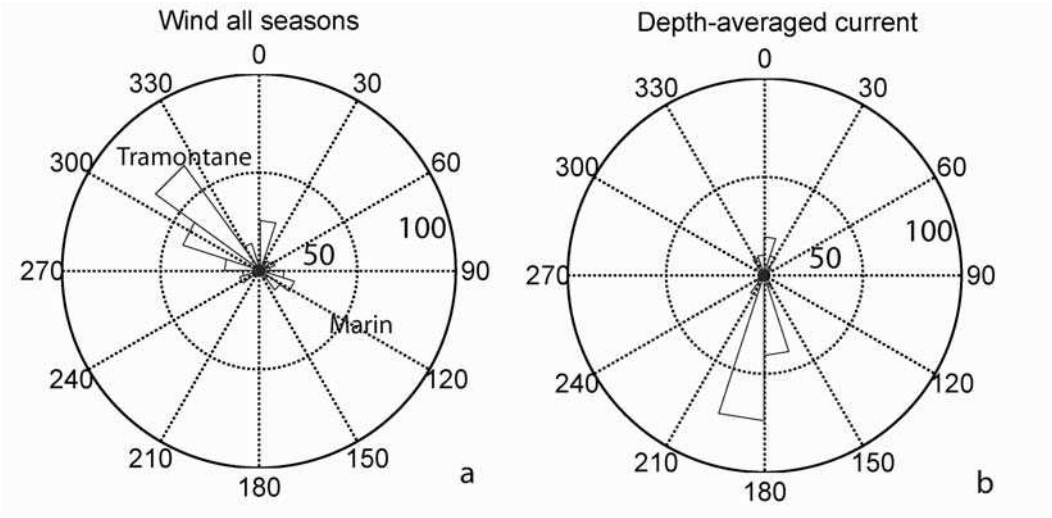

Figure 4-6 : (a) Rose diagrams of dominant winds measured at the weather station of Torreilles over the 2003-2005 period; and (b) Depth-averaged current direction at the POEM station measured over the 2003-2005 period. The units are frequency (0.25 = 25 %).

Along the Roussillon coastline, storms are associated with southeastern winds (Marin), which advect humid marine air over the coastal topography causing local precipitation. The high river discharges that occur later on are generally accompanied by continental winds (Tramontane) which favor the southward propagation of river plumes. Satellite pictures during storm and flood events show that the riverborn material is advected by alongshore currents southward before being exported outside the continental shelf at its southern tip through the canyons (**Palanques et al., 2006**). Numerical models confirm that a part of the sedimentary material deposited in small prodeltas is eroded and advected by near-bed currents toward the mid-shelf mud belt from 50 to 80 m water depth before being finally exported from the continental shelf (**Ulses, 2005**).

4.1.5 Conclusions

The Rhône River is the main input of freshwater and sediment to the Gulf of Lions, but small coastal rivers along the Languedoc-Roussillon coast, characterized by a strong inter-annual variability, can discharge large amounts of sedimentary material to the inner-shelf in a few days. The liquid and suspended solid discharges of all the coastal rivers to the Gulf of Lions are 4441 x 10^6 m^3/yr and 0.637 x 10^6 t/yr respectively and represent about 8 and 6.3 % of the liquid and suspended solid discharges of the Rhône River.

The sedimentation rates on the Têt and the Aude prodeltas, representative of Roussillon (western) and Languedocian (central) rivers of the Gulf of Lions, are small: 0.07 and 0.12 cm/yr respectively, compared to the Rhône prodelta (~20 cm/yr). Sediment budgets suggests that: (i) 20 % of the Têt River suspended solid discharge is trapped permanently in the Têt prodelta; and (ii) 45 % of the suspended solid discharges of the Aude, Orb and Hérault rivers are trapped permanently in the Aude prodelta. Most of the sediment introduced by coastal rivers in the inner-shelf of the Gulf of Lions mainly during flash-flood events thus bypasses the prodeltas and is advected southward.

Further studies are necessary to improve the estimation of the sediment supply of the coastal rivers to the Gulf of Lions. In particularly, estimation of sediment fluxes by the Aude River, the second larger river of the gulf in terms of sediment yield, could be improved, .e.g. by increasing the measurements of SSCs during flood events. More sediment analysis (both grain-size and geochronological analysis) must to be realized on prodeltas of the Gulf of Lions in order to improve the estimation of sediment trapped and thus pollutants and pathogens in those areas as well as in front of lagoon mouths.

Acknowledgements

This work was funded under the European program EUROSTRATAFORM (EVK3-CT-2002-00079, EU Fifth Framework Programme: Energy, Environment and Sustainable Development) and the French program of the Languedoc-Roussillon region, SYSCOLAG. The authors would like to thank Gérard Jeanty for the processing of radiochemical analyses at the CEFREM, Perpignan, France. Grain-size analyses were performed at the laboratory of Banyuls s/ Mer under the responsibility of Antoine Grémare. We also would like to thank the IRSN group from La Seyne s/ Mer, for the participation to the REMORA campaigns and the use of the sediment samples. We are grateful to Pierre Serrat and two other anonymous reviewers who contributed to greatly improve the manuscript.

Bibliography

Aloïsi, J.-C., Got, H., Monaco, A., 1973. Carte géologique du précontinent languedocien au 1/250000ième., Netherlands.

Aloïsi, J.-C., Millot, C., Monaco, A., Pauc, H., 1979. Dynamique des suspensions et mécanismes sédimentogénétiques sur le plateau continental du Golfe du Lion. C. R. Acad. Sc., 289(13) : 879-882.

Aloïsi, J.-C.,Monaco, A., 1975. La sédimentation infralittorale. Les prodeltas nord-méditerranéens. C.R. Acad. Sci., 280: 2833-2836.

Antonelli, C., Provansal, M.,Vella, C., 2004. Recent morphological channel changes in a deltaïc environment. The case of the Rhône River, France. Geomorphology, 57: 385-402.

Beaudouin, C., Suc, J.-P., Cambon, G., Touzani, A., Giresse, P., Pont, D., Aloïsi, J.-C., Marsset, T., Cochonat, P., Duzer, D., Ferrier, J., 2005. Present-Day Rhythmic Deposition in the Grand Rhône Prodelta (NW Mediterranean) According to High-Resolution Pollen Analyses. Journal of Coastal Research, 21(2): 292-306.

Courp, T., Monaco, A., 1990. Sediment dispersal and accumulation on the continental margin of the gulf of Lions: sedimentary budget. Continental Shelf Research, 9-11: 1063-1088.

Durrieu de Madron, X., Abassi, A., Heussner, S., Monaco, A., Aloïsi, J.C., Radakovitch, O., Giresse, P., Buscail, R., and Kerhervé, P., 2000. Particulate matter and organic carbon budgets for the Gulf of Lion (NW Mediterranean). Oceanologica acta, 23(6) : 717-730.

Durrieu de Madron, X., Panouse, M., 1996. Transport de matière en suspension sur le plateau continental du Golfe du Lion - Situation estivale et hivernale. C. R. Acad. Sc., 322: 1061-1070.

Fergusson, R.I., 1987. Accuracy and precision of methods for estimating river loads. Earth Surface Processes and Landforms, 12: 95-104.

Goldberg, E.D., 1963. Geochronology with 210-lead. Radioactiv. dating, I.A.E.A., Vienna: 121-131.

Guillén, J., Bourrin, F., Palanques, A., Durrieu de Madron, X., Puig, P., Buscail, R., 2006. Sediment dynamics during "wet" and "dry" storm events on the Têt inner shelf (SW Gulf of Lions). Marine Geology.

Lansard, B., 2004. Distribution et remobilisation du plutonium dans les sédiments du prodelta du Rhône (Méditerranée nord-occidentale). PhD Thesis, Univ. Méditerranée Aix-Marseille II, 344 pp.

Ludwig, W., 2003. Observatoire Régional Méditerranéen sur L'Environnement - Rapport final 2001-2003 et perspectives, 60 pp.

Miralles, J., Radakovitch, O., Aloïsi, J.-C., 2005. 210Pb sedimentation rates from the Northwestern Mediterranean margin. Marine Geology, 216: 155-167.

Monaco, A., 1971. Contribution à l'étude géologique et sédimentologique de plateau continental du Roussillon (Golfe du Lion). PhD Thesis, Université des Sciences et Techniques du Languedoc., Montpellier, 285 pp.

Monaco, A., 1975. Les facteurs de la sédimentation marine argileuse. Les phénomènes physico-chimiques à l'interface. BULL. B.R.G.M. (2), IV(3) : 147-174.

Monaco, A., 1987. Transferts littoraux en Méditerranée. Bull. Ecol., 18(2) : 225-228.

Palanques, A., Durrieu de Madron, X., Puig, P., Fabres, J., Guillén, J., Calafat, A., Canals, M., Heussner, S.,Bonnin, J., 2006. Suspended sediment fluxes and transport processes in the Gulf of Lions submarine canyons. The role of storms and dense water cascading. Marine Geology, 234(1-4): 43-61.

Pauc, H., 2005. Formation of the Aude, Orb and Hérault prodeltas and their characterisation using physicochemical and sedimentological parameters. Marine Geology, 222-223: 335-343.

Pont, D., 1997. Les débits solides du Rhône à proximité de son embouchure : données récentes (1994-1995). Revue de Géographie de Lyon, 72(1/97) : 23-33.

Pont, D., Simonnet, J.-P., Walter, A.V., 2002. Medium-term Changes in Suspended Sediment Delivery to the Ocean: Consequences of Catchment Heterogeneity and River Management (Rhône River, France). Estuarine, Coastal and Shelf Science, 54(1) : 1-18.

Radakovitch, O., 1995. Etude du dépôt et du transfert du matériel particulaire par le 210Po et le 210Pb. Application aux marges continentales du golfe de Gascogne (NE Atlantique) et du golfe du Lion (NW Méditerranée). PhD Thesis, Univ. Perpignan, 250 pp.

Radakovitch, O., Charmasson, S., Arnaud, M., Bouisset, P., 1999. ^{210}Pb and caesium accumulation in the Rhône delta sediments. Estuarine, Coastal and Shelf Science, 48: 77-92.

Roussiez, V., Aloïsi, J.-C., Monaco, A., Ludwig, W., 2005. Early muddy deposits along the Gulf of Lions shoreline: A key for a better understanding of land-to-sea transfer of sediments and associated pollutant fluxes. Marine Geology, 222-223: 345-358.

Serrat, P., 1999. Dynamique sédimentaire actuelle d'un système fluvial méditerranéen : l'Agly (France). Comptes Rendus de l'Académie des Sciences, 329: 189-196.

Serrat, P., Ludwig, W., Navarro, B., Blazi, J.-L., 2001. Variabilité spatio-temporelle des flux de matières en suspension d'un fleuve côtier méditerranéen : la Têt (France). Comptes Rendus de l'Académie des Sciences, 333: 389-397.

Sommerfield, C.K., Nittrouer, C.A., 1999. Modern accumulation rates and a sediment budget for the Eel shelf: a flood-dominated depositional environment. Marine Geology, 154: 227-241.

Ulses, C., 2005. Dynamique océanique et transport de la matière particulaire dans le Golfe du Lion : Crue, tempête et période hivernale. PhD Thesis, Université Paul Sabatier, Toulouse, 247 pp.

Wheatcroft, R.A., Drake, D.E., 2003. Post-depositional alteration and preservation of sedimentary event layers on continental margins, I. The role of episodic sedimentation. Marine Geology, 199: 123-137.

Les principaux résultats apportés dans le chapitre 4.1 sont les suivants :

1. Les fleuves côtiers du golfe du Lion sont marqués par une forte saisonnalité puisque l'essentiel des apports liquide et solide est apporté lors de crues-éclairs à l'automne et au printemps. Ils se distinguent du Rhône par leur torrentialité et les quantités des apports au golfe du Lion. Le fleuve Têt est un exemple de ces fleuves côtiers méditerranéens à caractère torrentiel.
2. Ces fleuves côtiers sont également marqués par une très forte variabilité interannuelle. Le débit liquide du Rhône varie d'un facteur 1 à 3 alors que les débits liquides des fleuves côtiers varient d'un facteur 1 à 10. Cette variabilité interannuelle est d'autant plus importante si l'on considère les débits solides de ces fleuves. Le débit solide du Rhône varie d'un facteur 1 à 50 alors que les débits solides des fleuves côtiers du golfe du Lion varient d'un facteur 1 à 300.
3. Les taux de sédimentation estimée à partir des mesures de $^{210}Pb_{xs}$ montrent des taux de sédimentation de l'ordre de 0.07 et 0.12 cm/an sur les prodeltas de la Têt et de l'Aude respectivement. Ces taux de sédimentation sont très faibles par rapport à ceux que l'on peut observer devant l'embouchure du Rhône (jusqu'à 20 cm/an). Le rapport entre les quantités de sédiments apportés par les fleuves côtiers et les quantités piégées dans la zone côtière du golfe du Lion montre qu'environ 20 % des apports du fleuve Têt sont piégés dans son prodelta et qu'environ 45 % des apports des fleuves Orb, Aude et Hérault sont piégés dans la zone prodeltaïque adjacente. Ce premier bilan montre que les prodeltas méditerranéens du golfe du Lion ne piège qu'une faible partie des sédiments apportés par les fleuves dans la zone côtière.

De ces résultats préliminaires découlent plusieurs questions. Si les prodeltas ne piègent qu'une partie des apports sédimentaires apportés par les fleuves, quel est le devenir du matériel restant ? Ensuite, ce premier bilan est une résultante des mécanismes hydro-sédimentaires qui se sont produits à l'échelle séculaire. Quels sont alors les mécanismes actuels haute-fréquence qui régissent la dynamique des prodeltas méditerranéens ?

Ainsi dans le **chapitre 4.2**, nous aborderons l'impact hydro-sédimentaire des évènements de crues et tempêtes extrêmes associés, dans un continuum Terre-Mer, généralisés à l'ensemble du golfe du Lion. Nous aborderons ensuite dans le **chapitre 4.3**, l'impact d'un évènement de crue et tempête isolé sur le prodelta de la Têt, et la relation côte-large des processus hydro-sédimentaires. Et enfin dans le **chapitre 4.4**, nous nous intéresserons à l'impact des

évènements hydro-climatiques extrêmes durant un hiver particulier, sur la dynamique sédimentaire de la zone prodeltaïque du fleuve Têt.

4.2 Dynamique sédimentaire durant les tempêtes « humides » et « sèches » sur le littoral de la Têt (Sud-ouest du golfe du Lion)

Sediment dynamics during wet and dry storm events on the Têt inner shelf (SW Gulf of Lions)

J. Guillén[a]	Redaction, Data (OBS,current meters)
F. Bourrin[b]	Redaction, Data (altimeters, ADCP currents and waves)
A. Palanques[a]	Redaction, Data (canyons mooring lines, sediment traps)
X. Durrieu de Madron[b]	Manuscript revision
P. Puig[a]	Manuscript revision
R. Buscail[b]	Manuscript revision, Data (sediment cores analysis)

[a] Instituto de Ciencias del Mar-C.S.I.C., Passeig Maritim de la Barceloneta, 37, 08003 Barcelona, Spain

[b] Centre de Formation et de Recherche sur l'Environnement Marin, Université de Perpignan 52, Avenue Paul Alduy, 66860 Perpignan, France

Soumis le 04/07/2005

Accepté le 05/09/2006

Marine Geology 234 (2006) 129–142

EUROSTRATAFORM VOL. 1: Source to Sink Sedimentation on the European Margin

Abstract

The importance of short-term processes, such as floods and storms, on sediment delivery and reworking on the Têt inner shelf was investigated. The Têt inner shelf is a small, event-dominated system located in the south-western part of the Gulf of Lions. The expected sedimentary scenario in this environment is that fluvial sediment should be deposited on the prodelta and later dispersed around the shelf and slope by waves and currents reworking during storms. This paper investigates differences in inner shelf sediment dynamics between storm events occurring during usual river discharges and those occurring during river floods.

Waves, current velocities, near-bottom water turbidity, bottom sediment grain-size and sea-floor erosion/accretion were concurrently measured at 28-m water depth on the Têt inner shelf from November 2003 to March 2004. Two major storms took place on 4 December 2003 and 21 February 2004, and two moderate storms occurred on 8 December 2003 and 14 March 2004. The two major storms displayed similar wave characteristics: maximum significant wave height (Hs) >7 m, peak period (Tp) >12 s and wave direction around 90°. The main environmental differences during the two major storm events correspond to the amount of sediment discharged from the Têt River. About 2×10^4 t of sediment was delivered by the river during the 4 December flood (wet storm) and less than 5×10^2 t during the 21 February storm (dry storm).

Sediment dynamics were quite similar during the storm events: resuspension caused by waves and sediment advection towards the southeast due to near-bottom shelf currents were the dominant sedimentary processes. The result was a bottom sediment erosion of several centimetres at the study site during both the wet and dry events. The main differences between the wet and dry events arose after the storm. Immediately after the peak of the wet storm, sediment supplied by the Têt River (and probably from other rivers) was deposited around the river mouth. A few days later, during a moderate storm, this unconsolidated sediment was resuspended, transported offshore and deposited on the inner shelf. In contrast, a moderate storm which occurred some days after the dry February storm caused bottom erosion on the inner shelf, because no fresh sediment was available on the shallower area. The results from this study indicate that the Têt inner shelf at 28-m water depth is mainly a bypass zone for sediment that is transported S–SE towards the middle–outer shelf and slope, although ephemeral sediment deposits may be favoured by the sediment supplied from flood events.

Sediment transport across the shelf, from the river to the slope, follows a complex, multi-step pattern that needs to be addressed using a multi-event approach.

Keywords

Wet storm; dry storm; near-bottom sediment dynamics; seabed erosion; inner shelf.

4.2.1 Introduction

The fate of sediment from rivers into the ocean and how the particles are dispersed and accumulated across different sedimentary environments of the continental margin has been studied during the last few decades. Research first focused on shelves located off the largest rivers (the Mississippi, the Amazon, etc) (**Wright and Coleman, 1974; Nittrouer and DeMaster, 1987**), but more recently it has shifted to areas dominated by medium-sized rivers (the Eel, Atchafalaya, Po, Rhône, etc.) (**Nittrouer, 1999; Allison et al., 2000; Trincardi and Syvitski, 2005**). In a general perspective, sediment dynamics on the shelf have been categorized into high and low-concentration regimes (**Fan et al., 2004**). The high-concentration regime is characterized by the occurrence of floods and storms that favour gravity driven seaward transport and the formation of inner shelf flood deposits when wave energy decays at the end of the storm. In the low-concentration regime, there is no recent flood deposition on the inner shelf and the dominant processes are the winnowing of fines and the bypass of sediment. The importance of short term processes like floods and storms on sediment delivery and reworking on the shelf has been addressed in these studies (e.g. **Ogston et al., 2004**), in addition to the probability of preservation of event strata (e.g. **Bentley and Nittrouer, 2003; Wheatcroft and Drake, 2003**). On the Eel shelf (probably as on most shelves around the world), sediment transport is dominated by waves and currents, and the suspended sediment concentration and wave-orbital velocity generally correlated during storms (**Ogston et al., 2000**) that occur without relevant continental runoff (i.e. dry storms). However, if the storm coincides with a period of high river discharge (i.e. a wet storm), the additional fluvial sediment can considerably increase the near-bottom suspended sediment concentration, which is unrelated to the orbital velocity on the shelf (**Ogston et al., 2000; Sommerfield et al., submitted**). For example, orbital velocity and suspended sediment concentration changes are comparable only at the beginning of a wet storm in winter 1995 but peak SSC occurs after that of orbital velocity, due to the supply of sediment from the Eel

River (**Cacchione et al., 1999**). Additionally, wet storms can produce widespread flood deposits on the shelf and slope (**Mullenbach and Nittrouer, 2000**) or favour the creation of fluid mud (**Traykovski et al., 2000**).

A conceptual model of sediment dynamics on the shelf can be summarized from previous studies that are based largely on the Eel system: the sediment supplied from rivers is trapped on the inner shelf (**Geyer et al., 2000, Crockett and Nittrouer, 2004**), usually in the form of an ephemeral (days–weeks) fine flood layer (**Wheatcroft and Borgeld, 2000**). This sediment is resuspended during storms, transported offshore as near-bottom fluid mud layers, and deposited on the middle shelf where the mud belt is typically located (**Traykovski et al., 2000**). Finally, the most energetic storms can resuspend this sediment as fluid muds, making it available for transport towards the outer shelf and upper slope (**Ogston et al., 2000; Puig et al., 2003; Fan et al., 2004**). In spite of the apparent simplicity of the conceptual model, many processes remain poorly understood and the field information is scarce in the Eel margin and absent in other areas. For instance, sedimentary processes on the inner shelf during the generation of fluid mud layers (**Traykovski et al., 2000**) and the ephemeral character of the inner shelf deposit (**Wheatcroft and Borgeld, 2000**) are not well documented.

One of the objectives of the EUROSTRATAFORM Project was to characterize the sedimentation processes involved in the transport of sediment in different European margins, from its origin in rivers to its deposition on deltas, shelves, canyons and open slopes. In the Mediterranean Sea, this work focused on two large rivers (the Rhône and the Po) and one small system (the Têt River). Note: the terms “large” and “small” are quite subjective, since “large” rivers in the Mediterranean have similar dimensions (drainage basin, water and sediment supplies) to “medium” rivers around the world, such as the Eel River. From a global perspective, the Têt is a “small” system typical of the Mediterranean. The aim of this work is to improve our knowledge of sediment dynamics on the inner continental shelf located off a small river during different storm events, in order to complement the previous findings on large and medium sized systems. The general goal is to study sediment dispersion and deposition on the Têt inner shelf during two consecutives major storms. The first storm (December 2003) occurred simultaneously to a river flood, whereas the second one (February 2004) was without relevant river inputs. The specific objectives were to compare resuspension, advective transport processes, event layer formation and seabed

erosion/deposition in both wet and dry storm events to determine the role of the inner shelf environment in controlling the fate of sediment supplied from small rivers.

4.2.2 Study area

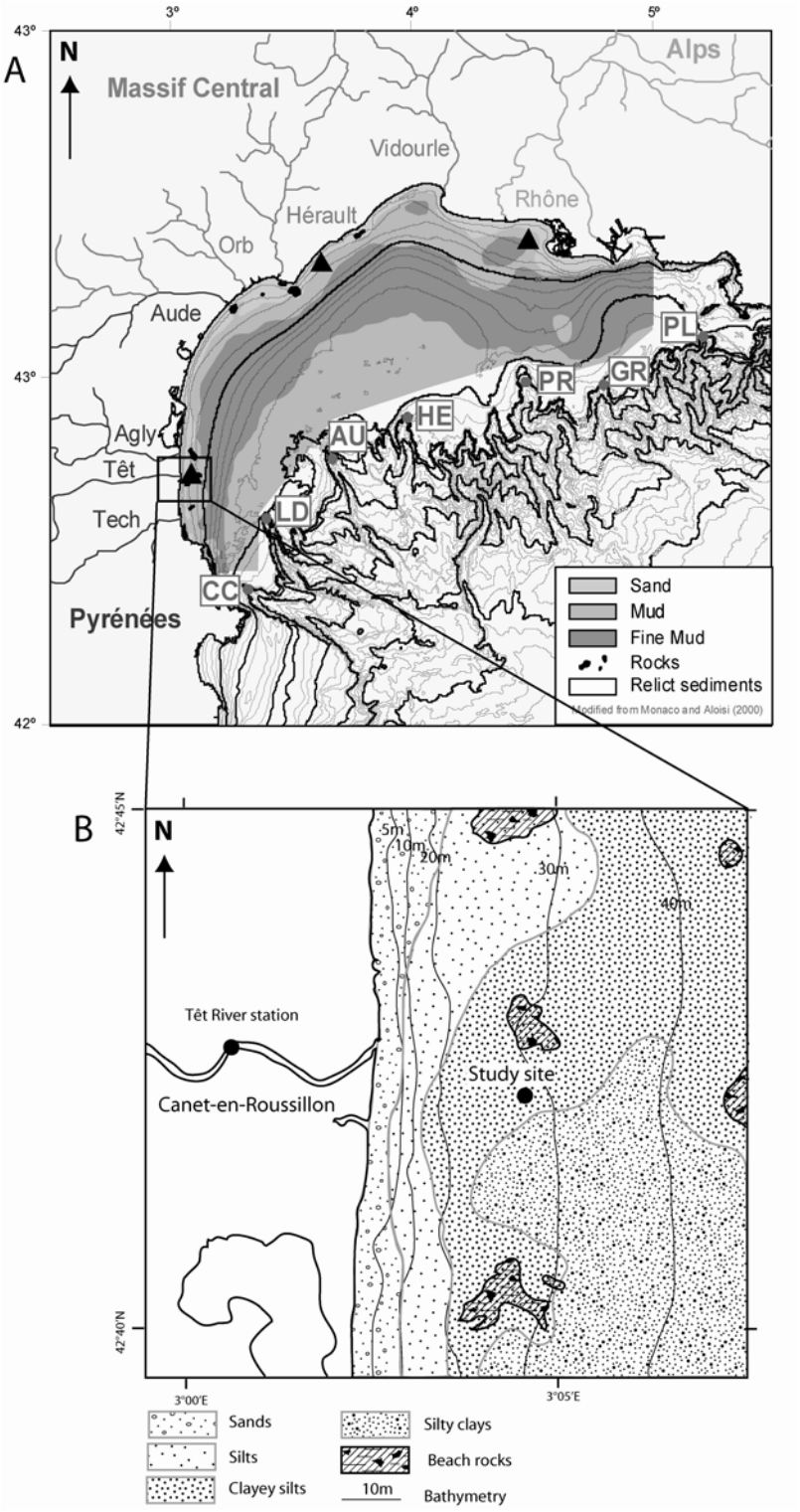

Figure 4-7 : The study area. (A) The Gulf of Lions showing main rivers and submarine canyons (from east to west: PL (Planier), GR (Grand Rhône), PR (Petit Rhône), HE (Hérault), AU (Aude), LD (Lacaze

Duthiers) and CC (Cap de Creus Canyon); and (B) the Têt system showing the location of the observational site at the inner shelf.

The Gulf of Lions (NW Mediterranean) is an example of a temperate, deltaic margin dissected by numerous canyons (**Figure 4-7**). This margin receives water and sediment from the Rhône River (now one of the largest river input into the Mediterranean Sea with the Po River) as well as from many smaller rivers (the Tech, Têt, Agly, Aude, Orb and Hérault, among others). The bottom sediment distribution displays a mid-shelf mud belt and the inner and outer shelf regions with mixed sandy mud deposits (**Aloïsi et al., 1973**). Fine-grained deposits are also located on the upper slope.

The general coastal circulation of the Gulf of Lions is relatively poorly understood because the circulation is highly variable and dependent on wind conditions. The main winds in the western part of the gulf are the northwesterly "Tramontane" and the southeasterly "Marin". **Estournel et al. (2003)** have shown that the Tramontane induces a cyclonic circulation, with the same pattern induced by southeasterly winds coming from the sea.

The Têt system is located in the south-western part of the Gulf of Lions (**Figure 4-7**). It is characterized by a small river that discharges water and sediment episodically onto the continental shelf, generating a prodelta deposit (**Courp and Monaco, 1990; Buscail et al, 1990, 1995; Guidi-Guilvard and Buscail, 1995; Roussiez et al., 2005**).

The Têt River discharges into the sea a daily average of 10 $m^3\ s^{-1}$, although instantaneous water discharge can reach 1800 $m^3\ s^{-1}$ during major floods associated with strong rainfall events (**Serrat et al., 2001**). The mean annual sediment discharge of the Têt River to the sea for the period from 1980 to 1999 was $5.3 \pm 1.6\times10^4$ t yr^{-1}, with maximum suspended sediment concentration values of about 47 g l^{-1} for the catastrophic 1940s flood event (**Serrat et al., 2001**). On the adjacent shelf, bottom sediment is composed mostly of sand between the shoreline and 25-m water depth and muddy-sand between 25 and 40 m (**Aloïsi et al., 1973**).

Waves are the main mechanism causing bottom sediment resuspension in the western Mediterranean as tidal currents are negligible. Major storms are associated with waves coming from the east. Large waves with Hs > 5 m and Tp > 9 s occur during autumn and winter. These are able to resuspend sediment on the inner and middle shelf and produce a

dominant sediment transport along-shelf towards the south (**Puig et al., 2001; Guillén et al., 2002; Palanques et al., 2002**). Mean waves in the south of the Gulf of Lions have Hs = 1.2 m and Tp = 4.8 s. Swells associated with southeasterly winds can generate waves with Hs > 6 m and Tp up to 12 s, causing bottom sediment resuspension such as that observed at 26-m water depth during one of these events (**Ferré et al., 2005**).

4.2.3 Methods

Time series of meteorological, sedimentological and hydrodynamic parameters were collected near the river mouth and on the inner shelf during the winter of 2003– 2004. Têt River water discharge was obtained from the HYDRO national data bank. The hourly river discharge is the sum of the Têt and the Basse River (a small tributary) discharge. Riverine suspended sediment concentration (SSC) is based on 311 measurements from water samples collected during the period 1971–1999 (**Serrat et al., 2001**). A relationship was established between SSC (in mg l^{-1}) and instantaneous river discharge (Qi in m^3 s^{-1}):

$\log C=0.5057 \log Qi^2-0.4537 \log Qi+1.087$ with $r^2=0.67$ (**Serrat et al., 2001**)

and was applied to the hourly water discharge data for the study period. The relationship has been verified through regular water samples since 1999.

An oceanographic station was installed 2 km off the mouth of the Têt River at 28-m water depth (42° 42.250 N–03° 04.006 E), close to the sand–mud transition (**Figure 4-7**). Oceanographic instruments were deployed on 26 November 2003 and retrieved in mid-March 2004.

4.2.3.1 Waves and currents

Continuous information about wave conditions was obtained by an autonomous ADCP RDI Sentinel 600 kHz model equipped with a wave pressure sensor and deployed at the study site. It was mounted on a bottom platform with an upward-looking configuration. Waves were measured during 20 min bursts at 2 Hz every 3 h. Currents were measured between wave burst measurements at 1 Hz and were averaged over that period. The ADCP collected data

between 26 November 2003 and 16 January 2004 and between 4 February and 26March 2004. Additional wave data were obtained from a Datawell wave buoy deployed 11 km south of the study area. Bottom shear stress (τ) was estimated using the combined wave-and-current boundary- layer model of **Grant and Madsen (1986)**. Inputs to the model were wave-orbital velocity (u_{rms}), obtained by applying linear wave theory from the ADCP Hs and Tp measurements, current speed (u_c) at 2 m above bottom (mab) and wave–current angle. The bottom was assumed to be flat and the bottom roughness was given by the sediment grain-size (D_{50}). Seabed observations using a video-lapse camera during deployments indicated that this assumption could be acceptable most of the time. Video observations showed small ripples at the beginning of the deployment (November 2003) and a flat bottom after storms. The flat bed assumption was also checked against different models predicting ripple formation (**Madsen, 1993; Wiberg and Harris, 1994**) using a range of sediment grain-sizes. These models predict formation of small ripples (height < 1 cm; wavelength < 10 cm) at the study site during short periods at the beginning and the end of storms, which are similar to the ripples observed by the video camera at the beginning of the deployment. During the peak of storms, models predict sheet flow conditions or upper plane bed conditions. Therefore, the form drag can be expected not to drastically modify shear stress estimations. However, bed roughness caused by saltating grains during high-energy conditions could increase the estimated shear stress during the peak of the storm.

4.2.3.2 Suspended sediment concentration and sediment fluxes

A bottom tripod was deployed at the study site from 26 November to 12 December 2003 and from 4 February to 18 March 2004. Current and water turbidity were measured using three EMF current meters (Delft Hydraulics) and three D&A Instruments Optical Backscatter Sensors (OBS-3) mounted on a frame at 0.15, 0.5 and 0.9 mab, collecting data every 3 h in 20 min bursts logging at 2 Hz. In the first deployment, the tripod was knocked over during the peak of a strong storm after 8 days sampling, but fortunately the OBS located closest to the bottom gave continuous useful information. OBS sensors were calibrated in the laboratory using bottom sediment collected at the tripod location prior to the deployments, and signals from these instruments were converted into SSC. Near-bottom suspended sediment fluxes were estimated from burst-averaged SSC and current velocity using sensors located about 0.15 meters above the bottom (mab). In order to estimate the near-bottom velocity when the tripod was knocked over during the first deployment, a linear regression (r^2 = 0.8) was

established between current intensity measured by the ADCP 2 mab and the lowest current metre of the tripod. In the second deployment, the tripod sank several centimetres into the seabed during the peak of the dry storm, and measurements of the lowest sensors were disturbed. Therefore, SSC and currents measured by sensors originally located at 0.5 mab were used for the estimation of suspended sediment fluxes after the peak of the storm.

4.2.3.3 Seabed erosion/deposition

Erosion/deposition events were monitored using an NKE ALTUS 2 MHz altimeter that measured the seabed position and water depth every 20 min during the study period. Instrument accuracy was ± 0.5 cm. Data were obtained from 26 November to 12 December 2003 and from 4 February to 18 March 2004. During the first deployment, the altimeter was mounted in a small tripod frame, whereas for the second deployment it was installed on the large tripod.

4.2.3.4 Sediment

Four sea-floor interface cores of undisturbed sediment were collected by divers using transparent Perspex tubes (7-cm diameter and 20-cm long) in order to obtain information about temporal variations of sediment properties. The cores were obtained on 26 November 2003, 12 December 2003, 11 February 2004 and 15 March 2004. The cores were sectioned at 1-cm intervals, except the first centimeter, which was sectioned at intervals of 0.5 cm. The samples were frozen and then freeze-dried in the laboratory a few hours after core subsampling. Grain-size was analyzed using a Malvern instrument Mastersizer 2000 equipped with a Hydro MU sample dispersion unit, and a laser diffraction system. Water content, expressed as percentage of water over the dry weight of sediment (% d.w.), was measured on microcores obtained with 2-ml truncated syringes. Additionally, a sequential sediment trap (12 bottles, 2–3 day collecting period) mounted on a tripod frame was deployed in order to obtain information about suspended sediment characteristics during the study period. Only five bottles had enough sediment to conduct grain-size analysis, corresponding to periods of storms and/or floods. Sediment grain-size was analyzed using a settling tube (sand fraction) and a Sedigraph 5100 (mud fraction).

4.2.4 Results

4.2.4.1 Forcing conditions during the experiment

4.2.4.1.1 River discharge

The Têt River water discharge was usually lower than 20 m^3 s^{-1} during the study period, although a flood occurred on 4 December 2003 with an average daily discharge of 235 m^3 s^{-1} (**Figure 4-8**). The flood, arbitrarily defined when the instantaneous water discharge was larger than 100 m^3 s^{-1}, lasted from 4 December at 00:00 to 5 December at 23:00. It reached the maximum (363 m^3 s^{-1}) on 4 December at 12:00.

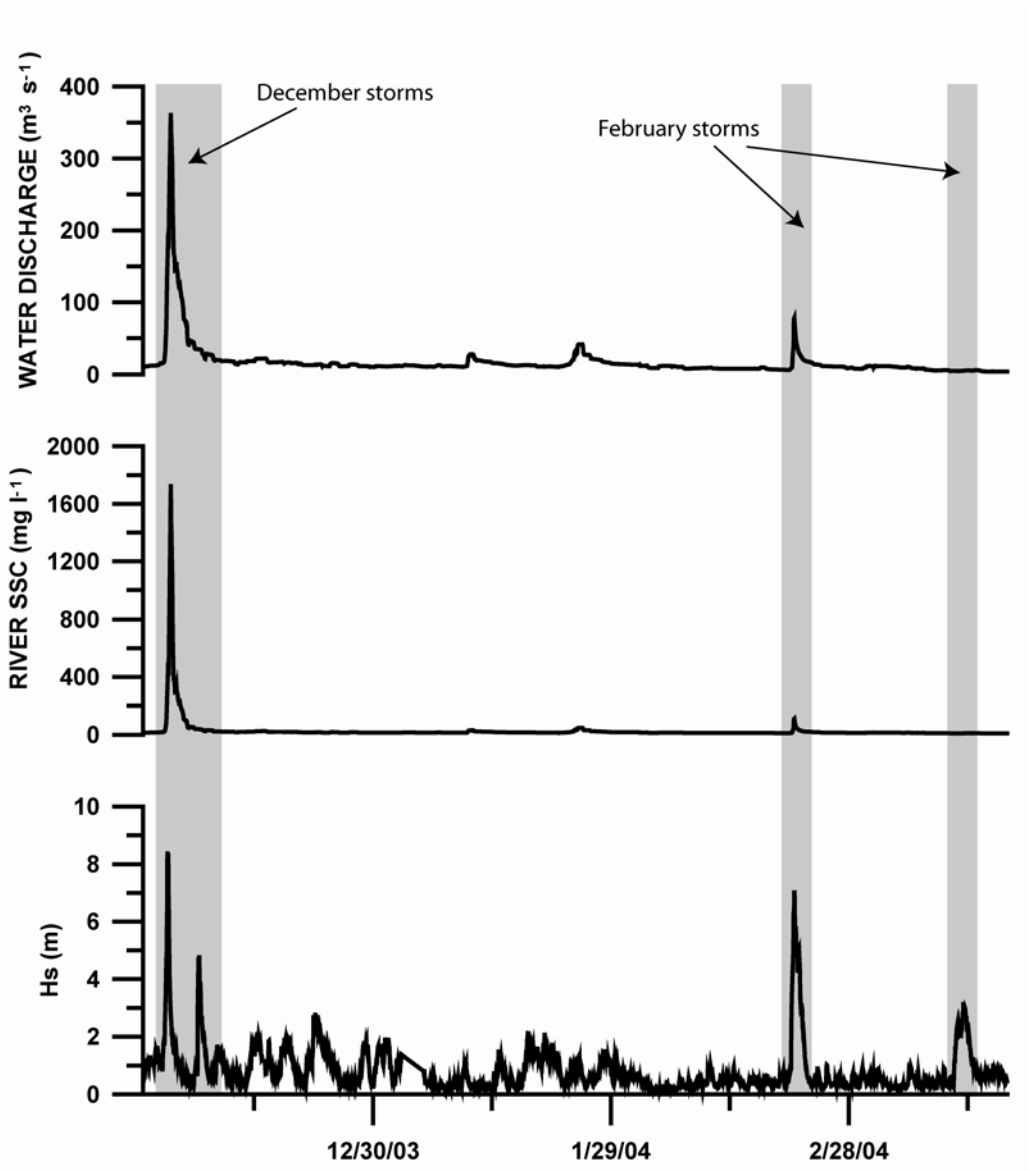

Figure 4-8 : Forcing conditions during the study period. Time series of a) Têt River water discharge, b) SSC on the river and c) wave height (Hs) at the study site.

The SSC in the river, calculated from the calibration equation (**Serrat et al., 2001**), ranged between 0.014 and 1.73 g l^{-1}. Based on these estimates, the amount of sediment supplied by the Têt River to the sea during the flood was about 2.15×10^4 t. The total sediment supplied over the study period (December 2003 to mid-March 2004) under non-flood conditions was about 3×10^3 t.

4.2.4.1.2 Waves and currents

There were two major eastern storm events (4 December 2003 and 21 February 2004) with Hs > 7 m, and two moderate easterly storm events (8 December 2003 and 12 March 2004), with Hs > 3 m (**Figure 4-8**). No major storms took place between 9 December 2003 and 20 February 2004. Near-bottom wave-orbital velocities at the study site were > 0.8 and 0.3 m s^{-1} during major and moderate storms respectively. Storm duration was arbitrarily defined when τ > 0.35 N m^{-2}. The four storm events generated a τ > 0.50 N m^{-2}, which theoretically could resuspend at least unconsolidated silt and fine sand fractions of the bottom sediment (**Figure 4-9 and Figure 4-10**).

Currents measured at 2 mab ranged between 0.02 m s^{-1} and more than 0.5 m s^{-1} during the peak of the storms (**Figure 4-9 and Figure 4-10**). The two major storms are identified clearly by the increase in current velocity (> 0.4 m s^{-1} in both storms). At least 10 events with a current speed > 0.2 m s^{-1} were observed. Typically, currents were directed towards the S–SE and became more intense after the peak of the storm.

4.2.4.2 Description of December storm events

4.2.4.2.1 The wet storm

On 4 December 2003 a storm event occurred together with a flood of the Têt River. The maximum near-bottom orbital velocity (u_b) during this event was 1.05 m s^{-1} and it was reached on 4 December at 02:00. SSC progressively increased in response to wave resuspension (**Figure 4-9**). A considerable increase in SSC at 0.15 mab was observed at the beginning of the storm (3 December at 17:00) with $\tau \sim 0.35$ N m^{-2}. SSC reached a maximum of about 2 g l^{-1} during the peak of the storm (τ = 8.7 N m^{-2}) (**Figure 4-9**). A second peak in SSC occurred between the storm peak and the flood maximum (4 December at 06:00). This

was caused by the advective transport of sediment from shallower areas towards the shelf, produced by currents directed towards the SE (**Figure 4-9**). Net seabed erosion of 4 cm was measured at the study site during the wet storm (**Figure 4-9**). Bottom erosion was progressive (17 h): it started on 3 December 2003 at 19:00 and finished on 4 December at 12:00, corresponding to $u_b > 0.25$ m s^{-1}. After the most energetic period of the storm, no changes to the seabed were observed for some hours (4 December 2003 at 12:00–17:00), until a 1-cm thick layer was deposited between 17:00 and 23:00 on the same day. The time series of u_b and river sediment discharge indicates that there was a lag (about 10 h) between the peak of the storm (02:00) and the peak of the river sediment discharge (4 December at 12:00) (**Figure 4-9**).

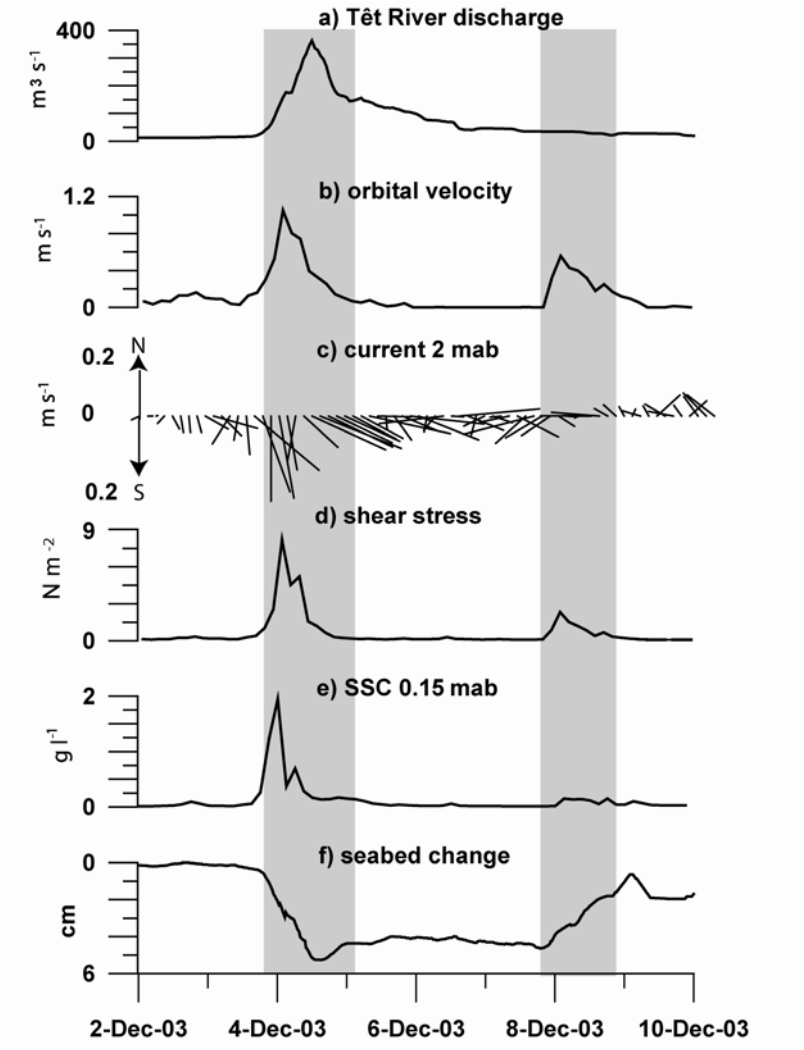

Figure 4-9 : Time series during the two storms of December 2003: a) Têt River water discharge, b) near-bottom orbital velocity, c) current speed and direction (2 mab), d) total shear stress, e) near-bottom SSC and f) seabed changes.

4.2.4.2.2 The moderate storm of December

A moderate, short-duration (18 h) storm, took place a few days after the wet storm. The storm started on 7 December 2003 at 23:00 and finished on 8 December at 17:00, reaching a maximum τ of 2.4 N m^{-2} on 8 December at 02:00 (**Figure 4-9**). Even though the total river sediment discharge was not important during this storm (< 180 t), a 4-cm thick seabed deposit was formed. Sediment deposition took place during and after the storm, beginning on 7 December at 23:00 and ending on 9 December at 04:00. Near-bottom current velocities < 0.17 m s^{-1} were directed towards the south, southeast and northwest during the sedimentation period, over which three peaks in SSC were identified (**Figure 4-9**).

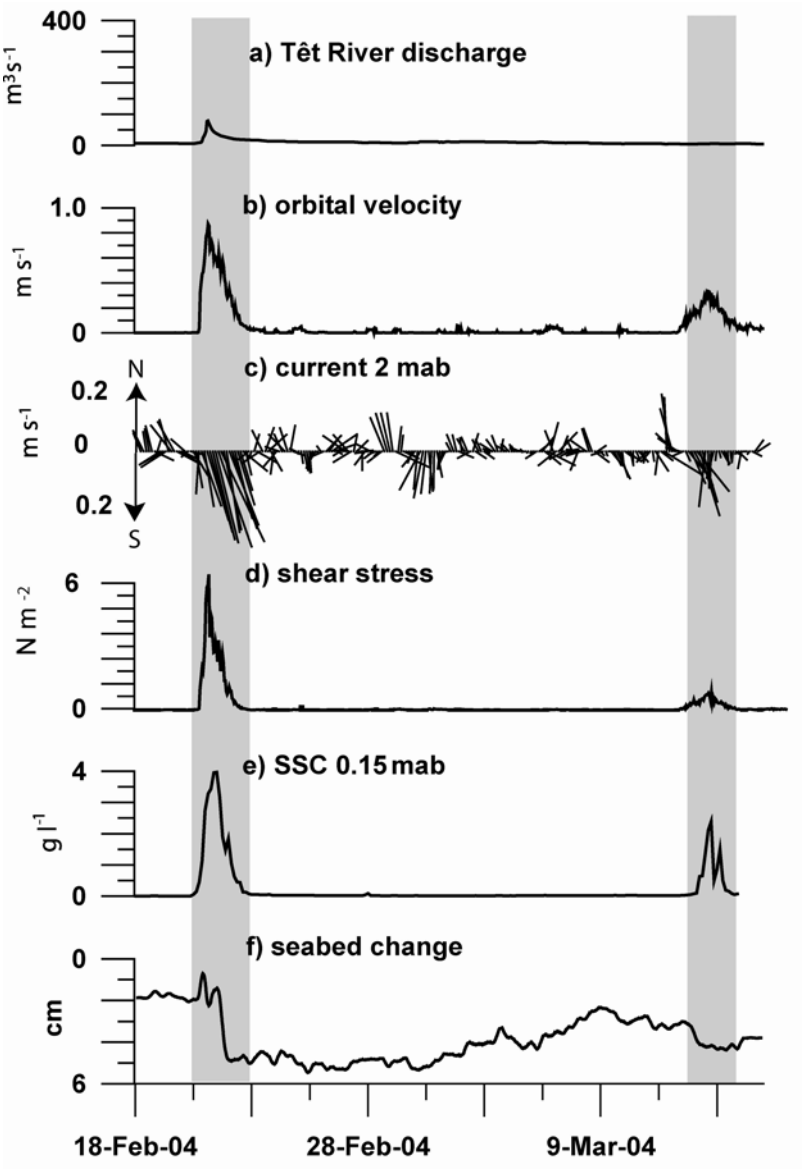

Figure 4-10 : Time series during the storms of February and March 2004: a) Têt River water discharge, b) near-bottom orbital velocity, c) current speed and direction (2 mab), d) total shear stress, e) near-bottom SSC and f) seabed changes.

A strong relation existed between SSC and orbital velocity at the beginning and during the peak of the storm, with maximum SSC values of about 0.15 g l−1 (**Figure 4-9**). A second SSC peak of equivalent magnitude was caused by sediment advection from shallower areas. Finally, a third SSC peak of lower intensity was observed at the end of the accumulation period, corresponding to an increase in current intensity directed towards the northwest.

4.2.4.2.3 Grain-size changes

Sediment cores taken before and after the December 2003 storms give additional information about sedimentary processes. The bottom sediment grain-size in both cores displayed a coarsening upward trend, with median sizes of about 20–30 μm at −20 cm from the bottom surface and 70–80 μm at the surface (**Figure 4-11**). The sediment deposition that occurred during the 8 December storm can be recognized in the core taken on 12 December 2003 by a 4–5 cm superficial layer of very fine sediment (D_{50} = 50 μm).

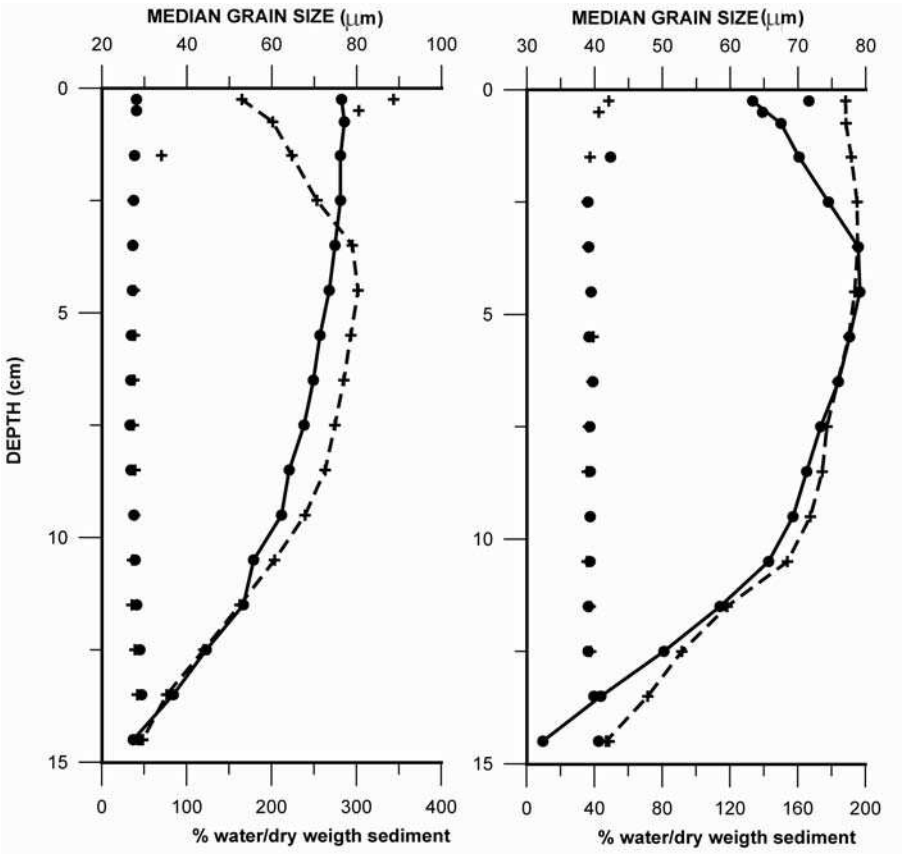

Figure 4-11 : Vertical sediment grain-size (lines) and water content distribution (dots) during the study period. Left: comparison between 26 November (circles) and 12 December 2003. Right: comparison between 11 February (circles) and 15 March 2004 (% w / d.w.: percentage of water over the dry weight of sediment).

This layer was enriched in water (320 % d.w.), suggesting the continental origin of this fresh sediment. This layer of fresh and fine sediment could be still recognized in the core taken on 11 February 2004, although the sediment was coarser (D_{50} = 65 μm).

The grain-size of the sediment collected in the sediment trap also showed major variations during this period (**Table 4-3**). The median grain-size of the sediment was quite similar during the storms on 4 and 8 December 2003 (32 μm), when most of the suspended sediment in the trap probably came from resuspension of the bottom sediment. However, sediment collected by the trap between the two storms increased the clay content from 18 to 33% of the total sediment and the grain-size was finer (D_{50} = 12 μm). This sediment must be mainly supplied by rivers.

Grain-size characteristics of the sediment collected in the trap

	Sediment collected	Sand	Silt	Clay	D50
	(g)	(%)	(%)	(%)	(μm)
3–4 Dec. 2003	74	27	55	18	32
5–6 Dec. 2003	12	22	45	33	12
7–8 Dec. 2003	37	22	59	19	32
20–22 Feb. 2004	95	14	61	24	14
23–25 Feb. 2004	5	3	44	53	3.6

Table 4-3 : Grain-size characteristics of the sediment collected in the trap

4.2.4.3 Description of February/March storm events

4.2.4.3.1 The dry storm

On 21 February 2004, a high-energy storm event occurred together with a slight increase in the Têt River water and sediment discharge (**Figure 4-10**). The sediment supplied from the river was 4.5×10^2 t during the 40 h of the storm duration ($\tau > 0.35$ N m^{-2}). The storm conditions remained between 20 February 2004 at 18:00 and 22 February 2004 at 11:00, with a maximum u_b of 0.87 m s^{-1} and an associated maximum τ of 6.2 N m^{-2} (21 February 2004 at 03:00) (**Figure 4-10**). Maximum near-bottom currents were about 0.4 m s^{-1} and directed towards the SE (160°) during the storm. At the beginning of the storm, the SSC increased quickly in response to wave activity. However, SSC at 0.15 mab reached a maximum of 4 g l^{-1} on 21 February 2004 at 12:00, about 9 h later than the peak of the storm, suggesting a

strong advective component of the suspended sediment (**Figure 4-10**). The result of the storm was net seabed erosion of 4 cm, although several short erosion/deposition events can be identified (**Figure 4-10**).

4.2.4.3.2 The moderate storm of March

A new storm occurred almost three weeks after the dry storm (**Figure 4-10**).Waves were moderate (the maximum u_b of about 0.33 m s^{-1} on 13 March 2004 at 15:00) and the duration of the storm was 39 h (from 12 March at 19:00 to 14 March at 10:00). Currents were oriented towards the north at the beginning of the storm and towards the SE after the peak of the storm, with a maximum current of 0.29 m s^{-1} measured on 14 March 2004 at 08:00. The Têt River sediment discharge was 22 t during this period. The SSC increases with the wave activity, reaching a peak of 2.5 g l^{-1} near to the maximum of the orbital velocity. A second peak in SSC (1.4 g l^{-1}) took place on 14 March at 03:00, due to sediment advection towards the SE. Changes in the sea bottom level were small, resulting in net erosion of 1 cm during the storm (**Figure 4-10**). The beginning of the storm (before the peak) caused an erosion of about 1.5 cm of sediment, whereas at the end of the storm there was deposition of about 0.5 cm.

4.2.4.3.3 Grain-size changes

The core taken on 15 March 2004 shows a vertical grain-size distribution equivalent to the pre-storm conditions because the finer sediment layer previously deposited was eroded during the February storm (**Figure 4-11**). The sediment trap collected 95 g of sediment during the 20 to 22 February 2004 storm period with a median grain-size of 14 μm. After the storm (from 23 to 25 February 2004), 5 g of sediment was retained in the bottle with D_{50} = 3.6 μm. (**Table 4-3**).

4.2.4.4 Near-bottom suspended sediment fluxes

The temporal evolution of near-bottom instantaneous suspended sediment fluxes on the Têt inner shelf is illustrated in **Figure 4-12**. The magnitude of fluxes at 0.15 mab ranged between 2×10^{-4} and 9.7×10^{2} kg m^{-2} h^{-1}, with the maximum instantaneous transport during the wet storm event (4 December 2003). Maximum instantaneous fluxes were progressively lower during the dry storm on 21 February 2004 (8.3×10^{2} kg m^{-2} h^{-1}) and the storm of 12 March

2004 (3.3×10^2 kg m^{-2} h^{-1}), and they were very small during the storm of 8 December 2003 (30 kg $m^{-}2$ h^{-1}). The cumulative transport of suspended sediment at 0.15 mab along and across the inner continental shelf shows that more than 90% of the transport during the study period occurred during the wet and dry storm events (**Figure 4-12**). Since isobaths on the shelf approximately follow a N–S direction (**Figure 4-7**), alongshelf and across-shelf components correspond to N–S and W–E directions respectively. In the wet storm event, the dominant transport was towards the south (13 t m^{-2}), with an important component towards the east (offshore) of about 3 t m^{-2}. The cumulative suspended sediment transport was higher during the dry storm and the alongshelf and across-shelf components were quite similar (16 and 15 t m^{-2} respectively).

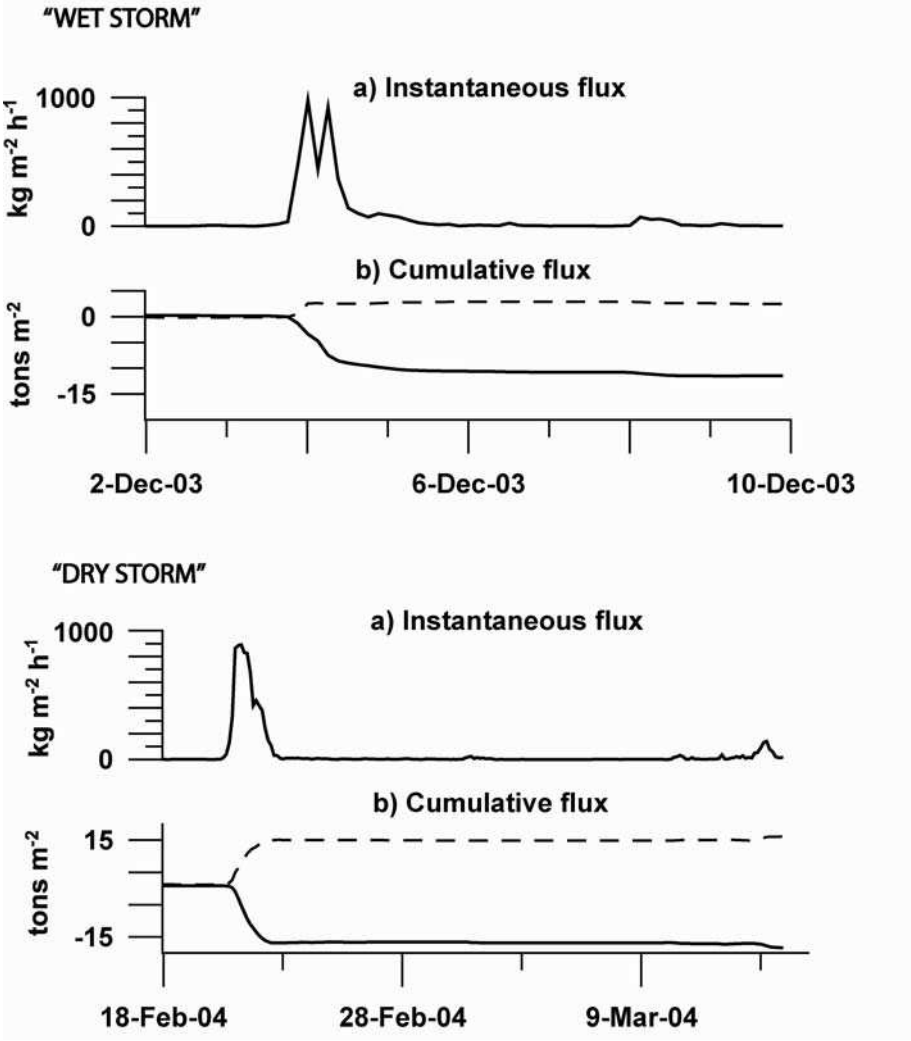

Figure 4-12 : Near-bottom sediment fluxes during storm events during the wet (above) and dry storms: a) instantaneous fluxes and b) cumulative along-shelf (continuous line) and across-shelf (dashed line) fluxes (positive towards North and East).

4.2.5 Discussion

The Têt River is a typical small Mediterranean river with episodic high water and sediment discharges that are usually induced by strong rainfall events. The magnitudes of the characteristic parameters of this system are smaller than those of other well-studied systems such as the Eel River (**Wheatcroft and Borgeld, 2000**). Comparing the Têt and Eel systems, the water discharge during floods (< 700 m^3 s^{-1} versus > 10,000 m^3 s^{-1} respectively), the flood duration (1–2 days versus > 5 days), the maximum river SSC (< 2 g l^{-1} versus > 10g l^{-1}) and even the storm duration (one day versus several days) are quite different. For these reasons, a distinctly different response between medium (e.g. Eel, Po, and Rhône) and small (e.g. Têt) systems should be expected.

The time series of near-bottom SSC on the Têt inner shelf displayed a similar evolution during the four storms (**Figure 4-9 and 4-4**): sediment resuspension began when $\tau > 0.35$ N m^{-2}, reaching a maximum close to the peak of the storm. Afterwards, wave shear stress decreased and a southeast current transported near-bottom suspended sediment seaward, generating a second minor peak in SSC. This pattern of SSC was independent of river inputs. From this perspective, there are no differences between dry and wet storms, and the behaviour of the Têt system is different from that of other shelves, where an increase in SSC and the formation of a flood deposit is frequently observed on the inner shelf (20–40 m water depth) (**Hill et al., 2000; Wheatcroft and Borgeld, 2000**). Moreover, strong storms caused about 4 cm of seabed erosion in both dry and wet storms on the Têt inner shelf. This is a large resuspension depth when compared with estimations on the Eel shelf (**Wiberg, 2000**) or observations on the Atchafalaya shelf (**Allison et al., 2000**). The main particularities of the Têt inner shelf for discussion are the formation of ephemeral layers, differences in suspended sediment dynamics during wet and dry storms, and the role of the inner shelf as a bypass area for the sediment.

4.2.5.1 Fluvial sediment delivery, accumulation and ephemeral layers

The amount of sediment introduced by the Têt River into the sea during the flood was about 2×10^4 t. This material, along with resuspended sediment from the nearshore and inner shelf areas, was transported offshore during the wet storm. Considering the bed erosion of 4 cm at the study site, and the fact that this erosion should be higher in shallower areas because of the more energetic action of waves, the sediment that bypassed the inner shelf and was

transported offshore should be mainly composed of resuspended sediment rather than fluvial inputs. After the wet storm, the Têt River maintained high sediment discharge for several hours. This sediment was mainly trapped in the nearshore zone near the river mouth favoured by slow currents and probably by aggregation of fine particles as observed in other areas (**Hill et al., 2000**). At the study site, there was a deposit < 1 cm accumulated at the end of the flood, which could be remobilized during the next storm. Therefore, one characteristic of the Têt system is that the riverine sediment is trapped in coastal areas. The shallow trapping of flood deposits seems to be typical of areas with low-intensity tidal currents such as the Atchafalaya (**Allison et al., 2000**) and Po (**Fox et al., 2004; Palinkas et al., 2005**) systems.

A 4-cm thick layer was deposited on the Têt inner shelf during a moderate storm that occurred four days after the flood. This storm was able to resuspend the unconsolidated and easily erodable sediment of the flood deposit located in the nearshore area and transport the sediment offshore to the inner shelf. The formation of this sedimentary deposit took place after the peak of the storm, when wave energy decayed and was unable to resuspend sediment at the study site. These observations on the Têt inner shelf suggest that some event strata identified as flood deposits on other continental shelves could, in fact, be storm deposits derived from previous, shallower flood deposits, or at least mixed deposits. Secondary flood deposits or "flood-associated" storm deposits have been identified on the central and outer shelf of the Eel system (**Fan et al., 2004**). In the Têt system, only the data from the altimeter deployed on the inner shelf enabled us to distinguish that the sediment that was deposited in December 2003, with typical characteristics of a fluvial origin, was in fact reworked sediment of a recent deposit formed four days earlier during the flood. The preservation of the flood deposit located in the nearshore area lasted only 4 days, which is the typical preservation period for inner shelf deposits on the Eel shelf (**Traykovski et al., 2000**). The preservation of the December storm deposit that is formed by sediment supplied during the flood was about two months, until a new energetic storm (the dry storm) occurred. Since most event deposits are defined on the basis of seasonal sampling strategies, but preservation periods could have a duration of days, flood-associated storm deposits may be prevalent in the inner shelf environment of other areas.

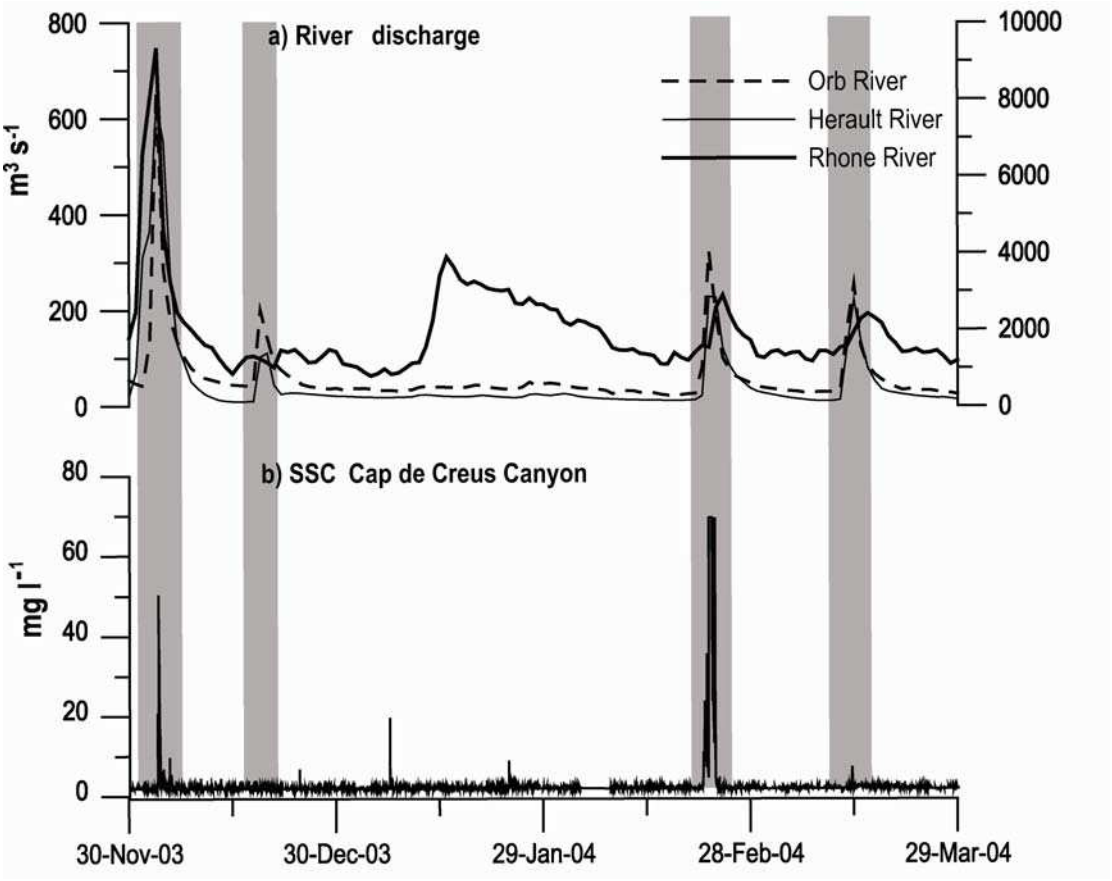

Figure 4-13 : a) Water discharge from other rivers discharging to the Gulf of Lions (water discharge of the Rhône River is scaled on the right axis) and b) SSC at the head of Cap Creus Canyon during the study period (modified from Palanques et al., 2006).

An intriguing topic in the study of sediment dynamics on the Têt inner shelf is the origin of sediment deposited after the flood. Can the sediment supplied by the Têt River during the tail of the flood (less than 1×10^4 t) and deposited on the nearshore area explain the 4-cm thick deposit observed at the study site? If the accumulated sediment was entirely formed by supplies from the Têt River, the event layer should be a small patch (about 0.09 km^2) around our study site. Although we do not have direct evidence, we believe that the sediment deposition event was a more general process, and consequently additional sources of fresh sediment were required. Rivers located northwards of the Têt River (in particular the Rhône River) also supplied large amounts of particulate matter to the gulf during the December storm (**Figure 4-13**). Satellite images suggest that the sediment supplied by the Gulf of Lions rivers can be trapped close to the coast by the general, cyclonic circulation that occurs during E–SE storms (**Figure 4-14**). Therefore, the SW part of the continental shelf received large inputs of sediment from other sources upstream. In this scenario, the formation and

characteristics of ephemeral deposits off the Têt River must be strongly dependent on sediment supplied by both the Têt and other rivers discharging into the Gulf of Lions. Consequently, the Têt system cannot be fully understood as an independent sedimentary system, but is also controlled by the general pattern of sediment dynamics around the Gulf of Lions.

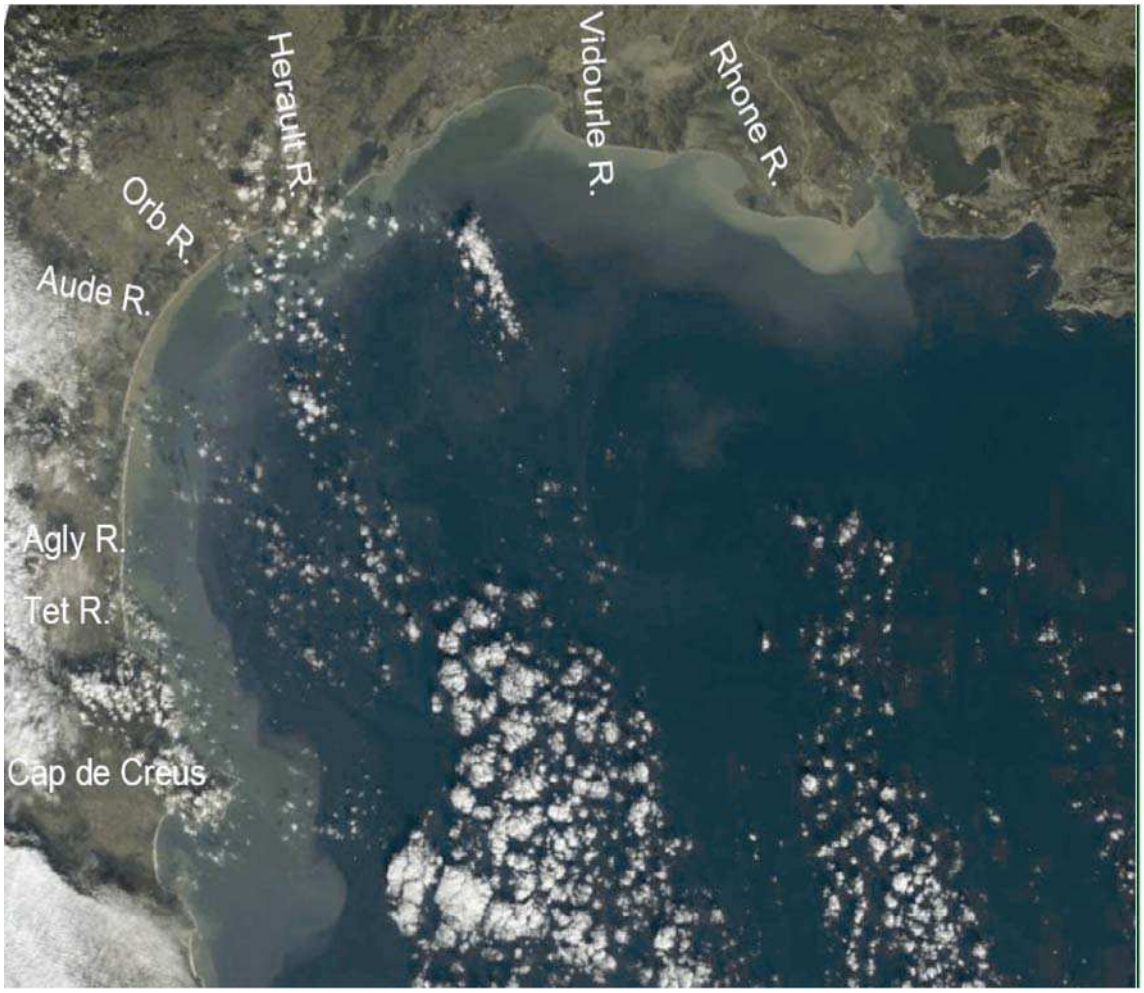

Figure 4-14 : MERIS image of the Gulf of Lions on December 8, 2003 showing across and alongshelf dispersion of the river plumes.

4.2.5.2 Influence of floods on suspended sediment concentration

River floods can modify the near-bottom SSC in two different ways (**Ogston et al., 2000; Fan et al., 2004**): a) enhancing the SSC associated with wave activity by incorporating river inputs in the suspension, and b) changing bed sediment characteristics and modifying the conditions for sediment resuspension and transport. On the Têt inner shelf the enhancement of

the SSC caused by the sediment delivered from rivers was not observed. Nevertheless, the flood-derived storm deposit observed on the Têt inner shelf had a strong influence on resuspension events because it represented a change in bottom sediment characteristics. At the study site, the median grain-size of the surficial (upper 1 cm) sediment before the wet storm was about 75 μm, whereas it was 55 μm at the beginning of the dry storm (**Figure 4-11**). In addition to the finer grain-size, the deposit was composed of fresh sediment with higher porosity and water content, and it was more easily erodable. Consequently, the near-bottom SSC was considerably higher during the dry storm than during the wet storm, although the bed wave shear stress was slightly lower.

Sediment dynamics at the study site were also different during the two moderate storms that occurred after the major events. A comparison between the December and March moderate events revealed that the deposition/erosion processes were the opposite during these two storms of equivalent energy because of differences in the previous events that occurred on the shelf. The first storm after the flood in December caused the deposition of a 4 cm thick layer, probably from the ephemeral deposit of sediment in very shallow water (<20 m depth). Conversely, the March storm caused a small erosion (1 cm) on the inner shelf because all the fine particles in shallow areas had already been winnowed by the preceding storm. Therefore, the "memory" of the past events on the shelf plays a crucial role in sediment dynamics and bed evolution, since the same storm can produce opposite results, depending on the sequence of previous flood and storm events. However, the influence of sediment delivered to the shelf during floods and the change in bottom characteristics are difficult to introduce in sediment transport models because the transport processes involved are not fully understood (**Cacchione et al., 1999; Harris and Wiberg, 2002**).

The chronology of events may also be relevant to the mode of seaward sediment transport on continental shelves, mainly associated with near-bottom sediment transport by advective currents and fluid muds. Fluid muds have recently been identified as a relevant process of sediment transport on the continental shelf, and are associated with very high (> 10 g l^{-1}) near-bottom SSC (**Traykovski et al., 2000**), usually in association with major floods and storms. No evidence of fluid mud has been found in the Têt inner shelf study, but some insights can be inferred from our observations. The maximum SSC on the inner shelf (about 4 g l^{-1} approximately at 0.1 mab after the tripod sunk) was measured during the dry storm, when a recently deposited storm/flood layer was resuspended. The wet storm, with equivalent

wave energy, reached lower values of SSC. Therefore, the best conditions for the occurrence of fluid muds on the Têt inner shelf seem to occur when a layer of unconsolidated fresh sediment recently supplied from the river is resuspended by a highly energetic storm.

4.2.5.3 From the river to the slope: the role of the inner shelf

Observations from the Têt inner shelf are a good example of the multi-event path of the sediment. It should be pointed out that, although the general circulation pattern in this area is mainly directed towards the south (along-shelf), the seawards component is quite relevant on the inner shelf during storm events and favours the escape of sediment towards deeper areas. For these reasons, sediment dynamics on the Têt inner shelf have strong implications for understanding the escape of sediment to deeper areas of the Gulf of Lions. The Cap de Creus canyon is located a few tens of kilometres towards the SE from the Têt River. Nearbottom SSC and currents were monitored simultaneously on the Têt inner shelf and within the Cap Creus canyon head (**Palanques et al., 2006**). Time series of near-bottom SSC at the head of the canyon showed two peaks of high SSC that correspond to the wet and dry storms described above (**Figure 4-13**). Other less energetic storms produced a negligible increase in SSC in the canyon. The SSC in the canyon was appreciably higher during the dry storm than during the wet storm, and these data are consistent with our observations on the inner shelf. Combining the information from the inner shelf and the head of the canyon, some comments on the escape of sediment from the inner shelf to the slope can be made. Firstly, a major escape of sediment from the inner shelf occurs during extreme storm events, and the proportion of sediment directly supplied by the Têt River (and other northern rivers of the Gulf of Lions) and reaching the slope during the flood is probably small, compared with the amount of sediment resuspended by waves and advected by currents. From this perspective, the inner shelf is a source of sediment for deeper regions. Secondly, moderate storms are not able to transport large amounts of sediment across the shelf towards the slope. However, they probably play a crucial role in the shallow shelf area, remobilizing the sediment from shallower areas and transporting it along and across the continental shelf. Here, suspended sediment particles settle on the seabed until they are remobilized by a more energetic storm or can be transported away by strong near-bottom flows, such as the ones caused by dense water cascading (**Palanques et al., 2006**).

The Têt inner shelf largely acts as a bypass area in this multi-event transport of sediment from the Têt River (as well as other fluvial sedimentary inputs coming from the north of the Gulf of Lions) towards the slope, although it can retain sediment during short periods of time (days–months). This inner shelf underwent a number of erosion and deposition events but without an appreciable net change in the seabed level during the study period. In the Têt system, the first step of the sequence of events is the flood deposit on the nearshore, followed by transport to the inner shelf by moderate storms. This is likely to be the case when small rivers discharge sediment to the ocean during floods.

In a medium- or long-term perspective, the Têt system falls into the category of a low-concentration regime because the discharge of fluvial sediment is low and the dominant processes on the inner shelf are typical of a low-concentration regime. Additionally, the vertical coarsening upwards sequence of the sediment on the inner shelf suggests a strong winnowing of the finer sediment affecting the superficial layer (**Figure 4-11**). In a short-term perspective, the behaviour of the sediment on the inner shelf during wet and dry storms has characteristics of low-concentration and high-concentration regimes respectively. These apparently contradictory definitions are due to the fact that the concept of dry and wet storms does not take into account the previous sequence of events, whereas the definition of high- and low-concentration regimes does. In practice, none of the typical characteristics defined for a wet storm (**Sommerfield et al., submitted**) were observed on the Têt inner shelf during the wet storm: enhanced near-bottom SSC, a higher second peak of SSC associated with advection processes, more favourable conditions for fluid mud development and formation of flood deposits on the inner shelf. However, some of these characteristics were observed during the successive dry storms. This is due to the small amounts of sediment supplied by the Têt River in comparison with the systems in which dry and wet storms were defined (**Ogston et al., 2000; Sommerfield et al., submitted**). In larger river systems, riverine inputs during floods are always dominant over the storm, whereas storms dominate in small rivers like the Têt. This dominance of storms over floods also has implications for the application of the term “oceanic flood” (**Wheatcroft, 2000**) to very small rivers, because river inputs can only be the main factor during catastrophic floods or when the flood occurs alone and does not correspond to a wet storm.

4.2.6 Summary

Time series collected on the Têt inner shelf during the winter of 2003–2004 support several conclusions.

- The seabed at 28-m water depth experiences erosion and deposition events of up to 4 cm thickness during eastern storm events. Major storms always produce erosional events, whereas moderate storms can produce erosion or accretion depending on the availability of sediment in shallower areas.

- Sediment supplied from the Têt River (and probably from other rivers of the Gulf of Lions) was deposited in the nearshore area after the wet storm. A few days later, this sediment was remobilized by a moderate storm and deposited on the inner shelf as a secondary flood deposit.

- Most near-bottom suspended sediment transport on the inner shelf occurred during major storm events. Sediment fluxes were directed towards the south (along-shelf) and east (seawards). Maximum SSCs (and sediment fluxes) occurred during the dry storm due to the presence of the secondary flood layer that favoured sediment resuspension and transport. Observations at the head of the Cap de Creus Canyon (**Palanques et al., 2006**) were consistent with sediment dynamics observed on the inner shelf.

- In the Têt River system, the discharge of fluvial sediment is low and storms are the dominant process on the inner shelf; consequently, wet storms display different characteristics to those defined for larger systems. In small river systems, some of the typical characteristics of a wet storm (higher near-bottom SSC and a higher second peak in SSC related to suspended sediment flux by currents from shallower areas) may be better recognizable in dry storms, depending on the previous sequence of events.

Acknowledgements

This study was supported by the EUROSTRATAFORM Project funded by the EU (EVK3-CT-2002– 00079), within EU Fifth Framework Programme: Energy, Environment and

Sustainable Development. We thank the officers and crew of the R/V “Nereis” for their help during surveys.

References

Allison, M.A., Kineke, G.C., Gordon, E.S., Goñi, M.A., 2000. Development and reworking of a seasonal flood deposit on the inner continental shelf off the Atchafalaya River. Cont. Shelf Res.

20, 2267–2294.

Aloïsi, J.C., Got, H., Monaco, A., 1973. Carte géologique du précontinent languedocien au 1/250000ième. International Institute for Aerial Survey and Earth Sciences (I.T.C.) (Eds.), Netherlands.

Bentley, S.J., Nittrouer, C.A., 2003. Emplacement, modification, and preservation of event strata on a flood-dominated continental shelf: Eel shelf, Northern California. Cont. Shelf Res. 23, 1465–1493.

Buscail, R., Pocklington, R., Daumas, R., Guidi, L., 1990. Fluxes and budget of organic matter in the benthic boundary layer over the northwestern Mediterranean margin. Cont. Shelf Res. 10, 1089–1122.

Buscail, R., Pocklington, R., Germain, C., 1995. Seasonal variability of the organic matter in a sedimentary coastal environment: sources, degradation and accumulation (continental shelf of the Gulf of Lions — NW Mediterranean Sea). Cont. Shelf Res. 15, 843–869.

Cacchione, D.A., Wiberg, P.L., Lynch, J.F., Irish, J.D., Traykovski, P., 1999. Estimates of suspended-sediment flux and bedform activity on the inner portion of the Eel continental shelf. Mar. Geol. 154, 83–98.

Courp, T., Monaco, A., 1990. Sediment dispersal and accumulation on the continental margin of the Gulf of Lions: sedimentary budget. Cont. Shelf Res. 10, 1063–1088.

Crockett, J.S., Nittrouer, C.A., 2004. The sandy inner shelf as a repository for muddy sediment: an example from northern California. Cont. Shelf Res. 24, 55–73.

Estournel, C., Marsaleix, P., Auclair, F., Julliand, C., Vehil, R., 2003. Observations and modelisation of the winter coastal oceanic circulation in the Gulf of Lions under wind

conditions influenced by the continental orography (FETCH experiment). J. Geophys. Res. 108 (C3), 8059.

Fan, S., Swift, D.J.P., Traykovski, P., Bentley, S., Borgeld, J., Reed, C.W., Niedoroda, A.W., 2004. River flooding, storm resuspension, and event stratigraphy on the northern California shelf: observations compared with simulations. Mar. Geol. 210, 17–41.

Ferré, B., Guizien, K., Durrieu de Madron, X., Palanques, A., Guillén, J., Grémare, A., 2005. Fine-grained sediment dynamics during a strong storm event in the inner-shelf of the Gulf of Lion (NW Mediterranean). Cont. Shelf Res. 25, 2410–2427.

Fox, J.M., Hill, P.S., Milligan, T.G., Boldrin, A., 2004. Flocculation and sedimentation on the Po River delta. Mar. Geol. 203, 95–107.

Geyer, W.R., Hill, P.S., Milligan, T.G., Traykovski, P., 2000. The structure of the Eel River plume during floods. Cont. Shelf Res. 20, 2067–2093.

Grant, W.D., Madsen, O.S., 1986. The continental shelf bottom boundary layer. Annu. Rev. Fluid Mech. 18, 265–305.

Guidi-Guilvard, L., Buscail, R., 1995. Seasonal survey of metazoan meiofauna and surface sediment organics in a non-tidal turbulent sublittoral prodelta (northwestern Mediterranean). Cont. Shelf Res. 15, 633–653.

Guillén, J., Jiménez, J., Palanques, A., Gracia, V., Puig, P., Sánchez- Arcilla, A., 2002. Sediment resuspension across a microtidal, low energy inner shelf. Cont. Shelf Res. 22, 305–325.

Harris, C.K., Wiberg, P., 2002. Across-shelf sediment transport; interactions between suspended sediment and bed sediment. J. Geophys. Res. 107 (C1), 12.

Hill, P.S., Milligan, T.G., Geyer, W.R., 2000. Controls on effective settling velocity of suspended sediment in the Eel River flood plume. Cont. Shelf Res. 20, 2095–2111.

Madsen, O.S., 1993. Sediment transport on the shelf. Lecture Notes. Ralph M. Parsons Laboratory for Water Resources and Hydrodynamics, Department of Civil Engineering, Massachusetts Institute of Technology, Cambridge, USA. 147 pp.

Mullenbach, B.L., Nittrouer, C.A., 2000. Rapid deposition of fluvial sediment in the Eel Canyon, northern California. Cont. Shelf Res. 20, 2191–2212.

Nittrouer, C.A., 1999. STRATAFORM: overview of its design and synthesis of its results. Mar. Geol. 154, 3–12.

Nittrouer, C.A., DeMaster, D.J. (Eds.), 1987. Sedimentary Processes on the Amazon Continental Shelf. Pergamon Press, Oxford. 379 pp.

Ogston, A.S., Cacchione, D.A., Sternberg, R.W., Kineke, G.C., 2000. Observations of storm and river flood-driven sediment transport on the northern California continental shelf. Cont. Shelf Res. 20, 2141–2162.

Ogston, A.S., Guerra, J.V., Sternberg, R.W., 2004. Interannual variability of near-bed sediment flux on the Eel River shelf, northern California. Cont. Shelf Res. 24, 117–136.

Palanques, A., Puig, P., Guillén, J., Jiménez, J., Gracia, V., Sánchez- Arcilla, A., Madsen, O., 2002. Near-bottom suspended sediment fluxes on the microtidal low-energy Ebro continental shelf (NW Mediterranean). Cont. Shelf Res. 22, 285–303.

Palanques, A., Durrieu de Madron, X., Puig, P., Fabres, J., Guillén, J., Calafat, A., Canals, M., Bonnin, J., 2006. Suspended sediment fluxes and transport processes in the Gulf of Lions submarine canyons. The role of storms and dense water cascading. Mar. Geol. 234, 43–61. doi:10.1016/j.margeo.2006.09.002.

Palinkas, C.M., Nittrouer, C.A., Wheatcroft, R.A., Langone, L., 2005. The use of 7Be to identify event and seasonal sedimentation near the Po River delta, Adriatic Sea. Mar. Geol. 222–223, 95–112.

Puig, P., Palanques, A., Guillén, J., 2001. Near-bottom suspended sediment variability caused by storms and near-inertial waves on the Ebro mid continental shelf (NW Mediterranean). Mar. Geol. 178, 81–93.

Puig, P., Ogston, A.S., Mullenbach, B.L., Nittrouer, C.A., Sternberg, R.W., 2003. Shelf-to-canyon sediment-transport processes on the Eel continental margin (northern California). Mar. Geol. 193, 129–149.

Roussiez, V., Aloïsi, J.C., Monaco, A., Ludwig, W., 2005. Early muddy deposits along the Gulf of Lions shoreline: a key for a better understanding of land-to-sea transfer of sediments and associated pollutant fluxes. Mar. Geol. 222–223, 345–358.

Serrat, P., Ludwig, W., Navarro, B., Blazi, J.-L., 2001. Variabilité spatio-temporelle des flux de matières en suspension d'un fleuve côtier méditerranéen : la Têt (France). C. R. Acad. Sci., Paris 333, 389–397.

Sommerfield, C.K., Ogston, A.S., Mullenbach, B.L., Drake, D.E., Alexander, C.R., Nittrouer, C.A., Borgeld, J.C., Wheatcroft, R.A., Leithold, E.L., submitted for publication. Chapter 4: Oceanic dispersal and accumulation of river sediment. In: Nittrouer et. al. (Eds.), STRATAFORM Master Volume Textbook, Blackwell Publishing, Continental-Margin Sedimentation: Transport to Sequence.

Traykovski, P., Geyer, W.R., Irish, J.D., Lynch, J.F., 2000. The role of wave-induced density-driven fluid mud flows for cross-shelf transport on the Eel continental shelf. Cont. Shelf Res. 20, 2113–2140.

Trincardi, F., Syvitski, J.P.M. (Eds.), 2005. Mediterranean Prodelta Systems. Mar. Geol., vol. 222–223, pp. 1–514.

Wheatcroft, R.A., 2000. Oceanic flood sedimentation: a new perspective. Cont. Shelf Res. 20, 2059–2066.

Wheatcroft, R.A., Borgeld, J.C., 2000. Oceanic flood deposits on the northern California shelf: large-scale distribution and small-scale physical properties. Cont. Shelf Res. 20, 2163–2190.

Wheatcroft, R.A., Drake, D.E., 2003. Post-depositional alteration and preservation of sedimentary event layers on continental margins, I. The role of episodic sedimentation. Mar. Geol. 199, 123–137.

Wiberg, P., 2000. A perfect Storm: formation and potential for preservation of storm beds on the continental shelf. Oceanography 13 (3), 93–99.

Wiberg, P.L., Harris, C.K., 1994. Ripples geometry in wave-dominated environments. J. Geophys. Res. 99, 775–789.

Wright, L.D., Coleman, C.H., 1974. Mississippi river mouth processes-effluent dynamics and morphologic development. J. Geol. 82 (6), 751–778.

4.3 Une crue océanique dans une mer sans marée dominée par les vagues : cas de la Têt dans le golfe du Lion (Nord-ouest de la Méditerranée, France)

An oceanic flood in a microtidal, storm dominated basin: the Têt, Gulf of Lions (NW Mediterranean, France)

Bourrin, F.[a]	Redaction, Data (CTD, suface SSCs)
Friend, P.L.[b1]	Redaction, Data (river water samples)
Amos, C.L.[b]	Redaction, Data (ADCP survey, bathymetry)
Durrieu de Madron, X.[a]	Manuscript revision
Thompson, C.E.L.[b]	Data and field logistic
Manca, E.[b]	Data (Gao and Collins sediment transport trends)
Ulses, C.[c]	Modelisation

[a] Centre de Formation et de Recherche sur l'Environnement Marin, Université de Perpignan, 52 Avenue de Villeneuve, 66860, Perpignan cedex, France

[b] School of Ocean and Earth Science, National Oceanography Centre Southampton, European Way, Southampton SO14 3ZH, UK

[1] Present address: Maersk Oil, Esplanaden 50, 1263 Copenhagen K, Denmark

[c] Pole d'Océanographie Côtière de l'Observatoire Midi-Pyrénées - Laboratoire d'Aérologie 14 Avenue Edouard Belin - 31400 Toulouse, France

Soumis le 09/05/2007

Continental Shelf Research

Gulf of Lions Special Issue

Abstract

This paper describes the first integrated study of an oceanic flood event in the Mediterranean Sea. An oceanic flood with a 5-year return interval occurred in the Têt River basin and adjacent inner-shelf in the Gulf of Lions, northwest Mediterranean, during April 2004. Data were collected during this flood as part of event-response investigations of the EU-funded Eurostrataform (European Margin Strata Formation) project. Southeasterly storm winds led to a flash-flood which directly modified the inner-shelf hydrodynamics. Sediment delivery to the coastal zone during this flood represented more than half of the mean annual discharge of the Têt River to the Gulf of Lions. This river transported a large amount of sand in suspension and as bedload, 34% and 12% respectively during this event. Sand introduced in the nearshore was transported northwards during the peak storm and nourished a well-developed delta. Fine sediments were separated from coarse sediments at the mouth, and were advected southwards and seawards by the counter-clockwise general circulation. Fine-grained sediments were transported via a hypopycnal plume along the coast towards the southern tip of the Gulf of Lions and the Cap Creus canyon. The along-shore currents, which intensified from north to south between the Cap Creus promontory and the Cap Creus canyon, favored the transfer of fine-grained sediments across the continental shelf of the Gulf of Lions towards the continental slope. Oceanic floods with a few-year return interval in small coastal rivers can play a significant role in the transport of sediments on continental margins and their export from the shelf through canyons.

Keywords

Oceanic flood, sediment transport, hypopycnal river plume, Têt River, Gulf of Lions, northwest Mediterranean.

4.3.1 Introduction

River floods are important processes in the land-to-sea transfer of sediment and associated contaminants (e.g. metals and pathogens). River floods can be classified into two different types: seasonal floods and flash-floods. Seasonal floods are generally associated with large systems such as the Amazon, South America, and the Huanghe (Yellow River, China) rivers,

and are characterised by seasonal increase in river discharge caused by prolonged snow melting or monsoon conditions. Occurring during several weeks or months, meteorological conditions that have caused these floods are not directly linked with conditions at the coast. By contrast, flash-floods are brief and violent events occurring during a few hours or days, and provoked under brief meteorological conditions. Flash-floods are common in the Mediterranean Sea, and are associated with small mountainous catchments influenced by brief meteorological marine storm events during which depressions over the sea induce rapid and extreme rain-fall over coastal relief. The result is a sudden river discharge of fresh water and sediment to the coastal zone. In this case, hydrological conditions in the inner-shelf are closely linked with local meteorological conditions. These floods affecting small coastal rivers under marine storm conditions are commonly named oceanic floods (**Wheatcroft, 2000**).

Oceanic floods occur over short time periods on small rivers, with the key aspect that the receiving-ocean basin is under the influence of the storm that leads to the flooding (**Wheatcroft, 2000**). Due to the event-driven nature of the discharge in small rivers, most sediment reaching the ocean usually does so during oceanic floods. As the annual load per basin area of small rivers is greater than that of moderate to large size rivers, it is particularly important for global sediment flux studies to investigate oceanic floods in which steep basin topography can give rise to a high potential sediment discharge (**Milliman and Syvitski, 1992**). Sediment delivered to the ocean during such floods may be stored transitionally in prodeltas or mid-shelf mud belts, or bypass these reaching the slope/canyon region and thence the abyssal plain. Globally, small rivers are estimated to account for around half the annual suspended sediment load to the sea (**Milliman and Syvitski, 1992**). River sediment fluxes are sensitive to reservoir construction, land clearance, land use change, soil and water conservation measures and climate change (**Walling and Fang, 2003**). Oceanic floods, due to their short duration and spatial scales, require novel sampling and modeling strategies (**Wheatcroft, 2000**).

Oceanic floods have been investigated in various small mountainous systems. Some studies have focused on the dynamics and the fate of sudden river inputs to the coastal zone (**Hill et al., 2000; Palinkas et al., 2005; Wheatcroft and Borgeld, 2000**). Others studies have focused on the river system (runoff, fresh water and solid fluxes) during flash-floods (**Gaume**

et al., 2004; Winston and Criss, 2002). Few studies have investigated both the processes in the river catchment and in the adjacent coastal zone. In this paper, an oceanic flood event (with a 5-year river flood return interval) in the Gulf of Lions, northwest Mediterranean, is described in terms of the water and sediment fluxes to the continental shelf edge; the sediment dynamics and the main conditions leading to these fluxes are described. The aim of the study is to quantify the contribution of oceanic floods with a relatively short return interval to land-ocean sediment fluxes. The contribution to the sediment fluxes in terms of bed load, suspended load or wash load is examined. In particular, the sediment flux across the prodelta under enhanced river discharge conditions is examined, as well as the sediment flux manifested at the shoreface/inner shelf, and the links between the shoreface/inner shelf and canyon heads. A source-to-sink approach is followed through the investigation of: (1) rainfall intensity and watershed localization; (2) coarse and fine-grained sediment transport by the river; (3) dispersal and deposition of both coarse and fine-grained sediment in the nearshore; and (4) dispersal of fine-grained sediment through the continental margin to the shelf edge and the canyons.

4.3.2 Regional settings

4.3.2.1 General circulation and waves

The coastal circulation in the western part of the Gulf of Lions is highly variable and dependant upon wind conditions. The main winds are the northwesterly “Tramontane” and the southeasterly “Marin”, which causes the extreme rainfall events. The coastal current induced by the prevailing northwesterly wind generally flows from north to south-southeast along the Roussillon coast (**Millot, 1976**). Circulation shifts are observed at the transition between northwesterly and southeasterly wind conditions. The southeasterly winds also induce coastal currents flowing from north to south, intensified in the Cap Creus zone where the shelf narrows (**Ulses, 2005**).

Waves are the main stirring mechanism causing bottom sediment resuspension in the western Mediterranean because tidal currents are negligible. Major storms are associated with waves coming from the east and southeast. Usually, large waves with significant wave height (Hs) >6 m and period (Ts) >12 s occur during autumn and winter. These are able to resuspend

sediment on the inner and middle shelf (**Ferré et al., 2005; Guillén, 2002; Palanques et al., 2002; Puig et al., 2001**). From analysis of long term meteorological observations and wave data series at Sète and Cap Bear (1949-1997), the biggest storms occur in the northern part of the Gulf of Lions, with most of the extreme events taking place during the last decade (1997, 1999, and 2003). Relatively, these storms have the same characteristics: Hs of 7 m and maximum wave height of 11 m; Ts of 10 to 12s generated by SE winds of up to 30 m s^{-1}, associated with a storm surge of up to 1 m in the harbours; and an estimated return interval of up to 20 years (**Durand, 1999**).

4.3.2.2 Freshwater inputs

The Têt River discharges into the southwestern part of the Gulf of Lions (**Figure 4-15 a**). The Têt catchment (1396 km^2) has a mean altitude of 1023 m, and a mean slope of 12.4° (**Ludwig et al., 2004**). Its maximum headwater elevation is at 2100 m and the river length is about 100 km (**Garcia-Esteves et al., 2007**). The Têt River basin can thus be considered as a small mountainous river (**Milliman and Syvitski, 1992**). Precipitation for the entire basin range is ~757 mm yr^{-1} (average over the 1980–2000 period); the rainfall pattern is characterised by long dry periods interrupted by short, violent oceanic events that can result, within a few hours, in oceanic floods. The average liquid discharge at the gauging station of Perpignan, 10 km upstream of the mouth, is 10.82 m^3 s^{-1}. Instantaneous discharge can reach 1,800 m^3 s^{-1} during major floods associated with extreme rainfall events (**Serrat et al., 2001**). Extreme oceanic floods (mean daily liquid discharge of up to 540 m^3 s^{-1}) have a 5-year return interval, whilst relatively smaller flood events (mean daily liquid discharge of 180 m^3 s^{-1}) have a return interval of 2 years. In order to reduce the intensity of peak floods, a retention dam was built in 1978 at Vinça, ~50 km upstream of the mouth, on the border between the mountainous part and the alluvial plain of the Têt River catchment.

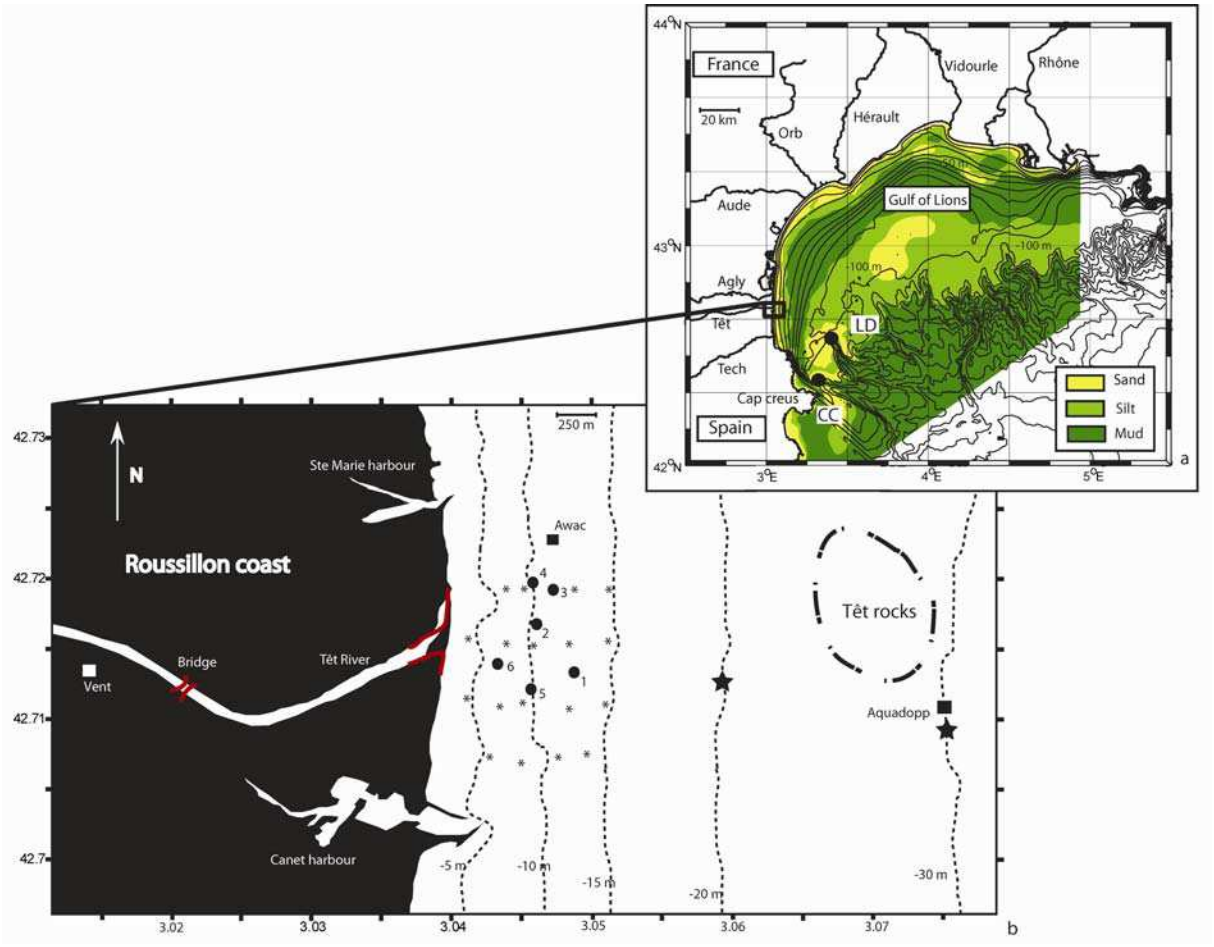

Figure 4-15 : Morpho-sedimentary map of the Gulf of Lions, NW Mediterranean, France, (redrawn from Aloïsi et al., 1973) indicating the location of the mooring lines in the Cap Creus (CC) and Lacaze-Duthiers (LD) canyons (a), and detailed map of the Têt River inner-shelf studied area along the Roussillon coast (b). The bridge water sampling site and the post-flood mouth configuration are shown in red. The black square represents the location of the AWAC and Aquadopp instruments deployed at 11 and 30 m water depth (42°43.23'N 3°02.89'E and 42°42.64'N et 3°04.86'E). Black circles represent the location of the CTD profiles; black asterisks represent the location of the grab samples in the near-shore; and black stars the location of the two 20 cm long cores at 20 and 30 m water depths.

4.3.2.3 Sediment input and prodelta deposits

Oceanic floods occur mainly during the autumn, at which time most of the total annual suspended load is transported to the Gulf of Lions: 78% of the total sediment flux between 1980 and 1999 occurred in only 50 days (0.7% of the total time). The mean annual suspended sediment discharge (1978 to 2004) is ~61 (± 18) x 10^3 t (**Bourrin et al., 2006**). The maximum suspended sediment concentration (47 g L^{-1}) was recorded during a catastrophic flood event in the 1940's (**Serrat et al., 2001**). An ephemeral fluid mud deposit, composed of silts and

clays, has often been observed on the inner-shelf in front of the Têt River mouth around 30 m depth after flood events (**Buscail et al., 1990; Buscail et al., 1995; Courp and Monaco, 1990; Guidi-Guilvard and Buscail, 1995**). This thin deposit forms the prodelta of the Têt River. The short residence time and/or the weak preservation of this deposit are mainly due to resuspension by waves and currents during high energetic events (**Guillén et al., 2006**).

4.3.2.4 Shelf sedimentation and export to canyons

The Gulf of Lions margin presents a sandy shoreline and a silty inner-shelf to about 50 m water depth (**Aloïsi et al., 1973**). Then a shore-parallel mid-shelf mud-belt develops between 50 and 80 m water depth and its thickness reflects the predominance of northeastern solid inputs of the Rhône River over the coastal rivers of the western Gulf of Lions (**Figure 4-15 a**). During generalised flooding periods of the Gulf of Lions rivers, fine-grained dispersal of sediment by hypopycnal plumes is influenced by the general along-shore circulation on the shelf, and preferential export occurs in the southwestern canyons (**Palanques et al., 2006; Ulses et al., 2007**).

4.3.3 Material and Methods

4.3.3.1 Meteorological measurements

The wind field was measured every 5 minutes with an ultrasonic wind sensor (Vaisala WAS425) installed on the roof of the waste station of Canet-en-Roussillon (Vent station, 42°42.82'N 03°00.70'E), at 6 m above the ground (**Figure 4-15 b**). Statistical parameters of the wind field (mean and maximum hourly speed and direction) were extracted from high frequency measurements. Rainfall was measured daily in 49 meteorological stations by the French National Meteorological Society (Météo France), covering the watershed of the Têt River. Mean rainfall over the catchment area was estimated from a biharmonic spline interpolation (**Sandwell, 1987**) of mean daily precipitation measured in the 49 meteorological stations over the entire surface basin area (**Figure 4-16**).

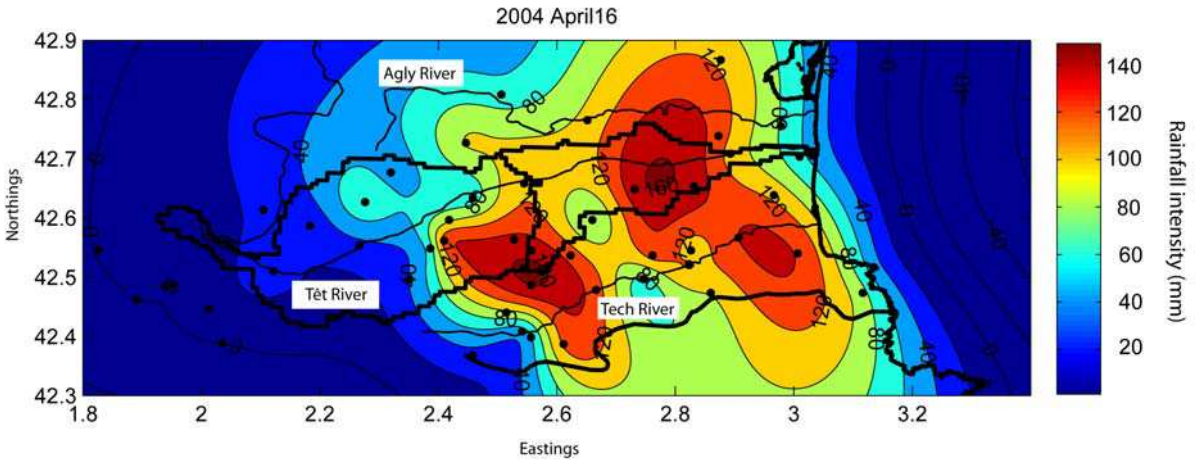

Figure 4-16: Rainfall intensity over the entire Têt River catchment on 16th April 2004. Black circles represent the 49 meteorological stations (Météo France) used for the biharmonic spline interpolation of mean daily rainfall data (Sandwell, 1987).

4.3.3.2 River measurements

Hourly water discharge of the Têt River was measured at the Perpignan gauging station (station Y0474040 in the national data bank, "Hydro"), 10 km upstream from the river mouth (42°42.21'N 02°53.58'E). Surface water samples were collected at 6-hourly intervals from 16-20 April 2004 with a bucket (~5 L) from a bridge ~2 km from the river mouth (see **Figure 4-15 b**). Surface water velocity was estimated at the same time by measuring the elapsed time of displacement of natural debris over a known distance. River surface height was measured simultaneously at the same bridge with a limnimetric scale (DDE Pyrénées Orientales). Water samples were filtered in the laboratories of the National Oceanography Centre Southampton, UK, using 2 µm Whatman GF standard filter paper. The mass of sediment retained was determined after drying at 100ºC for 12 hours, and the result used to derive the total suspended solids (TSS) concentration. Hourly water discharges, together with TSS concentrations, were used to derive TSS river fluxes. Sands and organic flocs >63µm were separated from silts and clays by gentle wet-sieving through a 63 µm sieve. The organics floc fraction was determined by weighing after heating for 12 hours at 450 ºC. Each of the remaining fractions was analysed for settling velocity and grain size using a settling column (sands) and a Coulter™ laser sizer (silts and clays).

4.3.3.3 Nearshore measurements

4.3.3.3.1 Seabed

Twenty sea bed samples were collected by van Veen grab on 18th April 2004 from the delta top and front areas (5-15 m depth), and 18 swash zone samples were collected from the beaches to the north and south of the river mouth (**Figure 4-15 b**). Sand and silt fractions were separated by gentle wet-sieving using a 63 μm sieve, and then analysed for settling velocity and grain size using a settling column and a Coulter™ laser sizer. Grain size trend analysis (**Gao, 1996; Gao and Collins, 1992**) was applied to the delta top and front samples. A 200 kHz single beam Lowrance echo-sounder survey was conducted on the inner shelf at 3-10 m water depths in the river mouth area on 18th April 2004 06:30-09:00 UT, and used to derive a detailed bathymetric map of the coastal zone. 2 sediment cores were also collected by SCUBA divers using transparent Perspex tubes (20 cm length, 4 cm diameter); at 20 and 30 m water depth the 28th April 2004. Grain-size analyses were performed on samples, sonicated for 5 min in MilliQ-filtered water, using a Malvern Mastersizer 2000 particle size analyser equipped with a sample dispersion unit.

4.3.3.3.2 Water column

A 600 kHz hull-mounted (RDI) ADCP survey was conducted on the inner shelf at 3-10 m water depths in front of the river mouth on 18th April 2004, 06:30-09:00 UT, at the same time as the bathymetric survey, in order to monitor the spatial structure of the river plume. CTD profiles of temperature, conductivity, turbidity and chlorophyll were made using an autonomous YSI 6600 EDS probe (1 Hz sampling rate) during the ADCP survey (**Figure 4-15 b**). Data were cleaned for pressure reversal and averaged in 0.5 dbar bins. Salinity was derived from conductivity and temperature probe measurements according to algorithms found in **Standard Methods for the Examination of Water and Wastewater (1989)**. Turbidity, acquired initially in NTU, was converted to TSS concentration, using gravimetric measurements of TSS from surface water samples collected within the turbid plume. In situ grain-size measurements were performed simultaneously with a sequoia LISST-100 type B (1.25-250 μm range). An upward-looking ADP AWAC (Nortek) equipped with a wave gauge was deployed near the survey area (**Figure 4-15 b**) at 11 m water depth (42°43.23'N, 3°02.89'E). Wave and current parameters were logged for 5 minutes every 30 minutes. A downward looking Aquadopp Profiler 600 kHz (Nortek) was installed on a buoy moored at

30 m water depth, 1.5 n.m. from the river mouth (42°42.59'N 03°04.78'E) to measure water column currents from the surface, every 5 minutes.

The Sediview program (**Land and Bray, 2000**) was used to derive TSS concentrations from the average backscatter signal of the RDI ADCP using an iterative method to solve a simplified version of the sonar equation (**Urick, 1975**):

$Log_{10}Mr = S [Ks + dB + 2r (\alpha_w + \alpha_s)]$

where Mr is the mass concentration per unit volume at range r, S is the relative backscatter coefficient, Ks is the site and instrument dependant factor, dB is the measured relative backscatter intensity corrected for spherical spreading, α_w is the water attenuation coefficient computed using observed temperature and salinity near the transducer, and α_s is the sediment attenuation coefficient estimated from the measured depth-averaged median grain size of the suspended particles from the LISST instrument. The calibration constants S and Ks are determined by fitting the ADCP measured backscatter intensities with the optical turbidity measurements of the YSI multiparameter probe at the same time. The efficiency of the calibration between acoustically- and optically-derived TSS was relatively good ($r^2 = 0.98$, n = 83) with fitted coefficient Ks = 41.5 and S = 33.

4.3.3.4 Shelf and canyon head measurements

The first satellite picture available after the passage of the low-pressure system over the studied area was taken the 26th April 2004 from the MERIS sensor of ENVISAT satellite. The spectral band of total suspended concentration was extracted from the satellite data and used to observe the dispersal of turbid river plumes in the southwestern Gulf of Lions.

Shelf-slope suspended sediment transport was monitored by deploying an Aanderaa RCM11 current meter equipped with a turbidimeter (OBS) on 2 moorings, 4 m above bottom, at 300 m water depths in the head of the Cap de Creus (CC) and Lacaze-Duthiers (LD) submarine canyons at the southern end of the Gulf, in April 2004 (**Palanques et al., 2006; Figure 4-15 a)**. The sampling interval of the current meter was 20 minutes. The turbidity signal, initially acquired in NTU, was converted in TSS following the relationship used in **Guillén et al. (2000)**.

4.3.4 Results

4.3.4.1 Meteorological and oceanic conditions

In April 2004, an anti-cyclonic depression over the NW Mediterranean, with southeasterly winds (**Figure 4-17 a**) and high rainfall, induced a major flood event in the Têt River (5-year return interval) with a maximum hourly liquid discharge of 683 m^3 s^{-1} on 16th April at 23:00 (**Figure 4-17 b**). Mean precipitation over the total catchment area was evaluated to be 80 mm and locally exceeded 160 mm, corresponding to 1/10 of the total annual precipitation. Precipitation was concentrated over the lower part of the basin area (**Figure 4-16**). The depression generated waves in the host sea of up to Hs = 5 m and Ts = 9 s (2-year return interval, **Figure 4-17 c**). Such waves are capable of resuspending bottom sediments to a depth of around 30 m (**Guillén et al., 2006**).

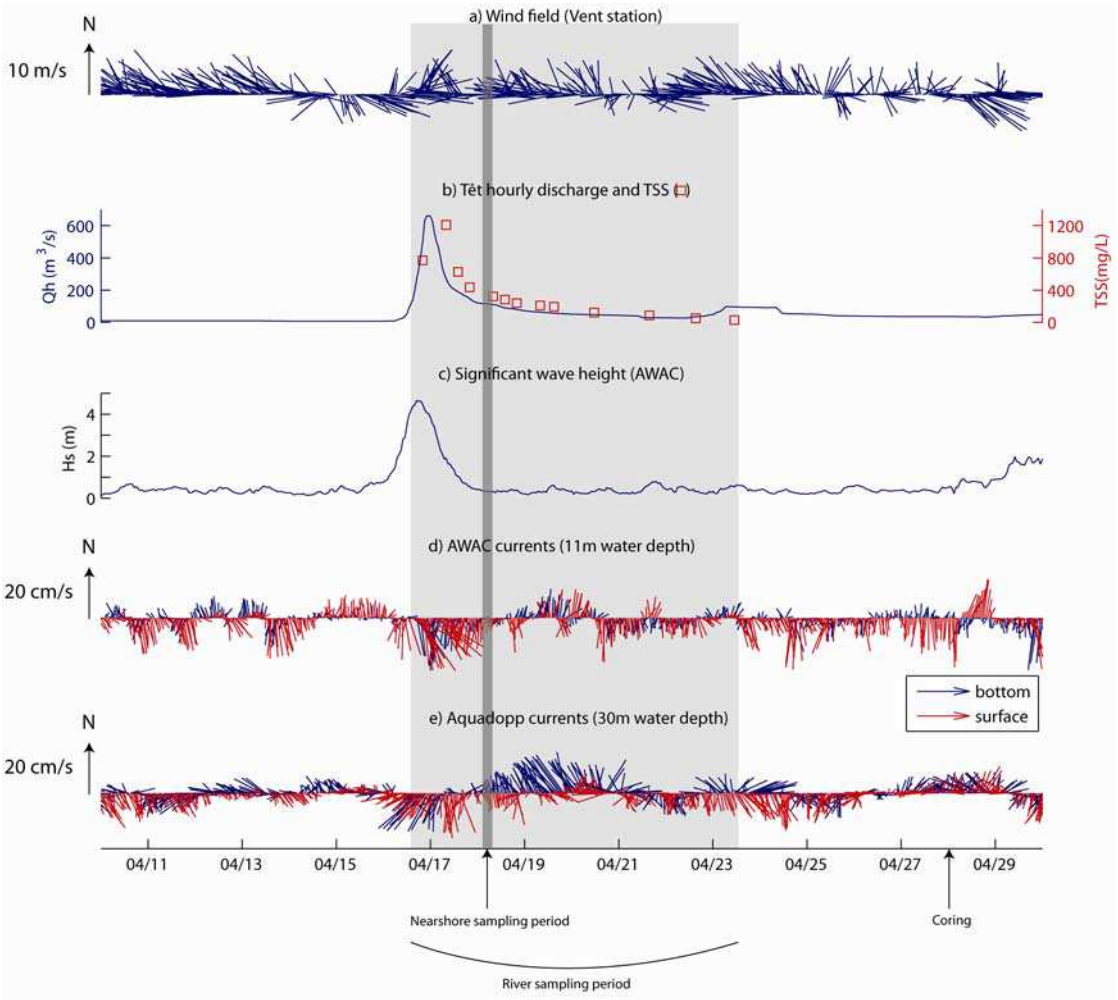

Figure 4-17: Time series of wind field at the Vent station (a), Têt River hourly discharge (Qh) and TSS concentrations (b), significant wave height (Hs) (c), bottom (in blue) and surface (in red) current stick plots at AWAC station (d) and the Aquadopp station (e). By convention, wind sticks represent the

direction from which the wind is blowing, and current sticks the direction in which the current is flowing. The river sampling and nearshore sampling periods are indicated by the shaded areas.

4.3.4.2 River sediment fluxes

4.3.4.2.1 Suspended sediment transport

The maximum TSS concentration of the surface river water was 1.2 g L-1, measured on 17th April at 08:00, i.e. after the peak liquid discharge (**Figure 4-17 b**). TSS concentrations decreased as the river flow and water level decreased (**Figure 4-17 b and Figure 4-18**). Using instantaneous measurements of TSS concentrations and corresponding water discharge, the total suspended solid load reaching the sea during this flood was estimated to ~34 x 10^3 t. Rating curves developed from long-term measurements of TSS concentrations and instantaneous river discharge give a slightly higher value of 35.5 x 10^3 t (**Bourrin et al., 2006**).

Figure 4-18 illustrates the temporal variation in concentration of silts (<63 μm), sands (>63 μm) and organic flocs (>63 μm) in the surface river water, as well as the surface current speed (m s^{-1}) and water level (m). The concentration of silts in suspension reached 1.08 g L^{-1} during peak discharge, and decreased as the surface water speed and water level decreased. Sand in suspension at the river surface (~0.15 g L^{-1}) was found during the peak river discharge, reaching about 10% of the total load, decreasing with the surface flow speed. Organic flocs were also present (5% at the river peak discharge, ~0.02 g L^{-1}). During the peak of the flood, the TSS comprised 85% silt, 10% sand and 5% organic flocs. After the flood peak, TSS composition was 80% silt and 20% sand. Maximum river flow speed of 1.93 m s^{-1} and water level of 2.14 m were measured the 17th April 2004, 8:00 after the flood peak (16th April, 23:00). At the end of the flood, flow speed and water level reached 1.04 m s^{-1} and 0.6 m respectively.

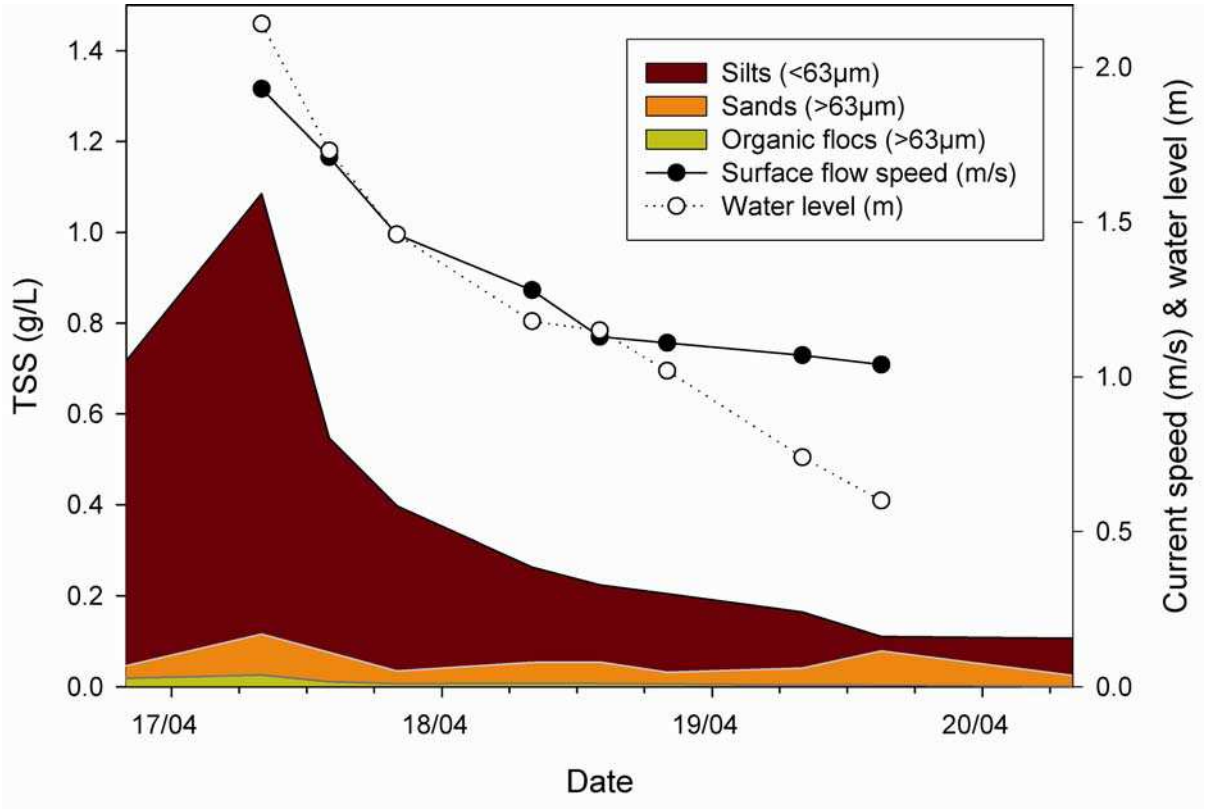

Figure 4-18: Concentration of surface suspended sediment by size fraction, surface current speed and water level in the Têt River, during the oceanic flood event of April 2004.

4.3.4.2.2 Sand transport

The Rouse equation, defining the vertical distribution of concentration c, in an open channel flow (**Rouse, 1937**) was used to estimate suspended sand transport in the Têt River during the April 2004 flood event (**Figure 4-19**):

$$\frac{c}{c_a} = \frac{(h-y)}{y} \cdot \left(\frac{a}{(h-a)} \right)^Z$$

where c_a is a reference concentration at a height a, above the bed; with a = y/h where h is the total water depth, and y is the height above the bed; $Z = w_s/(ku_*)$ is the Rouse number, w_s is the measured particle settling velocity, k = 0.4 is the von Karman constant, and u_* is the shear velocity estimated from log-law velocity profile.

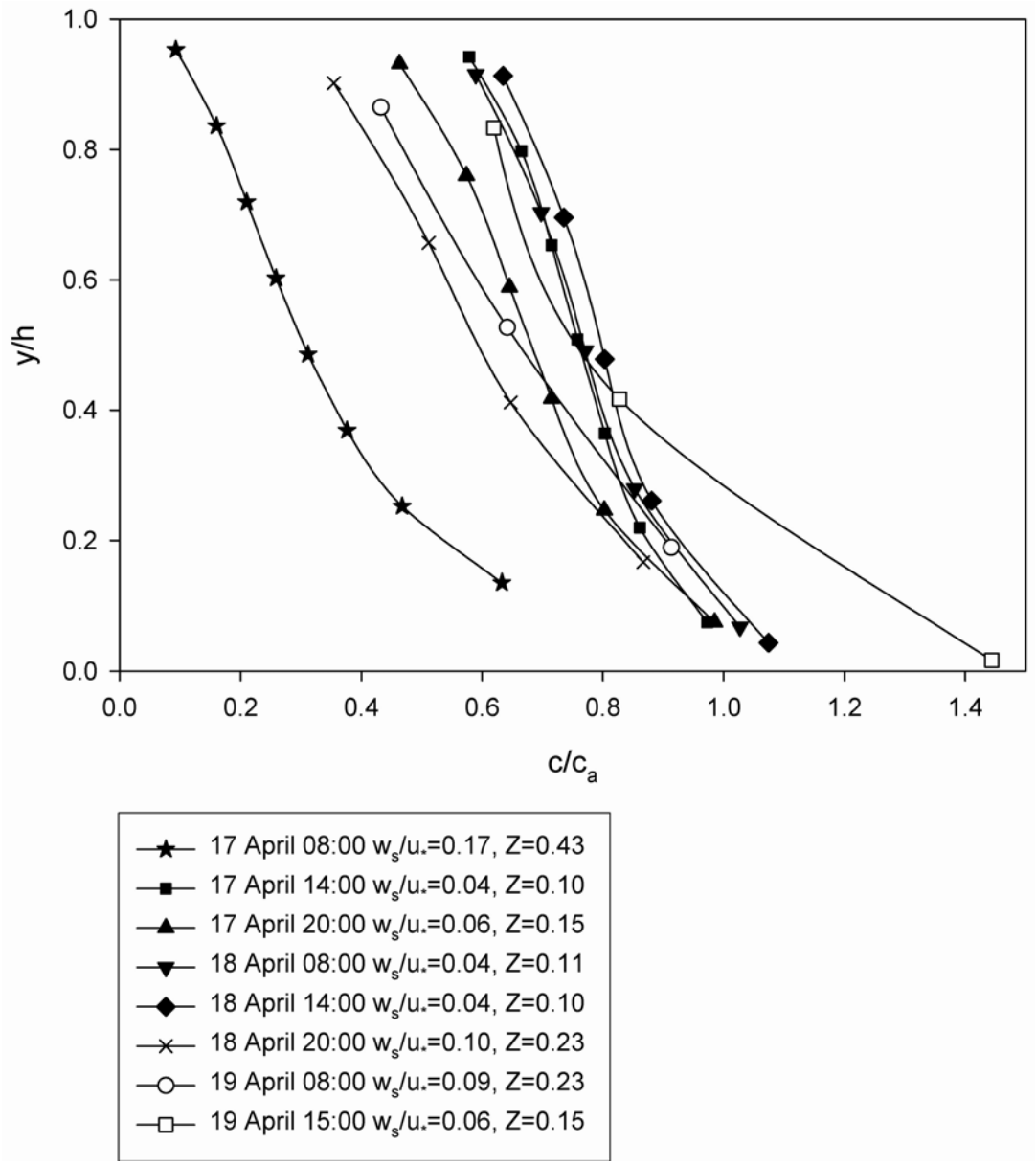

Figure 4-19: Rouse profiles derived from river surface water samples and velocity measurements during the Têt oceanic flood of April 2004. y is the height above the bed, h the total water depth, c the concentration at depth y and c_a the concentration at reference depth a (a=y/h) above the bed, w_s the measured settling velocity of suspended particles, and u_* the shear velocity.

Depth-integrated concentrations of sand during this event were derived from Rouse profiles, and the product of this and the instantaneous river discharge yields the total suspended load of sand. By this method it was estimated that ~11.4 x 10^3 t of sand were discharged in suspension to the coastal zone, representing ~34% of the total suspended load during this flood. SEDTRANS96 model (**Li, 2001**), was used to estimate the river bedload transport following the algorithm of **Yalin (1963)**. The model prediction gives a value of ~4 x 10^3 t of

sand discharged as bedload to the coastal area, which represents ~12% of the total suspended solid discharge during this oceanic flood event.

4.3.4.3 Near shore hydrology

Current profiles measured with the AWAC in 11 m water depth and with the Aquadopp in 30 m water depth (**Figure 4-17 d and Figure 4-17 e**), show a similar directional pattern through the water column in the study area, but of differing intensity. Surface and bottom currents were usually orientated towards the south at both sites, except during short-term southeasterly wind events, when currents veered towards the north. Before the storm event, currents associated with southeasterly winds were orientated towards the north (until the 16th April 2004, 03:00). During the flood, currents were orientated towards the south and the wind blew from the north (until the 19th April 2004, 05:00). After the event, currents were once again orientated towards the north.

The surface current reached a maximum speed (0.73 and 0.57 m s^{-1} at the 11 and 30 m water depth measurement sites, respectively) during the storm peak (16th April 2004, 18:00) when the northerly winds were well established. Bottom currents also reached a maximum (0.43 and 0.30 m s^{-1} at the 11 and 30 m water depth measurement sites, respectively) during the peak of the storm. Sedimentary material resuspended by near-bed orbital currents during the storm would thus be advected mainly towards the southeast by bottom currents. The maximum wave orbital velocity reached 1.9 m s^{-1} (corresponding to Hs = 5 m, **Figure 4-17 c**) at the storm peak, and could therefore resuspend sands of at least medium size (160 μm at the AWAC site).

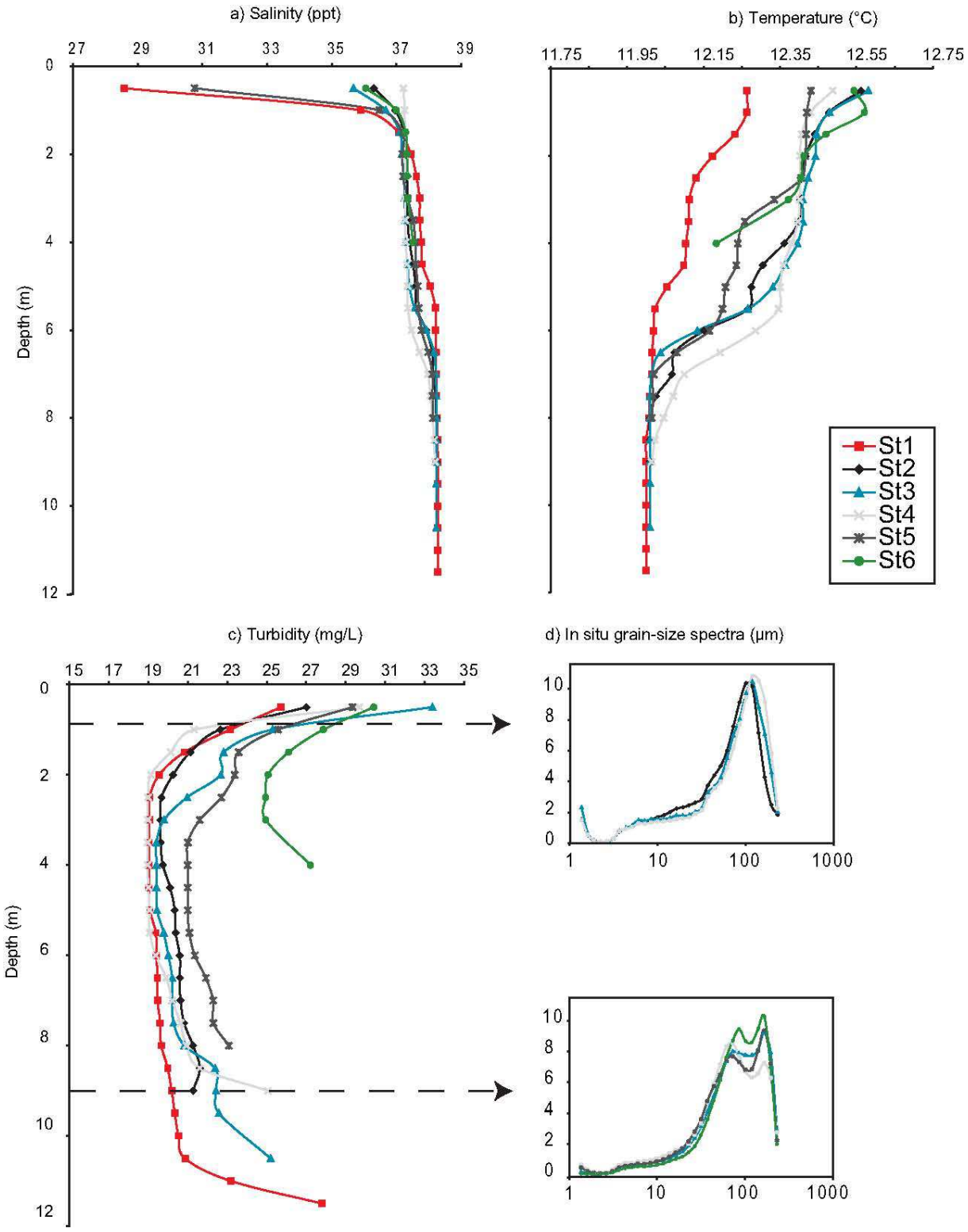

Figure 4-20: CTD profiles (6 stations) measured on 18th April 2004 06:30-09:00 UT, in the vicinity of the Têt River mouth. Parameters measured are (a) salinity in ppt, (b) temperature in °C, and (c) turbidity in mg L^{-1}. In situ grain-size spectra measured with the LISST are indicated for the surface and bottom layers (d).

CTD profiles monitored at different locations in front of the river mouth (**Figure 4-15b**) were used to characterise the structure of the water column during the sampling period (18th April 2004, 06:00-09:30). A surface layer about 2 m thick, was identified with low salinity (~29-31 ppt, **Figure 4-20a**), and relatively high temperature (~12.4 °C, **Figure 4-20b**). Below this surface layer, the water column appeared to be weakly stratified to the bottom.

4.3.4.4 Fine-grained dispersal in the nearshore

In the nearshore, high turbidity values (~30 mg L^{-1}, **Figure 4-20c**) and chlorophyll content (~12 µg L^{-1}, not shown) were measured with the CTD probe in the surface layer. In addition, a bottom layer, also about 2 m thick, was observed with high TSS concentrations (~20 mg L^{-1}) and low chlorophyll values (~6 µg L^{-1}). In situ grain-size measurements with the LISST (**Figure 4-20d**) show that the surface layer contained mainly flocs of ~110 µm diameter. The bottom layer was composed of a broad range of discrete and composite particles with sizes between 80 and 160 µm.

The ADCP survey took place the 18th April, after the peak flood during a period of northwesterly winds and southward currents. Turbidity maps were derived from interpolation of TSS concentrations estimated from ADCP backscatter measurements (**Figure 4-21**). At ~2 m below the surface, (**Figure 4-21a**) the dispersion towards the southeast of the turbid river plume near the mouth can be seen. Maximum turbidity reached ~40 mg L^{-1} at the river mouth and close to the harbour entrance. At 5 mab which is the mid-water column depth (**Figure 4-21b**), no turbidity maximum was present, whereas at ~2m above the bottom (**Figure 4-21c**), turbidity maxima were seen at the river mouth (~30 mg L^{-1}) and at the harbour entrance (~20 mg L^{-1}). Bottom turbidity remained relatively high in the entire area surveyed. Currents were orientated mainly towards the south at all depths during the survey, veering from the southeast at the surface to the south at the bottom. Current intensities decrease from 11 cm s^{-1} at the surface to 6 cm s^{-1} at the bottom during the survey (**Figure 4-21**).

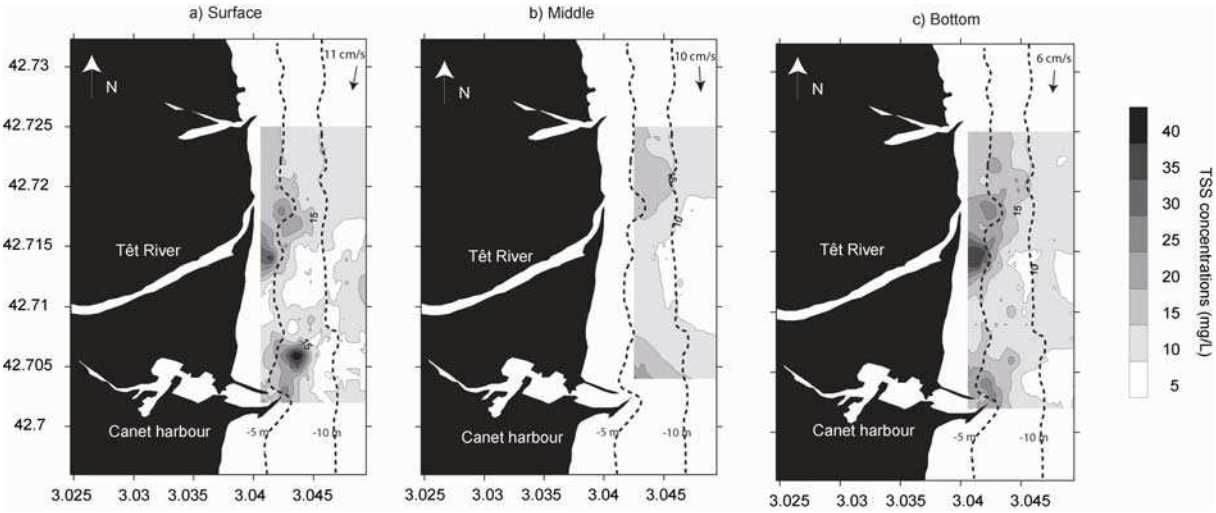

Figure 4-21: TSS repartition at several depths (surface, a; mid-water depth, b; and bottom, c) in the vicinity of the Têt River mouth on 18th April 2004 06:30-09:00 UT. TSS concentrations are derived from treatment of the backscattered intensities measured by the mounted ADCP. Current trend vectors and corresponding intensities are also indicated in the top-right corner of each figure.

4.3.4.5 Seabed imprint

The sand grain size distributions were mainly unimodal. Delta and shore sands were of fine or medium grain size; the river bed sand had a variable mean grain size from fine to coarse. Sands from the north beach were coarser than those from the south. Sands were generally very well- to well-sorted, with sorting improving with distance from the mouth for both the northern and southern beaches. The Gao and Collins (**Gao, 1996; Gao and Collins, 1992**) trend analysis indicated that sand transport was generally in a northerly direction (**Figure 4-22**). By contrast, the mud content of bottom sediment (3-10 m water depth) indicates that the fall out of suspended matter from the surface plume is greatest south of the river mouth. Thus there is a divergence in size population of sediment at the river mouth. Two additional sediment cores sampled at 20 and 30 m water depths show the presence of a superficial (~2 cm) flood layer composed of fluffy material only at 20 m water depth.

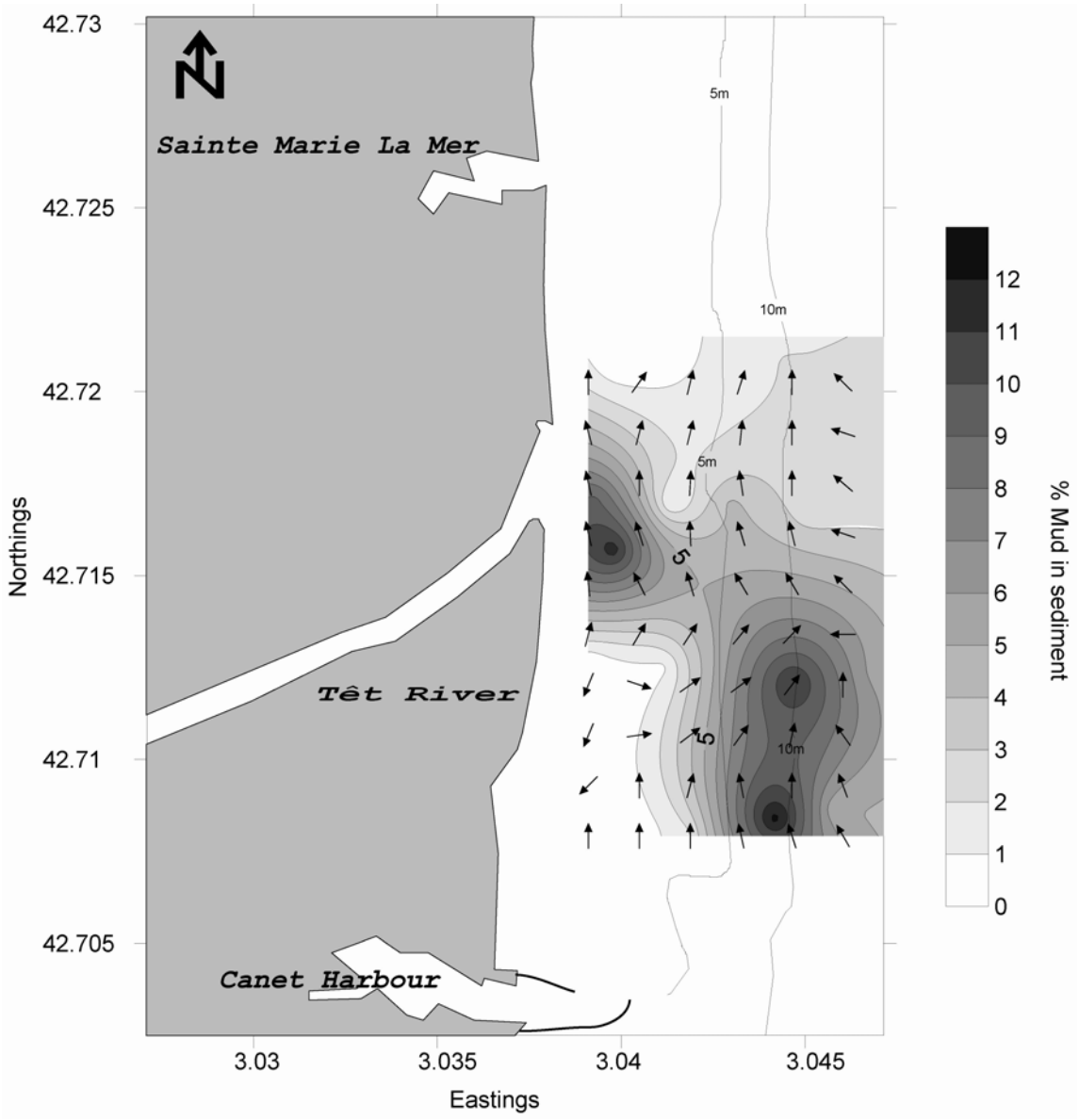

Figure 4-22: Black arrows represent residual sand transport vectors from Gao & Collins model. The size of the vectors is a measure of how probable that trend is. The residual sand transport vectors are characterised by a unitary length. Iso-lines of mud content (<63 µm fraction) in surface sediment are also illustrated in the vicinity of the Têt River mouth.

4.3.4.6 Canyon response to the event

The marine storm of April 2004 induced major floods both on the Têt and Tech rivers, and a minor flood on the Agly River further north (onset of flood discharge on the Têt, Qh >100 m^3 s^{-1}, 16th April 12:00, with flood peak on 16th April 23:00, Qh=683 m^3 s^{-1}, **Figure 4-23b**). Precipitation was concentrated in the southern catchments of the Roussillon coast (**Figure 4-16**).

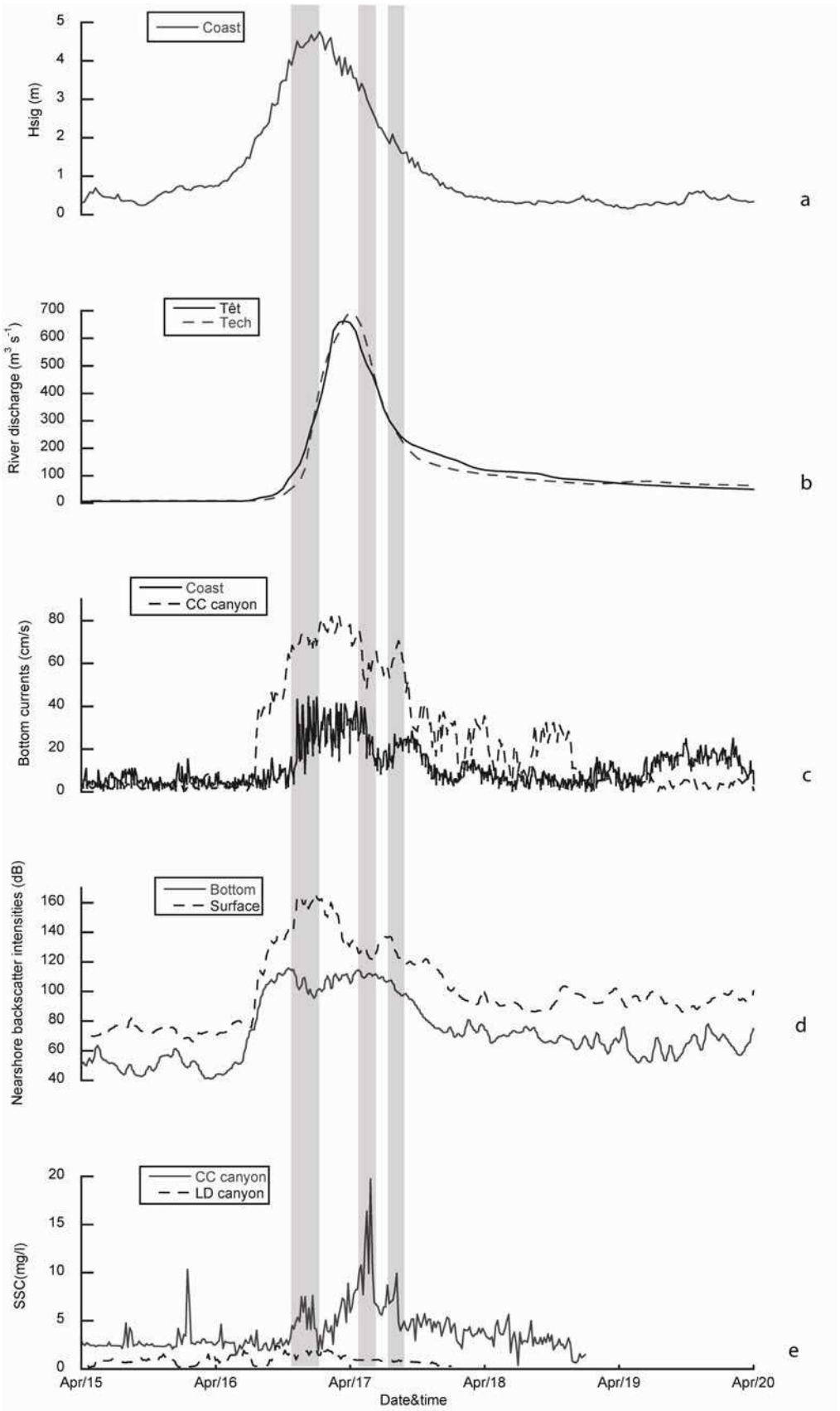

Figure 4-23: Detailed time-series of (a) hourly significant wave height (Hs in m) measured at the AWAC station (Figure 4-15b), (b) hourly river discharge (Qh) of the Têt and Tech rivers extracted from the national data bank "Hydro", (c) hourly averaged bottom current speed measured at the AWAC station

(Coast) and in the canyon head of the Cap Creus canyon, (d) nearshore TSS dependant backscatter intensities (1 hr average) from the AWAC 1 m above the bottom and at the surface, and TSS (mg/L) signal measured by OBS deployed in the canyon heads of the Cap Creus and Lacaze-Duthiers canyons. Northward and southward (shaded area) current regimes are indicated at the top of the figure with arrows. Canyon turbidity peaks are delimited with shaded areas.

Bottom current intensity measured near the Têt River mouth in the coastal area, lagged the coastal current increase by ~6 hours, and reached intensities of 40 cm s^{-1} for more than half a day. At the head of the Cap Creus canyon, about 50 km south, maximum bottom current magnitude reached about 80 cm s^{-1}, and current intensities >60 cm s^{-1} were measured for about 20 hours (**Figure 4-23**c). Backscatter intensities measured by the Acoustic Doppler Profiler (AWAC) in the nearshore zone are directly related to the quantity of suspended material in the water column. In the nearshore, two peaks of the backscatter intensity were measured: the first peak occurred during the waxing phase of the storm, the second was measured during the peak of flood discharge (**Figure 4-23**d). At the canyon head, a first turbidity peak concomitant to the peak of the storm (Hs = 5 m, 16th April 02:00) was measured on 16th April 16:00 with concentrations of ~8 mg L^{-1}, (**Figure 4-23**d). A second turbidity peak was measured on 17th April 04:00, with concentrations of ~20 mg L^{-1}, 14 hours after the peak of the storm (**Figure 4-23**d). A third turbidity peak was measured on 17th April 08:00 with concentrations of ~10 mg L^{-1}, 9 hours after the peak flood of coastal rivers. No turbidity anomaly was measured in the Lacaze-Duthiers canyon further north.

4.3.5 Discussion

4.3.5.1 Sediment contribution of coastal rivers to the shelf

4.3.5.1.1 Total inputs to the shelf

Total solid discharge of the Têt River was estimated to be ~34 x 10^3 t during the April 2004 flood event. This corresponds to more than the half of the total mean annual suspended load of the Têt River (~61 x 10^3 t), discharged in 3 days. The mean annual solid discharge of the coastal rivers of the Gulf of Lions is ~0.65 x 10^6 t yr^{-1} compared to 10.2 x 10^6 t yr^{-1} for the Rhône River (**Bourrin et al., 2006**). However, during severe oceanic flood events, the suspended sediment contribution to the Gulf of Lions by small coastal rivers can have a major

importance in comparison to the Rhône, the largest river of the Gulf. For example, during the oceanic flood of April 2004, the Têt and the adjacent Tech rivers together discharged ~70 x 10^3 t (+ ~15 x 10^3 t for the Agly River) of sediment to the coastal zone, representing 7 times the discharge of the Rhône during the same period.

4.3.5.1.2 Importance of sand transport fraction (suspended and bedload)

The percentage of sand in suspension, measured in surface water of the Têt River reached values of ~20% of the total load during the flood. We estimated that about 34% of the total suspended load was composed of sand (~11.4 x 10^3 t). The bedload transport of sand, estimated using SEDTRANS96 (**Li and Amos, 2001**), represented an additional load of 4 x 10^3 t. **Garcia-Estevez (2005)** has shown that about 40% of TSS are retained by the dam, built between the alluvial plain and the mountainous part of the catchment, about 50 kms upstream to the river mouth, to prevent flooding (**Figure 4-16**). This dam should preferentially retain the coarser fraction of solids in suspension such as sands and silts. But the flood of April 2004 occurred mainly in the lower part of the Têt River catchment, as indicated by the location of the cells of maximum rainfall (**Figure 4-16**). In this part of the catchment, the dam appears to have no effect on the TSS concentrations in river water. Precipitation in the lower part of the catchment promoted erosion of sediments from easily-erodible land on the plain and the transport of alluvial sediment in suspension towards the mouth and the coastal zone.

By comparison, the Eel River, a larger mountainous river on the Californian margin, delivers ~24% of its total discharge as sand in suspension (**Crockett and Nittrouer, 2004**). The Rhône River generally discharges ~5% of the total load of sand in suspension. This percentage can reach ~15% during flood events **(Antonelli, 2002)**. Estimates based on global sediment budget from worldwide rivers to the global ocean give a bedload value of about 10% of the total load **(Milliman and Meade, 1983)**, which represents about 3.4 x 10^3 t for the Têt River during this event. For the Rhône River, estimates of bedload from **IRS (2000)** give values of 0.8 to 1.6 x 10^6 t yr^{-1}, representing about 10% of the total suspended discharge (2 to 17 x 10^6 t yr^{-1}, from **Antonelli, 2002** and **Pont et al., 2002**). **Serrat (1999**) estimated that the bedload transport for a similar river located northward to the Têt River, the Agly River, is minimal (~1% of the total load). Thus, the Têt River appears to deliver a higher fraction of sand both in suspension and as bedload than size-comparable rivers (Agly) and larger rivers (Rhône and Eel).

4.3.5.2 Sediment pathways in the nearshore

4.3.5.2.1 Coarse sediment transport

No evidence of sandy deposits related to this flood was found close to the river mouth from the bathymetric survey (**Figure 4-24**). Most of the sand introduced in the coastal zone probably bypassed the mouth through the bypass channel. Sand was caught by the northwards littoral drift during the peak storm, and nourished the modern sandy delta north of the mouth. A relict delta was also observed from the bathymetric survey (**Figure 4-24**) north from the river mouth, and was probably active during major floods of the last century (**Delpont and Motti, 1994**).

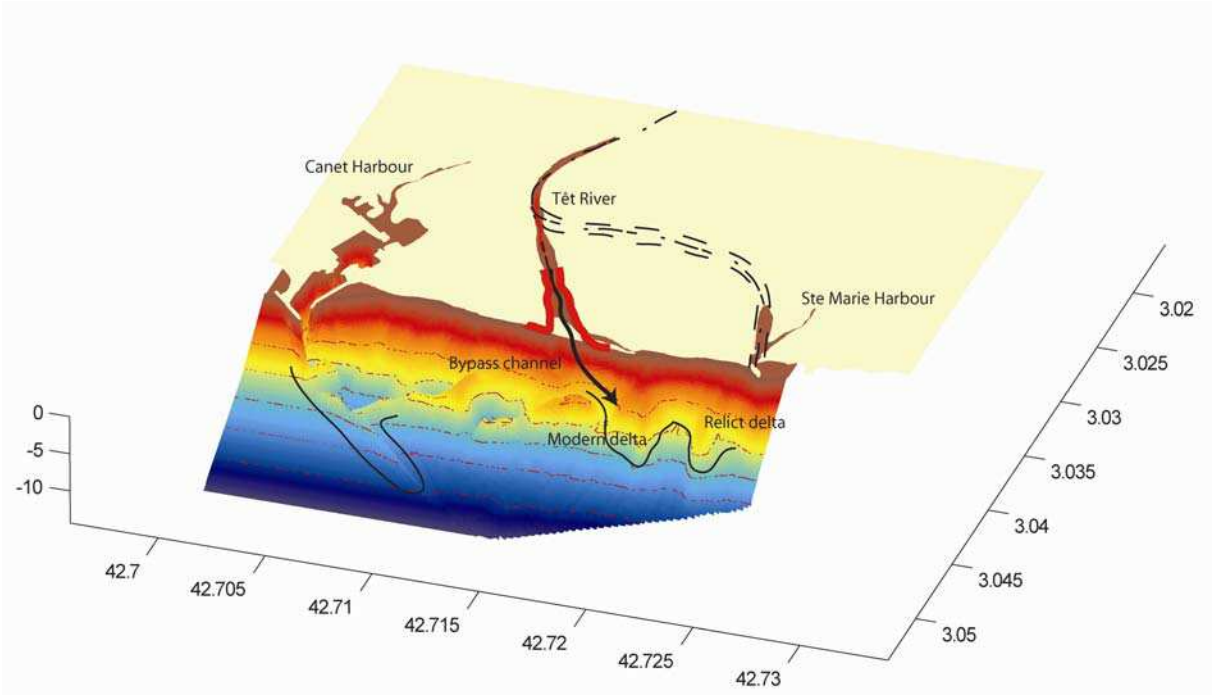

Figure 4-24: Bathymetric map of the study area showing the position of the bypass river channel, the modern and relict delta.

The Gao and Collins model in this case can only give an indication of the sand transport direction which appears to be mainly northwards in the nearshore area of the Têt River (**Manca, 2005**). The resulting direction of the trend vectors depends strongly upon the density of sampling and the size of area sampled. This is problematic in a small deltaic environment, which is highly variable over short distances. For these reasons, results may be ambiguous. Nevertheless, the northerly transport of sands is supported by other evidence. Previous studies

(**Anguenot and Monaco, 1967; Certain, 2002; Delpont and Motti, 1994; Durand, 1999**) refer to a counter current along the Roussillon coast opposite to the general counterclockwise circulation in the southwestern Gulf of Lions (**Figure 4-15a**). **Anguenot and Monaco (1967)** monitored a northwards net sediment transport of radioactive sand in the nearshore of the Roussillon inner-shelf, associated with SE storms, and weaker southern net sediment transport associated with NW continental winds. **Delpont and Motti (1994)** showed the development of sand spits growing northwards at river mouths by studying satellite images at different periods of time. These authors also demonstrated that the configuration of the river mouth changed after the flood events. In April 2004, the sand spit attached to the southern side of the Têt River mouth was removed from its position shown in marine charts. Indeed, the river mouth has two different configurations according to the river discharge regime. During low river discharge (few m^3 s^{-1}), a sand spit grows from south to north following the northward littoral drift. During high flooding conditions, river flow breaks through this sand spit. **Delpont and Motti (1994)** also observed local sand-trapping on the south side of Canet-en-Roussillon and Sainte Marie harbours, suggesting a net northwards littoral drift. The bathymetric survey of the area conducted in April 2004 (**Figure 4-24**), indicated that the orientation of sand bars does not appear to be a good indicator of the net sand transport direction because they are perturbed by the presence of the artificial dike of the leisure harbour of Canet-en-Roussillon. The dike promoted the development of a sand spit growing from its southern tip toward the north. Sand accretion was observed in the southern exposure and erosion in its northern exposure. The position of the nearshore submarine deltas (modern and relict), located north of the river mouth seems to indicate a net northwards littoral drift. A bypass channel orientated northwards is located between the river channel and the modern delta zone. The non-active delta observed further north of the modern delta is believed to be active during extreme flooding as was the case during the "Aiguat" event of 1940, one of the biggest events ever known. These features confirm the northwards trend of the littoral drift of sand.

4.3.5.2.2 Flood layer deposits

Concerning the transport of fine-grained sediment, mud patches were observed in the nearshore area of the Têt River after the oceanic flood of April 2004. High mud content was measured in surface sediment directly in front of the river mouth and towards the south (**Figure 4-22**) to a water depth of 10 m. Sediment cores, taken after the flood event on 28th

April 2004 showed a flood deposit at 20 m water depth, however this was absent at 30 m water depth. The southwards current regime occurring during this oceanic flood (**Figure 4-17**) restricted the dispersion of fine-grained sediment offshore. TSS concentrations measured in surface river water were not high enough to overcome the stratification between freshwater and saltwater, and produce bottom hyperpycnal flows (**Mulder and Syvitski, 1995**). Part of the fine sediments settled near the mouth; the remainder was advected with the surface hypopycnal plume southwards along the coast. Likewise, on others prodeltas associated with larger rivers (Rhône, Miralles et al., 2006; Po, Palinkas et al., 2005; Atchafalaya, **Allison et al., 2000**), no flood deposit was observed below 40 m water depth after certain flood events. The depth reached by these deposits depends on: (1) the strength of the flood in terms of liquid and solid discharges; (2) the wave climate of the receiving basin; and (3) the current regime during and following the peak discharge.

4.3.5.3 Fine-grained dispersal

4.3.5.3.1 Shelf transport

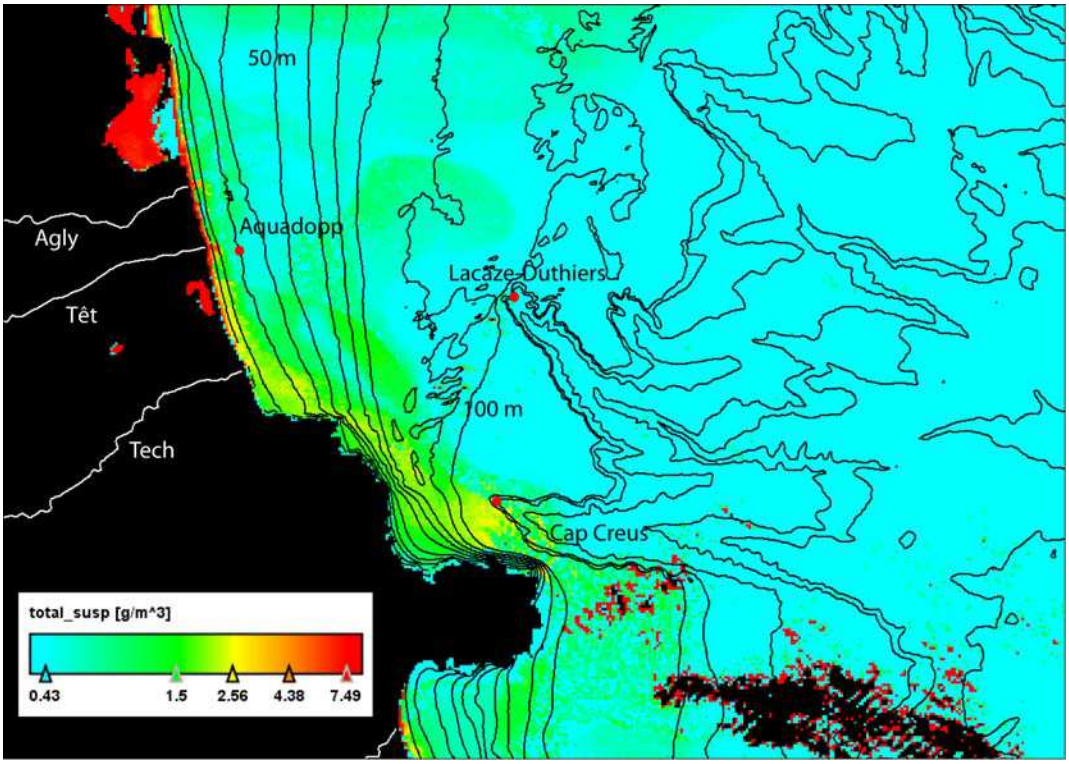

Figure 4-25: Satellite image of the southwestern Gulf of Lions along the Roussillon coast, taken on 26th April 2004 from MERIS sensor, with the courtesy of the European Space Agency through APISCO program. The spectral band corresponding to surface TSS concentrations was extracted. The color bar on

the bottom right corner is expressed in g m^{-3}. Hydrography and bathymetry are also represented, as well as the sampling stations with red circles.

The southwards plume orientation revealed by grain-size analysis of the bed near the Têt River mouth is also evidenced by satellite image. The MERIS picture (**Figure 4-25**) taken after the peak flood the 26th April 2004, shows the southwards dispersion of river plumes along the Roussillon coast. In this image, it is possible to distinguish the dispersion of several hypopycnal plumes from the Agly, Têt and Tech rivers on the shelf towards the southwestern canyons of the Gulf of Lions. River mouth plume events and their dispersal in the northwestern Mediterranean Sea have already been observed in large systems such as the Rhône and the Ebro (**Arnau et al., 2004**), but no observations have been investigated in the smaller systems. In this case, satellite imagery was possible only several days after the flood event, due to cloud cover during the passage of a low pressure system (**Wheatcroft, 2000**) and could reflect different oceanic conditions in the Têt inner-shelf.

Following **Trump and Marmorino (2003)**, in which vessel-mounted acoustical backscatter measurements were used to map river front structure, the southwards orientation of the Têt surface plume was evidenced from the water column acoustical backscatter data measured on 18th April 2004 (**Figure 4-21**). Surface turbidity maxima were first observed at the entrance of the Canet-en-Roussillon harbour, corresponding to the draining of the harbour basin in response to the flood and the relaxation phase of the water mass after the storm induced surge in the harbour. Surface turbidity maxima were also observed south of the Têt River mouth, confirming the dispersal of the river plume towards the south, following the general circulation in the Gulf of Lions.

4.3.5.3.2 Sediment export from the shelf

Surface currents modeled in the southwestern part of the Gulf of Lions (16th April 2004, **Figure 4-26**) predicted strong surface currents flowing along the coast towards the southern tip of the continental margin and the Cap Creus canyon head. Surface velocities reached a maximum of 80 cm s^{-1} on 16th April 2004 during the peak of the storm. Fine particles entering the coastal area through hypopycnal plumes from the Roussillon coastal rivers (Agly, Têt and Tech) were thus rapidly advected southwardly by the general counter-clockwise circulation, thereby reaching the canyon head in less than a day. Near bottom measurements in the Cap

Creus canyon head at the SW end of the Gulf indicate an increase of the current intensity and suspended sediment concentration shortly after the storm and river flood (**Figure 4-23**).

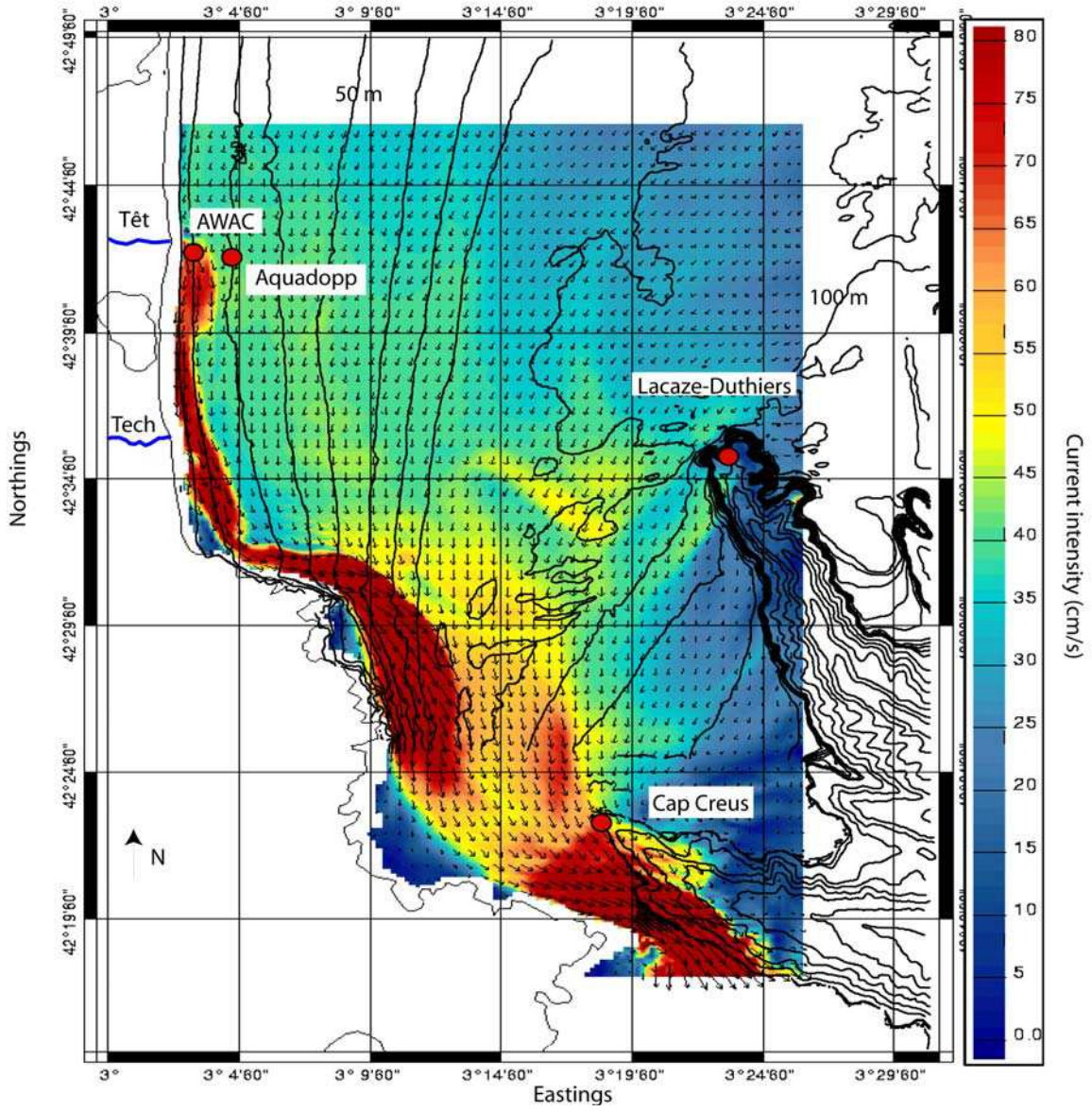

Figure 4-26: Surface currents extracted from Symphonie model (Ulses, 2005), 16th April 2004, in the southwestern Gulf of Lions along the Roussillon coast. Current intensity is proportional to the size of black dots. Color scale bar of current intensity is represented in cm s^{-1} on the right. Sampling stations are indicated with red circles.

Exported sediment originated both from the river input of fine-grained material, but also from the resuspension of shelf sediment. On one hand, our estimates of fine-grained supply by the three adjacent rivers (Agly, Têt and Tech) to the southwestern Gulf of Lions amounted to approximately 85 x 10^3 t. On the other hand, **Ulses et al. (submitted)** estimated from models that the export primarily took place through the Cap Creus canyon and the southernmost shelf,

and amounted to 180 x 10^3 t, of which a large part originated from the shelf sediment resuspension. This implies that rivers input contributed little to the off-shelf export of suspended sediment during that event, because it was diluted by the large storm –induced resuspension that occurred on the shelf.

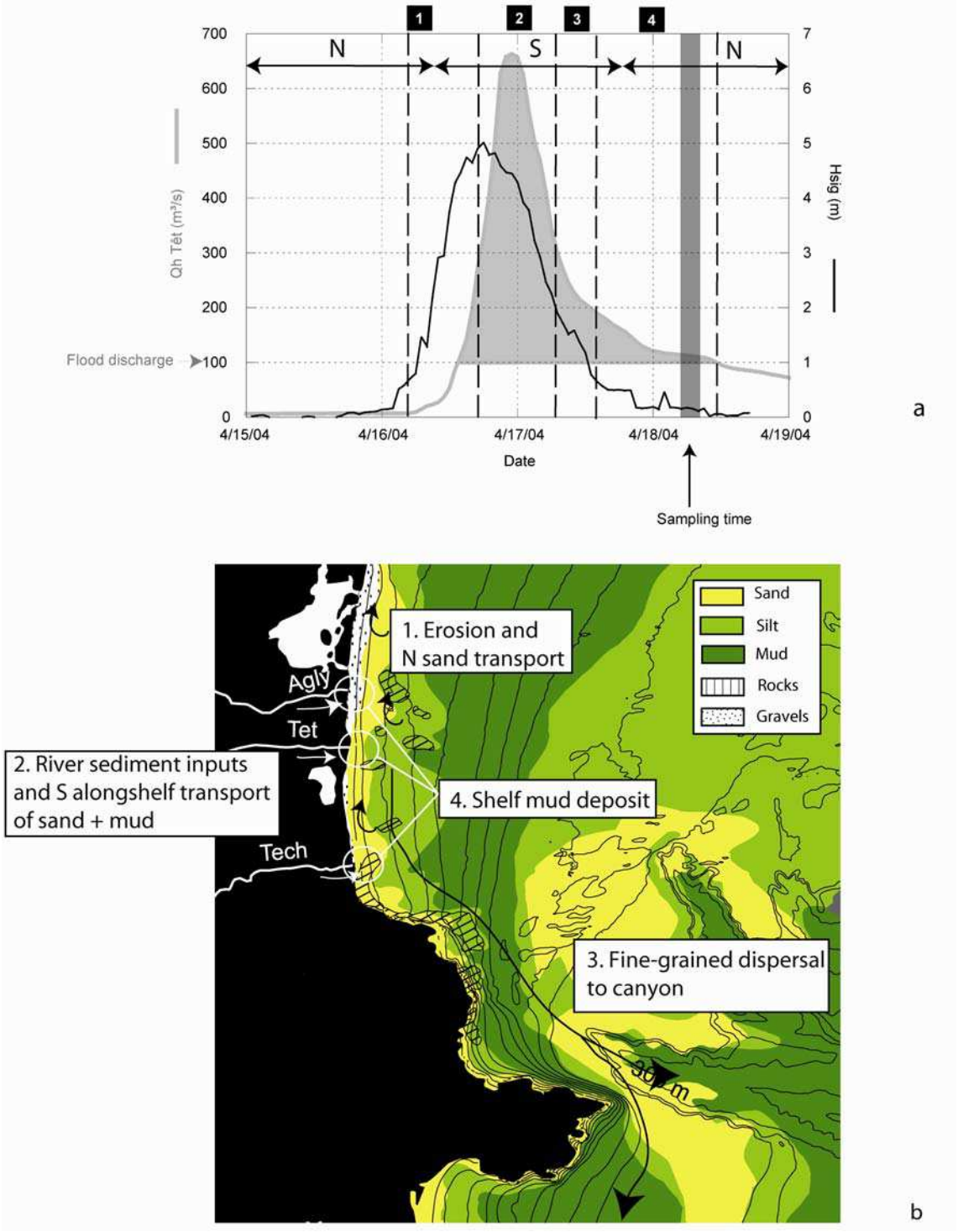

Figure 4-27: Sketch of the mechanisms (sediment transport and deposition), and pathways occurring during the oceanic flood event of April 2004. a, Timing of the storm and flood phenomena. The direction of the alongshelf coastal current is represented at the top of the figure (N: northwards and S: southwards).

b, Sediment transport pathways replaced in a spatial scale from the river mouth to the outer shelf and the canyons in the southwestern Gulf of Lions. The numbers refer to the different steps of the sediment transport on the Roussillon coast. Sedimentological features are also represented (redrawn from Aloïsi et al., 1973).

A schematic diagram of the sediment transport and deposition mechanisms of a typical oceanic flood event on a microtidal margin dominated by storms is presented in **Figure 4-27**a. (1) A depression over the sea induces SE marine winds which promote a typical storm event associated with a coastal storm surge. Waves induce sea bed erosion in the coastal zone to about 20-30 m water depth. In the nearshore (0-10 m water depth), sand is transported northwards as bedload in the breaker zone; (2) a few hours after the onset of the storm, precipitation in the catchment occurs causing an oceanic flood. Sand and mud are transported by rivers to the coastal area. The marine winds cease, and northeasterly winds invert the coastal current direction that veers from a southerly to a northerly direction. Coastal currents and wave energy remain strong enough to maintain fine sediments in suspension, which bypass the coastal area and are advected directly southwards along the coast; (3) the storm passes, and fine-grained hypopycnal plumes flow southwards along the coast, and reach the Cap Creus area; (4) the river discharge remains high and alongshore currents decrease; mud is deposited in the inner-shelf south of the river mouth. Thus, according to our observations replaced in a regional setting (**Figure 4-27b**), coarse-grained sediment transport is restricted to the nearshore. Part of the fine-grained sediment settles close to river mouths on prodeltas; part is advected directly southwards to the Cap Creus canyon head and along the coast. Prodeltas constitute early muddy deposits at river mouths (**Roussiez et al., 2005**) and feed the mid-shelf mud belt in a multi-step pathway following storm events (**Guillén et al., 2006**). Oceanic flood events with relatively short return intervals on small mountainous rivers can thus play a significant role in the supply of coarse sediment to the inner shelf, and contribute to the dispersal and export of fine-grained sediment across the shelf and, through the canyons, to the continental slope. The fine-grained sediment transport across the shelf thus occurred directly towards the continental slope during oceanic floods through hypopycnal plumes, and in multi-step pathways from the erosion of prodeltas and the mid-shelf mud belt during storm events.

4.3.6 Conclusions

The most important findings of this work are as follows. An oceanic flood event was observed in April 2004 on the Têt River. About half of the annual load was discharged in a few days during this oceanic flood. The dam in the middle of the Têt River catchment did not appear to prevent sand transport to the coastal zone during this event. Maximum precipitation cells were localized in the lower part of the basin promoting erosion of easily erodible lands. Large amounts of sand in suspension were thus carried to the coastal zone. River sand was trapped in the nearshore and was subsequently moved alongshore to the north as bedload as indicated by a well-developed delta and bedforms. At the same time, river fines were separated at the mouth: a part settles towards the south and the finest fraction is advected towards the Cap Creus canyon through hypopycnal plume, where it exits the shelf within a few hours after the flood peak. Next to major flood events of large-size rivers, e.g. the Rhône, small mountainous rivers can play a significant role in the supply of sediment to continental shelves and, in the case of the NW Mediterranean Sea, can contribute significantly to the export of sediment from the continental margin.

Sediment transport from continental margins to the shelf edge has been investigated extensively during extreme flood events on large-size rivers (e.g. the Rhône) in the Gulf of Lions and on other continental shelves (e.g. the Eel and the Po). However, until the present contribution, no study has investigated the ability of coastal mountainous rivers under oceanic flood conditions to transport sediment across the continental shelf towards the slope. There is a paucity of data on oceanic flood events on European continental margins; this is the first scientific study of one such event in a microtidal setting within Europe.

Acknowledgements

The authors would like to thank the “Communauté d'Agglomération Perpignan Méditerranée” for providing wind, current and wave data, initially measured during the construction of a waste water pipe in the coastal area of the Têt River. This work was supported by the European project Eurostrataform (contract number EVK3-CT-2002-00079).

References

Allison, M.A., Kineke, G.C., Gordon, E.S., Goñi, M.A., 2000. Development and reworking of a seasonal flood deposit on the inner continental shelf off the Atchafalaya River. Continental Shelf Research, 20 (16): 2267-2294.

Aloïsi, J.C., Got, H., Monaco, A., 1973. Carte géologique du précontinent languedocien au 1/250000ième., International Institute for Aerial Survey and Earth Sciences (I.T.C.) (Eds.), Netherlands.

Anguenot, F., Monaco, A., 1967. Etude de transits sédimentaires, sur le littoral du Roussillon, par la méthode des traceurs radioactifs. Cahiers Océanographiques, 19 (7) : 579-589.

Antonelli, C., 2002. Flux sédimentaires et morphogenèse récente dans le chenal du Rhône aval. PhD Thesis, Université Aix-Marseille I, 279 pp.

Arnau, P., Liquete, C., Canals, M., 2004. River mouth plume events and their dispersal in the Northwestern Mediterranean Sea. Oceanography, 17 (3): 22-31.

Bourrin, F., Durrieu de Madron, X., Ludwig, W., 2006. Contribution of the study of coastal rivers and associated prodeltas to sediment supply in North-western Mediterranean Sea (Gulf of Lions). Vie et Milieu, 56 (4) : 1-8.

Buscail, R., Pocklington, R., Daumas, R., Guidi, L., 1990. Fluxes and budget of organic matter in the benthic boundary layer over the northwestern Mediterranean margin. Continental Shelf Research, 10 (9-11): 1089-1122.

Buscail, R., Pocklington, R., Germain, C., 1995. Seasonal variability of the organic matter in a sedimentary coastal environment: sources, degradation and accumulation (continental shelf of the Gulf of Lions-northwestern Mediterranean Sea). Continental Shelf Research, 15 (7) : 843-869.

Certain, R., 2002. Morphodynamique d'une côte sableuse microtidale à barres : le Golfe du Lion (Languedoc-Roussillon). PhD Thesis, Université Perpignan, 209 pp.

Courp, T., Monaco, A., 1990. Sediment dispersal and accumulation on the continental margin of the Gulf of Lions: sedimentary budget. Continental Shelf Research, 9-11: 1063-1088.

Crockett, J.S., Nittrouer, C.A., 2004. The sandy inner shelf as a repository for muddy sediment: an example from Northern California. Continental Shelf Research, 24 (1): 55-73.

Delpont, G., Motti, E., 1994. Monitoring by remote sensing of the geomorphological evolution of a part of the Roussillon coastal layout (France). OCEANIS 94 OSATES, pp. 44-47.

Durand, P., 1999. L'évolution des plages de l'ouest du Golfe du Lion au XXème siècle. PhD Thesis, Université Lumière Lyon 2, 461 pp.

Ferré, B., Guizien K., Durrieu de Madron X., Palanques A., Guillén J., Grémare, A., 2005. Fine-grained sediment dynamics during a strong storm event in the inner-shelf of the Gulf of Lion (NW Mediterranean). Continental Shelf Research, 25: 2410-2427.

Gao, S., 1996. A FORTRAN program for grain-size trend analysis to define net sediment transport pathways. Computers and Geosciences, 22 (4): 449-452.

Gao, S., Collins, M., 1992. Net sediment transport patterns inferred from grain-size trends, based upon definition of "transport vectors". Sedimentary Geology, 81 (1-2): 47-60.

Garcia-Esteves, J., Ludwig, W., Kerherve, P., Probst, J.-L., Lespinas, F., 2007. Predicting the impact of land use on the major element and nutrient fluxes in coastal Mediterranean rivers: The case of the Têt River (Southern France). Applied Geochemistry., 22 (1) : 230-248.

Garcia-Estevez, J., 2005. Géochimie d'un fleuve côtier méditerranéen : la Têt en Roussillon. Origines et transferts de matières dissoutes et particulaires de la source jusqu'à la mer. PhD Thesis, Université Perpignan, 263 pp.

Gaudin, M., Berne, S., Jouanneau, J.M., Palanques, A., Puig, P., Mulder, T., Cirac, P., Rabineau, M., Imbert, P., 2006. Massive sand beds attributed to deposition by dense water cascades in the Bourcart canyon head, Gulf of Lions (northwestern Mediterranean Sea). Marine Geology, 234 (1-4) : 111-128.

Gaume, E., Livet, M., Desbordes, M., Villeneuve, J.-P., 2004. Hydrological analysis of the river Aude, France, flash flood on 12 and 13 November 1999. Journal of Hydrology, 286 (1-4): 135-154.

Guidi-Guilvard, L.D. and Buscail, R., 1995. Seasonal survey of metazoan meiofauna and surface sediment organics in a non-tidal turbulent sublittoral prodelta (northwestern Mediterranean). Continental Shelf Research, 15 (6) : 633-653.

Guillén, J., Bourrin, F., Palanques, A., Durrieu de Madron, X., Puig, P., Buscail, R., 2006. Sediment dynamics during wet and dry storm events on the Têt inner shelf (SW Gulf of Lions). Marine Geology, 234 (1-4) : 129-142.

Guillén, J., Jiménez, J. A., Palanques, A., Garcia, V., Puig, P., Sanchez-Arcilla, A., 2002. Sediment resuspension across a microtidal, low-energy inner shelf. Continental Shelf Research, 22: 305-325.

Guillén, J., Palanques, A., Puig, P., Durrieu De Madron, X., Nyffeler, F., 2000. Field calibration of optical sensors for measuring suspended concentration in the western Mediterranean. Scientia Marina, 64 (4): 427-435.

Hill, P.S., Milligan, T.G., Geyer, W.R., 2000. Controls on effective settling velocity of suspended sediment in the Eel River flood plume. Continental Shelf Research, 20 (16) : 2095-2111.

IRS, 2000. Etude globale pour une stratégie de réduction des risques dus aux crues du Rhône. Etude du transport solide, 1ère étape, rapport de synthèse, Institution interdépartementale des bassins Rhône-Saône, Valence, France.

Land, J.M., Bray, R.N., 2000. Acoustic measurement of suspended solids for monitoring of dredging and dredged material disposal. Journal of Dredging Engineering, 2 (3): 1-17.

Li, M.Z., Amos, C. L., 2001. SEDTRANS96: the upgraded and better calibrated sediment-transport model for continental shelves. Computers and Geosciences, 27: 619-645.

Ludwig, W., Serrat, P., Cesmat, L., Garcia-Esteves, J., 2004. Evaluating the impact of the recent temperature increase on the hydrology of the Têt River (Southern France). Journal of Hydrology, 289 (1-4): 204-221.

Manca, E., 2005. La dinamica sedimentaria nell'ambiente deltizio del flume Têt (Francia Meridionale). Master Thesis, University of Genova.

Milliman, J.D., Meade, R.H., 1983. World-wide delivery of sediment to the oceans. Journal of Geology, 91 (1): 1-21.

Milliman, J.D., Syvitski, J.P.M., 1992. Geomorphic/Tectonic Control of Sediment Discharge to the Ocean: The Importance of Small Mountainous Rivers. Journal of Geology, 100 (5): 525-544.

Millot, C., 1976. Specific features of the sea-shore circulation near Cap Leucate. Mémoires Société Royale des Sciences de Liège, 6e série (tome X) : 227-245.

Miralles, J., Arnaud, M., Radakovitch, O., Marion, C., Cagnat, X., 2006. Radionuclide deposition in the Rhône River Prodelta (NW Mediterranean Sea) in response to the December 2003 extreme flood. Marine Geology, 234 (1-4): 179-189.

Mulder, T., Syvitski, J.P.M., 1995. Turbidity currents Generated at river Mouths during Exceptional Discharges to the world Oceans. Journal of Geology, 103: 285-299.

Palanques, A., Durrieu de Madron, X., Puig, P., Fabres, J., Guillén, J., Calafat, A., Canals, M., Heussner, S., Bonnin, J., 2006. Suspended sediment fluxes and transport processes in the Gulf of Lions submarine canyons. The role of storms and dense water cascading. Marine Geology, 234 (1-4): 43-61.

Palanques, A., Puig, P., Guillén, J., Jimenez, J., Gracia, V., Sanchez-Arcilla, A., Madsen, O., 2002. Near-bottom suspended sediment fluxes on the microtidal low-energy Ebro continental shelf (NW Mediterranean). Continental Shelf Research, 22 (2): 285-303.

Palinkas, C.M., Nittrouer, C.A., Wheatcroft, R.A., Langone, L., 2005. The use of ^{7}Be to identify event and seasonal sedimentation near the Po River delta, Adriatic Sea. Marine Geology, 222-223: 95-112.

Pont, D., Simonnet, J.-P., Walter, A.V., 2002. Medium-term Changes in Suspended Sediment Delivery to the Ocean: Consequences of Catchment Heterogeneity and River Management (Rhone River, France). Estuarine Coastal and Shelf Sciences, 54 (1): 1-18.

Puig, P., Palanques, A., Guillén, J., 2001. Near-bottom suspended sediment variability caused by storms and near-inertial internal waves on the Ebro mid continental shelf (NW Mediterranean). Marine Geology, 178 (1-4): 81-93.

Rouse, H., 1937. Modern conceptions of the mechanics of fluid turbulence. Transactions of the American Society of Civil Engineering, 102 (463-554).

Roussiez, V., Aloïsi, J.-C., Monaco, A., Ludwig, W., 2005. Early muddy deposits along the Gulf of Lions shoreline: A key for a better understanding of land-to-sea transfer of sediments and associated pollutant fluxes. Marine Geology, 222-223: 345-358.

Sandwell, D.T., 1987. Biharmonic spline interpolation of GEOS-3 and Seasat altimeter data. Geophysical Research Letters, 14 (2) : 139-142.

Serrat, P., 1999. Dynamique sédimentaire actuelle d'un système fluvial méditerranéen : l'Agly (France). Comptes Rendus de l'Académie des Sciences Paris Série D, 329: 189-196.

Serrat, P., Ludwig, W., Navarro, B., Blazi, J.-L., 2001. Variabilité spatio-temporelle des flux de matières en suspension d'un fleuve côtier méditerranéen : la Têt (France). Comptes Rendus de l'Académie des Sciences Paris Série D, 333: 389-397.

Standard Methods for the Examination of Water and wastewater. Ed. 1989, 17 th.

Trump, C.L., Marmorino, G.O., 2003. Mapping Small-scale Along-front Structure using ADCP Acoustic Backscatter Range-bin Data. Estuaries, 26 (4) : 878–884.

Ulses, C., 2005. Dynamique océanique et transport de la matière particulaire dans le Golfe du Lion : Crue, tempête et période hivernale. PhD Thesis, Université Paul Sabatier, Toulouse, 247 pp.

Ulses, C., Estournel, C., Bonnin, J., Durrieu de Madron, X., Marsaleix, P., 2007. Impact of storms and dense water cascading on shelf-slope exchanges in the Gulf of Lion (NW Mediterranean). Journal of Geophysical Research, Accepted.

Ulses, C., Estournel, C., Durrieu de Madron, X., Palanques, A., Submitted, submitted. Suspended Sediment Transport in the Gulf of Lion (NW Mediterranean): Impact of Extreme Storms and Floods. Continental Shelf Research.

Urick, R.J., 1975. Principles of Underwater Sound. McGraw Hill, N.Y., 384 pp.

Walling, D.E., Fang, D., 2003. Recent trends in the suspended sediment load of the world's rivers. Global Planetary Change, 39 (111-126).

Wheatcroft, R.A., 2000. Oceanic flood sedimentation: a new perspective. Continental Shelf Research, 20(16): 2059-2066.

Wheatcroft, R.A., Borgeld, J.C., 2000. Oceanic flood deposits on the northern California shelf: large-scale distribution and small-scale physical properties. Continental Shelf Research, 20(16): 2163-2190.

Winston, W.E., Criss, R.E., 2002. Geochemical variations during flash flooding, Meramec River basin, May 2000. Journal of Hydrology, 265(1-4): 149-163.

Yalin, M.S., 1963. An expression for bedload transportation. Journal of the Hydraulics Division, ASCE 89(HY3): 221-250.

4.4 Impact de la circulation hivernale et de la formation des eaux denses sur l'érosion du plateau dans le golfe du Lion

Impact of winter Dense Water Formation on shelf sediment erosion (evidence from the Gulf of Lions, NW Mediterranean)

François Bourrin[1]*	Redaction, Data
Xavier Durrieu de Madron[1]	Redaction, Data
Claude Estournel[2]	Modelisation
Serge Heussner[1]	Manuscript revision

[1] Centre de Formation et de Recherche sur l'Environnement Marin, UMR 5110 CNRS Université de Perpignan, 52 Avenue de Villeneuve, 66860, Perpignan cedex, France

[2] Pôle d'Océanographie Côtière de l'Observatoire Midi-Pyrénées - Laboratoire d'Aérologie 14 Avenue Edouard Belin - 31400 Toulouse, France

Soumis le 13/07/2007

Continental Shelf Research

Gulf of Lions Special Issue

Abstract

A 1-yr survey of sediment dynamics on the Têt inner-shelf in the southwestern part of the Gulf of Lions was conducted as part of the EuroStrataform program from October 2004 to October 2005. Several bottom instruments (ADCP, wave gauge and altimeters) were deployed at 28 m water depth on the Têt prodelta to measure forcing responsible for sediment erosion and transport on the inner-shelf.

The survey period was characterized by low river inputs of the coastal rivers, the absence of severe E-SE storms, but the occurrence of intense cold dense water formation along the inner-shelf due to strong and persistent continental winds. The strong (> 20 cm/s) and prolonged (4 months) southwards alongshore currents taking place during the preconditioning and formation phases of dense shelf water generated a continuous sediment erosion of several centimetres on the Têt prodelta and significant suspended sediment transport. Hydrodynamical modelling shows that the core of the flow predominantly affects the inner shelf, but occasionally spreads over the mid-shelf mud belt and the outer-shelf, due the variable intensity of the NW wind (Tramontane).

The impact of this N-NW wind-driven process in terms of resuspension rates and suspended sediment transport clearly differs from that of extreme E-SE storms observed during the previous winter at the same site (**Guillén et al., 2006; see chapter 4.2**). However due to their different duration, both led to significant erosion of the inner shelf sediment.

Keywords

Sediment erosion, dense water flow, inner-shelf, continental shelf, Têt River, Gulf of Lions, Mediterranean Sea

4.4.1 Introduction

Modern sediment dynamics on continental shelves are essentially dependant upon sediment inputs by adjacent rivers and hydrodynamical conditions. The number and strength of sediment sources, which essentially occurs during floods, control the sedimentation rate on the inner-shelf and on prodeltas, the submarine part of continental deltas directly off the river mouths (**Milliman and Syvitski, 1992)**. On micro-tidal inner-shelves, waves are considered the main stirring mechanism causing bottom sediment resuspension. The wind-driven

circulation then advects the sediment in suspension and control the bottom shelf sediment distribution (**McCave, 1972; Drake, 1976**).

This general scheme applies to the Gulf of Lions (GoL) shelf, in the northwestern Mediterranean Sea. The major sedimentary units (sandy inner shelf and mid-shelf muddy belt) reflect the impact of waves on the inner shelf and the southwestward dispersal by the shelf circulation of the sediment inputs from the Rhône River and the small coastal rivers (**Aloïsi, 1986**). Recent observations (**Ferré et al., 2005; Guillén et al., 2006; Palanques et al., 2006; Bourrin et al, submitted; see chapter 4.3**) and modelling (**Ulses et al., submitted**) emphasized the role of severe E-SE storms. Their associated large waves (H_s > 7 m and T_p > 12 s) create significant resuspension on the shelf and subsequent transport towards the Cap de Creus Canyon at the SW end of the gulf. Erosion of a sediment layer up to 5 cm thick and cumulative near-bottom transport up to 16 t/m^2 were observed during the December 2003 and February 2004 large storms on the Têt inner-shelf at 28 m water depth (**Guillén et al., 2006; see chapter 4.2**).

The E-SE storms have a marked seasonal impact with a maximum occurrence during autumn and winter. This period is also characterized by the progressive disappearance of summer stratification and cooling of the shelf water, which eventually leads to the formation of homogeneous coastal water denser than the offshore water (**Dufaud-Julliand et al., 2004; Ulses et al., accepted**). The cold dense coastal water forms a bottom-arrested gravity plume that propagates on the shelf and, once it reaches the shelf edge, cascades down the continental slope following topographic depressions down to its horizon of equilibrium density. E-SE storm and dense shelf water transport can interact and enhance the off-shelf export, as shown by **Palanques et al (2006)** and **Ulses et al (submitted)**, but they require adverse conditions to develop. River floods generally associated to large storms decrease the salinity of surface waters and thereby limit the density increase of coastal water. Conversely, the strongest dense water formations are observed for very dry and windy winters, which are not favorable to E-SE storms.

During the cold and windy 2004-05 winter, **Canals et al. (2006) and Puig et al. (submitted)**, showed that intense dense shelf water cascading in the nearby Cap de Creus Canyon was able to entrain sediment given the high velocity (up to 80 cm/s) of the dense water plume. In the

present study, we assess the impact of the winter 2004-05 dense shelf water formation and propagation on the coastal sediment erosion and transport, and compare it with the effect of large S-SE storms that dominated during the previous 2003-04 winter.

4.4.2 Material and methods

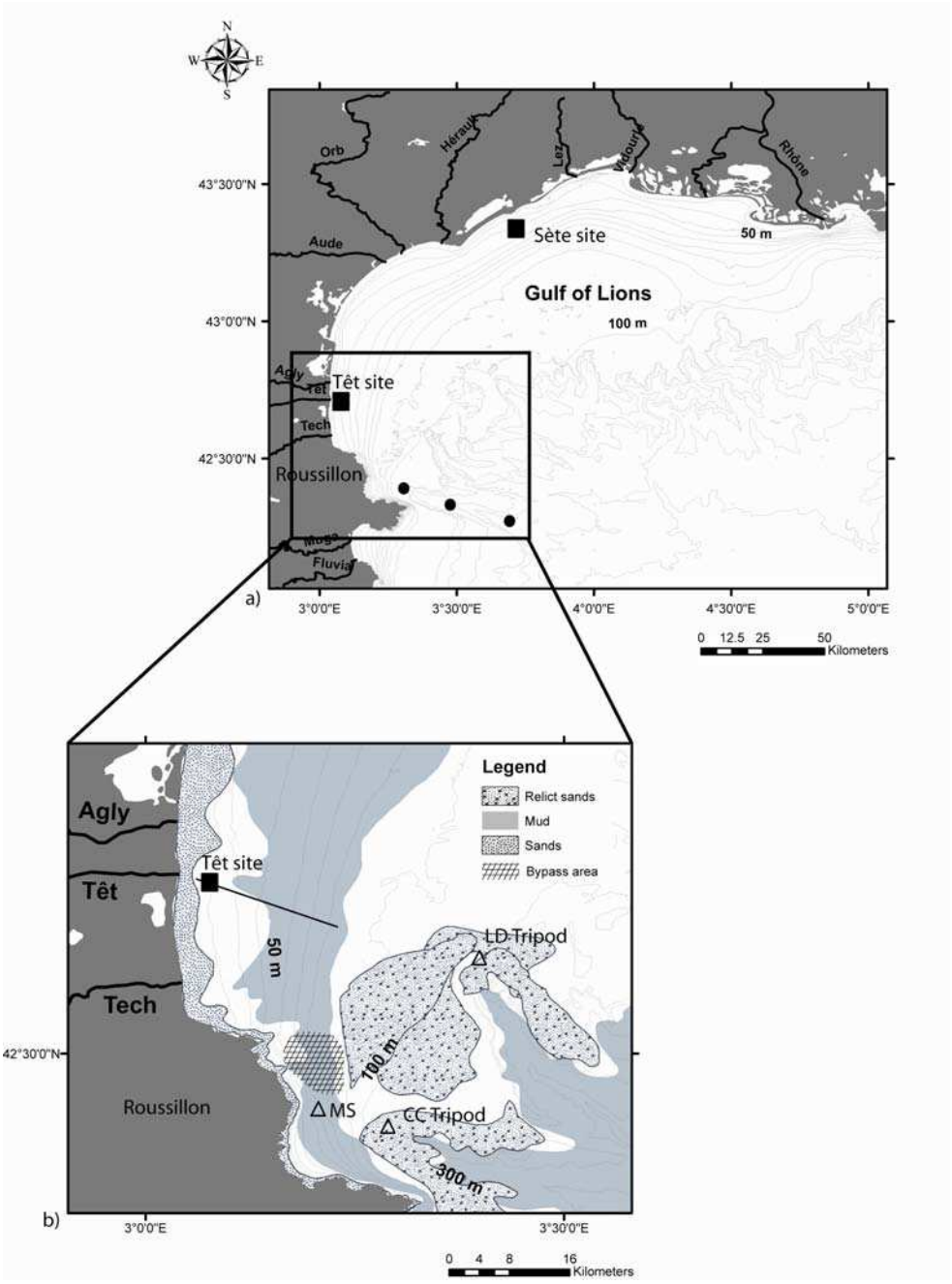

Figure 4-28 : a) Morpho-bathymetric map of the whole Gulf of Lions (redrawn from Berné et al., 2002). the black circles represent the measurement sites from Puig et al. (submitted), and the black squares represent the Sète and Têt sites; and b) detailed bathymetric and sedimentological map of its southwestern tip (redrawn from Aloïsi et al., 1973) showing the Têt site at 28 m water depth. The triangles represent the

measurement sites from Ogston et al. (submitted) in the Cap de Creus (CC) and Lacaze-Duthiers (LD) canyons respectively and the location of the mid-shelf tripod (MS). Details about the bypass area are given in DeGeest et al. (submitted).

A 1-yr investigation of waves, currents, suspended sediment concentrations (SSC) and fluxes, and bed level measurements was conducted on the Têt inner-shelf, at the SW end of the GoL, from October 2004 to October 2005. It was part of a larger experimental setup designed to study the sediment dynamics at the shelf edge and within nearby canyons (**Figure 4-28**).

4.4.2.1 Measurement site

The meteorological buoy of the "Plateforme d'Observation de l'Environnement Méditerranéen – Littoral Languedoc-Roussillon" (POEM-L2R), installed at 28 m water depth, 1.5 n.m. off the Têt River mouth (42°42.210'N, 003°04.012'E), was the base site of the coastal zone monitoring (**Figure 4-28**). This coastal platform is located at the exit of the GoL where the shelf narrows, intensifying currents and receiving sediment fluxes by rivers further north along the coastline. This buoy has a 3-point helicoidal anchoring tightly linked to mid-water depth flotation to prevent any sediment resuspension (**Figure 4-29**). This buoy shelters a seabed area allowing the deployment of benthic instruments and preventing them from trawling.

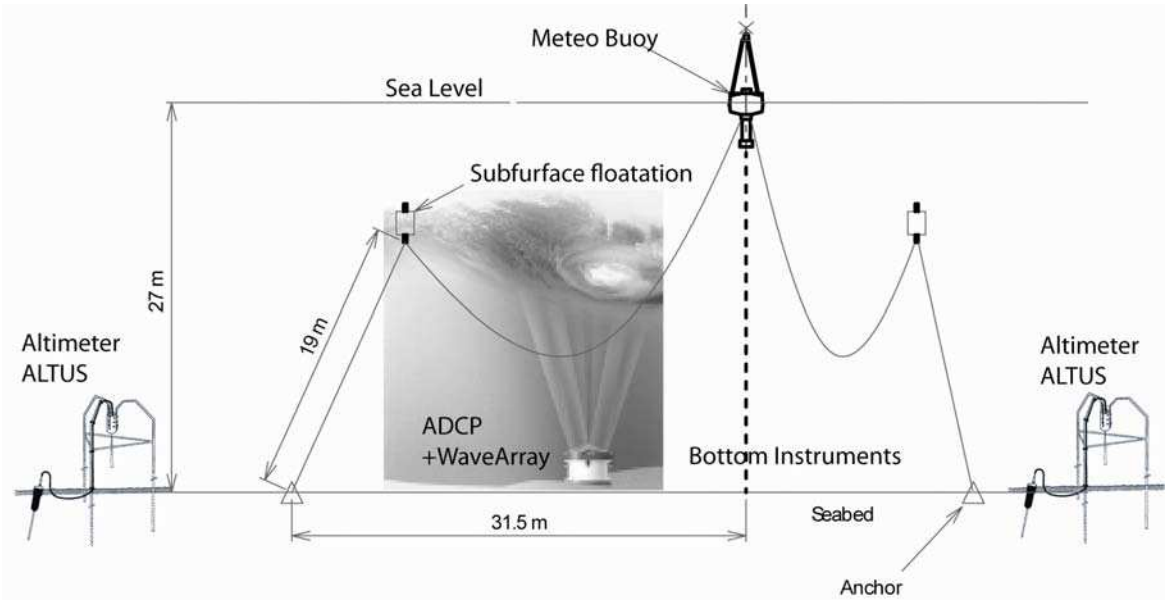

Figure 4-29 : Scheme of the buoy of the POEM platform, installed on the Têt prodelta at 28 m water depth, showing the position of the instruments on the seabed (ADCP and altimeters) on the sheltered area of the buoy.

4.4.2.2 Wind and river discharges measurements

A Young Wind Monitor Model 05106 anemometer (RM Young Compagny), installed at 4 m above the sea surface on the top of the buoy, measured wind speed and direction every 15 minutes. Data from the nearest Météo France meteorological station in Torreilles (code 66212001, location 42°45.379'N, 02°58.781'N), were used to fill the measurements gaps at the buoy site during maintenance. Hourly liquid discharge at the Têt River mouth next to the study site was obtained by adding the discharge of the Têt River measured at Perpignan (code Y0474030) and its last tributary, the Basse River (code Y0475610). These data, collected by "DDE de l'Aude", are available through the website of the National Data Bank "HYDRO" (http://www.hydro.eaufrance.fr/accueil.html). Hourly liquid discharges of the Rhône River were measured by the "Compagnie Nationale du Rhône" (CNR) during the study period at the Beaucaire gauging station.

4.4.2.3 Hydrodynamical measurements

Currents and waves were monitored on the Têt prodelta at 28 m water depth from October 2004 to October 2005 using a 600 kHz RDI upward looking ADCP equipped with a wave gauge, deployed on a bottom frame in the sheltered area of the buoy (**Figure 4-29**). Two maintenance periods were necessary to change the battery and download the data in March (15^{th} to 19^{th}) and July (6^{th} to 22^{nd}) 2005, defining 3 deployment periods over the whole year. High-frequency measurements of near-surface wave orbital velocities, surface track and pressure were used to compute directional wave characteristics (**RD Instruments, 2001**). Waves were measured during 20-min bursts every 3 hours. Currents were measured at 1 Hz in 1 m depth cells from 2 to 27 mab, between wave burst measurements and were averaged every 3 hours.

4.4.2.4 Hydrology, turbidity and grain-size measurements

Temperature was measured at the head of the ADCP instrument at the coastal site, at 28 m water depth. CTD profiles were measured from the research vessels Oceanus and Endeavor on October 10^{th} 2004 and February 22^{nd} 2005 along a cross-shelf transect between the coastal site and the shelf edge (**Figure 4-28b**). A LISST type B (Sequoia Scientific) was deployed on the INSEECT tripod on April 2005 (**Curran et al., 2007**) and was set to take measurements

every 15 min at 1.5 mab. Grain-size measurements of suspended material were investigated in the range 1.25 – 250 µm.

4.4.2.5 Estimation of SSC from backscatter intensities

Backscatter intensities were measured by ADCP along the 4 transducers in depth cells of 1 m through the whole water column. Relative backscatter intensity is directly dependant of the quantity of suspended material in the water column (**RD Instruments, 1996)**. The Sediview program (**Land and Bray, 2000**) was used to derive suspended sediment concentrations (SSC) from the average backscatter signal of the RDI ADCP using an iterative method to solve a simplified version of the sonar equation (**Urick, 1975**):

$Log_{10}Mr = S\,[Ks + dB + 2r\,(\alpha_w + \alpha_s)]$

where Mr is the mass concentration per unit volume at range r, S is the relative backscatter coefficient, Ks is the site and instrument dependant factor, dB is the measured relative backscatter intensity corrected for spherical spreading, α_w is the water attenuation coefficient computed using measured temperature and salinity near the transducer, and α_s is the sediment attenuation coefficient. Information concerning the grain-size of the suspended particles at the coastal site was provided by measurements from the LISST type B instrument attached on the instrumented platform INSEECT deployed in April 2005 (**Curran et al., 2007**). The calibration constants S and Ks were determined by fitting the averaged backscatter intensities measured by the ADCP with optical turbidity measurements of an OBS during a previous deployment in February 2004 at the same site. Fitted coefficient Ks = 35 and S = 25 were used for the calibration of the data at the coastal site. **Ferré et al. (2005)** showed that the relative backscatter coefficient S did not vary through time, but slight variations of Ks can be observed in relation to some changes in the nature of suspended particles. Suspended sediment concentration profiles were obtained from 2 to 27 mab. This profile was completed between the bottom and the first cell of acoustical measurements (2 mab), using the Rouse equation, defining the vertical distribution of concentration c, in an open channel flow **(Rouse, 1937)**:

$$\frac{c}{c_a} = \frac{(h-y)}{y}.\left(\frac{a}{(h-a)}\right)^Z$$

where c_a is a reference concentration at a height a above the bed with a = y/h, h is flow depth, y is height above the bed, $Z = w_s / (ku_*)$ is the Rouse number, w_s is the particle settling

velocity (measured for 80 µm particles at the study site), k = 0.4 is the von Karman constant, and u_* is the shear velocity estimated from log-law velocity profile. Suspended sediment concentrations above 20 mab were not used because of air bubbles that confuse the measurements close to the sea surface.

4.4.2.6 Bed-level monitoring

ALTUS (NKE) sonic altimeters were deployed at 28 m water depth on the buoy site to measure bed-level variations from 30th September 2004 to 8th November 2005 (**Figure 4-28b**). Three deployment periods were investigated to monitor one whole year. The ALTUS instrument is a 2 MHz acoustic altimeter with a transmitter/receiver transducer (3.6° opening at -3 dB). The altimeters were independently mounted on light tripod frames at ~ 40 cm above the bed, preventing any sediment scouring under the transducer (**Bassoullet et al., 2000; Jestin et al., 1998**). The tripods legs were tightly screwed into the sediment. The separate battery container also hosts a pressure sensor, which allows to measure bed-level variations every 20 min during several months. Instrumented frames were deployed by SCUBA divers under the buoy. Each instrument was located 1 m in front of each helicoidal buoy anchor (**Figure 4-29**). Three altimeters were used during the first deployment (September 2004 to March 2005), and two for the following deployments because the memory of one altimeter was damaged during the first deployment. ALTUS altimeters show a 0.6 mm resolution in the 20-200 cm measurement range and 2 mm accuracy in the 20-70 cm range. Net erosion fluxes (integrating erosion and deposition) were calculated from the thickness of eroded sediment Δh through time and the sediment density ρ measured from sediment cores sampled during the 2003-04 (**Guillén et al., 2006**) and 2004-05 (this study) periods. The sediment density did not vary more than 10% during the study period, which was confirmed by in situ measurements from a benthic tripod deployed during one month on the study site (**Meuerer et al., submitted**). Sediment density was thus considered as constant during the 2004-05 period. Net erosion fluxes (EF) were calculated from:

$$EF = \frac{\rho.\Delta h}{\Delta t}$$

where Δt (= 20 min) is the sampling interval of the altimetric measurements.

EF were related to the effective shear stress due both to waves and currents τ_{cws}, calculated from the SEDTRANS model (**Li and Amos, 2001**).

4.4.2.7 Hydrodynamic modelling

The three-dimensional model SYMPHONIE was used to simulate dense water formation and cascading during the winter 2005. This model was previously used to study dense water cascading in the Gulf of Lions (**Dufau-Julliand et al., 2004**) and the effect of marine storms on the exportation of shelf water during winter 2004 (**Ulses et al., accepted**). The horizontal resolution was set at 1.5 km. Vertical resolution is refined near the surface and the seafloor. This high-resolution coastal simulation is nested in a 3-km resolution regional simulation with the same model, itself initialized and forced at its lateral open boundaries by the OPA model applied at the Mediterranean scale in the frame of the MFS project (http://www.bo.ingv.it/mfstep/). At the sea surface, air-sea fluxes were calculated from the atmospheric parameters calculated by the limited-area numerical weather prediction model ALADIN from Météo-France at the 0.1° resolution and from the SST of the ocean model through bulk formulae. The simulation was initialized in December 2004.

4.4.3 Results

4.4.3.1 External forcing

From October 2004 to October 2005, 72 windy days were recorded with mean daily wind speed > 10 m/s (and 204 days with mean daily wind speed > 5 m/s). The wind direction during these windy days was SE (Marin wind) for one day, and NW (Tramontane) for the 71 other days (**Figure 4-30a**). The NW wind is the main wind blowing in the southwestern part of the GoL that induces southwards alongshelf currents (**Estournel et al., 2003; Millot, 1976**). It is also responsible for the cooling and mixing of shelf water during winter, initiated at the coast and generating dense shelf water flowing along the slope to the shelf edge and the canyons (**Dufau-Julliand et al., 2004**).

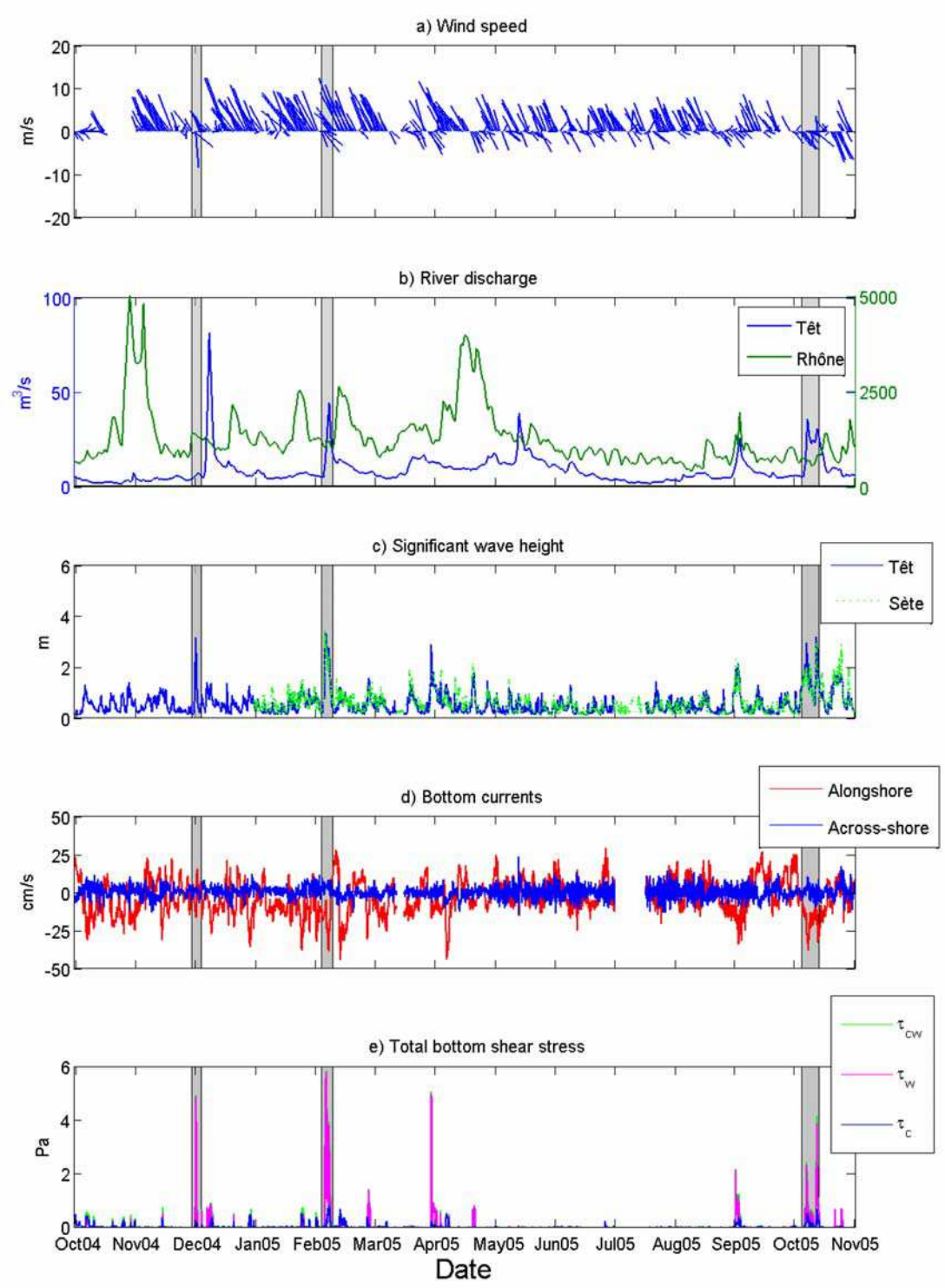

Figure 4-30 : a) Stick plot of wind speed and direction, b) time-series of daily discharge of the Têt and Rhône rivers, c) significant wave height at the Têt and Sète sites (Figure 4-28), d) near-bottom currents in the alongshore and across-shore directions, and d) bottom shear stresses due to currents alone (τ_c), waves alone (τ_w), and due to both currents and waves (τ_{cw}), estimated from SEDTRANS model (Li and Amos, 2001) measured at the buoy POEM at 28 m water depth from October 2004 to October 2005.

The Têt River is the main distributary of water and sediment to the coastal experimental site (28 m water depth). Between October 2004 and October 2005, the daily discharge varied from 1.5 to 81.2 m^3/s (**Figure 4-30b**). No significant flood event occurred during this period (Q = 180 m^3/s for 2-yr recurrence interval floods). The contribution of the Têt River to the coastal zone was very low compared to the previous year during which several extreme flood events occurred (**Bourrin et al., submitted**). No significant flood of the northern coastal rivers along the GoL coastline occurred. The Rhône River, the major input to the GoL, was however characterized by two periods of relatively high discharge in October 2004 and April 2005 with maximum daily discharges of 4500 and 3000 m^3/s respectively (2-yr recurrence interval flood = 5300 m^3/s).

4.4.3.2 Coastal measurements

4.4.3.2.1 Hydrology and temperature

The water temperature at 28 m water depth at the coastal site showed two different patterns during the study period (**Figure 4-31a**). The summer situation showed high water temperature (up to 22°C) during October 2004 and from May to the end of October 2005, cut by periods of variable temperature during episodes of strong continental winds. The autumn 2004 and winter 2005 periods showed a progressive decrease of the temperature down to 9°C, which produced a significant increase of the water density. Modelling indicated that the coastal water started to get denser than the offshore shelf water in late December when coastal water temperature decreased below 11.5 °C. Thus, the preconditioning phase (mixing and initial cooling of the shelf water) lasted from October to late December 2004, and the formation of dense shelf water lasted from January to early April 2005.

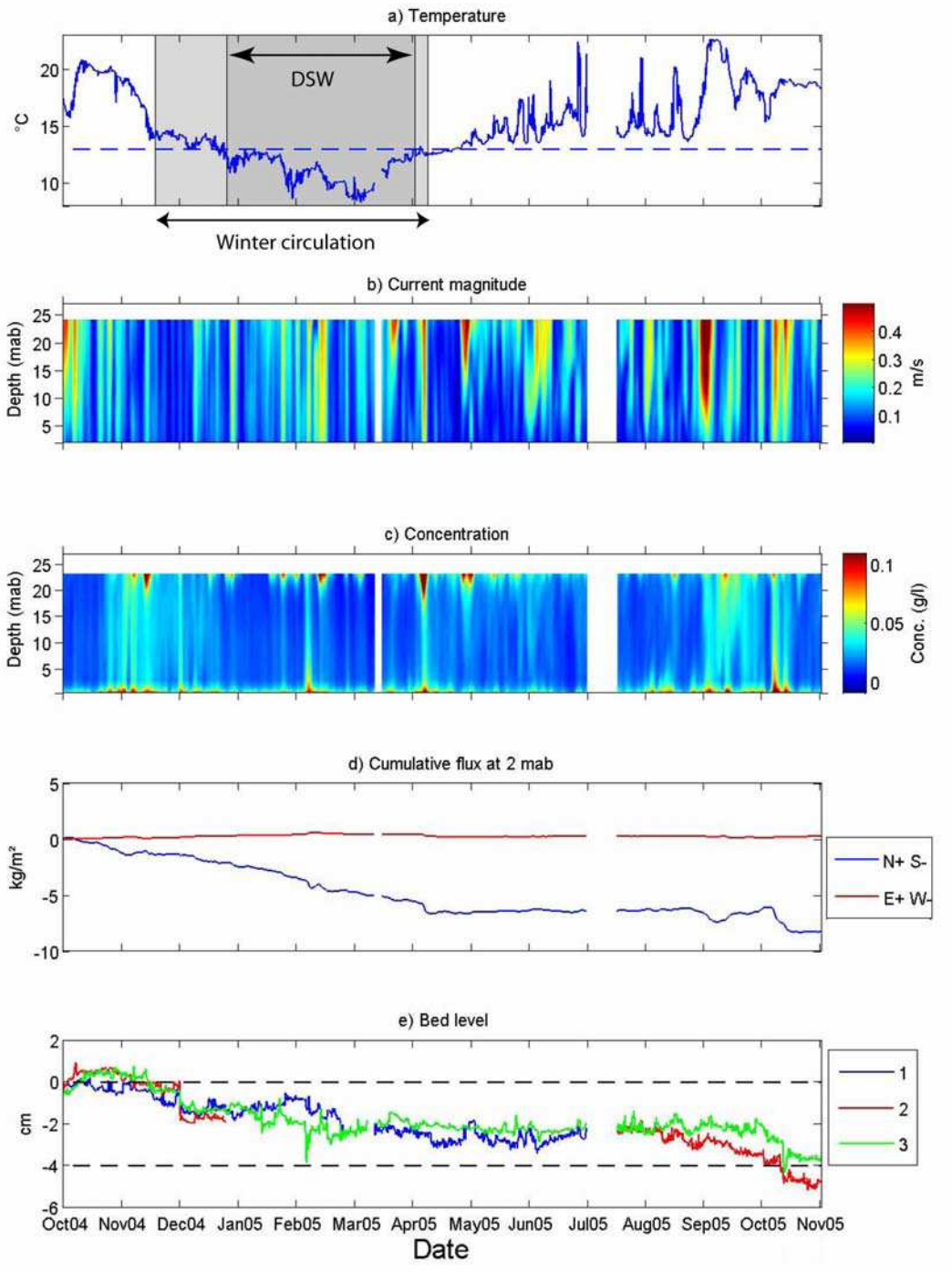

Figure 4-31 : a) Time-series of the temperature 2 mab, the dotted line is the temperature from which the water density at the coast overwhelm the water density on the shelf, b) colour plot of the current magnitude from 2 to 23 mab, c) colour plot of the concentration derived from acoustical measurements from 2 to 23 mab, d), cumulative suspended sediment horizontal fluxes measured at 2 mab and e) evolution of the seabed level measured at the Têt site at 28 m water depth.

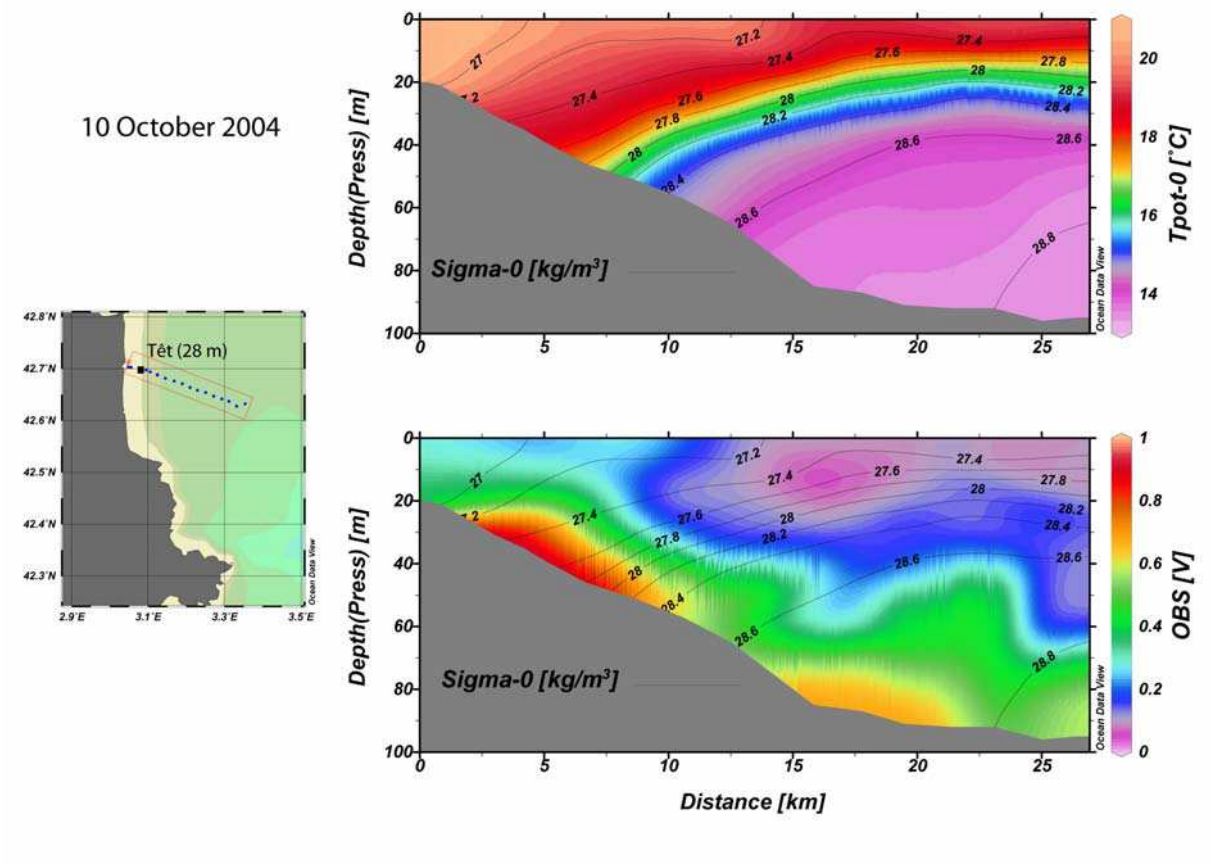

Figure 4-32 : Potential temperature (top) and turbidity (bottom) transects derived from CTD profiles made in October 10th 2004 from the Têt site to about 100 m water depth near the shelf edge. Data were plotted using the visualisation program Ocean Data View (Schlitzer, 2007).

CTD and turbidity data collected in October 2004 and February 2005 characterized the dramatic change of the hydrological conditions prevailing on the shelf, shifting from stratified conditions during summer and autumn to unstratified conditions during winter and early spring. The CTD transect in October 10th 2004 (**Figure 4-32**) showed a strong stratification both in temperature and density from the coast to the shelf edge. The thermocline appeared around 50 m water depth at 8 km from the coastline. Maximum temperature at the coast was up to 20°C and minimum was about 14°C below the thermocline around 100 m water depth.

Turbidity measurements revealed the presence of a benthic nepheloid layer of several meters above the bottom all across the shelf. The maximum turbidity area was located just above the thermocline between 25 and 55 m water depth. In February 22nd 2005 (**Figure 4-33**), the temperature distribution across the shelf showed two distinct areas separated by a stratification front located at a water depth of about 70 m. The coastal area was characterized

by homogenised temperature of 9.5-10°C. The deeper area showed warmer homogenised water temperature of 11-12°C. The turbidity distribution across the shelf was rather homogeneous (**Figure 4-33**).

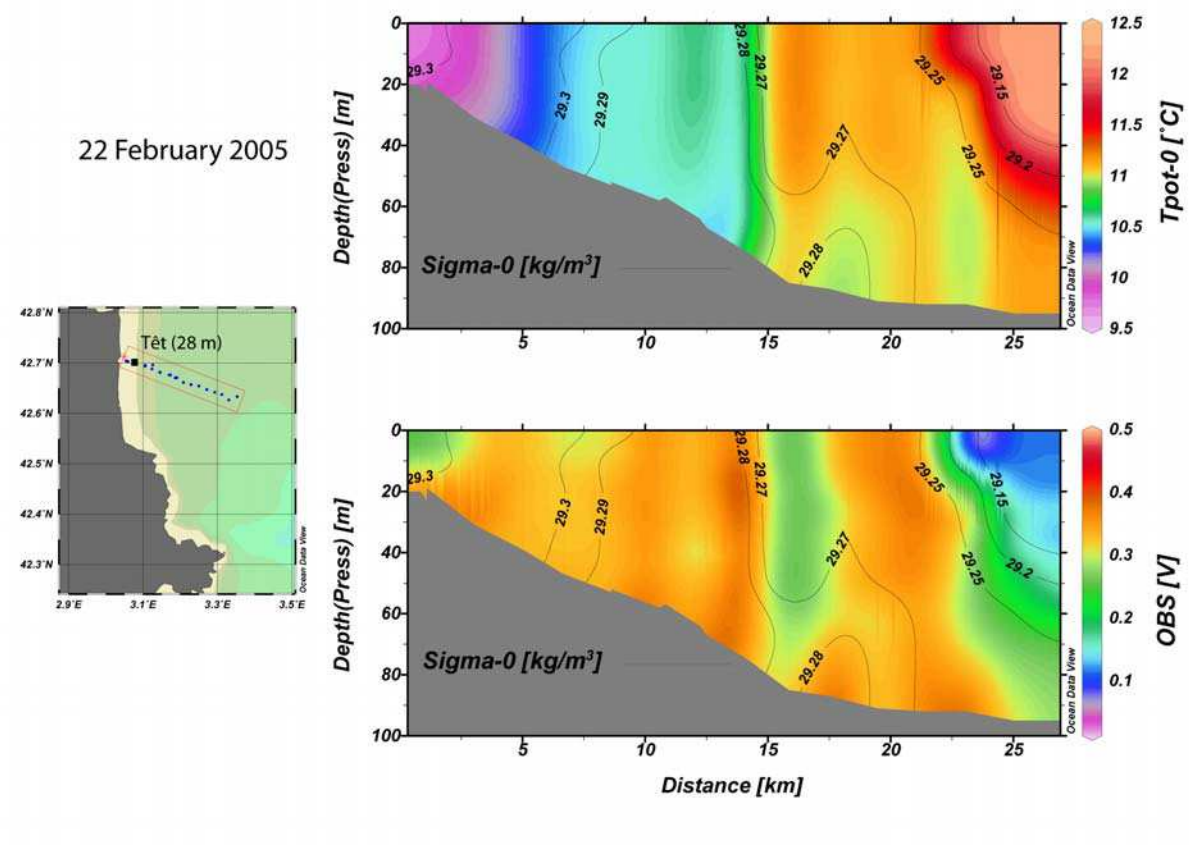

Figure 4-33 : Potential temperature and turbidity transect derived from CTD profiles made in February, 22nd 2005 from the Têt site to about 100 m water depth near the shelf edge. Data were plotted using the visualisation program Ocean Data View (Schlitzer, 2007).

4.4.3.2.2 Waves and currents

Waves are the main stirring mechanism causing bottom sediment resuspension in the Mediterranean Sea. Three storm events with significant wave height (Hs) > 3m and period (Tp) = 9 s were recorded during the study period (**Figure 4-30c**). These moderate storm events are usual in the GoL (Hs = 5.5 m for 2-yr recurrence return interval storm).

Bottom currents measured at the coastal site (POEM) during the study period are represented on **Figure 4-30d**. The alongshore current component was largely predominant over the cross-shore component. Currents measured at the coastal site were generally homogeneous over the water column during winter, indicating that the shelf water propagated along the inner shelf

mostly as a barotropic flow. Near-bottom currents (2 mab) were oriented mainly towards the south with a mean magnitude of 10 and 4 cm/s, in winter and summer respectively. Maximum near-bottom currents were observed in winter during short periods with maximum values up to 40 cm/s, and were directed southwards. From January to mid-April 2005, bottom currents were continuously > 20 cm/s.

Three events characterized by high total shear stress were observed through the monitoring period and having an impact on bottom SSC, fluxes and seabed level (**Figure 4-30e**). Two of these events occurred during the winter period 2004-05 (November 2004 and February 2005) and the other one in October 2005 and were associated to E-SE storm events. The shear stress due to currents (τ_c) exceeded the shear stress due to waves (τ_w) for most of the monitoring period. τ_c exceeded the critical value for sediment resuspension (τ_{crit} = 10 cm/s, D_{50} = 80 µm) for more than 10% of the time in winter.

4.4.3.2.3 Suspended sediment concentration, cumulative fluxes and seabed level monitoring

Estimated near-bed SSC (0.1 mab) at the POEM site varied from a few mg/L to about 1.5 g/L during high wave and current speed events (**Figure 4-31c**). Suspended sediment concentrations rapidly decreased with increasing distance from the seabed. Maximum SSC at 1 and 10 mab reached 0.21 and 0.08 g/L respectively during energetic events. Suspended sediment fluxes measured at 2 mab (**Figure 4-31d**) showed that the across-shelf component was negligible, whilst the alongshelf southward component continuously increases through the winter period 2004-2005. Suspended sediment fluxes were stable in summer and the increasing southward trend started again in October 2005 at the end of the monitoring period.

Seabed level measurements showed a net sediment erosion of about 4 to 5 cm between October 2004 and October 2005 (**Figure 4-31e**). This trend was observed for all altimeters located under the buoy at the POEM site. After a low sediment accretion period in October 2004, sediment erosion of about 2 cm was observed from November 2004 to February 2005. The spring-summer period (March to August 2005) was characterized by a relative stability of the bed level. A second period of sediment erosion of about 2 cm was then observed at the end of the monitoring period (September-October 2005). The largest variations occurred during the mild storms (with higher wave energy) in November 2004, February and October

2005 (**Figure 4-31e**). Net sediment erosion of about 1 cm was measured after these events except in February when no significant change was observed.

4.4.4 Discussion

4.4.4.1 Seasonal and interannual variability of shelf sediment erosion

Seabed level variations monitored at the coastal site (Têt prodelta) show a strong seasonality. Seabed erosion only occurred during autumn and winter. Comparison with the hydrodynamical forcing (**Figure 4-31**) reveals two different regimes associated to waves and currents (E-SE storms), or to currents alone (cold dense shelf water – DSW - flow). Whereas storm events induced brief (~ 1 d) and large (~ 1 cm) changes of the seabed level, the strong and prolonged (~ 2 months: Jan. – Feb. 2005) alongshore DSW flow induced a slow but continuous erosion (~ 2 cm) of the seabed. The relatively stability observed in summer suggests that there is no significant erosional trend - because of the absence of storm event and the weakness of the near-bottom currents - and therefore no significant deposition, deriving from river input or settling of marine biological material.

During the 2004-05 autumn and winter periods, the DSW flow appears as the predominant erosion mechanism. During the previous 2003-04 autumn and winter periods, at the same coastal site, **Guillén et al. (2006)** showed that the sediment erosion by storms largely exceeded the sediment erosion by currents alone. Large storms provoked sediment erosion of up to 5 cm, generally followed by a deposition of similar amplitude (**Figure 4-34**). The net erosion of the seabed during both periods varied between ~ 1 cm in Nov 2003 – Mar 2004 and 4 cm in Sept 2004 – Nov 2005 (**Figure 4-34**).

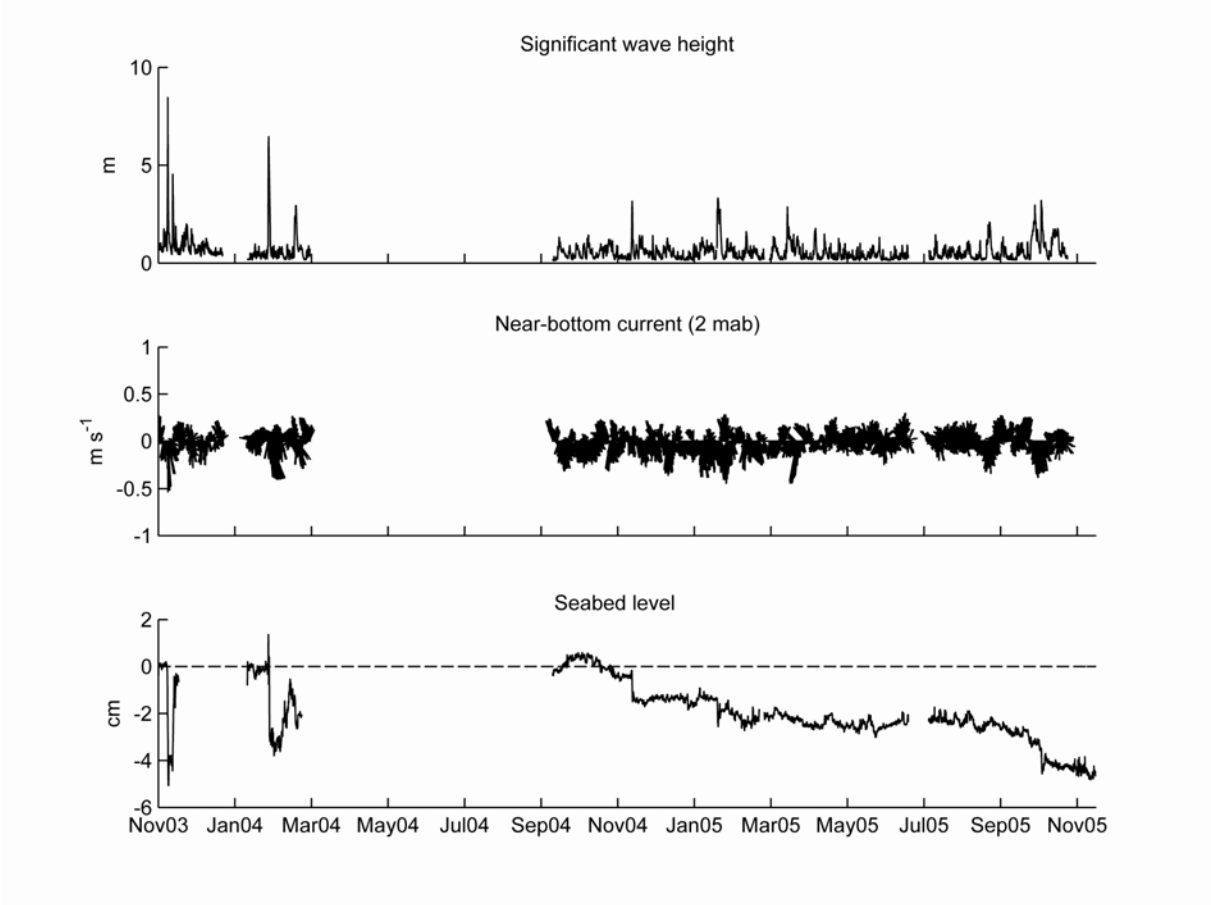

Figure 4-34 : a) Significant wave height, b) near-bottom currents and c) mean seabed level measured at the Têt site during monitoring periods 2003-04 and 2004-05.

It is worthy to note that the 2003-04 and 2004-05 periods are distinguished by unusually energetic hydro-climatic conditions. The 2003-04 autumn and winter periods were characterized by two large (Hs > 7 m) and 3 moderate (Hs > 3 m) storms as well as several extreme floods of the Rhône and the coastal rivers. Mild dense shelf water formation took place during that period (**Ulses et al., accepted**). The 2004-05 autumn and winter periods were characterized by very intense dense shelf water formation and only two moderate storms. The typical interval return period of extreme dense shelf water formation (**Béthoux et al., 2002; Canals et al., 2006**) and of extreme storm (Hs > 7 m) events in the GoL is between 5 and 10 years. Extreme flood events such as the Dec. 2003 Rhône flood event, has an interval return period of about 100 years. Thus, the 2003-04 and 2004-05 experiments allowed us to assess the impact of extreme events on the seabed level. The centimetric annual erosion induced by these extreme events is likely to be the main factor that restrict the secular sedimentation rate, estimated in the Têt inner-shelf to ~0.1 cm/yr (**Bourrin et al., in press**),

despite the local and upstream rivers inputs. This fact also suggests that accretion should dominate during less energetic periods to balance the erosion observed during these two consecutive years.

4.4.4.2 Net erosion fluxes, suspended sediment concentration and transport

Altimetric measurements allowed us to estimate the EF for the mixed sediment at the coastal station (sand fraction = 65 - 70 % and porosity = 60 – 70 % in the 0-2 cm layer) for a large range of bottom shear stress (0-9 Pa). The effective bottom shear stress range was much higher in 2003-04 (0-9 Pa) than in 2004-05 (0-1 Pa). Considering the whole data set (**Figure 4-35a**), one observes a rapid increase of EF up to 1.2 g/m²/s with increasing τ_{cws} up to 2 Pa. Beyond that limit, the increase of EF with bottom shear stress is lower and reached 1.8 g/m²/s for τ_{cws} = 9 Pa. Bed armouring, which limits the amount of fine-grained sediment available for resuspension, could be one reason to explain the lower increase of EF at high shear stress (**Wiberg et al., 1994**). **Ferré et al. (2005)** suggested from numerical simulations on a shallower and sandier site close to the present study site, the impact of the bed armouring on the bottom sediment. During a storm event, the bed armouring limits the resuspension of fine-grained sediment after the winnowing of the superficial sediment layer.

Net erosion fluxes for the 2003-04 period are 3 to 4 times lower than the 2004-05 period at low bottom shear stress (τ_{cws} < 0.5 Pa, **Figure 4-35b**), but are comparable for higher shear stress (up to 1 Pa) (**Figure 4-35a**). This different behaviour at low shear stress could result from the change in the surface sediment porosity, which significantly varied during the 2003-04 period as a results of floods and storms (**Bourrin et al., in press**) but were rather constant during the 2004-05 period (**Meuerer et al., submitted**). Fine-grained sediment deposits consecutive to flood events and reworking of the sediment by storms temporarily increase the surface layer porosity and thus enhance the subsequent resuspension at low shear stress. This difference vanishes at higher shear stress as the thickness of the eroded layer increases and reaches level where sediment porosity is more constant.

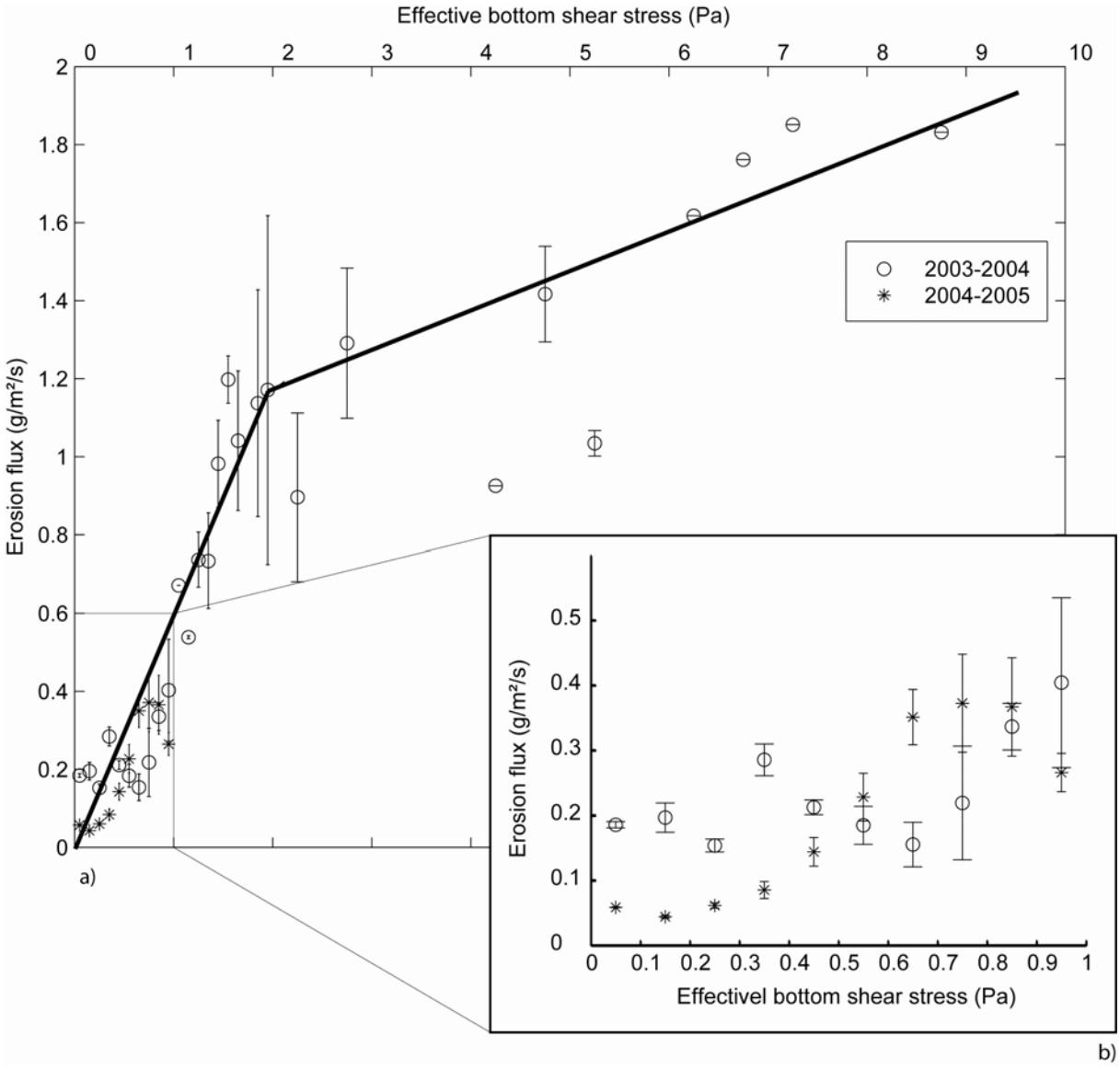

Figure 4-35 : Plot of the net erosion fluxes (EF) versus the effective bottom shear stress estimated from SEDTRANS model, and measured at the Têt site during monitoring periods 2003-04 and 2004-05. a) 0-10 Pa range and b) zoom on 0-1 Pa range.

The two major resuspension regimes (moderate storms, or currents alone) observed during the 2004-05 experiment have a different response in terms of SSC in the water column. While significant increases of SSC are observed within the last 10 mab during storm-induced resuspension, no significant increases of SSC are observed during the prolonged erosion phase induced by dense shelf water flow (**Figure 4-31c**). However, the impact of the latter mechanism is well evidenced on the sediment transport (**Figure 4-31d and Figure 4-31e**). Net erosion and alongshore sediment transport during the winter 2004-05 show very similar trends. Storm-induced resuspension and subsequent SSC increase do not affect significantly

the seasonal trend of the alongshore transport. During that winter, resuspension and transport associated to dense shelf water flow dominates the sediment dynamics on the Têt inner-shelf. The cumulative alongshore suspended sediment transport during the Nov. 04 – Mar 05 period was estimated to ~ 0.5 t/m² at 0.15 mab. This value has to be compared with the 13 and 16 t/m² at 0.15 mab estimated during the extreme storms of Dec. 03 and Feb. 04 respectively (**Guillén et al., 2006**). These latter values, which probably represent the upper range of the alongshore sediment transport associated to extreme hydrodynamical conditions, clearly evidence the predominant impact of extreme storms on the sediment transport. Nevertheless, in view of the comparable sediment thickness (few cm) eroded by both type of events, it is likely that the discrepancy between storm-induced and DSW -induced sediment transport results from the area affected by this events upstream of the Têt shelf. Storms impact on the entire inner-shelf of the GoL (**Ulses et al., submitted**), and the cyclonic alongshore current - which incorporates the resuspended sediment all along its pathway – yields a large transport on the Têt shelf. Conversely, as it will be shown in the next paragraph, the region impacted by DSW upstream of the Têt shelf has a lower expansion that limits the downstream increase of suspended sediment transport.

4.4.4.3 Region impacted by dense shelf water flows

Hydrodynamical modelling made during the study period allows to investigate the expanse and variability of the DSW plume (**Figure 4-36 and Figure 4-37**). The two consecutive daily snapshots of temperature and velocity flow field 10 mab at the Gulf scale (**Figure 4-36c and Figure 4-36d**), illustrate the typical features of this current. Both outputs evidence the presence of cold and dense water along the coast.

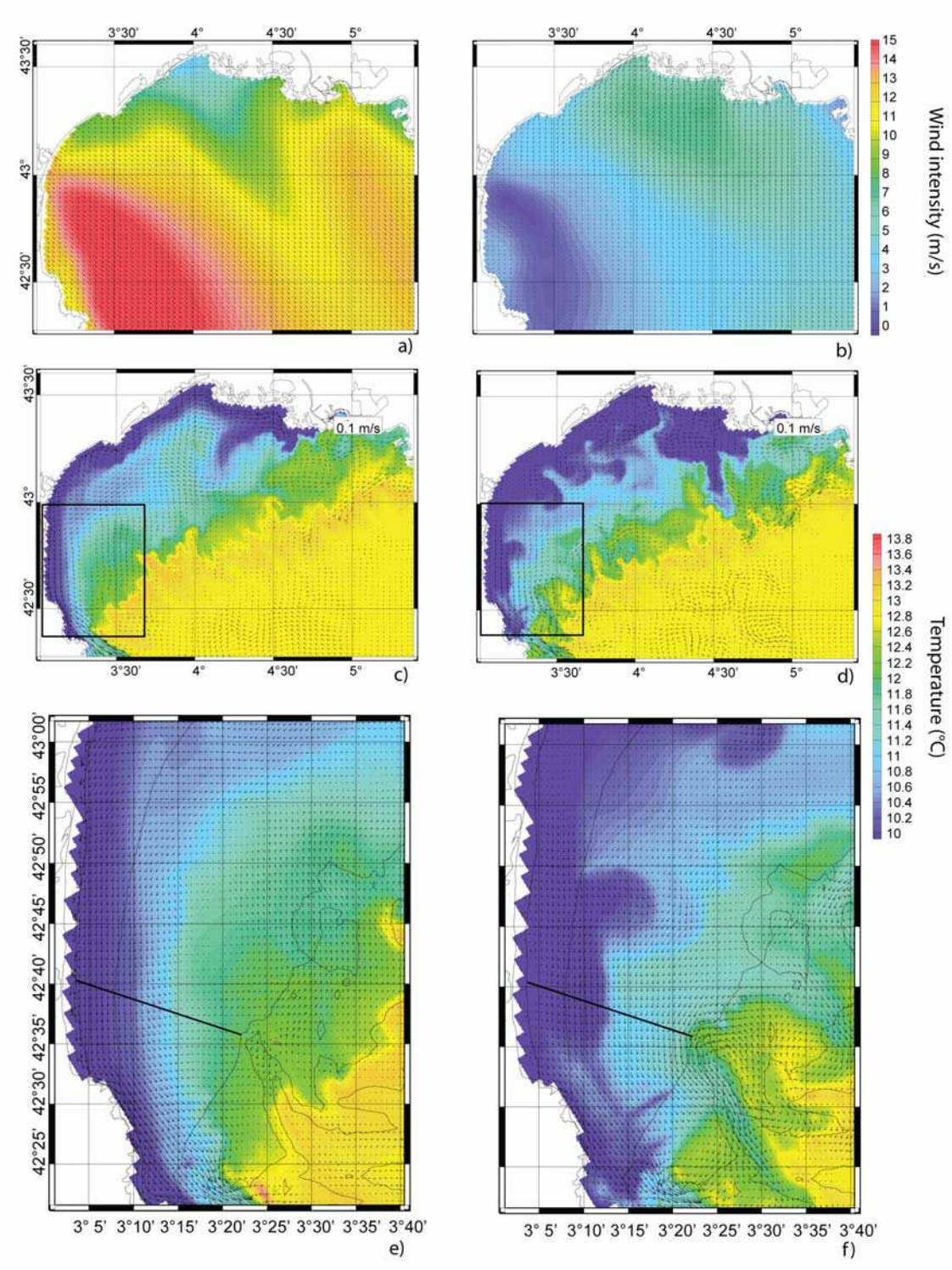

Figure 4-36 : a), b) Wind field over the Gulf of Lions for two contrasted conditions (19 and 26 February 2006); c), d) corresponding current field and temperature at 10 mab over the Gulf of Lions' shelf, and e), f) corresponding current field and temperature at 10 mab on the southwestern part of the Gulf.

The dispersal of this shallow water is controlled by several mesoscale circulations. In the southwestern part of the Gulf, a well defined southwards coastal current, starting around 43°N

(**Figure 4-36c and Figure 4-36d**) advects the cold and dense water formed near the shore. The intensity of the alongshore component of the DSW core is about 4 cm/s on the Têt shelf, and increase significantly near the Cap de Creus headland due to the narrowing of the shelf. (**Figure 4-36e and Figure 4-36f**).

The width of the core on the Têt shelf is clearly influenced by the presence or absence of a northwards wind-driven counter-current on the outer shelf, which originates from the intrusion of slope waters near the Lacaze-Duthiers Canyon. The decrease of the Tramontane intensity at one week interval (**Figure 4-36a and Figure 4-36b**), leads to the vanishing of counter current and to the widening of the southward DSW flow from the 30 to the 50 m isobath (**Figure 4-36e and Figure 4-36f**). The sequence of temperature and currents shown in **Figure 4-37** illustrates the fluctuations of the cross-shelf width of the DSW core during a 2-week period (Feb. 15 – Mar. 1, 2005) encompassing the hydrological observations (Feb. 22) depicted in **Figure 4-33**. It shows the progressive transition between an initial situation, with a strong northwards counter-current that confined the DSW core to the 30 m isobath, to a final situation where a bottom DSW plume reached the 90 m isobath. The offshore extension of the bottom plume started with the weakening of the northwards counter-current, which cannot balance the cross-isobath component of the DSW flow. This plume eventually separates from the main DSW core on the inner shelf to form a distinct filament on the mid and outer shelf. These results show that while the inner-shelf of the southwestern gulf is continuously affected by the DSW flow, the mid and outer shelves are affected only intermittently. During these latter episodes, the alongshore suspended sediment transport is likely to be larger since the DSW flow impacts the more easily erodible mid-shelf mud belt.

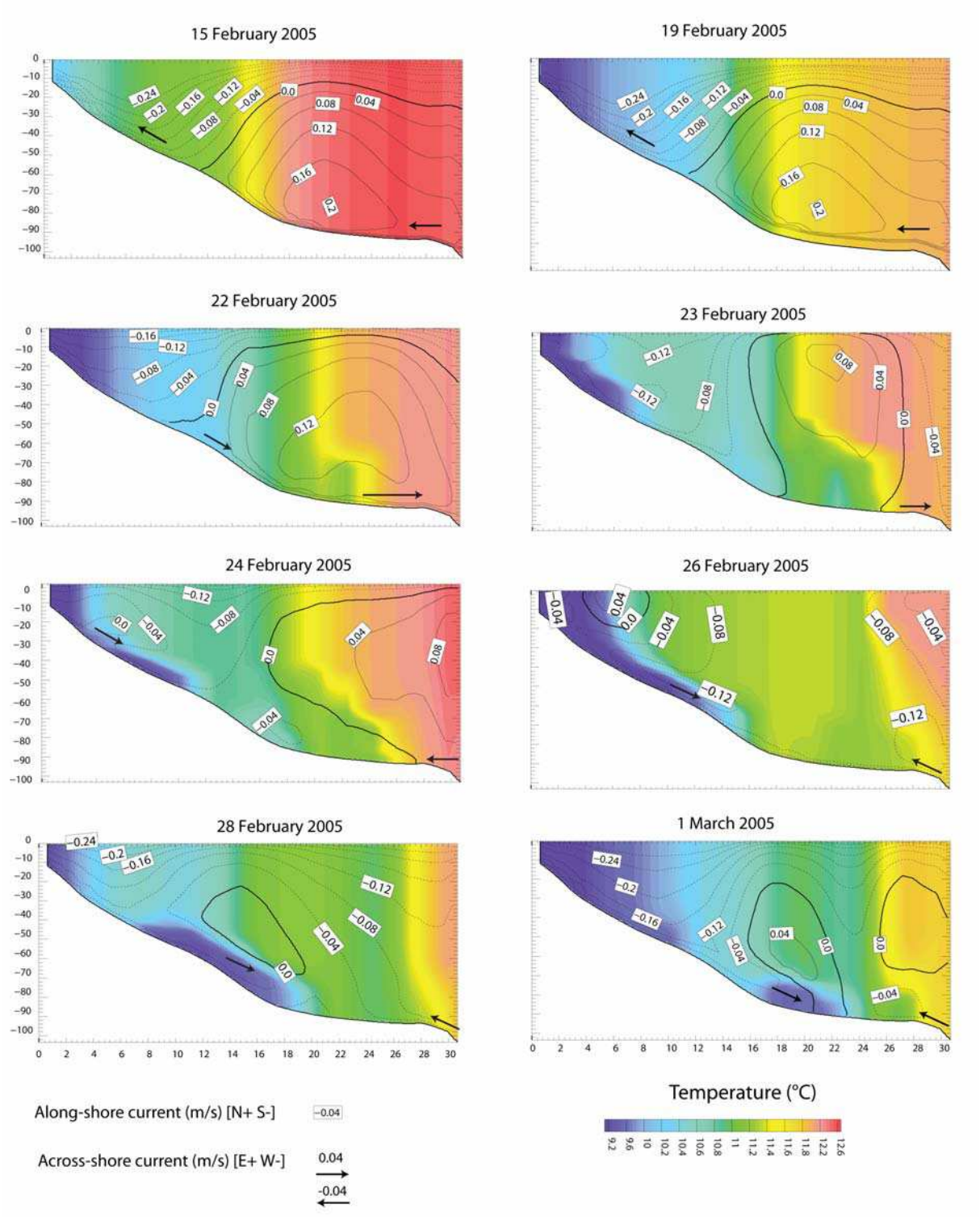

Figure 4-37 : Temperature and currents transects from 15th February 2005 to 1st March 2005, across the Roussillon's shelf (position of the transect on Figure 4-36e and Figure 4-36f).

Coastal measurements of temperature, current and sediment transport are well correlated to measurements made in the head of the southwestern Lacaze-Duthiers and Cap de Creus Canyons (**Ogston et al., submitted; Puig et al., submitted)**, confirming the potential of

DSW flows to carry and resuspend sediment. Moreover, **Ogston et al. (submitted)** show that DSW flows were more episodic and weaker in the Lacaze-Duthiers Canyon that in the Cap de Creus Canyon; emphasizing the preferential pathway of DSW flow toward the southern end of the GoL. **Puig et al. (submitted)** show the impact of DSW flows on the seabed erosion deeper in the Cap de Creus Canyon.

4.4.5 Conclusion

This paper investigated the impact of winter wind-driven circulation and cold dense water flows on the sediment dynamics on the Têt prodelta in the southwestern Gulf of Lions' shelf. The most important findings of this work are the following:

- Sediment erosion of several centimetres occurred on the Têt prodelta during the winter period 2004-05 due to the strong wind-driven current flowing southwards along the coast. During winter, this current transforms into a gravity current due to the large cooling and subsequent increase of its density. This winter was an unusual cold and dry winter that only occurred 3 times in the last decade. Conversely, sediment erosion measured at the same site during the previous winter 2003-04, an unusual winter with extreme storms and floods, was nearly balanced by river inputs. During these two consecutive winters, the Têt prodelta underwent a net erosion of ~ 4 cm that is much higher and opposite to the local secular apparent sedimentation rate (~ 0.1 cm/yr).
- Net erosion fluxes were measured in situ at high and very high effective shear stresses compared to those measured in laboratory. Net erosion fluxes for the lower shear stresses (0 – 2 Pa) clearly appear to depend on the sediment history, whereas they are more constant at higher shear stresses. The largest net erosion fluxes, which are linked to the extreme storm events, are possibly limited by bed armouring.
- Severe dense shelf water flow is an important winter mechanism for sediment erosion and southwards alongshore transport. The area impacted by dense shelf water flows is variable, depending on the wind-driven circulation on the shelf. The DSW core continuously eroded the inner-shelf but impacted more episodically the mid and outer-shelf. Dense shelf water flow measurements on the shelf are well correlated to contemporary measurements made in the southwestern canyons of the Gulf.

Acknowledgements

The authors acknowledge the support of the SysCoLag program from the Regional Council of Languedoc-Roussillon and the EC-funded program EuroStrataform (EVK3-CT-2002-00079, EU Fifth Framework Program: Energy, Environment and Sustainable Development). They warmly thank the captain and crews of the R/V Téthys II, Oceanus and Endeavor. Special thank is addressed to the technical staff of CEFREM.

References

Aloïsi, J.C., Got, H., Monaco, A., 1973. Carte géologique du précontinent languedocien au 1/250000ième., International Institute for Aerial Survey and Earth Sciences (I.T.C.) (Eds.), Netherlands.

Bassoullet, P., Le Hir, P., Gouleau, D., Robert, S., 2000. Sediment transport over an intertidal mudflat: field investigations and estimation of fluxes within the "Baie de Marennes-Oleron" (France). Continental Shelf Research, 20 (12-13): 1635-1653.

Berné, S., Satra, C., Aloïsi, J.C., Baztan, J., Dennielou, B., Droz, L., Dos Reis, A.T., Lofi, J., Méar, Y., Rabineau, M., 2002. Carte morphobathymétrique du Golfe du Lion, notice explicative. Ifremer, Brest.

Béthoux, J.P., Durrieu de Madron, X., Nyffeler, F., Tailliez, D., 2002. Deep water in the western Mediterranean: peculiar 1999 and 2000 characteristics, shelf formation hypothesis, variability since 1970 and geochemical inferences. Journal of Marine Systems, 33-34: 117-131.

Bourrin, F., Friend, P.L., Amos, C.L., Thompson, C.E.L., Manca, E., Durrieu De Madron, X., Ulses, C., submitted. An Oceanic Flood in a microtidal, Storm dominated basin: the Têt, Gulf of Lions (NW Mediterranean, France). Continental Shelf Research.

Bourrin, F., Monaco, A., Aloïsi, J.-C., Sanchez-Cabeza, J.-A., Lofi, J., Heussner, S., de Madron, X.D., Jeanty, G., Buscail, R., Saragoni, G., in press. Last millennia sedimentary record on a micro-tidal, low-accumulation prodelta (Têt NW Mediterranean). Marine Geology.

Canals, M., Puig, P., de Madron, X.D., Heussner, S., Palanques, A., Fabres, J., 2006. Flushing submarine canyons. Nature, 444 (7117) : 354-357.

Curran, K.J., Hill, P.S., Milligan, T.G., Mikkelsen, O.A., Law, B.A., Durrieu de Madron, X., Bourrin, F., 2007. Settling velocity, effective density, and mass composition of

suspended sediment in a coastal bottom boundary layer, Gulf of Lions, France. Continental Shelf Research, 27: 1408-1421.

DeGeest, A.L., Mullenbach, B.L., Puig, P., Nittrouer, C.A., Drexler, T.M., Durrieu de Madron, X., Orange, D.L., submitted. Sediment accumulation in the western Gulf of Lions, France: The role of Cap de Creus Canyon in linking shelf and slope sediment dispersal systems. Continental Shelf Research.

Drake, D.E., 1976. Suspended sediment transport and mud deposition on continental shelves. In: D.J. Stanley, Swift, D.J.P. (Editor), Marine Sediment Transport and Environmental Management. Wiley-Interscience Publication, pp. 602.

Dufau-Julliand, C., Marsaleix, P., Petrenko, A., Dekeyser, I., 2004. 3D Modeling of the Gulf of Lion's Hydrodynamics (NW Med.) during January 1999 (MOOGLI3 Experiment) and Late Winter 1999: Western Mediterranean Intermediate Water (WIW)'s Formation and Its Cascading over the Shelf Break. Journal of Geophysical Research, 109 (C11).

Estournel, C., Durrieu de Madron, X., Marsaleix, P., Auclair, F., Julliand, C., Vehil, R., 2003. Observation and modeling of the winter coastal oceanic circulation in the Gulf of Lion under wind conditions influenced by the continental orography (FETCH experiment). Journal of Geophysical Research, 108 (C3): 8059, doi: 10.1029/2001JC000825.

Ferré, B., Guizien K., Durrieu de Madron X., Palanques A., Guillén J., Grémare, A., 2005. Fine-grained sediment dynamics during a strong storm event in the inner-shelf of the Gulf of Lion (NW Mediterranean). Continental Shelf Research, 25: 2410-2427.

Guillén, J., Bourrin, F., Palanques, A., Durrieu de Madron, X., Puig, P., Buscail, R., 2006. Sediment dynamics during wet and dry storm events on the Têt inner shelf (SW Gulf of Lions). Marine Geology, 234 (1-4) : 129-142.

Guillén, J., Palanques, A., Puig, P., Durrieu De Madron, X., Nyffeler, F., 2000. Field calibration of optical sensors for measuring suspended concentration in the western Mediterranean. Scientia Marina, 64 (4) : 427-435.

Jestin, H., Bassoullet, P., Le Hir, P., L'Yavanc, J., Degres, Y., 1998. Development of ALTUS, a high frequency acoustic submersible recording altimeter to accurately monitor bed elevation and quantify deposition or erosion of sediments., Oceans'98-IEEC/OES Conference, Nice (France), pp. 189-194.

Land, J.M., Bray, R.N., 2000. Acoustic measurement of suspended solids for monitoring of dredging and dredged material disposal. Journal of Dredging Engineering, 2 (3): 1-17.

Li, M.Z., Amos, C.L., 2001. SEDTRANS96: the upgraded and better calibrated sediment-transport model for continental shelves. Computers & Geosciences, 27: 619-645.

Meuerer, A.M., Wiberg, P.L., Wheatcroft, R.A., Milligan, T.G., Law, B., Hill, P.S., submitted. Across-shelf variations in erodibility, bed properties and sediment transport potential in the western Gulf of Lions. Continental Shelf Research.

Milliman, J.D., Meade, R.H., 1983. World-wide delivery of sediment to the oceans. Journal of Geology, 91 (1): 1-21.

Milliman, J.D., Syvitski, J.P.M., 1992. Geomorphic/Tectonic Control of Sediment Discharge to the Ocean: The Importance of Small Mountainous Rivers. Journal of Geology, 100, 5: 525-544.

Millot, C., 1976. Specific features of the sea-shore circulation near Cap Leucate. Mémoires Société Royale des Sciences de Liège, 6e série (tome X) : 227-245.

Ogston, A., Drexler, T.M., Puig, P., submitted. Sediment delivery, resuspension, and transport characterizing canyon environments in the southwest Gulf of Lions. Continental Shelf Research.

Palanques, A., Durrieu de Madron, X., Puig, P., Fabres, J., Guillén, J., Calafat, A., Canals, M., Heussner, S., Bonnin, J., 2006. Suspended sediment fluxes and transport processes in the Gulf of Lions submarine canyons. The role of storms and dense water cascading. Marine Geology, 234 (1-4): 43-61.

Puig, P., Palanques, A., Orange, D., Canals, M., submitted. Dense shelf water cascading and furrows formation in the Cap de Creus submarine canyon, northwestern Mediterranean margin. Continental Shelf Research.

RD Instruments, 1996. Acoustic Doppler Current profilers - Principles of Operation: A Practical Primer, RD Instruments, San Diego, Ca., USA.

RD Instruments, 2001. Waves User's Guide.

Rouse, H., 1937. Modern conceptions of the mechanics of fluid turbulence. Transactions of the American Society of Civil Engineering, 102 (463-554).

Schlitzer, R., 2007. Ocean Data View, http://odv.awi.de.

Ulses, C., Estournel, C., Bonnin, J., Durrieu de Madron, X., Marsaleix, P., accepted. Impact of storms and dense water cascading on shelf-slope exchanges in the Gulf of Lion (NW Mediterranean). Journal of Geophysical Research.

Ulses, C., Estournel, C., Durrieu de Madron, X., Palanques, A., submitted. Suspended Sediment Transport in the Gulf of Lion (NW Mediterranean): Impact of Extreme Storms and Floods. Continental Shelf Research.

Urick, R.J., 1975. Principles of Underwater Sound. McGraw Hill, N.Y., 384 pp.

Wiberg, P.L., Drake, D.E., Cacchione, D.A., 1994. Sediment resuspension and bed armoring during high bottom stress events on the northern California inner continental shelf: measurements and predictions. Continental Shelf Research, 14 (10-11) : 1191-1219.

Dans les **chapitres 4.2, 4.3 et 4.4** nous avons caractérisé l'impact des évènements hydro-climatiques extrêmes sur la dynamique sédimentaire du prodelta de la Têt grâce à des mesures haute-fréquence. Deux hivers particulièrement intenses du point de vue hydrodynamique ont été suivis. L'hiver 2003-2004 (**chapitres 4.2 et 4.3**) a été caractérisé par 2 tempêtes extrêmes (décembre 2003 et février 2004) et 3 tempêtes modérées (décembre 2003, mars et avril 2004), ainsi que par 2 crues extrêmes du fleuve Têt (décembre 2003 et avril 2004). L'hiver 2004-2005 a été caractérisé par une circulation côtière intense induite par les forts vents continentaux entre décembre 2004 et avril 2005, et par la formation et l'écoulement d'eaux denses depuis la zone côtière jusque sur le plateau et son extrémité sud-ouest où se situent les canyons du Cap de Creus et du Lacaze-Duthiers.

Les résultats principaux de cette quatrième partie sont les suivant :

1. Les tempêtes extrêmes de l'hiver 2003-2004 sont capables de créer une érosion du fond sédimentaire du prodelta de la Têt sur une épaisseur de 4 cm (**chapitre 4.2**). Les tempêtes modérées peuvent créer de l'érosion ou de l'accrétion suivant l'histoire des événements hydro-climatiques précédents. Un dépôt de crue a été observé après une crue généralisée des fleuves de l'ensemble du golfe du Lion. Ce dépôt a été rapidement remanié par une tempête déplaçant ce matériel sédimentaire depuis le prodelta vers la vasière médiane du plateau et le large. Les évènements de tempêtes d'E-SE sont les acteurs majeurs de la resuspension et du transport du matériel fin vers le S-SE le long du littoral roussillonnais.
2. Le suivi d'un épisode de crue isolé au système Têt-littoral roussillonnais a été observé en avril 2004 (**chapitre 4.3**). Il a été mis en évidence que le fleuve Têt peut transporter une quantité importante de sable à la zone côtière pendant les crues torrentielles. Le sable se dépose dans la zone côtière au niveau du delta de la Têt et est mobilisé par les fortes houles de tempêtes le long du littoral vers le nord. Le matériel fin apporté par les crues est quant à lui transporté vers le sud : une partie se dépose dans la zone littorale et le reste est transporté sous la forme d'un panache de surface vers le sud et les canyons à l'extrémité du plateau.
3. Le suivi haute-fréquence de l'hiver 2004-2005 a montré que la circulation hivernale intense et la formation d'eaux denses sur le plateau était un autre processus hydro-climatiques intenses agissant sur la dynamique sédimentaire du prodelta de la Têt (**chapitre 4.4**). L'érosion créée par les tempêtes extrêmes a été équilibrée par les

apports fluviaux durant l'hiver 2003-2004. Par contre, l'hiver 2004-2005 a été caractérisé par une érosion nette de plusieurs centimètres du fond du prodelta de la Têt. La résultante nette sur ces deux hivers extrêmes est négative (~ - 4 cm) et contraste avec les taux de sédimentation mesuré (**chapitre 4.1**, ~ 0.1 cm/an). Les flux net d'érosion dépendent de l'histoire des évènements hydro-climatiques précédents pour les faibles contraintes de cisaillement et ils semblent être limités par la quantité de matériel fin disponible dans les sédiments (pavage) pour les contraintes plus importantes. Enfin, les eaux denses formées dans la zone côtière du plateau roussillonnais s'écoulent le long du littoral du nord vers le sud. Elles érodent ainsi continuellement la zone côtière mais peuvent affecter le plateau médian et extérieur suivant les conditions de vent. L'écoulement des eaux denses mesurées sur le plateau est confirmé par les mesures faites dans les têtes de canyon du sud-ouest du golfe du Lion.

La dynamique sédimentaire a été suivie à haute fréquence sur le prodelta de la Têt durant deux hivers extrêmement énergétiques mais différents en termes de processus. Ces deux années sont caractérisées par une érosion nette du fond sédimentaire du prodelta de la Têt qui est à opposer aux taux de sédimentation d'ordre séculaire mesurés dans cet environnement dynamique. Ces taux de sédimentation sont estimés à partir des mesures de ^{210}Pb dans les sédiments et d'un modèle basé sur un taux constant d'apport (**Goldberg, 1963**). Ce modèle est utilisé par défaut car considéré comme induisant le moins d'erreurs. Mais que signifient ces taux de sédimentation dans un environnement aussi énergétique que celui du prodelta de la Têt ? Quel est l'enregistrement du signal sédimentaire du prodelta de la Têt aux échelles séculaire et pluriséculaire ? Et enfin, comment cet enregistrement sédimentaire, s'il y en a un, évolue en fonction des modifications anthropiques de la zone côtière et du changement climatique global ? Nous essaierons de répondre à ces questions dans le **chapitre 4.5**.

4.5 Enregistrement sédimentaire des derniers milliers d'années sur un prodelta à faible taux d'accumulation dans une mer sans marée

Last millennia sedimentary record on a micro-tidal, low-accumulation prodelta (Têt, NW Mediterranean)

François Bourrin[1*]	Redaction, Data (grain-size and sequential analysis)
André Monaco[1]	Redaction
Jean-Claude Aloïsi[1]	Redaction
Joan-Albert Sanchez-Cabeza[2]	Manuscript revision and Data (^{14}C analysis)
Johanna Lofi[3]	Manuscript revision
Serge Heussner[1]	Manuscript revision
Xavier Durrieu de Madron[1]	Manuscript revision
Gérard Jeanty[1]	Data (^{210}Pb and estimation of sedimentation rates)
Roselyne Buscail[1]	Data (Sediment cores analysis)
Gilles Saragoni[1]	Sediment cores recovery by scuba diving

[1]Centre de Formation et de Recherche sur l'Environnement Marin
UMR 5110 CNRS - Université de Perpignan Via Domitia
52, Avenue Paul Alduy - 66860 Perpignan Cedex, France
[2]IAEA-Marine Environment Laboratories
4, Quai Antoine 1er - MC 98000 Monaco
[3]LGHF ISTEEM
CC56 - Université Montpellier 2 - 34095 MONTPELLIER cedex 05

Soumis le 19/12/2006 *Marine Geology*
Accepté le 16/03/2007

Abstract

Statistical sequential analysis was performed on a series of sediment cores collected from the Têt prodelta in the Gulf of Lions, northwestern Mediterranean Sea, between October 2003 and October 2004. Seabed changes during that period were correlated to hydrodynamic conditions (waves and currents) and river discharge. Low sediment supply prevents full preservation of new sediment strata on this low-accumulation prodelta located on a microtidal, storm-dominated inner shelf. Severe meteorological events caused a rapid succession of erosion and deposition phases. For example, the December 2003 flood and storm produced a flood layer deposit that persisted for two months with only slight transformations due to early diagenesis and/or bioturbation, until a new storm event eroded this layer. A typical sedimentary sequence was observed for the secular deposits composed of a 10 cm-thick sandy layer overlaying silty-clayey layers. These characteristic features were used to analyse the last millennia sedimentary record of the Têt prodelta. The low preservation of freshly deposited sediments and variable sedimentation rates during the last millennia period yield a sedimentary sequence formed by the outcropping of muddy prodeltaic units intersected by heterogeneous silty-sandy units similar to those formed under present day hydrodynamic conditions. No flood layer was found related to catastrophic flooding of the last century in the sedimentary record. The Little Ice Age (~1550-1850 AD) probably favoured the formation of a well-developed muddy prodelta in the mouth of the Têt River. Later on, the decrease of sediment supply by rivers due to climate change and/or human activities (damming, irrigation), and the increase of the number of high-energy storms reaching the coast, induced a coarsening of the top sediment layer on this prodelta. This modern change of the substrate is also observed in the composition of benthic biota found in the substrate.

Keywords

Prodelta, sedimentology, sedimentary sequence, radiocarbon, *Turitella communis*, Mediterranean Sea, Gulf of Lions, ^{210}Pb.

4.5.1 Introduction

Small rivers contribute a significant amount of the total sediment load to the global marine systems (**Milliman and Syvitski, 1992; Mulder and Syvitski, 1995**) and most of the sediment entering shallow coastal areas is entrapped in deltas. Prodeltas are the subaqueous

part of aerial deltas located in water depth below the storm wave base action (**Coleman and Wright, 1975**). Prodeltas correspond to preferential depositional areas of riverborne and organic material. They are composed of fine grained deposits (clays and silts) (**Aloïsi and Monaco, 1975**), and are commonly found off river mouths at depths ranging from 20 to 50 m, where wave and current energy decrease and flocculation by purely physico-chemical processes may cause nearshore mud accumulation on the shelf (**Drake, 1976**). Nevertheless, it has been demonstrated that waves and current energy remain occasionally strong enough to induce a part of resuspension and transport prodeltaic material seawards (**Smith and Hopkins, 1972**). For these reasons, prodeltas do not constitute static reservoirs of fine sediment, but are temporal deposit areas of clays and silts located in the sediment transport pathway between the turbid nearshore zone and the middle and outer shelf mud deposits.

Whatever the amount of sediment input from the nearby river, the prodelta records a trace of hydrological and biological changes, notably meteorological events such as floods and storms (**Nittrouer and Wright, 1994**). It is now well understood that in prodeltas of flood-prone rivers, well-preserved sedimentary strata are rather easy to identify, e.g. offshore of the Eel River, northern California (**Sommerfield and Nittrouer, 1999**), the Mississippi-Atchafalaya deltaic system (**Allison et al., 2005**); the Rhône River in the Gulf of Lions (**Beaudouin et al., 2005**), or the Po River (**Trincardi et al., 2004**). Conversely, sedimentary features of small flood-prone prodeltas are presumed to be more complex, due to slow accumulation rates and the low preservation potential of deposits. To date, only a limited number of studies round the world have addressed the modern to last millennia (century to millennial time-scale) sedimentary record in such small prodeltaic environments (**Ingram et al., 1996**), which are common in the Mediterranean. However, none of these studies addressed the sedimentary record itself, nor estimated the shelf mass accumulation rates over longer timescales. Are the conditions in small prodeltaic environments favourable to the formation of new sediment strata? Is there an identifiable sedimentary record and what is the structure of the record in small prodeltas from the last century to the last millennia period?

As part of the Eurostrataform project, which investigated the transfer of sediment from sources (catchment areas) to sinks (deep basins), this study aims at better understanding the formation and evolution of new sediment strata on continental shelves under the influence of meteorological events (floods, storms). Starting with the relationship between hydrodynamic forcing and resulting sedimentological and geochemical characteristics, an attempt is made to

define the last millennia record on a prodelta located on a microtidal continental shelf influenced by small rivers and dominated by storms.

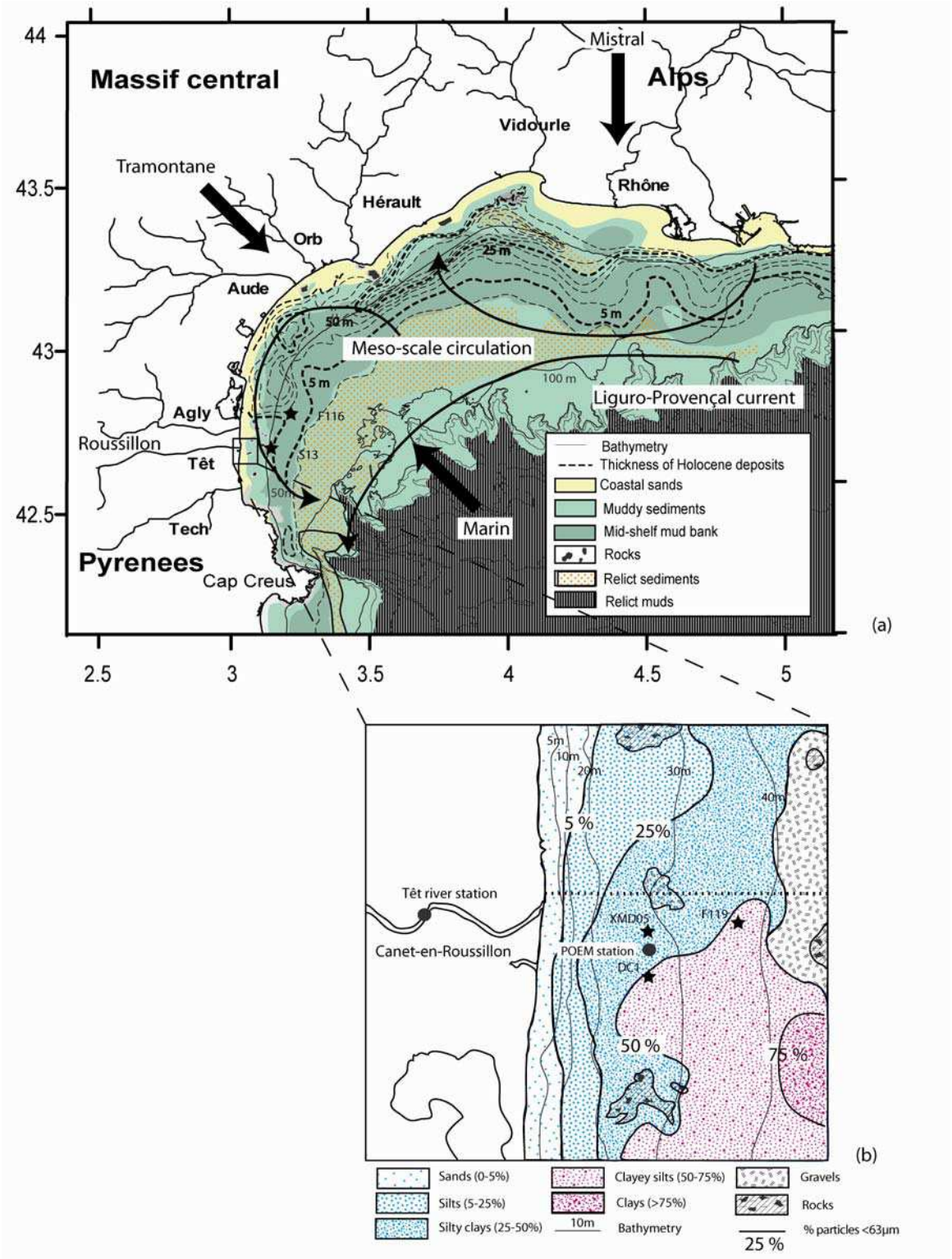

Figure 4-38 : (a) Sedimentary map of the continental margin of the Gulf of Lions (adapted from Monaco and Aloïsi, 2000, Observatoire Régional de l'Environnement Méditerranéen, http://medias.obs-mip.fr/orme/). The general and mesoscale circulations (black arrows) as well as the dominant winds (big

arrows) are shown; (b) Detailed sedimentary map of the Têt prodelta (redrawn from the Geological Map of Perpignan, 1/50,000e).

4.5.2 Regional setting

The Gulf of Lions, in the northwestern part of the Mediterranean Sea, is a large continental margin incised by numerous canyons. Its modern sedimentation is largely controlled by sedimentary inputs from several river systems (**Figure 4-38a**): the Rhône River, the largest Mediterranean river in terms of liquid (~56 x 10^6 m^3 yr^{-1}) and solid discharges (10 ± 3 x 10^6 t yr^{-1}), and several small torrential rivers (the Vidourle, Lez, Hérault, Orb, Aude, Agly, Têt and Tech rivers). The Rhône contributes more than 90% of the total annual liquid and solid discharges of the rivers to the Gulf of Lions (**Bourrin et al., 2006**). But small torrential rivers can discharge large amounts of material to the coastal area in a few days during flash flood events (**Serrat et al., 2001**). This amount of sediment can play a significant role in the sedimentation of the Gulf of Lions.

The predominant northwesterly ("Tramontane" and "Mistral") and southeasterly winds ("Marin") control variable mesoscale eddy circulations on the continental shelf (**Estournel et al., 2003**). The Tramontane as well as the Marin winds generally induce cyclonic circulation in the western part of the continental margin (**Millot, 1990**). Flood events are frequently associated with SE storms, which advect humid air inland and promote strong rains over the coast. Floods follow these storms a few hours later (**Ferré et al., 2005; Palanques et al., 2002; Puig et al., 2001**).

The location of continental sources and hydrodynamic processes control sediment distribution on this continental shelf. A decrease in grain-size is observed from the inner shelf to the outer shelf (**Figure 4-38a**). The coastal area is sandy and the sand-mud transition overlaps the average wave action limit at around 30 m water depth (**Jago and Barusseau, 1981**). Numerous rocky formations are found in the study area and present various mixed facies. A well-developed mid-shelf mud deposit follows the mean shelf circulation pattern from north to south. The outer-shelf is characterized by lowstand sandy shoreface deposits (**Jouet et al., 2006**).

The late-Holocene deposits form an alongshore muddy wedge (**Figure 4-38a**). This geometry predominantly reflects the dispersal of the Rhône River inputs by coastal circulation. The main depocentre is located directly in front to the mouth of the Rhône and decreases further west (**Aloïsi, 1986**).

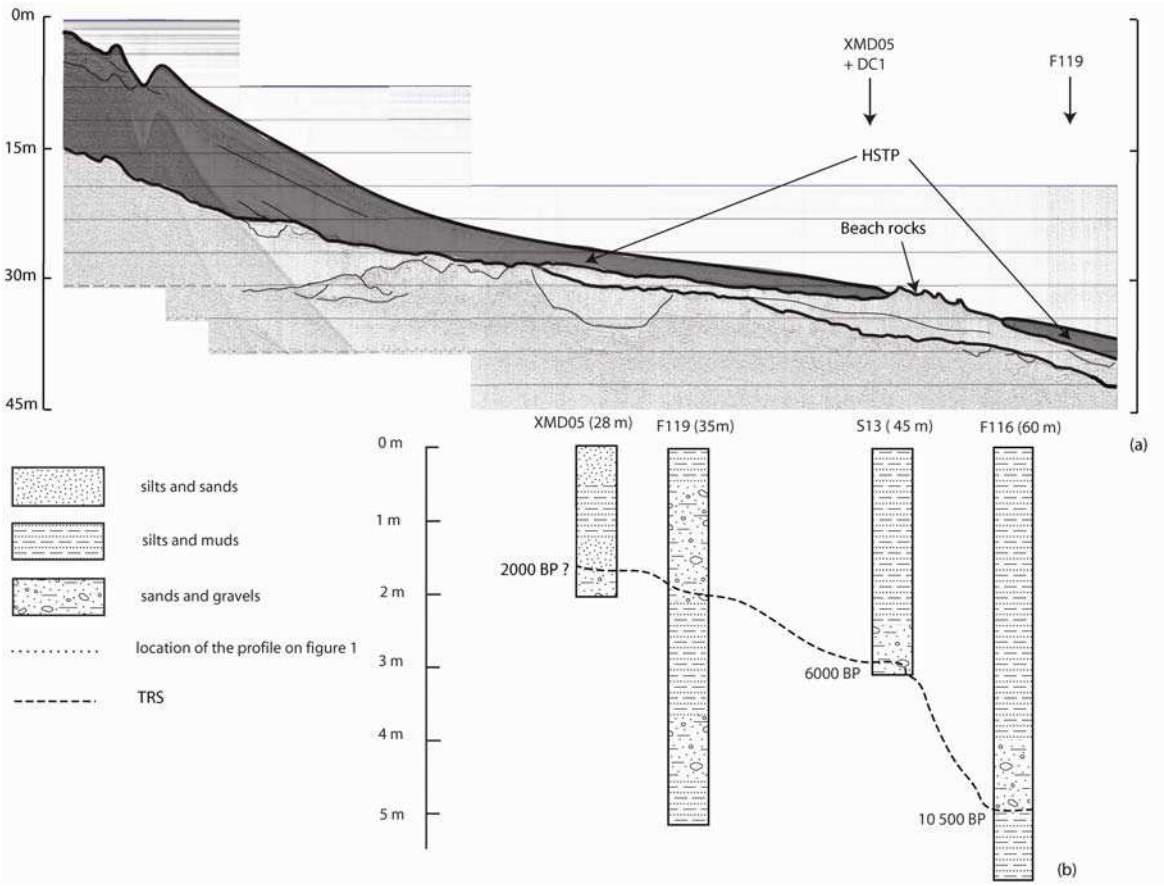

Figure 4-39 : (a) Dip-oriented seismic profile (see the location on the Têt prodelta map, Fig. 4-38b showing the architecture of the sedimentary deposits on the inner shelf (modified from Labaune et al., 2005). In dark grey colour, the Highstand Systems Tract Prism (HSTP) characterised by gently steeping foresets, where beach rocks outcrop locally. (b) Lithology of cores sampled close to this seismic profile are also shown in Fig. 1 [F119, S13 and F116 (Mear, 1984; Monaco, 1971); XDM05 (Bourrin, unpubl. data; DC1, this study)]. The dotted line represents the possible Transgressive Ravinement Surface (TRS) and shows the different stages of the last marine transgression.

The thickness of the late-Holocene deposit diminishes towards the southwestern part of the Gulf, confirming that the western torrential rivers are less important sediment sources. Seismic profiles off the Têt River (Roussillon area) (**Labaune et al., 2005**) have shown that, at 30 m water depth, the entire Holocene (the last 10,000 years) is found in a sediment layer a few meters thick (**Figure 4-39**). However, the thickness of these deposits is highly variable and depends on the underlying morphology of the Transgressive Ravinement Surface (TRS)

corresponding to the last Holocene transgression. The late-Holocene prodeltaic system, corresponding to the Highstand Systems Tract (HST), is wedge-shaped and pinches out seaward around 30 m depth where beach rocks are located (**Figure 4-39a**). These rocky formations are composed of gravels and pebbles as well as aeolian sandstones. Dating in these sandstones gives an age of 27,200 +/- 1,000 cal years BP, but these formations were reworked during slight standstill during the Holocene transgression around 6,000 and 8,000 cal years BP (**Monaco et al., 1972**). Sediment cores sampled at >40 m water depth (F116 and S13) showed a homogeneous muddy facies of several meters (**Figure 4-39 b**) characterizing the mid-shelf mud belt (Mear, 1984). At the base of these cores, gravels and coarse sand layers characterize the surface of marine transgression from the last glacial period, and allow dating of the different stages of relative sea level rise during this period. Other sediment cores (XDM05, **Bourrin, unpubl. data** and F119, **Monaco, 1971**) sampled at 28 m and 35 m water depth show alternations of fine sandy layers and silty-clayey layers and characterize a more complex organisation of the late-Holocene to last millennia sedimentary record (**Figure 4-39 b**).

The detailed map of the study site (**Figure 4-38 b**) shows an increase of the fine particle fraction (<63 μm) in the sediment from the coastline (5 %) to the mid-shelf mud belt (>75 %) (**Aloïsi and Monaco, 1975**). As a result of the predominance of along-shore southward currents in this area, the highest content of muddy sediment is not found directly in front of the river mouth but south-eastward, at a water depth >30 m, and between the beach rocks. Mineralogical analysis demonstrated that despite their bathymetric location, the prodeltas are enriched with the finest clays (smectite). This mineral is commonly observed in the Pliocene formations of the western drainage basins of the Gulf of Lions and often forms aggregates with organic compounds and pollutants (**Roussiez et al., 2005**).

4.5.3 Materials and methods

4.5.3.1 "Source" to "sink" approach

River fluxes, meteorological forcing, currents, waves and near-bed total suspended solids (TSS) were monitored between October 2003 and October 2004 by a multi-instrumented system ("Plateforme d'Observation de l'Environnement Méditerranéen – Littoral Languedoc-

Roussillon", POEM-L2R) (**Figure 4-38 b**). This system includes an automatic river sampler that collects 2 km upstream of the Têt River mouth (42°42.831'N, 002°59.615'E) and a meteo-oceanic buoy moored at 28 m water depth in the prodelta, at about 1.5 nm off the river mouth (42°42.210'N, 003°04.012'E), sheltering an area on the seabed to deploy instruments.

4.5.3.1.1 River fluxes

The river sampler was programmed to collect 1 L of water at 80 cm below the surface, once a day during normal periods, and automatically switch to hourly sampling during flood events. The water samples were filtered through 0.45 µm Nuclepore filters and dry-weighted in the laboratory to estimate the TSS concentration. The hourly liquid discharge was measured by the "Agence de l'eau de l'Aude" at the hydrological station of Pont Joffre in Perpignan (codeY0474030, data available on the website http://www.hydro.eaufrance.fr/accueil.html) located 10 km upstream from the mouth (42°42.205'N 02°53.583'E). Estimations of flood return periods were done from long term measurements of river discharge (1977-2004) following the momentum adjustments method of the Gumbel law. A rating curve was established based on long-term measurements (1980-1999 period from **Serrat et al., 2001**) combined with new data (this study) of daily TSS concentration and river discharge measurements (**Figure 4-40**). The following equation:

$\log TSS = 0.294 \log(Q)^2 + 0.0951 \log(Q) + 0.9839$ ($R^2 = 0.5553$, $n = 1400$)

was applied to mean daily river discharges to obtain mean annual fluxes corrected with the Fergusson method (**Fergusson, 1987**).

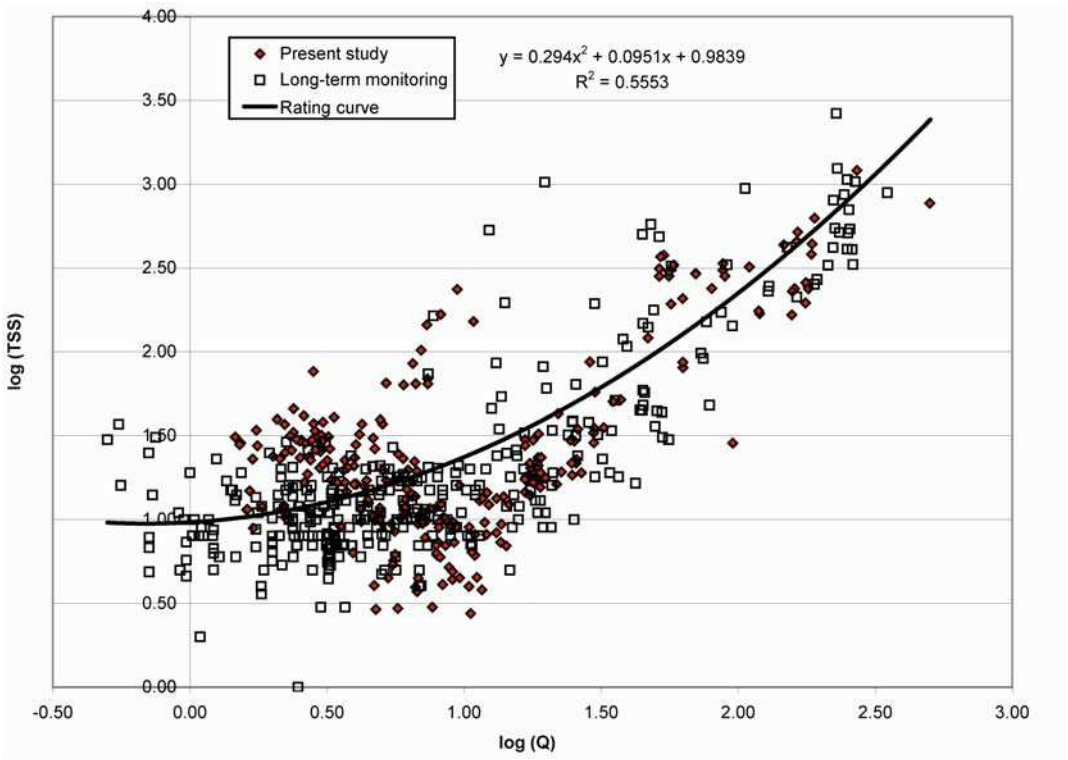

Figure 4-40 : Rating curve fitting logarithmically changed TSS concentrations versus daily river discharge of the Têt River (Qd)

4.5.3.1.2 Meteorological forcing

An anemometer (Young Wind Monitor Model 05106) mounted at 4 m above the sea surface on the buoy measured wind speed and direction. A bottom-mounted RDI ADCP 600 kHz equipped with a wave gauge was deployed at 28 m depth beneath the buoy. It recorded current profiles (magnitude and direction) over the entire water column along 1-m depth-cells, as well as wave orbital velocity below the surface and pressure. Surface height and directional spectrum of waves were derived from the combination of these measurements (**RD Instruments, 2001**). Estimations of storm return periods were done from long term measurements of wave characteristics in the whole Gulf of Lions (1996-2005) and following the momentum adjustments method of the Gumbel law. Near-bed currents and wave's characteristics were used to estimate the total shear stress at the bottom due to both mean current and waves, following **Grant and Madsen (1986)**. Results were used to estimate sediment resuspension events.

4.5.3.1.3 Prodelta seabed monitoring

One NKE ALTUS sonic altimeter (2 MHz), mounted on a small tripod, was deployed on the seabed by SCUBA divers to monitor erosion/deposition events by measuring the seabed position every 15 min from 26 November to 12 December 2003, and from 4 February to 18 March 2004. Factory instrument accuracy is ± 0.5 cm. Water turbidity was measured using a D&A Instruments Optical Back-scatter Sensors (OBS-3) mounted on a frame at 0.15 mab, collecting data every 3 h in 20 min bursts logging at 2 Hz. OBS sensors were calibrated in the laboratory using bottom sediment collected at the tripod location prior to the deployments, and signals from these instruments were converted into TSS concentrations.

4.5.3.2 Sediment sampling & analysis

From October 2003 to October 2004, 2 sediment cores at 28 m water depth were collected by SCUBA divers once a month using transparent Perspex tubes (20 cm length, 4 cm diameter) at the buoy site (**Figure 4-38**). A longer sediment core (1 m length, 8 cm diameter) was also collected using the same method at this site in May 2005. A small core was also sampled in May 2005 to check the integrity of the surface layer in the long core. Each core was sectioned into 1 cm-thick slices, except for the first cm which was sectioned into two 0.5 cm layers. Grain-size analyses were performed on sonicated samples during 5 min with MilliQ-filtered water using a Malvern Mastersizer 2000 particle size analyser equipped with a sample dispersion unit. Total carbon (TC) and organic carbon (OC) contents (% sediment dry weight) were obtained by combustion in a LECO CN 2000 analyser after acidification with HCl 2N to remove carbonates in the case of OC analysis.

The size spectra obtained from the different sediment samples were analysed following the Entropy method, which classifies the spectra on the basis of their morphology (**Johnston and Semple, 1983**). This classification has been used to describe grain-size changes in sediment cores and explain sediment erosion, transport and deposition by assuming that spectra with the same shape characterize sediments exposed to the same forcing conditions (**Woolfe et al., 2000; Woolfe and Michibayashi, 1995**). Entropy analysis, a statistical sequential analysis, classifies the size spectra into groups based on a measure of variance between groups relative to the total variance of the whole set of size spectra. The number of groups is empirically determined and its optimal value is reached when the variance explained by the distribution of the spectra into the different groups is minimum. The grouping is more effective when the inter-group variance relative to the intra-group variance is larger. In this study, an optimal

effectiveness of the spectral group classification of up to 70% was reached for 4 groups. The spectra were thus grouped into classes with similar grain-size properties. Each spectral group characterizes a typical sediment unit defined by a mean spectrum, a median grain-size (D_{50}) and a pelitic index (% <63 µm).

4.5.3.3 Geochronology

4.5.3.3.1 ^{210}Pb

Fine fraction of sediment samples (<63 µm) were freeze-dried, homogenized using a mortar and pestle, and totally dissolved according to a wet ashing technique using various mineral acids [HNO3 65%; HNO3/HClO4 mixed (v/v); HF 48%, HCl 32%]. The following methodology was taken from **Radakovitch (1995)**. After solubilisation in 250 mL of 0.3 M HCL, 0.1g ascorbic acid was added to reduce Fe (III) to Fe (II) at 90°C. Polonium from the resulting solution was spontaneously deposited onto polished silver discs at 60-65°C for about 16 hours while stirring. After auto-plating, the disk was rinsed with water and dried at room temperature. Chemical recoveries of ^{210}Po ranged from 97% to 99%. ^{210}Po activities deposited on each side of the silver disc were determined in a photomultiplier counter by measuring photons produced on a photophore screen by alpha emission. Activities were corrected for the decay of ^{210}Po between plating and counting, and the decay of ^{210}Pb between sampling and plating. Corrected ^{210}Po activities were assumed to be equal to ^{210}Pb activities. Excess ^{210}Pb ($^{210}Pb_{xs}$) activity was determined by subtracting from the total activity the supported ^{210}Pb activity, determined as the mean ^{210}Pb concentration at the base of the sediment core. Mean mass-accumulation rates (R in g cm^{-2} yr^{-1}) were calculated using the Constant Rate of Supply (CRS) model of **Goldberg (1963)**:

$$R = \frac{\lambda S}{A_{exces}} \text{ with } S = \int_z^Z \rho A_{exces} dz$$

where S is the cumulative concentration of $^{210}Pb_{xs}$ (Bq m^{-2}) in a sedimentary layer of thickness z, and A_{exces} is the $^{210}Pb_{xs}$ activity (Bq kg^{-1}). This method takes into account down-core variations of sediment density, and constant supply of ^{210}Pb through time is assumed. Mean apparent sediment accumulation rates (cm yr^{-1}) were determined by normalizing the sediment profile to the density measured for each sediment sample.

4.5.3.3.2 Radiocarbon dating

Shells of the gastropod *Turitella communis* sampled from sediment cores were used to perform radiocarbon dating in order to estimate ^{14}C based sediment accumulation rates and ages in the modern sedimentary record (small cores) and the paleo-sequence (long core) on the Têt prodelta. **Kershaw and co-workers (1988)** showed that dating shells of *Turitella communis* is a more reliable method to estimate sediment accumulation rates than dating the carbonate fraction of bulk sediment. In each shell we performed two sections perpendicular to the shell axis with a circular diamond-coated saw in order to obtain an aliquot of *circa* 100 mg. Each aliquot was first sonicated during 5 min with H_2O_2 30% v/v and then etched with 0.1 M HCl during 3 min. Samples were then carefully rinsed with distilled water, dried overnight at 60ºC and stored in an inert atmosphere. The samples, ranging from 25-68 mg, were then sent to the Woods Hole Oceanographic Institution's NOSAMS Facility for radiocarbon analysis. Special care was taken to obtain the calendar age of each sample. **Siani and co-workers (2000)** report for the Gulf of Lions a regional correction of the marine reservoir effect (400 y) of 118 ± 30 y (database available at http://calib.qub.ac.uk/marine/) This reservoir correction was used in the CALIB 5.0 code (**Stuiver and Reimer, 1993; Stuiver et al., 2005**) to convert radiocarbon ages to calibrated ages using the calibration data set marine 04.14c (**Hughen et al., 2004**). Age intervals with maximum probabilities were used as best age estimators (**Table 4-4**).

Core	Depth (cm)	Sediment unit	NOSAMS code	Radiocarbon age (yr)	Calendar age interval (AD)
DC1	3–4	Unit III	OS-53715	455±35	[1896 :1953*]
DC1	8–9	Unit II	OS-53716	535±35	[1871 :1951*]
DC1	13–14	Unit II	OS-53717	550±30	[1866 :1951*]
DC1	38–39	Unit II	OS-53718	815±35	[1555 :1658]
230604/1112S	11–12	Unit II	OS-53719	560±30	[1858 :1950*]
230604/1112G	11–12	Unit II	OS-53720	580±35	[1836 :1950*]
280404/78S	7–8	Unit III	OS-53753	560±30	[1858 :1950*]
280404/78G	7–8	Unit III	OS-53721	580±35	[1836 :1950*]
230604/1617SG	16–17	Unit I	OS-53722	640±30	[1710 :1852]

Table 4-4 : Radiocarbon ages of Gastropods Turitella communis. * The year 1950 is considered as the modern limit of the radiocarbon dating method.

4.5.4 Results

4.5.4.1 River inputs

During the study period, the mean daily Têt River discharge was 18 m^3 s^{-1} (mean pluri-annual daily discharge = 10 m^3 s^{-1}) with a mean TSS concentration of 30 mg L^{-1}. From long-term based rating curve and daily river discharge measurements, the total solid discharge between October 2003 and October 2004 was estimated to be 88,000 t (mean annual ~61,000 t). On the basis of the annual discharges between 1980 and 2004, the period analysed during this study can be considered as one of the wettest of the last 25 years. Between October 2003 and October 2004 three major floods of the Têt River, related to southeasterly winds, occurred with daily discharge exceeding 200 m^3 s^{-1} (2-year recurrence interval flood). During these three floods, which lasted eight days, 85% of the annual solid discharge of the Têt River was exported to the coastal zone. The largest flood, in April 2004, had an estimated return period of 5 years (Q_d > 280 m^3 s^{-1}, **Figure 4-41 b**), and delivered about 35,000 t of sediments in 3 days, i.e. 40% of the annual discharge (**Figure 4-41 c**).

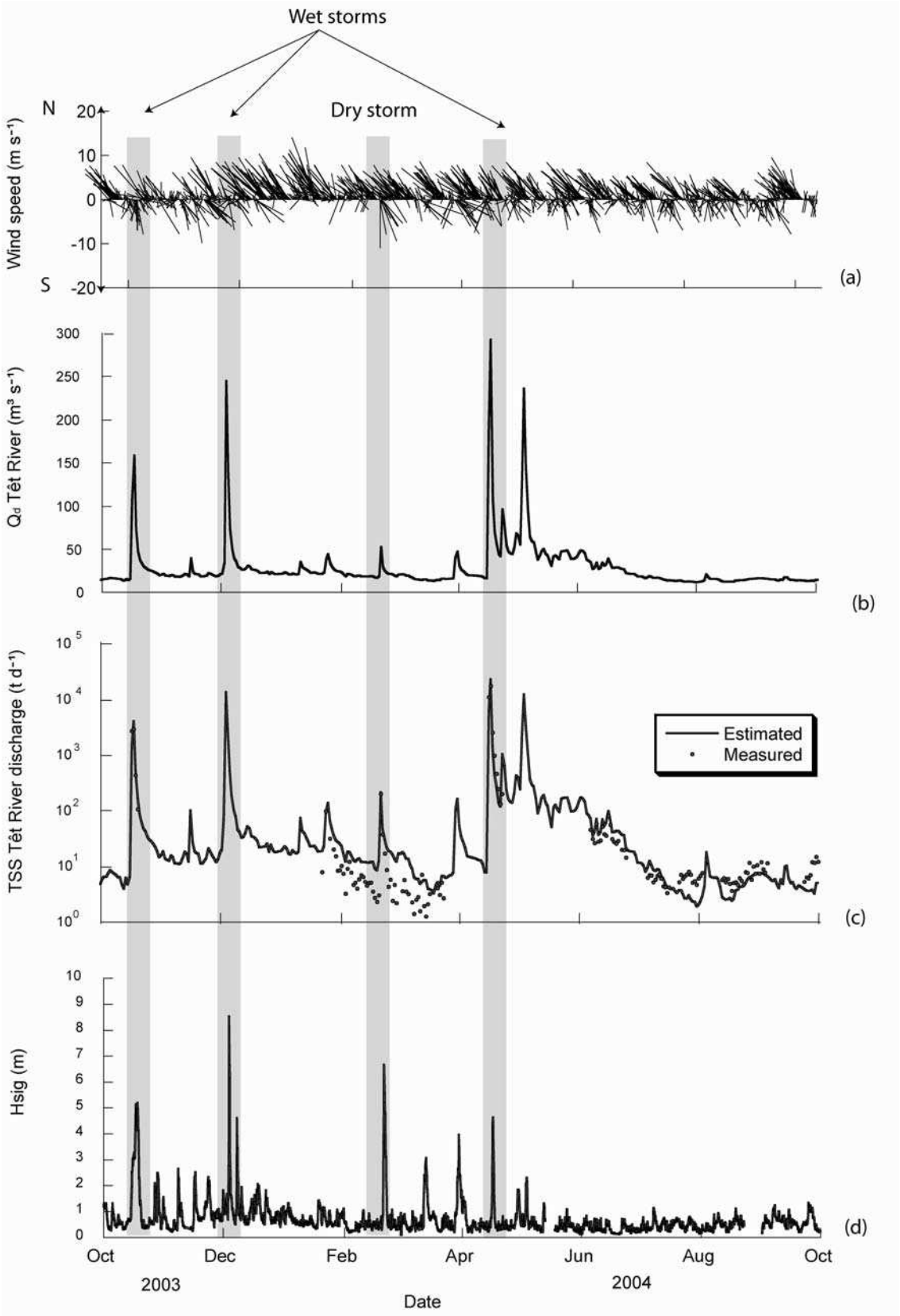

Figure 4-41 : Time-series of (a) Wind speed (in m s^{-1}) measured at the Meteo France meteorological station of Torreilles (code 66212001) located near the Têt River mouth (42°45.379'N 02°58.781'E), (b) Daily river discharge of the Têt River (Q_d in m^3 s^{-1}), (c) Daily discharge of Total Solids in Suspension (TSS discharge in tons d^{-1}) of the Têt River estimated from Serrat et al. (2001) and measured at the POEM

station 1.5 km upstream to the river mouth, (d) Significant wave height (H_{SIG} in m) measured at the POEM site 1.5 nm off the Têt River mouth, from October 2003 to October 2004. The dark grey areas correspond to the south-eastern storm events.

4.5.4.2 Hydrodynamics on the inner shelf

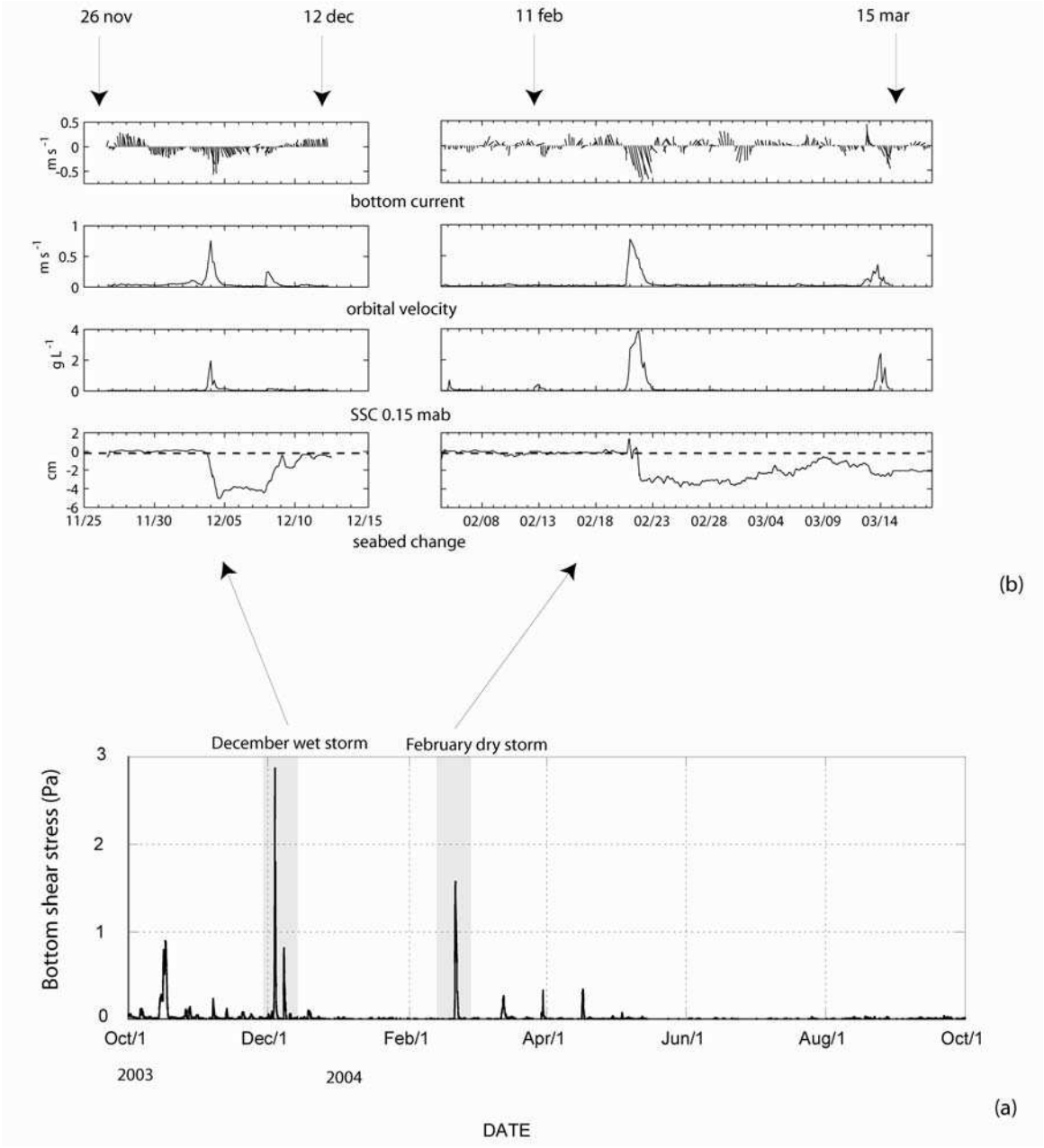

Figure 4-42 : (a) Time-series of bottom shear-stress due to current and waves estimated from GM 86 model (Grant and Madsen, 1986) from October 2003 to October 2004, and (b) Detailed stick plot of bottom currents (m s^{-1}), time-series of near-bed orbital velocities (in m s^{-1}), suspended solids concentration at 0.15 mab (in g L^{-1}) and seabed changes (cm) during December 2003 and February 2004, in the POEM

site off the Têt River mouth. The black arrows indicate the date when sediment cores were sampled from the prodelta.

The observation period was also particularly energetic and characterised by several SE storms (**Figure 4-41d**). Three SE events had significant wave height (H_{SIG}) >5 m (2-year recurrence interval) and 4 SE annual events with H_{SIG} >3 m. The largest storm in December 2003 (H_{SIG} > 8.5 m) had a > 20 yr return period. The calculated mean bed orbital velocity, was 3 cm s^{-1} during the whole experiment, and reached maximum >80 cm s^{-1} during the December 2003 and February 2004 storms (**Figure 4-42a**). Orbital velocities >35 cm s^{-1} (corresponding shear stress 0.12 Pa) were sufficient to erode at least unconsolidated silts or fine sands (D_{50} = 80 μm). Such conditions occurred about 5% of the time, mainly in winter during SE storms.
Typical bottom shear stresses were measured in laboratory with an annular Mini Flume (**Amos et al., 2000**) from sediment of the Têt inner shelf. Threshold values of 0.03 and 0.12 Pa were obtained, which correspond to the resuspension threshold for clays and fine sands, respectively (**Bourrin et al., 2004**). Effective bottom shear stress during these major storms reached respective values of 3 and 1.5 Pa (**Figure 4-42a**), and near-bed suspended solids concentrations reached values of 2 and 4 g L^{-1} during the storm peaks in December 2003 and February 2004 (**Figure 4-42b**). Currents measured 2 m above the bottom ranged between 2 and 50 cm s^{-1} and were mainly directed southwards.

4.5.4.3 Sediment dynamics

Storms associated with floods were qualified as “wet” storms (October and December 2003, and April 2004) and storms without floods were qualified as “dry” storms (February 2004). Such a distinction was established on the difference of their impact on sediment transport in the inner shelf of the Roussillon shelf (**Guillén et al., 2006**). Altimetric measurements of the seabed in this area at 28 m water depth showed that a sediment layer of 4 to 6 cm was eroded by wave resuspension during the most severe storms (the 4th December 2003 and the 21st February 2004, **Figure 4-42b**). Few hours after the peak of the wet storm, a one cm thick flood layer was immediately deposited in the Têt inner shelf. A second moderate storm (8th December 2003) provokes three days after, the accretion of ~4 cm of sediment. After the dry storm, no flood layer was deposited in the inner shelf. Continuous accretion of ~3 cm of sediment was observed several days after the dry storm (from 2nd to 9th March 2004). A

second moderate event (15th March 2004) finally occurred enhancing sediment erosion until 1 cm depth.

4.5.4.4 Sediment core analysis

4.5.4.4.1 Statistical sequential analysis

The sediment monitoring of the Têt prodelta provided a series of eight 20 cm-long sediment cores (**Figure 4-43**).

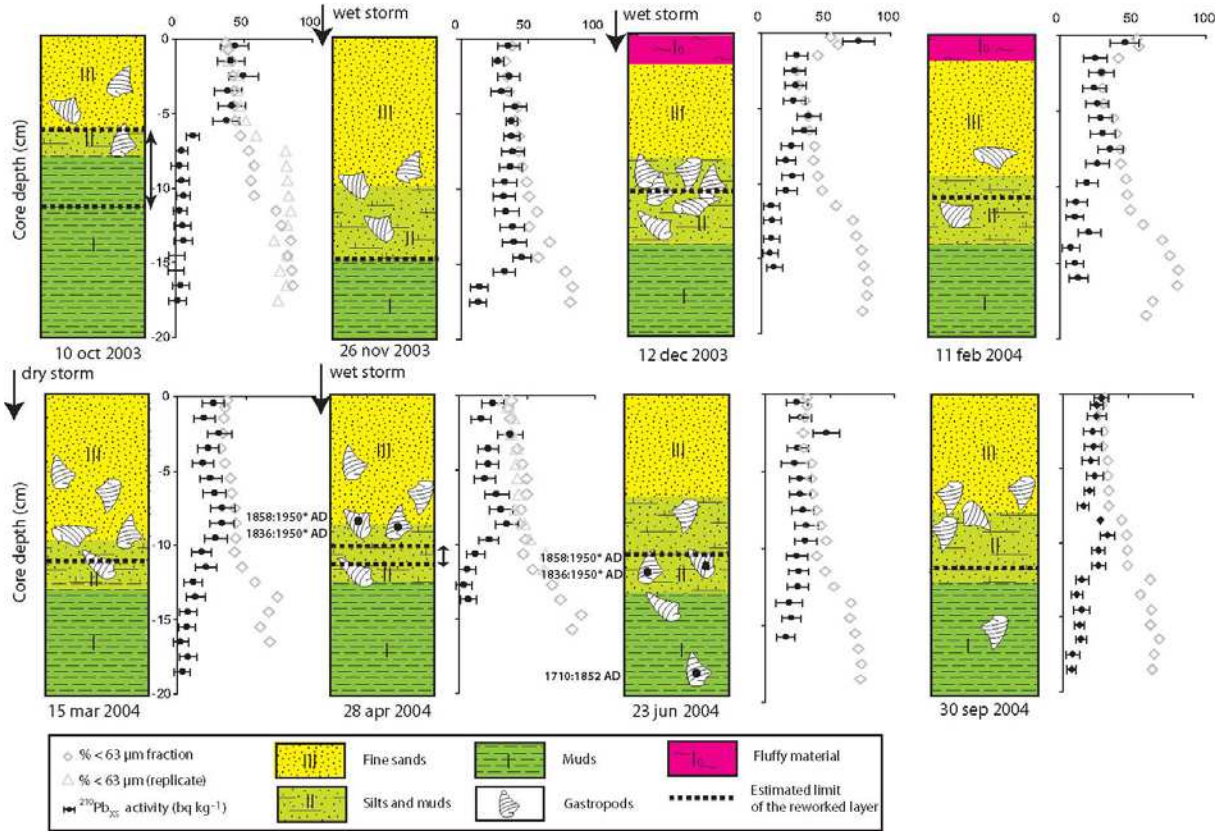

Figure 4-43 : Sedimentary logs of high-frequency monitoring cores sampled from October 2003 to October 2004 showing down-core profiles of the pelitic index (fraction of particles < 63 µm) and $^{210}Pb_{xs}$ activities.

Based on, facies analysis and grain-size characteristics, the sedimentary logs revealed 4 sediment types. We used the Entropy analysis method to confirm this observation. The first three distinct sediment units were labelled I, II and III from bottom to top of each core (**Figure 4-44**). Unit I (below 14 cm depth, **Figure 4-44b**) contains principally clayey material (mode grain size = 15 µm) and silts (mode = 60 µm). The average median grain size (D_{50}) of

this unit is 30 µm and has up to 60% pelitic fraction. Unit II (9 to 14 cm depth, **Figure 4-44b**) is composed of clays (mode = 15 µm) and silts or very-fine sands (mode = 70 µm). The D_{50} of this unit is about 50 µm and its pelitic fraction is comprised between 50 and 60%. The gastropod *Turitella communis* is often found in this unit. Unit III (0 to 9 cm depth, **Figure 4-44b**) is formed by very-fine, well-sorted sands, with D_{50}= 80 µm, and <40% pelitic fraction.

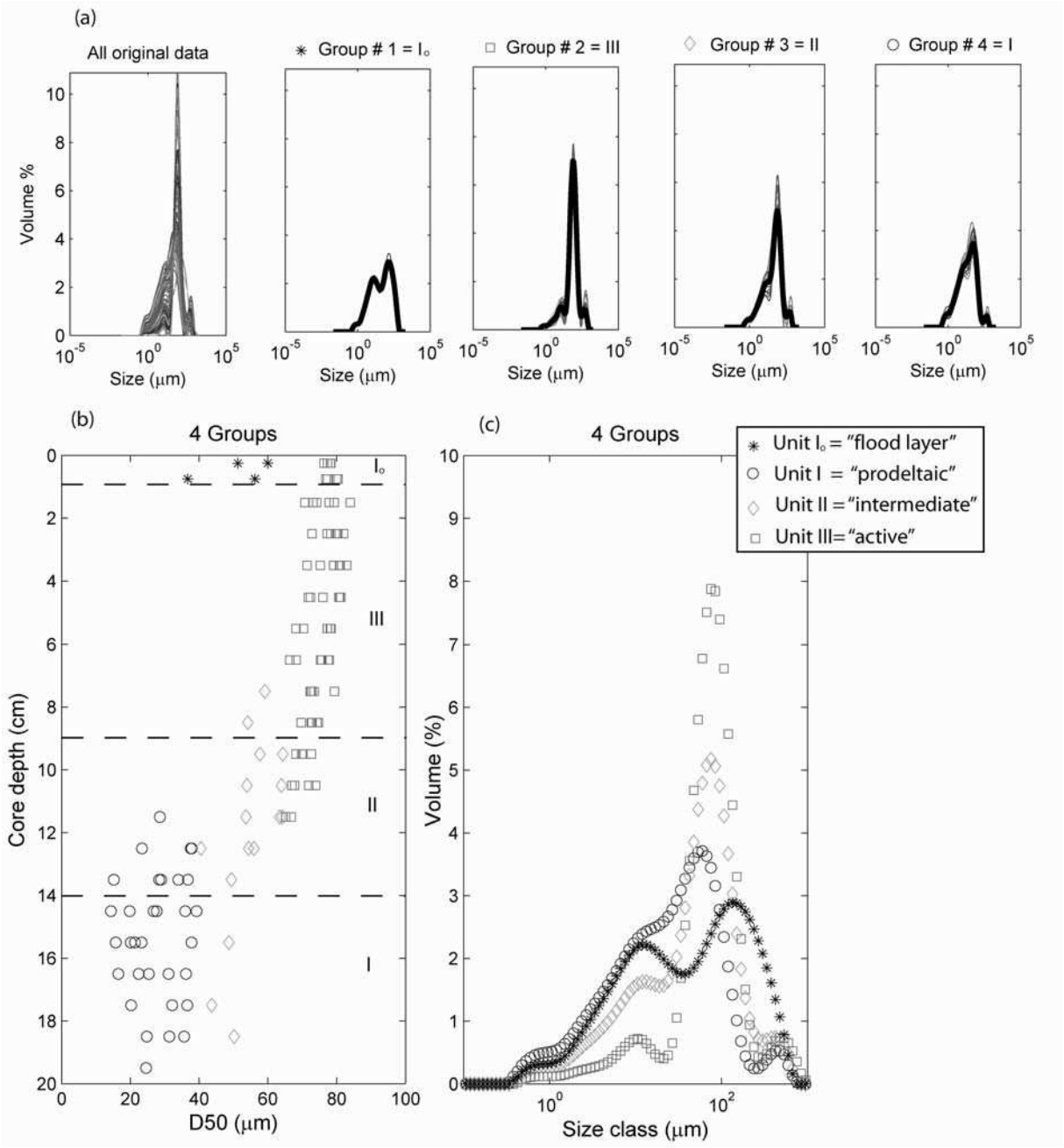

Figure 4-44 : Identification of the 4 different units in the small cores from the high-frequency monitoring, based on the Entropy method spectral analysis. (a) The original data and the four groups identified and corresponding mean spectra (bold); (b) Mean grain size (D_{50}) of each spectra as a function of the core depth; (c) Mean spectra of the four units identified.

The same granulometric modes of silts, around 20 µm, and fine sands, around 70 µm, were found in these three units but with various proportions. The 4th unit, labelled I_0, was observed at the top of Unit III in two cores collected in December 2003 and February 2004. This unit, less than 3 cm thick, is composed of fluffy sediments corresponding to a mixture of mud (mode = 15 µm) and organic material (2.96 and 1.49% organic carbon for December and February respectively) and has a high water content (70.5 and 49.6% respectively). The D_{50} of this unit is about 50 µm and has a pelitic fraction ~60%.

4.5.4.4.2 Annual evolution

The thickness of the units described above changed throughout the experimental year because of the impact of the different storm events. Erosion / deposition sequences directly affected the thickness of Unit III, which varied between 6 and 15 cm, and it is thus qualified as an active unit (**Figure 4-43**). The 2 cm thick fluffy layer (Unit I_0) was first observed at the top of the core sampled in December 2003 and it was still present in February 2004. Its persistence is probably linked to low waves during this period, whereby speeds were <15 cm s^{-1} recorded between mid-December and mid-February. This flood-related layer disappeared after the dry storm event of 21st February 2004 when maximum bottom orbital velocities reached 80cm s^{-1}. No significant changes were noticed in the thickness of the other units. After that storm, the sedimentary sequences from March to September 2004 did not show any perceptible difference in grain size despite a period of high river discharge in April-May 2004 linked to spring snow melting. Only small changes were observed in the thickness of these units, probably related to small-scale spatial variability. Grain-size analysis on replicate cores (10th October 2003 and 28th April 2004, **Figure 4-43**) sampled a few meters from each others show weak variability in the grain-size profiles. This variability can nevertheless affect the determination of the different units by the statistical sequential analysis over a few cm.

4.5.4.4.3 Ecological patterns

The gastropod *Turritella communis* preferentially lives in terrigenous muddy environments such as prodeltas, where frequent inputs of fine sediment and fresh organic matter occur (**Sartenaer, 1959**). During the sampling period, SCUBA divers observed accumulations of *Turritella communis* on the seabed surface (28 m water depth), and especially in the depressions formed by bottom currents or by biological activity. Several *Turritella communis*

shells were found at different depths in the cores. Based on the light salmon colour of their shells, living or recently dead gastropods were commonly observed at the surface of the sediment or within the first cm of the top unit (Unit III). Also dead gastropods, characterized by dark colours (**Sartenaer, 1958**), were found between 3-4 cm and 15-16 cm depths. In the 2 cores sampled after the December and February severe storms, accumulations of *Turritella communis* were found at the base of the reworked layer (Unit III) from 6 to 12 cm depth (**Figure 4-43**).

4.5.4.4.4 Age of the sequence

The radioisotope ^{210}Pb ($T_{1/2}$=22.3 years) provides important information both about the degree of reworking of the top sediment layer (Unit III) on a century time scale, and about the input of fresh continental material in the same time. In all short cores except for the first one (10th October 2003), the top sediment layer is characterized by higher and rather homogeneous $^{210}Pb_{xs}$ activities down to ~10 cm, corresponding approximately to the thickness of the reworked layer (Unit III) during extreme storms (**Figure 4-43**). Mixing can be produced by physical processes such as near-bed currents or biological processes such as burrowing or feeding activities by benthic organisms (**Nittrouer and Sternberg, 1981**). The four sedimentary units identified in the small cores (**Figure 4-43**) are also distinguishable in the ^{210}Pb profiles. The mean value of $^{210}Pb_{xs}$ activity in the top unit (Unit III) was 25 Bq kg^{-1}. The intermediate Unit II presented an almost linear decrease of $^{210}Pb_{xs}$ activities from 25 to 5 Bq kg^{-1} activity found in the Unit I. The flood layer (Unit I_0, **Figure 4-43**) was characterized by high $^{210}Pb_{xs}$ activities reaching 80 Bq kg^{-1} in December 2003.

Radiocarbon dating of *Turritella communis* shells was performed on Units III, II, I in small cores collected in April 2004 and June 2004 (**Table 4-4**). All the shells in Unit III located from surface to 8 cm depth showed similar recent ages from 1836 to 1950* AD (modern). We obtained the same interval of ages for the shells in Unit II located between 8 and 14 cm depth (**Figure 4-43**). Radiocarbon dating at the base of Unit I gives an age of 1710-1852 AD. Radiocarbon and ^{210}Pb dating thus suggest that the top sequence of about 10 cm thick was formed during a period of about one century.

4.5.4.5 Long-term sedimentary signal

The 85-cm long sediment core (DC1) was also analysed using the Entropy method (**Figure 4-46**). Based on the characteristics of Units I, II, III of the small cores, three larger sedimentary sequences can be identified. The uppermost sequence, from 0 to 20 cm deep, consists of a succession of the three units described above and identical to the units of the small cores and represents the modern sedimentary sequence. Indeed, radiocarbon dating in the top unit (Unit III) of this sequence yielded ages ranging from 1866-1953 AD (modern, **Figure 4-46a** and **Table 4-4**). The next sequence, from 20 to 45 cm deep, is formed by the succession of Units III, II, I and constitutes a fining-up sequence. Shell fragments, mud clasts and organic debris were observed at around 30 cm. in the Unit II. Radiocarbon dating at the base of this unit (38-39 cm) showed an age of 1555-1658 AD. The lowest sequence extends from 45 cm deep to the bottom of the core. It is formed by a coarsening-up sedimentary sequence and lies on a gravel and pebble layer containing mollusc shells. Grain-size trends of the small core and the long core show similar increase of the % of <63 μm sediment fraction from the surface (**Figure 4-46d**).

As in the short cores, the top of DC1 is characterized by higher $^{210}Pb_{xs}$ activities (**Figure 4-46c**). No surface mixed layer was found in the long core. Below that layer, the linear decrease of $^{210}Pb_{xs}$ activities are the same until supported ^{210}Pb is reached at around 12 cm depth, corresponding to the secular limit of the sedimentary sequence. Based on $^{210}Pb_{xs}$ profile and from CRS model, apparent mean sedimentation rate of 0.085 cm yr^{-1} was found for the long core. Radiocarbon ages provided mean accumulation rates of 0.035 cm yr^{-1} at 3-4 cm depth and 0.123 cm yr^{-1} at 39 cm depth, thus confirming the slow and variable accumulation rate on the Têt prodelta during the late-Holocene.

4.5.5 Discussion

4.5.5.1 Modern strata formation in inner-shelf environments

4.5.5.1.1 Preservation of flood layers

The main mechanisms leading to the formation of new sediment layers in front to river mouths were recently investigated in the Gulf of Lions (**Pauc, 2005; Guillén et al., 2006;**

Maillet et al., 2006) and in other continental shelves (**Wheatcroft and Borgeld, 2000; Curran et al., 2002; Wheatcroft et al., 2006**). The larger fraction of riverborne particles (silts and very-fine sands) is first deposited during a flood in the vicinity of the mouth. The finer fraction flowing in the surface hypopycnal plume settled after electro-chemical flocculation processes and can reach few tens of kilometres in the case of small rivers (**Drake, 1976**). The resulting bottom flood layer is then composed of a thin layer of silts and very-fine sands, overlaid by a fine particle layer enriched in organic matter. Time-series observations of cores clearly showed the presence a few cm-thick fluffy deposit (Unit I_0) at the top of the core the 12th December 2003, on the Têt prodelta after the wet storm (4th December 2003) and the consecutive moderate storm event (8th December 2003) (**Figure 4-45a**). But sediment cores only give information on the record of past events and the sequence of the events is difficult to analyse with such information. Details are provided by altimetric measurements (**Figure 4-45b**) and showed that a 1-cm flood layer was previously deposited following the flood event of the 4th December 2003.

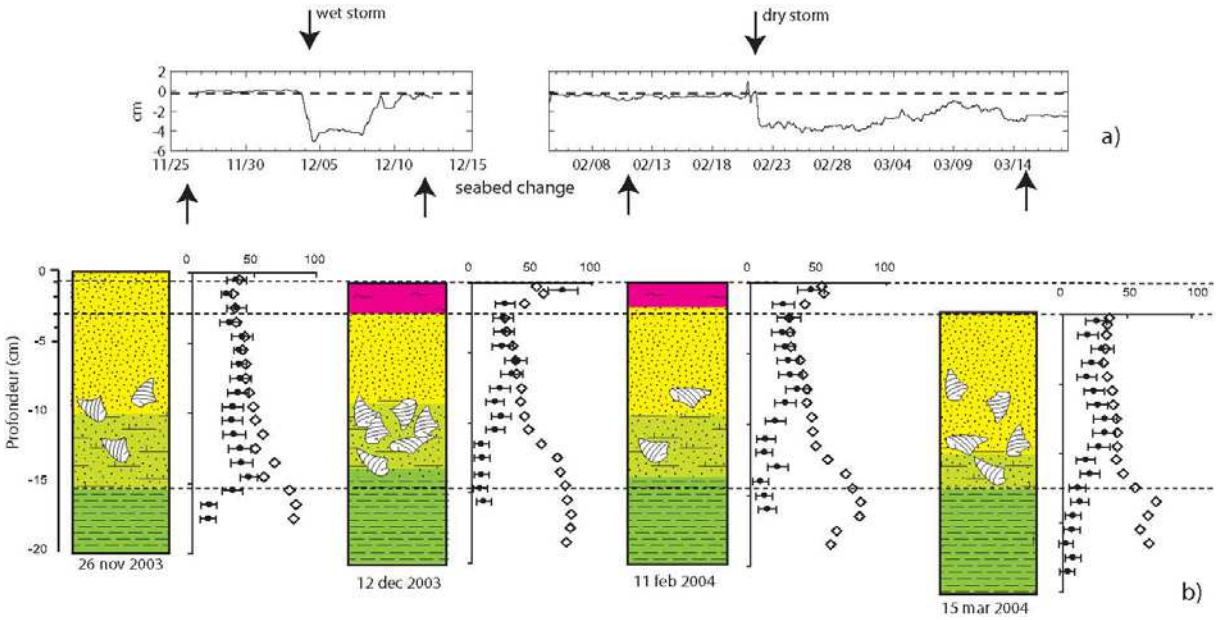

Figure 4-45 : (a) Altimetric measurements and (b) adjusted sediment cores from November 2003 to March 2004 at the base of Unit II where a sediment grain-size drop is observed in each core. The legend is the same as Figure 4-43.

Then a moderate second storm induced sediment accretion at least to the pre-storm seabed level. This storm, not associated with significant river discharge, promoted the advection of shallower material previously deposited in the nearshore during the flood to the inner-shelf in the Têt prodelta. This flood layer persisted only two months before a new storm event totally

swept away this freshly deposited and non-consolidated sediment material. During the second event (dry storm), no flood occurred and few material was available in the nearshore zone to be advected to the inner-shelf. The conditions to observe the deposit of a flood layer on the Têt inner-shelf thus depend strongly on the pre-flood conditions and the succession of the events (flood and storm) (**Guillén et al., 2006**). The adjustment of each sediment core at base of the Unit II, where a drop in sediment grain-size is observed, clearly shows the similarity between high-frequency altimetric measurements and core sampling (**Figure 4-45**). This sequence of events confirms previous observations on the inner shelf of the Têt River, which showed the presence of an ephemeral fluid mud layer that persisted for only 1 month (**Courp and Monaco, 1990**). The only way modern sediment strata can be created on this type of inner shelf characterized by energetic wave conditions, would be by an increase in flood events over very short time periods. Deposition of a new flood layer on top of a recently deposited layer could prevent the latter from being eroded and/or bioturbated in the surface mixed layer (**Wheatcroft and Drake, 2003**).

4.5.5.1.2 Storm bed thickness

Another important topic to discuss about sediment dynamics in the Têt River inner-shelf is the storm bed thickness. Preferential accumulation of dead gastropods was observed in Unit III (**Figure 4-45a**) and can be explained by the reworking of the upper sediment layer during the most severe storms (i.e., 8th December 2003 and 21st February 2004). While fine sediment particles were rapidly winnowed during the onset of the storms, coarser sandy particles and shells could be remobilised during the peak of the storm with maximum orbital speeds of up to 80 cm s^{-1}. During the declining phase of the storm, coarse particles and shells settle first, and were thus found at the base of the reworked layer (Unit III). These shells were subsequently covered by a mixture of sediment advected from shallower areas and from the Têt River. Accumulation of gastropod shells at the base of Unit III seems therefore to be a good marker for estimating the depth at which sediment was reworked by bottom currents. As other have noted (**Wiberg, 2000**), storm bed thickness depends on current and waves conditions. For the conditions that occurred in December 2003 (u_b > 1m/s and u > 0.4 m/s towards the southeast) and February 2004 (u_b > 0.9 m/s and u > 0.4 m/s towards the southeast) on the Têt prodelta, the model of **Wiberg (2000)** predicts a storm bed thickness of about 1-2 cm at 50 m depth. Measured storm bed thickness in this study is significantly higher. These values depend on in-situ altimetric measurements at a shallower site (28 m),

and show sediment erosion of ~5 cm during severe storm events. Furthermore, there is no net deposition immediately during the wane of the storm. Only deposition of a thin flood layer was observed with a time lag of a few hours after the dry storm. Winnowing of the fines and advection toward the southeast, few fresh materials available for advection from the nearshore, was explained for the sediment divergence creating such erosion levels at the study site.

4.5.5.2 Multi-scale sedimentary record

4.5.5.2.1 Secular sediment budget

Prodeltas of the northwestern Mediterranean Sea characterized by a high content of clay minerals were extensively mapped in the 1980s (**Aloïsi and Monaco, 1975**) and more recently, on the basis of trace metals at the seabed surface (**Roussiez et al., 2005**). Prodelta surface areas in the western Gulf of Lions were thus calculated from the integration of such data in GIS software (**Bourrin et al., 2006**). The depth where supported ^{210}Pb activities are reached corresponds approximately to the lower limit of the sedimentary record of these prodeltas of the last century (~12 cm depth on the Têt prodelta, **Figure 4-45a**). **Bourrin et al. (2006)** have estimated that only a small fraction (~20%) of the fine sediment freshly deposited on the prodelta area remained in place. In a nearby similar prodelta influenced by sediment supply from three coastal rivers (the Aude, Orb and Hérault), sediment retention was estimated to be ~40% using the same method based on ^{210}Pb mass accumulation rates The mean ^{210}Pb mass accumulation and sedimentation rates calculated from the whole series of small cores is 0.11 g cm^{-2} yr^{-1} (min=0.09, max=0.16) and 0.07 cm yr^{-1}, respectively. ^{210}Pb mass accumulation rates from others cores sampled in this area give similar values (**Roussiez, 2006**; **Table 4-5**) and thus comfort the estimated retained sediment fraction in these prodeltas. Thus, under present day conditions, most of the sediment entering the western Gulf of Lions by small coastal rivers, bypasses prodelta areas and is advected southward and seawards on century time scales. In this type of prodelta, the secular sedimentation rate results from the predominance of hydrodynamic forcing over the discontinuous and weak sediment supply, and only a limited fraction (~20%) of sediment is trapped in the proximal portion of the dispersal system.

Core	Location (degrees)	Depth (m)	^{210}Pb mass accumulation rate (g/cm^2/an)
35	42.716N, 3.065E	26	0.14
POEM	42.704N, 3.067E	28	0.11 (0.09–0.16)
351 bis	42.699N, 3.090E	33	0.182
353	42.712N, 3.152E	51	0.21
37 bis	42.582N, 3.206E	81	0.15

Table 4-5 : Core sampled close to the study site POEM (name, Location, Depth) taken from Roussiez (2006), and corresponding ^{210}Pb mass accumulation rate.

The balance between the total amount of fresh sedimentary material introduced into the coastal area and the frequency and strength of resuspension events in the inner shelf of continental margins can lead to various sedimentary records in prodeltaic environments. In prodeltas where large inputs of fresh material occur, the sediment accumulation rate is greater than the erosion rate and a sedimentary signal can be preserved (**Aloïsi, 1986; Fernandez, 1984; Wheatcroft et al., 2006**). It has been shown using high-resolution pollen analyses that proximal to the mouths of large rivers (.e.g. the Rhône), entire sedimentary sequences representing seasonal variations can be retained (**Beaudouin et al., 2005; Touzani and Giresse, 2002**). Nevertheless, the number of disturbed or incomplete sequences showed that about 50% of the total amount of sediment freshly deposited in the Rhône prodelta is subsequently resuspended by near-bed orbital currents. Also, off the flood-prone mountainous Eel River, a maximum of 20% of sediment introduced into the coastal area is generally retained on event and century time scales (**Sommerfield and Nittrouer, 1999; Wheatcroft et al., 1997**). However, geochronology reveals that catastrophic flash-floods can generate long-term accumulation layers of fine-grain sediment near river mouths. In the case of small event-dominated prodeltas influenced by flash floods, such as the Têt prodelta, the sedimentary record seems to be more complex. A large number of meteorological events can rework the same active, few-cm-thick layer. As an example, during the last century, the biggest flood event ever described in this area, "the Aïguat" of 1940 (**Desailly, 1990**), provided such a huge quantity of sediment to the inner shelf that the aerial delta prograded by more than 250 m into the sea. A comparison of aerial photographs before and after this catastrophic flood event clearly showed that the delta had been eroded since then by the littoral drift and, in fact, in the prodeltaic sedimentary record there is no evidence of such an event. The flood layer deposited on the prodelta has probably been levelled eroded by wave resuspension and redistributed

southward (**Delpont and Motti, 1994**). In present day conditions, the low inputs of sediment to the coastal area are not sufficient to counterbalance enhanced erosion during storms, reducing the preservation potential. In this case, the sedimentary record is assumed to be merely a low frequency signal of the meteorological events affecting the system. The variation of sediment characteristics with depth is then the expression of long-term variations of the prodelta dynamics due to climatic changes and/or changes in mean sea level.

4.5.5.2.2 Secular to late-Holocene sedimentary record

The high-frequency analysis of Têt prodelta modern sequence has been extrapolated to analyse the long-term sedimentary record in the same environment (DC1 core, **Figure 4-46**). Sediments exposed to the same hydrodynamic conditions in modern or geological timescales have the same grain-size characteristics (**Figure 4-46 c**). The modern (upper) sequence of the Têt prodelta is expressed by the succession of Units III, II, I overlapped by a flood layer (Unit I_0). Unit I is found several times in the Têt prodelta long-term sedimentary record. Unit I is found between 14 and 20 cm depth and shows a radiocarbon age of 1710-1852 AD (**Figure 4-43**). This unit is interpreted as the expression of more continuous sedimentation in the coastal zone compared to the present day. It appears from the literature (**Benech, 1993**) and archives (**Desailly, 1990**) that the period of the Little Ice Age (~1550-1850 AD) was characterized by an increase in the number of severe flooding events in the catchment area of the Roussillon rivers area linked to the Pyrenees mountains. The same events were recorded for the Rhône during the same period (**Sabatier et al., 2006**). This period of enhanced precipitation was also accompanied by human deforestation activities in the catchment area inducing higher continental sediment inputs to the coastal area (**Vella et al., 2005**). This period was thus favourable to the progression of the sandy coast and the build-up and conservation of a muddy prodelta on the Roussillon inner shelf. It is suggested that Units II and III, at the top of the modern sediment sequence, were formed from the muddy Unit I by mechanical transformation and winnowing of the fine fraction during successive storm events, at a time of limited sediment supply from rivers and increased number of storms. Unit II was then formed from Unit I and Unit III from Unit II by the same mechanism. The bottom units would be progressively isolated from surface hydrodynamics as sedimentation develops.

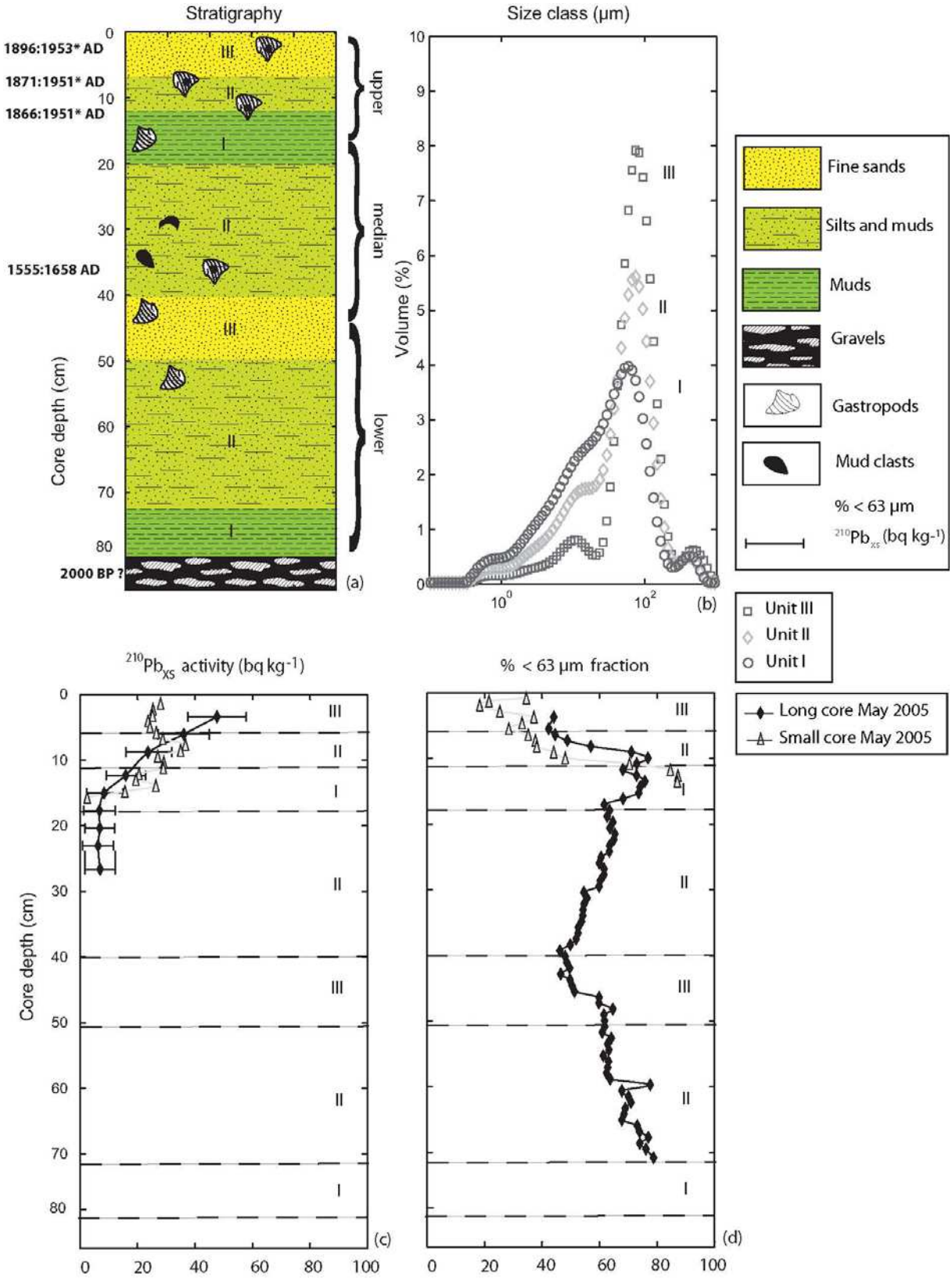

Figure 4-46 : (a) Sedimentary log of the DC1 core; (b) identification of the 3 units from spectral analysis by the Entropy method; (c), down-core profiles of $^{210}Pb_{xs}$ activity, and (d) pelitic index (% of particles < 63 µm) for 2 representative small cores sampled in May 2004 and May 2005 and the long core (DC1, May 2005).

In fact, the top sediment layer becomes coarser as it is depleted of its fine fraction during successive storms reaching the coastal zone. The low sediment accumulation rate on the Têt prodelta would then result from a build up of mixed and sorted sediment within a frequently reworked layer of about 10 cm thick. The coarsening of the surface layer was also observed by biologists who have observed a generalized change in the benthic macrofaunal populations in the coastal zone since the 1960s (**Grémare et al., 1998**). They hypothesized that this modification could have been caused by temporal changes of the sediment inputs from the Rhône and the small coastal rivers and by the frequency of easterly storms. **Durand (1999)** found evidence of an increase in the number and strength of storms in the Gulf of Lions from the 1980s onwards. Furthermore, river bed mining and the construction of flood-control dams (**Ludwig and Probst, 1998**) has substantially decreased continental inputs from rivers. The preservation of a muddy layer would then be the expression of the close juxtaposition of two flood events (**Wheatcroft and Drake, 2003**), and/or a long-term predominance of strong sediment supply by rivers over hydrodynamic conditions, suchas during the Little Ice Age.

Two other sequences composed of the succession of Units III, II, and I are found in the long-term record of the Têt prodelta and could have been formed under similar conditions to those of the present day. The sedimentary sequence found under the modern sequence (between 20 and 45 cm depth) is formed by heterogeneous layers of silts and clays. This median sequence, with an age ranging between 1555 and 1658 AD, is a coarsening-up sequence and suggest dynamic conditions different to those prevailing during the formation of the modern and basal sequences. This could be due to a change in sediment river supply due to climatic conditions, or to local variations in coastal morphology related to a change in the mean sea level. If present-day dynamic processes are extrapolated to this sequence, Units III and II at 45 and 60 cm depth, respectively, could have been formed by the reworking of the underlying prodeltaic unit (Unit I). The lowest prodeltaic unit (Unit I), located at the base of the lower sequence (at ~70 cm depth), could be the expression of a high sedimentation period between the higher than present sea-level stand (+ 2 m at 4.500 cal years BP) in western Mediterranean sea and the present day sea-level, stabilized some 2,000 cal years BP in the Roussillon coastal zone (**Aloïsi et al., 1978**). The bottom layer, formed by sands and gravels, at the base of core DC1, is similar to an old beach facies described at other locations in the Gulf of Lions, the base layer of part of the Holocene sedimentary record in this region (**Monaco, 1971; Tesson et al., 2005**). The coarsening of the basal sequence could be related to a deceleration of sediment inputs from local rivers and/or to a period of upsurge in the number of storms in the area as

under present day conditions. If we assume an age of ~2,000 cal years BP for this base layer and a mean sedimentation rate of ~0.1 cm yr^{-1} for the whole sedimentary record of the Têt prodelta, we certainly have some lacks of sedimentation. This sedimentary record of a small prodelta thus render a complex signal of the last millennia to the late-Holocene period. Others sediment cores sampled in the Têt inner-shelf also have a complex organisation (**Figure 4-39**), and the base of these cores could correspond to a base layer of the Holocene period. Others cores sampled seaward (**Figure 4-39**) have a more continuous record and can be used to analyse the sedimentation of the continental margin during the whole Holocene period. The interpretation of the sedimentary record of such small coastal systems to analyse past conditions must then be done very carefully because of the presence of discontinuity, as in the signal of the last millennia.

4.5.6 Conclusions

Deposition of fine riverborne particles after extreme floods appears to be the main mechanism governing the formation of new sediment strata on the Têt prodelta. Their preservation is conditioned by the intensity of post-depositional reworking by wave events. On the Têt prodelta, flood layers were often observed after flood events and their residence time was less than 2 months due to waves resuspension by SE marine winds, showing that present day hydrodynamic conditions do not allow the preservation of intact sediment strata on the Têt inner shelf. The secular ^{210}Pb sedimentation rate is very low (0.07 cm yr^{-1}), and only ~ 20 % of the continental material entering the coastal zone is retained in the inner shelf. The modern sedimentary record of the Têt prodelta is a complex signal resulting from the balance between few sedimentary inputs and the frequency and strength of storm events. This record builds up as mixed and sorted sediments within a frequently reworked layer about 10 cm thick. In present day conditions, sediment in the top sediment layer of the Têt prodelta is characterised by a grain-size coarsening due both to the decrease of solid river discharge since the end of the XIX^{th} century and the winnowing of fine particles during severe storm events.

Older preserved muddy prodeltaic units were observed in the Têt prodelta last-millennia sedimentary signal. These phases are interpreted as periods of river sediment load increase or by extreme flash-flood events, and thus as periods of higher potential for the preservation of muddy sediment on the prodelta area. As an example, the Little Ice Age (~1550-1850 AD) as

a period during which human activities in the mountainous catchment areas led to deforestation and more easily erodible lands. This period, also observed in similar Mediterranean environments, was favourable to the increase of suspended solid river discharges and the formation of a muddy prodelta on the Têt inner shelf.

The last-millennia sedimentary record of the Têt prodelta is characterised by preserved prodeltaic units during phases of high sedimentation intersected by heterogeneous sedimentation phases during energetic periods as under present day conditions. The formation mechanisms of such environments, and thus their sedimentary record, should be the same for prodeltas located in microtidal seas influenced by meteorological events such as floods and storms. Thus, small prodeltas record the long-term succession of meteorological events as a low frequency signal. But we have to be very careful when analysing and interpreting this signal in terms of long-term variations of climate change and/or human impact. If no complete signal is available elsewhere in front of large systems, then it can be interesting to analyse sedimentary records in front of small-size systems. Independently of the river size, deltaic/prodeltaic environments on inner shelves, lagoons or lakes, develop sedimentary records that can be used to analyse the variability of past environmental conditions.

Acknowledgements

We would like to thank the captains and crews of the R/Vs Téthys II and Néréis for their assistance in the sampling work. Sincere thanks are also given to the scuba divers of the Observatoire des Sciences de l'Univers of Banyuls-sur-Mer for their assistance in sediment coring. This research conducted through a PhD program was supported under Languedoc-Roussillon Regional Council's SysCôLag Program and the European Union's Eurostrataform Project (EC Contract No. EVK3-CT-2002-00079). NOSAMS operates at the Woods Hole Oceanographic Institution with National Science Foundation sponsorship. Laval Liong Wee Kwong, from IAEA Marine Environment Laboratories, performed the sample preparation for radiocarbon analysis. The IAEA is grateful for the support provided to its Marine Environment Laboratories by the Government of the Principality of Monaco. Authors are also grateful to Michel Tesson and Robert Wheatcroft who greatly participated to improve the manuscript from their valuable comments.

References

Allison, M.A., Sheremet, A., Goñi, M.A., Stoneb, G.W., 2005. Storm layer deposition on the Mississippi–Atchafalaya subaqueous delta generated by Hurricane Lili in 2002. Cont. Shelf Res., 25: 2213-2232.

Aloïsi, J.C., 1986. Sur un modèle de sédimentation deltaïque. Contribution à l'étude des marges passives. PhD Thesis, Université de Perpignan, 162 pp.

Aloïsi, J.-C., Monaco, A., 1975. La sédimentation infralittorale. Les prodeltas nord-méditerranéens. C.R. Acad. Sci. D, 280: 2833-2836.

Aloïsi, J.C., Monaco A., Planchais, N., Thommeret, J., Thommeret, Y., 1978. The Holocene transgression in the golfe du Lion, southwestern France: paleogeographic and paleobotanical evolution. Géogr. Phys. Quat., Montréal, XXXII(2) : 145-163.

Amos, C.L., Cloutier, D., Cristante, S., Cappucci, S., 2000. The Venice lagoon study (F-ECTS)-February, 1999. . Geological Survey of Canada Open File Report 3904: 47 pp.

Beaudouin, C., Suc, J.-P., Cambon, G., Touzani, A., Giresse, P., Pont, D., Aloïsi, J.-C., Marsset, T., Cochonat, P., Duzer, D., Ferrier, J., 2005. Present-Day Rhythmic Deposition in the Grand Rhone Prodelta (NW Mediterranean) According to High-Resolution Pollen Analyses. J. Coastal Res., 21(2) : 292-306.

Benech, C., 1993. Des risques naturels dans les P.O., DDAF 66.

Bourrin, F., Durrieu de Madron, X., Ludwig, W., 2006. Contribution of the study of coastal rivers and associated prodeltas to sediment supply in North-western Mediterranean Sea (Gulf of Lions). Vie Milieu, 56(4) : 1-8.

Bourrin, F., Ulses, C., Thompson, C.E.L., Friend, P.L., 2004. A comparison of the characteristics of the sediment from the Rhône and the Têt rivers using a mini cylindric flume., Joint Eurodelta - Eurostrataform Annual Meeting 2004, Venice, Italia., pp. 82.

Curran, K.J., Hill, P.S., Milligan, T.G., 2002. Fine-grained suspended sediment dynamics in the Eel River flood plume. Cont. Shelf Res., 22: 2537-2550.

Coleman, J.M., Wright, L.D., 1975. Modern river deltas: variability of processes and sand bodies. In: M.L. Broussard (Editor), Deltas Models for Exploration Houston Geological Society, Houston, pp. 99–149.

Courp, T., Monaco, A., 1990. Sediment dispersal and accumulation on the continental margin of the Gulf of Lions: sedimentary budget. Cont. Shelf Res., 9-11: 1063-1088.

Delpont, G., Motti, E., 1994. Monitoring by remote sensing of the geomorphological evolution of a part of the Roussillon coastal layout (France). OCEANIS 94 OSATES, pp. 44-47.

Desailly, B., 1990. Crues et inondations en Roussillon. Le risque et l'aménagement fin du XVIIe siècle - milieu du XXe siècle. PhD Thesis, Univ. Paris X - Nanterre, 352 pp.

Drake, D.E., 1976. Suspended sediment transport and mud deposition on continental shelves. In: D.J. Stanley, Swift, D.J.P. (Editor), Marine Sediment Transport and Environmental Management. Wiley-Interscience Publication, pp. 602.

Durand, P., 1999. L'évolution des plages de l'ouest du Golfe du Lion au XXème siècle. PhD Thesis, Univ. Lyon, 461 pp.

Estournel, C., Durrieu de Madron, X., Marsaleix, P., Auclair, F., Julliand, C., Vehil, R., 2003. Observation and modeling of the winter coastal oceanic circulation in the Gulf of Lion under wind conditions influenced by the continental orography (FETCH experiment). J. Geophys. Res., 108(C3) : 8059, doi : 10.1029/2001JC000825.

Fernandez, J.M., 1984. Utilisation de quelques éléments métalliques pour la reconstitution des mécanismes sédimentaires en Méditerranée Occidentale : apport du traitement statistique. PhD Thesis, Univ. Perpignan, 230 pp.

Ferré, B., Guizien K., Durrieu de Madron X., Palanques A., Guillén J., Grémare, A., 2005. Fine-grained sediment dynamics during a strong storm event in the inner-shelf of the Gulf of Lion (NW Mediterranean). Cont. Shelf Res., 25: 2410-2427.

Goldberg, E.D., 1963. Geochronology with 210-lead radioactive dating, I.A.E.A., Vienna.

Grant, W.D., Madsen, O.S., 1986. The continental shelf bottom boundary layer. Annu. Rev. Fluid Mech., 18: 265-305.

Grémare, A., Amouroux, J.M., Charles, F., Medernach, L., Jordana, E., Nozais, C., Viéton, G., Colomines, J.C., 1998. Temporal changes in the biochemical composition of particulate organic matter sedimentation in the Bay of Banyuls-sur-mer. Oceanol. Acta, 21: 783-792.

Guillén, J., Bourrin, F., Palanques, A., Durrieu de Madron, X., Puig, P., Buscail, R., 2006. Sediment dynamics during wet and dry storm events on the Têt inner shelf (SW Gulf of Lions). Mar. Geol., 234(1-4): 129-142.

Hughen, K., Baillie, M., Bard, E., Bayliss, A., Beck, J., Bertrand, C., Blackwell, P., Buck, C., Burr, G., Cutler, K., Damon, P., Edwards, R., Fairbanks, R., Friedrich, M., Guilderson, T., Kromer, B., McCormac, F., Manning, S., Bronk Ramsey, C., Reimer, P., Reimer, R., Remmele, S., Southon, J., Stuiver, M., Talamo, S., Taylor, F., van der

Plicht, J., Weyhenmeyer, C., 2004. Marine radiocarbon age calibration, 26 - 0 ka BP. Radiocarbon, 56: 1059-1086.

Ingram, B.L., Ingle, J.C., Conrad, M.E., 1996. A 2000 yr record of Sacramento–San Joaquin river inflow to San Francisco Bay estuary, California. Geology, 24(4): 331-334.

Jago, C.F., Barusseau, J.P., 1981. Sediment entrainment on a wave-graded shelf, Roussillon, France. Mar. Geol., 42: 279-299.

Johnston, R.J., Semple, R.K., 1983. Classification using information statistics. CATMOG, 37.

Jouet, G., Berne, S., Rabineau, M., Bassetti, M.A., Bernier, P., Dennielou, B., Sierro, F.J., Flores, J.A., Taviani, M., 2006. Shoreface migrations at the shelf edge and sea-level changes around the Last Glacial Maximum (Gulf of Lions, NW Mediterranean). Mar. Geol., 234(1-4): 21-42.

Kershaw, P.J., Swift, D.J., Denoon, D.C., 1988. Evidence of recent sedimentation in the eastern Irish Sea. Mar. Geol., 85(1): 1-14.

Labaune, C., Tesson, M., Gensous, B., 2005. Integration of high and very high-resolution seismic reflection profiles to study late Quaternary deposits of a coastal area in the western Gulf of Lions, SW France. Mar. Geophys. Res., 26(2-4): 109-122.

Ludwig, W., Probst, J.L., 1998. River sediment discharge to the oceans: present-day controls and global budgets. Am. J. Sci., 296: 265–295.

Maillet, G.M., Vella, C., Berne, S., Friend, P.L., Amos, C.L., Fleury, T.J., Normand, A., 2006. Morphological changes and sedimentary processes induced by the December 2003 flood event at the present mouth of the Grand Rhone River (southern France). Mar. Geol., 234(1-4) : 159-177.

Mear, Y., 1984. Séquences et unités sédimentaires du glacis rhodanien (Méditerranée occidentale). . PhD Thesis, Univ. Perpignan, 214 pp.

Milliman, J.D., Syvitski, J.P.M., 1992. Geomorphic/Tectonic Control of Sediment Discharge to the Ocean: The Importance of Small Mountainous Rivers. J. Geol., 100, 5: 525-544.

Millot, C., 1990. The Gulf of Lions' hydrodynamics. Cont. Shelf Res., 10(9-11): 885-894.

Monaco, A., 1971. Contribution à l'étude géologique et sédimentologique de plateau continental du Roussillon (Golfe du Lion). PhD Thesis, Université des Sciences et Techniques du Languedoc., Montpellier, 285 pp.

Monaco, A., Thommeret, J., Thommeret, Y., 1972. L'âge des dépôts quaternaires sur le plateau continental du Roussillon (Golfe du Lion). C.R. Acad. Sci. D, 274: 2280-2283.

Mulder, T., Syvitski, J.P.M., 1995. Turbidity currents Generated at river Mouths during Exceptional Discharges to the world Oceans. J. Geol., 103: 285-299.

Nittrouer, C.A., Sternberg, R.W., 1981. The formation of sedimentary strata in an allochthonous shelf environment: The Washington continental shelf. Mar. Geol., 42(1-4): 201-232.

Nittrouer, C.A., Wright, L.D., 1994. Transport of particles across continental shelves. Rev. Geophys., 32: 85-113.

Palanques, A., Puig, P., Guillén, J., Jimenez, J., Gracia, V., Sanchez-Arcilla, A., Madsen, O., 2002. Near-bottom suspended sediment fluxes on the microtidal low-energy Ebro continental shelf (NW Mediterranean). Cont. Shelf Res., 22(2): 285-303.

Pauc, H., 2005. Formation of the Aude, Orb and Hérault prodeltas and their characterisation using physicochemical and sedimentological parameters. Mar. Geol., 222-223: 335-343.

Puig, P., Palanques, A., Guillén, J., 2001. Near-bottom suspended sediment variability caused by storms and near-inertial internal waves on the Ebro mid continental shelf (NW Mediterranean). Mar. Geol., 178(1-4) : 81-93.

Radakovitch, O., 1995. Etude du dépôt et du transfert du matériel particulaire par le ^{210}Po et le ^{210}Pb. Application aux marges continentales du golfe de Gascogne (NE Atlantique) et du golfe du Lion (NW Méditerranée). PhD Thesis, Univ. Perpignan, 250 pp.

Radakovitch, O., Charmasson, S., Arnaud, M., Bouisset, P., 1999. ^{210}Pb and caesium accumulation in the Rhône delta sediments. Estuar. Coast. Shelf S., 48: 77-92.

RD Instruments, 2001. Waves User's Guide.

Roussiez, V., 2006. Les éléments métalliques. Traceurs de la pression anthropique et du fonctionnement hydro-sédimentaire du golfe du Lion. PhD Thesis, Univ. Perpignan, 247 pp.

Roussiez, V., Aloïsi, J.-C., Monaco, A., Ludwig, W., 2005. Early muddy deposits along the Gulf of Lions shoreline: A key for a better understanding of land-to-sea transfer of sediments and associated pollutant fluxes. Mar. Geol., 222-223: 345-358.

Sabatier, F., Maillet, G., Provansal, M., Fleury, T.-J., Suanez, S., Vella, C., 2006. Sediment budget of the Rhone delta shoreface since the middle of the 19th century. Mar. Geol., 234(1-4) : 143-157.

Sartenaer, P., 1959. Premières recherches taphonomiques, en scaphandre autonome, sur le facies a Turritella tricarinata forme communis de la vase molle terrigène du golfe de Fos. Rec. Trav. Sta. mar. Endoume, 26(16): 15-38.

Serrat, P., Ludwig, W., Navarro, B., Blazi, J.-L., 2001. Variabilité spatio-temporelle des flux de matières en suspension d'un fleuve côtier méditerranéen : la Têt (France). C. R. Acad. Sci., 333: 389-397.

Siani, G., Paterne, M., Arnold, M., Bard E, Métivier, B., Tisnerat, N., Bassinot, F., 2000. Radiocarbon reservoir ages in the Mediterranean Sea and Black Sea. Radiocarbon, 42: 271-280.

Smith, J.D., Hopkins, T.S., 1972. Sediment transport on the continental shelf off of Washington and Oregon in light of recent current measurements. In: H.a.R. Dowden, Inc., Stroudsburg, Pennsylvania (Editor), Shelf Sediment Transport: Process and Pattern, pp. 143-180.

Sommerfield, C.K., Nittrouer, C.A., 1999. Modern accumulation rates and a sediment budget for the Eel shelf: a flood-dominated depositional environment. Mar. Geol., 154: 227-241.

Stuiver, M., Reimer, P.J., 1993. Extended ^{14}C data base and revised CALIB 3.0 ^{14}C Age calibration program. Radiocarbon, 35(1): 215-230.

Stuiver, M., Reimer, P. J., Reimer, R. W., 2005. CALIB 5.0. [WWW program and documentation].

Tesson, M., Labaune, C., Gensous, B., 2005. Small rivers contribution to the Quaternary evolution of a Mediterranean littoral system: The western gulf of Lion, France. Mar. Geol., 222-223: 313-324.

Touzani, A., Giresse, P., 2002. The Rhône River Prodelta: Short-Term (10^0-10^3 Year) sedimentation Patterns and Human Impact. J. Coastal Res., 18(1): 102-117.

Trincardi, F., Cattaneo, A., Correggiari, A., 2004. Mediterranean Prodelta Systems. Oceanography, 17(4).

Vella, C., Fleury, T.J., Raccasi, G., Provansal, M., Sabatier, F., Bourcier, M., 2005. Evolution of the Rhône delta plain in the Holocene. Mar. Geol., 222-223: 2350-2365.

Wheatcroft, R.A., Sommerfield, C.K., Drake, D.E., Borgeld, J.C., Nittrouer, C.A., 1997. Rapid and widespread dispersal of flood sediment on the northern California margin. Geology, 25(2): 163-166.

Wheatcroft, R.A., Borgeld, J.C., 2000. Oceanic flood deposits on the northern California shelf: large-scale distribution and small-scale physical properties. Cont. Shelf Res., 20(16): 2163-2190.

Wheatcroft, R.A., Drake, D.E., 2003. Post-depositional alteration and preservation of sedimentary event layers on continental margins, I. The role of episodic sedimentation. Mar. Geol., 199: 123-137.

Wheatcroft, R.A., Stevens, A.W., Hunt, L.M., Milligan, T.G., 2006. The large-scale distribution and internal geometry of the fall 2000 Po River flood deposit: Evidence from digital X-radiography. Cont. Shelf Res., 26(4): 499-516.

Wiberg, P.L., 2000. A Perfect Storm: formation and potential for preservation of storm beds on continental shelf. Oceanography, 13(3): 93-99.

Woolfe, K.J., Larcombe, P., Stewart, L.K., 2000. Shelf sediments adjacent to the Herbert River delta, Great Barrier Reef, Australia. Aust. J. Earth Sci., 47(2): 301-308.

Woolfe, K.J., Michibayashi, K., 1995. "Basic" Entropy grouping of laser-derived grain-size data: an example from the great barrier reef. Comput. Geosc., 21(4): 447-462.

5 SYNTHÈSE ET CONCLUSIONS GÉNÉRALES

5.1 Synthèse

Les prodeltas constituent des unités sédimentaires fonctionnelles de la zone côtière du golfe du Lion, au même titre que le cordon littoral, la vasière médiane et le domaine du large. Ces unités sont localisées à proximité immédiate des fleuves et graus, et sont donc sous l'influence combinée et concurrente des apports fluviatiles et des forçages marins. L'étude de ces unités ne peut se faire qu'en étudiant à la fois le domaine continental (bassin-versant) et le réceptacle marin (zone côtière). L'étude des prodeltas fait donc intervenir différentes disciplines allant de la géologie et la géochimie, à l'hydrologie continentale et marine, à la physico-chimie et à la biologie.

Dans ce contexte scientifique original, le site retenu a été celui de la Têt et du littoral roussillonnais pris comme exemple des prodeltas associés à des fleuves torrentiels dans le golfe du Lion. Durant cette étude, nous nous sommes attachés à :

- Caractériser et localiser les prodeltas du golfe du Lion associés aux fleuves côtiers à caractère torrentiel, identifier leur fonctionnement et faire un premier bilan sédimentaire sur les quantités apportées et stockées dans les prodeltas (**Partie 4.1**).
- Estimer l'impact des évènements hydro-climatiques extrêmes sur la dynamique sédimentaire du prodelta de la Têt, évaluer la variabilité saisonnière et interannuelle, ainsi que son fonctionnement (**Parties 4.2, 4.3 et 4.4**).
- Mesurer le signal (enregistrement) sédimentaire du prodelta de la Têt et estimer la variabilité séculaire et pluriséculaire de ce signal (**Partie 4.5**).

Pour répondre à ces objectifs, j'ai participé à la mise en place d'une plateforme instrumentée composée d'une station fluviatile couplée à une station côtière. Au niveau du fleuve, on vient d'atteindre 3 années complètes de suivi (1000^{e} prélèvements) et la station est en cours d'automatisation complète. Au niveau de la zone côtière, la maintenance de la station a été plus compliquée car on a dû faire face à des dégâts matériels importants et le remplacement des instruments endommagés a été rendu difficile par des fournisseurs pas toujours éclairés. Cependant le savoir-faire que j'ai acquis au cours de la mise en place et de l'automatisation de

cette bouée côtière permettra de pérenniser cette station sur le long terme et de l'appliquer à d'autres environnements. Plusieurs expériences de terrain fructueuses ont été menées autour de cette plateforme durant deux années de suivi intensives. Une première année (2003-2004) a permis de caractériser les apports des fleuves côtiers et leur devenir dans la zone côtière, ainsi que la dynamique sédimentaire au niveau du prodelta de la Têt, au cours d'évènements de tempêtes/crues extrêmes. Une deuxième année de mesure complète (2004-2005) a permis de caractériser cette dynamique durant une période de circulation côtière intense. Les données de ces expériences ont été corrélées aux analyses de prélèvements sédimentaires continus sur le prodelta de la Têt. Les principaux résultats sont résumés et discutés dans cette synthèse.

5.1.1 Le prodelta de la Têt : source ou puits de matière ?

5.1.1.1 Les mécanismes de dépôt

Le prodelta a été défini comme une zone de dépôt préférentielle du matériel fin d'origine fluviatile dans la zone côtière. Il est situé en dessous de la limite d'action des vagues de tempête et des forts courants, vers 30 m de profondeur. Durant la période étudiée, plusieurs dépôts de crue ont été observés. La **crue généralisée** à l'ensemble des fleuves du golfe du Lion de décembre 2003 a engendré un dépôt de crue d'une épaisseur d'environ 2 cm, observé au niveau de la bouée vers 30 m de profondeur. La crue isolée du fleuve Têt d'avril 2004 qualifiée de **crue océanique** en raison de son impact immédiat sur l'hydrologie de la zone côtière (**Wheatcroft, 2000**), a provoqué un dépôt de crue observé entre 0 et 20 m de profondeur. Aucun dépôt n'a été observé au niveau de la bouée (30 m de profondeur) durant cette crue. Ainsi deux mécanismes principaux de dépôt et de transfert du matériel fin continental depuis l'embouchure vers le large en passant par la zone prodeltaïque ont été observés au cours de notre étude (**Figure 5-1**). Dans le cas de la crue isolée du fleuve Têt en avril 2004, le prodelta a été soumis aux apports de matériel fin du fleuve Têt qui se sont déposés d'abord dans la zone très littorale (0-20 m) (**Figure 5-1, étape 1**). Ces dépôts ont ensuite été remaniés par les tempêtes suivantes et advectés par les courants vers le prodelta (à partir de 30 m de profondeur) (**Figure 5-1, étape 2**). Les dépôts ainsi observés au niveau du prodelta précédemment identifié, sont souvent des **dépôts secondaires** issus du remaniement de dépôts précoces dans la zone très littorale, pratiquement au niveau du cordon sableux. Dans le cas de la crue généralisée à l'ensemble des fleuves du golfe du Lion en décembre 2003, le prodelta a également été soumis aux apports de matériel fin des fleuves situés plus au

nord, dont le Rhône (**Figure 5-1, étape 3**). Le matériel déposé au niveau du prodelta n'a été remanié qu'en cas de tempêtes ou de courants extrêmes. Le matériel ainsi érodé a été advecté vers la vasière médiane (**Figure 5-1, étape 4**) et/ou exporté vers le large et vers le sud-est (**Figure 5-1, étape 5**).

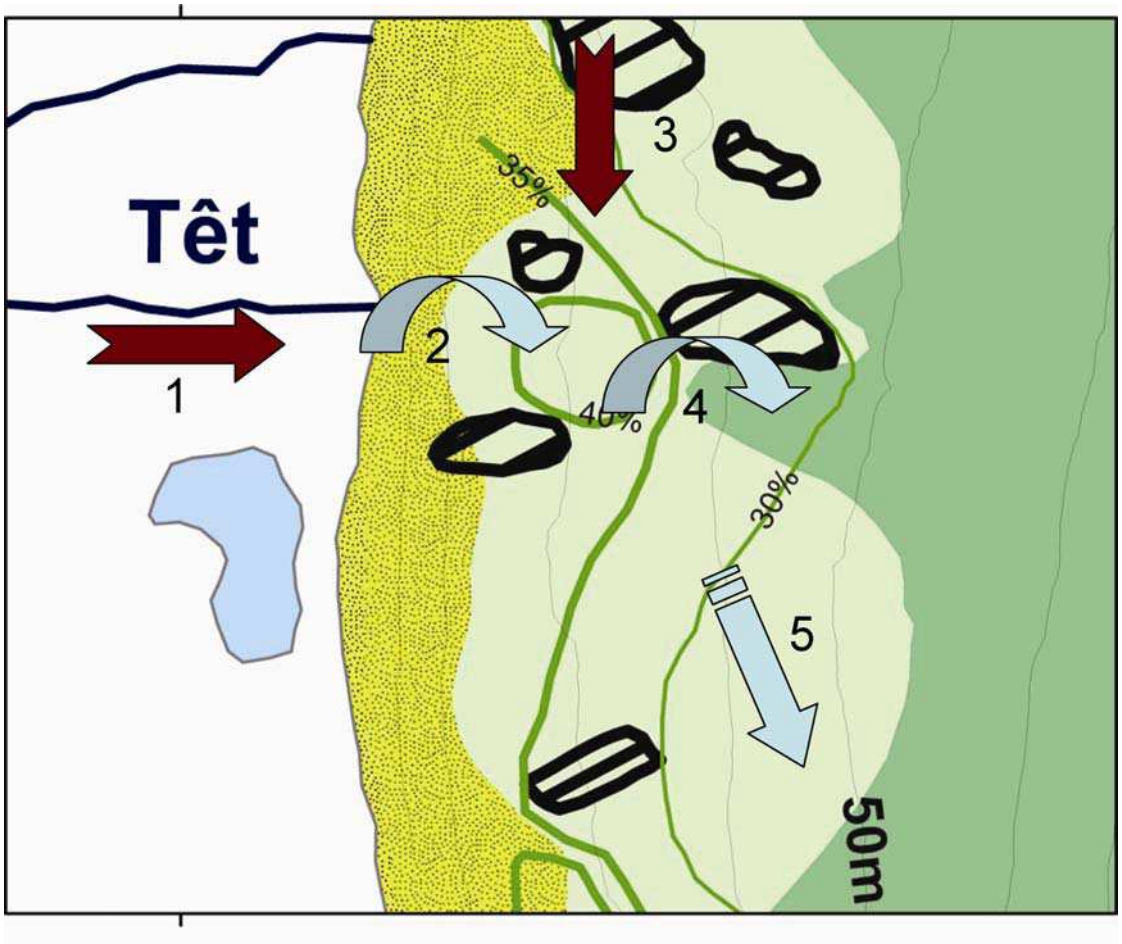

Figure 5-1 : Schéma du transfert du matériel fin d'origine fluviatile dans la zone côtière de la Têt. Les isolignes en vert indiquent les concentrations en argiles. Les plus fortes concentrations limitent l'extension du prodelta. Les étapes du transfert sont détaillées dans le texte : 1. apports fluviatiles, 2. resuspension par les tempêtes et advection vers le prodelta, 3. advection vers le prodelta, 4. resuspension et advection vers la vasière médiane et 5. advection et exportation vers le large.

Le temps de résidence des dépôts précoces dans la zone proche littoral (0-20 m) n'est que de quelques jours (**Traykovski et al., 2000**) en raison des forts courants et tempêtes agissant dans cette zone. Par contre, le temps de résidence des dépôts de crue (directs ou secondaires) au niveau du prodelta est plus important et peut atteindre plusieurs mois. Le dépôt de crue de décembre 2003 a ainsi été observé jusqu'en février 2004 au niveau du prodelta de la Têt

subissant des transformations diagénétiques plus ou moins importantes (compaction, bioturbation,…) (**Wheatcroft and Drake, 2003**). Le temps de résidence de ces dépôts est donc conditionné par l'occurrence des phénomènes érosifs. La conservation d'un dépôt de crue sur le prodelta de la Têt n'est possible que si son temps de résidence est suffisamment important afin de le consolider ou bien s'il est isolé de la surface par le dépôt d'une couche de crue consécutive. Cependant, la conservation et l'enregistrement d'un dépôt de crue n'a pas été observé sur le prodelta de la Têt au cours de cette étude.

5.1.1.2 Les mécanismes d'érosion

Les principaux mécanismes d'érosion mis en évidence au niveau du prodelta de la Têt durant cette étude sont les courants engendrés par les vagues de tempête et ceux engendrés par la circulation induite par les vents. Au niveau des tempêtes, les **tempêtes extrêmes** (Hs > 7 m et Tp > 10 s, décembre 2003 et février 2004) ont provoqué une érosion de plusieurs centimètres au niveau du fond du prodelta de la Têt. Les **tempêtes modérées** (Hs > 3 m et Tp > 8 s, décembre 2003 et mars 2004) ont eu un effet différent sur le fond, en fonction de l'histoire précédente des évènements hydro-sédimentaires du prodelta. Lorsqu'il n'y a pas eu d'apports sédimentaires significatifs à la zone littorale, une tempête modérée crée une érosion nette d'1cm maximum au niveau du prodelta. Par contre, lorsqu'un évènement de crue est intervenu auparavant et que du matériel frais facilement érodable est disponible, une tempête modérée a provoqué une advection de matériel sédimentaire depuis la zone très littorale (0–20 m) vers le prodelta (>30 m), et engendre ainsi un dépôt significatif (décembre 2003).

Le deuxième mécanisme d'érosion identifié au niveau du prodelta de la Têt est la circulation côtière hivernale particulièrement intense durant l'hiver 2004-2005, engendrée par les forts vents continentaux. Ceux-ci peuvent être à l'origine de la formation et de l'écoulement d'eaux denses sur le plateau. Cette circulation intense avec des vitesses au fond > 20 cm/s pendant plusieurs semaines voire plusieurs mois, a créé une érosion continue de plusieurs centimètres sur le fond du prodelta. Le matériel érodé est ainsi advecté par la circulation côtière le long de littoral vers le sud/sud-est et la sortie du golfe du Lion.

Il se détache ainsi deux mécanismes d'érosion/transport suivant le régime des fleuves et la quantité de matériel disponible érodable dans la zone littorale (**Figure 5-2**). En régime de crue, le système multicouche des apports des rivières (**Aloïsi, 1986**) a été identifié au niveau

de l'embouchure de la Têt pendant la crue d'avril 2004 (**Figure 5-2, haut**). Du matériel fin se déplace au sein d'un panache (hypopycnal) de surface vers le sud/sud-est (**Figure 1-3 et Figure 4-25**). Le matériel en suspension se dépose au fur-et-à-mesure de la progression et de la dilution du panache. Une couche de fond est alimentée par le fleuve et des mécanismes continus d'apports, dépôt, resuspension par les tempêtes et redépôt, permettant le déplacement de ce matériel depuis la zone côtière vers la vasière médiane et le domaine du large (**Figure 5-2, haut**). En régime de tempête ou fort courant côtier (cas des plongées d'eaux denses), le matériel sédimentaire disponible est érodé dans la zone littorale par les tempêtes (0-50 m) et jusqu'en bordure du plateau (0-100 m) par les forts courants côtiers et l'écoulement des plongées d'eaux denses (**Figure 5-2, bas**). Le matériel est advecté vers le sud/sud-est le long des isobathes vers la sortie du golfe du Lion et le canyon du Cap de Creus principalement (**Ulses, 2005**).

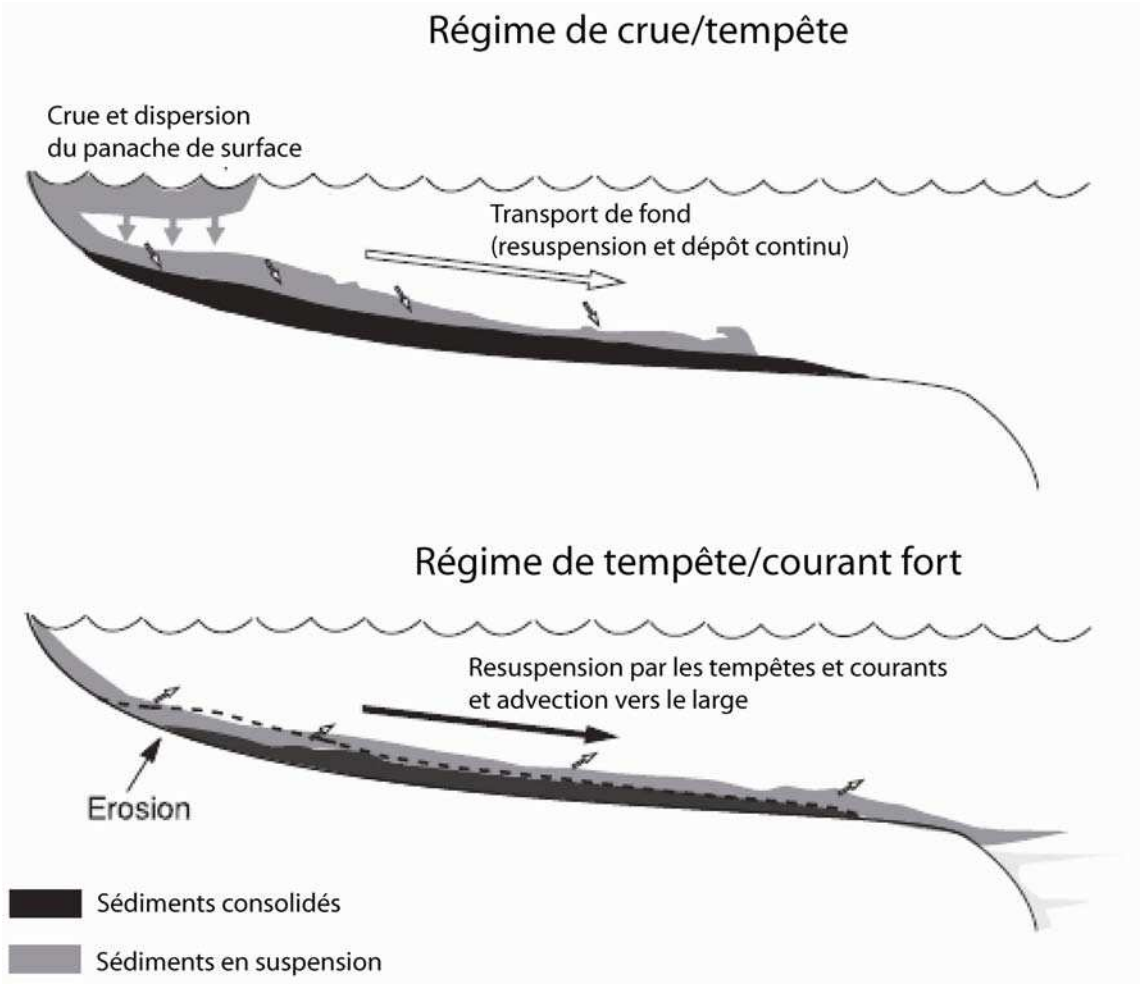

Figure 5-2 : Mécanismes d'érosion/transport intervenant dans le cas d'un régime de crue (en haut) et dans le cas d'un régime de tempête seule ou de forts courants côtiers (circulation induite par le vent et plongées d'eaux denses) (en bas). Repris d'après Fan et al. (2004).

5.1.1.3 Bilan sédimentaire

La balance sédimentaire du prodelta de la Têt est conditionnée par la quantité des apports sédimentaires et l'intensité des mécanismes érosifs. Les années d'observation de cette étude ont été faites durant deux hivers extrêmement énergétiques. Les mécanismes d'érosion ont été concentrés sur la période hivernale. Durant la première année d'observation (2003-2004), caractérisée par des tempêtes et crues extrêmes, le bilan net est pratiquement nul. En effet, l'érosion engendrée lors des évènements de tempêtes (dont une tempête avec une période de retour supérieure à 10 ans) a été équilibrée par les apports sédimentaires des fleuves. Durant la deuxième année d'observation (2004-2005), caractérisée par une circulation côtière hivernale très intense, le bilan net a été une érosion d'environ 4 cm. Le bilan net sur ces deux années extrêmes a donc été fortement négatif. Ce bilan est à opposer aux taux de sédimentation estimés par les mesures de ^{210}Pb, qui sont certes faibles (~0.1 cm/an) mais qui sont le témoin d'un certain enregistrement sédimentaire. Pour équilibrer ce bilan et obtenir de tels taux de sédimentation, ces deux années de mesure au bilan sédimentaire négatif devraient alterner avec des années hydrodynamiquement plus faibles et aux apports sédimentaires plus importants.

5.1.2 L'enregistrement sédimentaire du prodelta de la Têt

5.1.2.1 L'échelle séculaire

Au cours de notre étude, nous avons mis en évidence une **séquence type** d'un prodelta soumis aux apports discontinus d'un fleuve côtier torrentiel et sous l'influence des tempêtes et des forts courants côtiers hivernaux, dans une mer sans marée. Le signal sédimentaire moderne du prodelta de la Têt est composé d'une couche d'environ 10 cm continuellement remaniée par les évènements de tempêtes, et alimentée par le fleuve Têt et les apports des autres fleuves situés plus au nord dans le golfe du Lion. Cette séquence moderne forme une séquence granocroissante vers le haut se terminant par une couche de sables fins (0 - 5 cm) mélangée à des silts et vases (65 -70 % de sables), reposant sur une couche de silts intermédiaire (5 - 10 cm) et d'une couche de vases fines (10 – 15 cm) à la base. Cette couche de base de la **séquence moderne** est caractéristique d'une période d'apports sédimentaires fins prédominants (**Figure 5-4**).

En se référant à la littérature sur l'histoire des crues du fleuve Têt (**Delorme, 1980 ; Desailly, 1990**), on remarque plusieurs évènements catastrophiques qui ont fortement modifié le cours du fleuve ainsi que la position de son embouchure. Ces évènements ont certainement laissé une trace au niveau de l'enregistrement sédimentaire du fleuve. En effet, la crue de 1940 nommée « aiguât », est la plus importante des crues de la Têt de mémoire humaine. Son débit maximum a été évalué à 1800 m^3/s (~ débit moyen du Rhône) avec une charge de 48 g/L et les quantités apportés à la mer ont été colossales (5 à 8 Mt selon **Pardé, 1941** ; contre 2 x 10^4 t en décembre 2003). L'embouchure du fleuve Têt a largement été modifiée après cet évènement comme en témoigne l'avancée de plus 250 m du delta de la Têt et sa double embouchure (**Figure 5-3**). Actuellement, cette avancée à la mer a été gommée par l'érosion littorale et l'embouchure située plus au nord a été comblée.

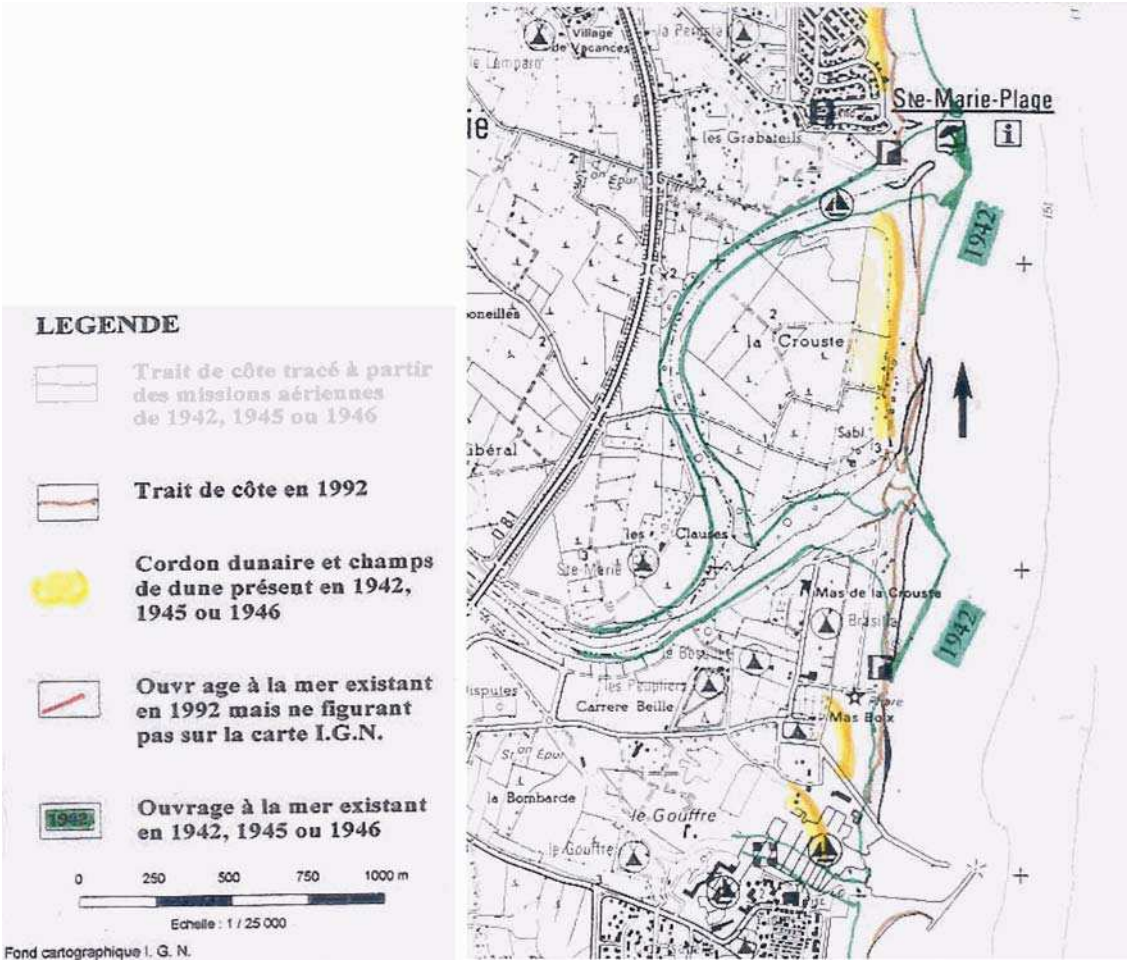

Figure 5-3 : Carte morphologique de l'embouchure de la Têt montrant la position des embouchures de la Têt en 1942 (en vert) et la position actuelle du trait de côte et de l'embouchure de la Têt (en 1992, en marron).

A la lumière des datations au ^{14}C, on s'aperçoit que si cette crue avait laissée une empreinte dans le signal sédimentaire du prodelta de la Têt, celle-ci serait visible dans les premiers centimètres. En effet, la séquence moderne d'âge séculaire atteint sa limite inférieure dès que le ^{210}Pb supporté est atteint (**Figure 5-4**), soit entre 15 et 20 cm de profondeur. Or aucune trace n'est visible. Cela signifie que soit les dépôts sédimentaires liés à cet évènement ont été érodés depuis, soit les dépôts ont été stockés ailleurs. Vu que les stocks sableux au niveau du trait de côte ont disparu, il semblerait que l'hypothèse d'érosion prédomine. Ainsi, une seule crue, aussi forte soit-elle, ne suffit pas à créer un dépôt qui s'enregistre dans la séquence sédimentaire du prodelta de la Têt. Il faudrait alors une période longue de plusieurs centaines d'années au cours de laquelle un nombre important de crues provoque le dépôt de multiples couches de vases fines qui isoleraient les couches sous-jacentes et les protègent de l'érosion.
Actuellement, il semblerait que les apports des fleuves côtiers ne soient pas assez importants pour contrebalancer l'impact des tempêtes et courants. On observerait la formation d'une couche de surface composée de sédiments de plus en plus sableux dépourvue de ses particules les plus fines, tempête après tempête. Cet accroissement de la taille des particules dans les sédiments de surface du prodelta de la Têt est à mettre en relation avec (1) la baisse des apports sédimentaires en rapport avec la construction d'un barrage écrêteur de crue au milieu du bassin, et (2) l'augmentation du nombre de tempêtes suggéré par **Durand (1999)** depuis quelques dizaines d'années. Les zones prodeltaïques étant des oasis pour les organismes benthiques qui y trouvent une source de matière organique fraîche d'origine continentale, une modification de cet environnement liée au changement climatique serait donc préjudiciable pour cette faune mais aussi pour tout l'écosystème associé. En effet, les biologistes ont déjà remarqué un changement des caractéristiques de la macrofaune benthique depuis plusieurs décennies (**Grémare et al., 1998; Labrune et al., sous presse**) en relation avec les variations climatiques à l'échelle régionale. Les prodeltas constituent donc des oasis de vie fragiles qui sont à prendre en compte dans la gestion intégrée de la zone côtière. L'impact anthropique et le changement climatique actuel modifient cet environnement fragile au même titre que la position du trait de côte qui est certes plus préocuppante aux yeux des décideurs locaux.

5.1.2.2 L'échelle pluriséculaire

Le prodelta de la Têt dans sa forme moderne semble se transformer sous l'impact des facteurs cités précédemment. Les apports sédimentaires ne sont plus assez importants pour contrebalancer l'hydrodynamisme de la zone côtière. Mais cela n'a pas toujours été le cas. En

effet, une couche de vases fines située en dessous du signal sédimentaire séculaire est située vers 15-20 cm de profondeur (**Figure 5-4**). Cette couche est le témoin d'une période où les apports sédimentaires fins étaient plus importants et peut-être plus réguliers. Cette période a été rapprochée au Petit Age Glaciaire (1550-1850), marqué par un grand nombre de crues et une activité humaine intense dans le bassin versant laissant supposer un pouvoir érosif plus important. Cette période a déjà été identifiée au niveau du Rhône où l'enregistrement sédimentaire est continu, mais son identification au niveau des Pyrénées était jusque là plus incertaine.

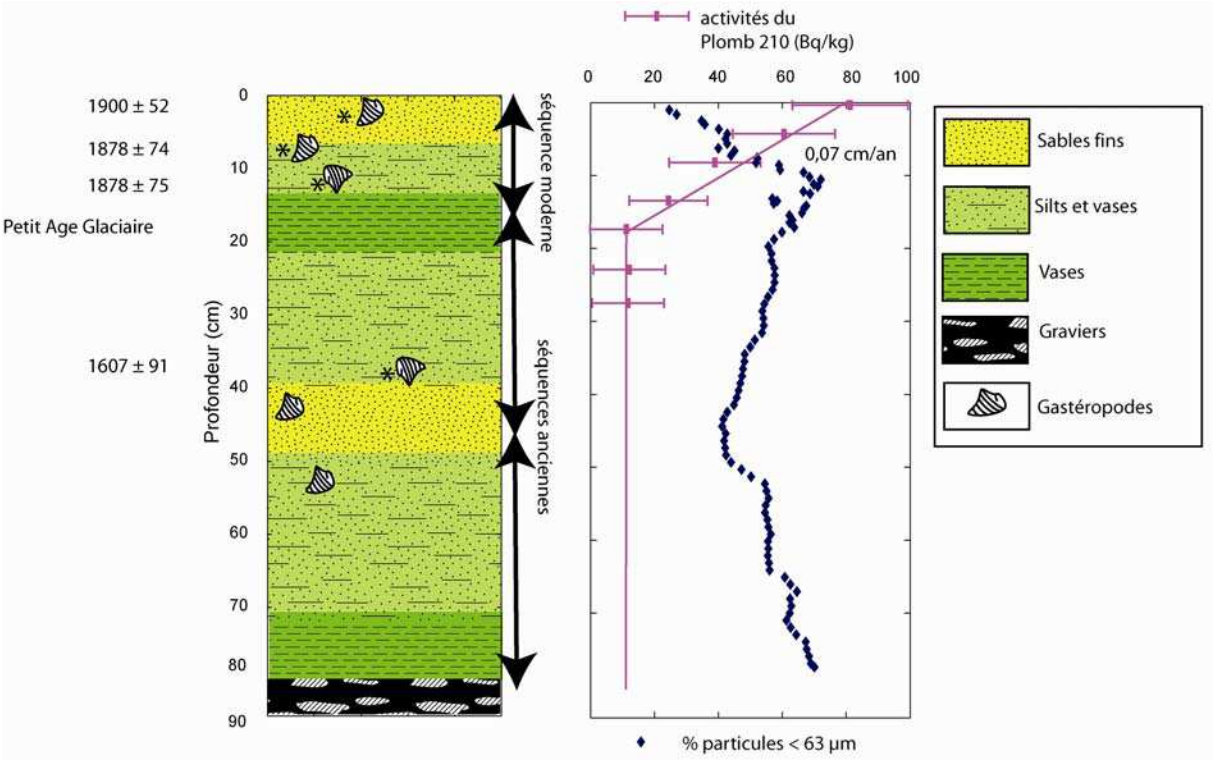

Figure 5-4 : Signal sédimentaire sur le prodelta de la Têt.

Le signal sédimentaire du prodelta de la Têt est également composé de séquences plus anciennes en dessous de la séquence moderne qui témoigne de la variabilité des apports sédimentaires et de l'hydrodynamisme dans cette zone à l'échelle pluriséculaire. Cette séquence sédimentaire représentée sur la **Figure 5-4** repose sur une couche de cailloutis qui serait un des niveaux de base du signal Holocène du prodelta de la Têt.

5.1.3 Généralisation au golfe du Lion

La quantification des apports sédimentaires au golfe du Lion a souvent été limitée aux apports par le Rhône. Bien qu'il contribue en moyenne annuelle à environ 92 et 94 % des apports liquides et solides (**Partie 4.1**), les fleuves côtiers peuvent apporter des quantités non négligeables durant les crues-éclairs. En effet, si l'on considère la contribution des débits journaliers du Rhône par rapport à ceux des fleuves côtiers, on remarque de brefs évènements où la contribution des fleuves côtiers devient significative et même supérieure dans certains cas, qui restent cependant assez rares (**Partie 4.1** et **Figure 5-5**).

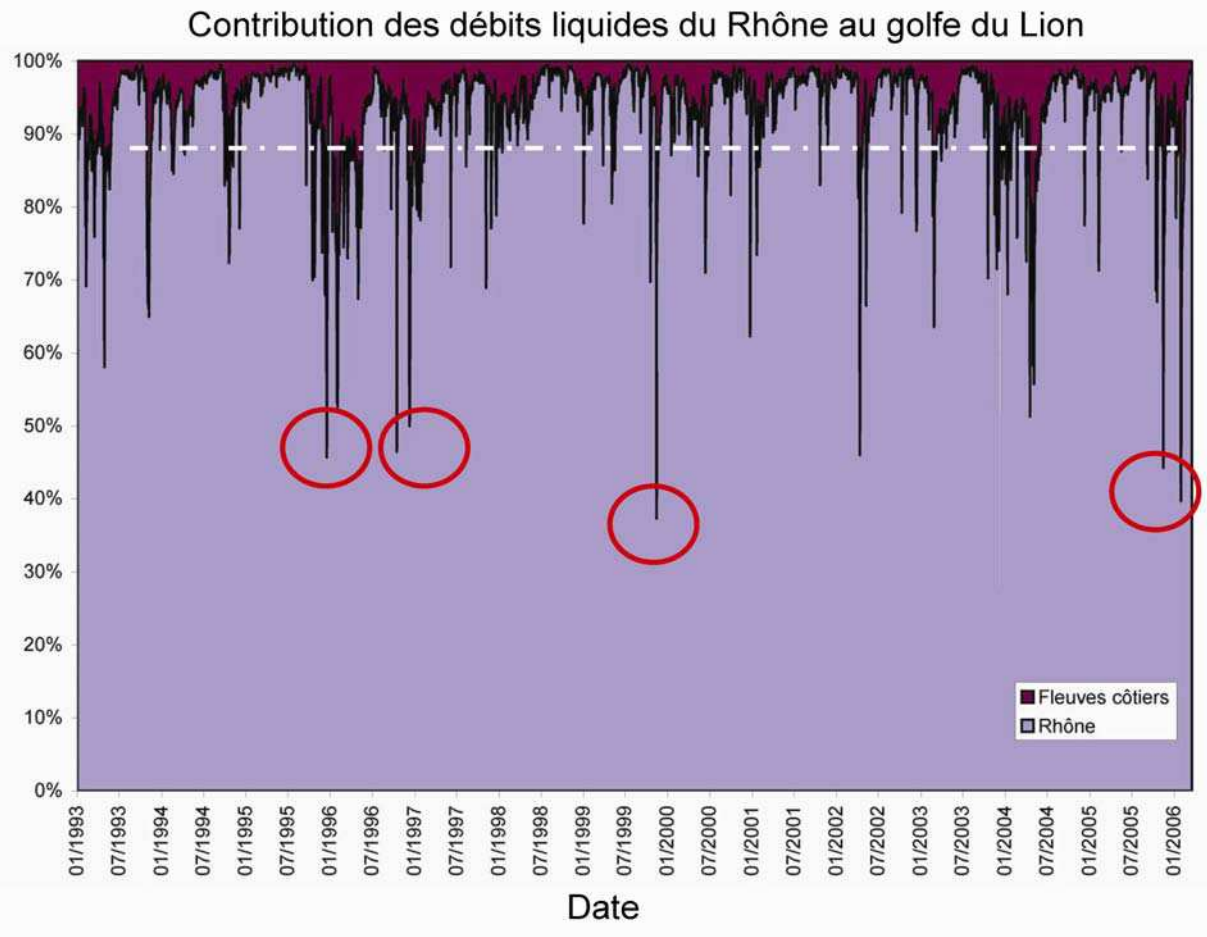

Figure 5-5 : Contribution des débits liquides du Rhône par rapport à ceux des fleuves côtiers au golfe du Lion de 1993 à 2001. La ligne en pointillés blancs représente la moyenne de la contribution du Rhône (~ 95 %) et les cercles rouges représentent les évènements où la contribution des fleuves côtiers est supérieure à celle du Rhône.

Sur les dernières décennies, les apports annuels du Rhône correspondent à environ 10 Mt, mais ils ne seraient plus que de 7-8 Mt actuellement (**Antonelli et Provansal, 2002**). En recoupant les travaux de divers auteurs (**Beaudouin et al., 2005; Durrieu de Madron et al.,**

2000; Lansard, 2004; Radakovitch et al., 1999), on peut considérer qu'environ 50% des ces apports sont stockés dans le prodelta (soit environ 2 Mt), où les taux de sédimentation peuvent atteindre des valeurs de 20 cm/an en face de l'embouchure (**Radakovitch et al., 1999**). Concernant les fleuves côtiers, les fleuves situés au nord du golfe du Lion (Lez et Vidourle) apportent 0.05 Mt, les fleuves centraux (Orb, Aude et Hérault) 0.39 Mt et les fleuves du sud du golfe 0.19 Mt, soit un total de 0.64 Mt/an. Le prodelta de l'Aude stocke 45% des apports adjacents, soit 0.18 Mt, alors que le prodelta de la Têt en stocke 20% soit 0.04 Mt. Cependant les taux de sédimentation restent faibles dans ces zones prodeltaïques (0.12 et 0.07 cm/an respectivement) montrant ainsi la prépondérance des forçages hydrodynamiques sur les apports sédimentaires. Les taux de stockage dans les prodeltas de ces fleuves côtiers montrent également qu'une grande partie du matériel sédimentaire d'origine fluviatile contourne la zone prodeltaïque au profit des zones du large.

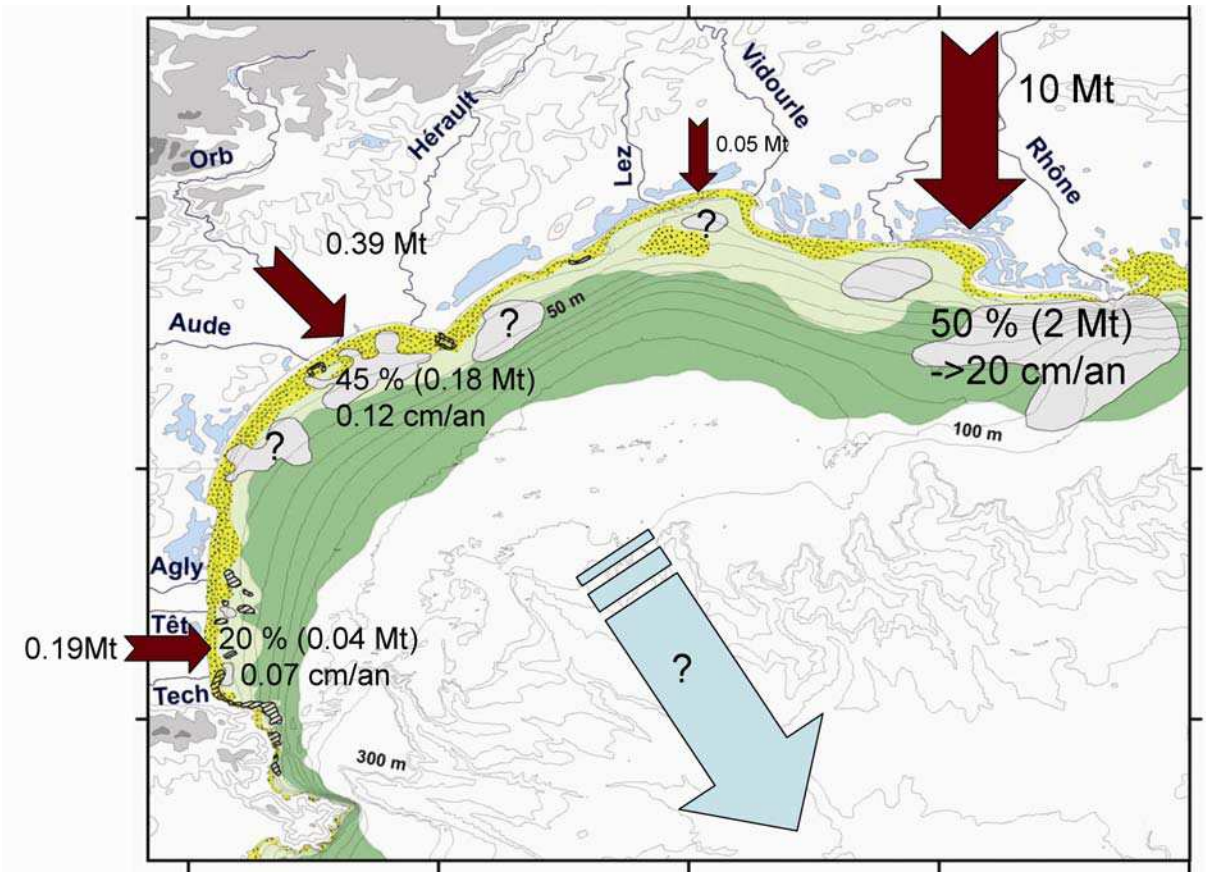

Figure 5-6 : Schéma du bilan des apports sédimentaires (moyennes annuelles) dans le golfe du Lion et des quantités stockées dans les prodeltas. Les prodeltas sont représentés en gris clair, les sables littoraux en jaune et la vasière médiane en vert.

Il reste cependant quelques inconnues dans ce bilan comme les quantités stockées en face du Lez et du Vidourle au niveau de son prodelta bien identifié dans le golfe d'Aigues-Mortes (**Aloïsi and Monaco, 1975**). Il existe dans cette zone une circulation côtière particulière qui pourrait favoriser le stockage des apports fluviaux fins dans la zone littorale (**Denamiel, 2006**). D'autres zones prodeltaïques actives ou inactives sont également présentes en face de l'étang de Thau et en face des étangs de Sigean. Leur fonctionnement actuel reste mal défini.

La fonction de stockage des prodeltas et de la vasière médiane est donc bien établie. Par contre, les quantités échangées entre les deux et le rôle de source pour la zone du large restent mal appréciés (**Figure 5-6**). Les quantités apportées par les fleuves et stockées dans les prodeltas et la vasière médiane présentent une forte variabilité interannuelle. **Monaco (1971)** avait établi que 80% des apports des fleuves étaient stockés dans la zone côtière. Cependant, durant une année extrêmement énergétique et propice aux crues, **Ulses (2005)** a montré par la modélisation qu'environ 8 Mt de sédiments ont été apportés par les fleuves en 2003-2004 et que la même quantité a été exportée hors du plateau par les canyons du sud-ouest du golfe. Une simulation sur l'année 1998-1999 (**Ferré et al., soumis**), caractérisée par une circulation hivernale intense montre également que la zone du Cap de Creus est la sortie du golfe du Lion en termes de transport Les prodeltas seraient donc à la fois des puits de matière dans la zone côtière mais également des sources de matière pour le reste de la plateforme continentale et le domaine du large.

5.1.3.1 Connexion avec les autres unités de la zone côtière

Le prodelta de la Têt est une zone de stockage et d'échange de matière dans la zone côtière. En effet, les apports des fleuves y sont stockés soit directement soit secondairement après advection de matériel précédemment déposé dans la zone proche littorale. Une fois stocké ce matériel sédimentaire fin peut être remanié et déplacé sur le fond vers la vasière médiane puis progressivement vers la sortie du golfe du Lion tempête après tempête (**Figure 5-7**). Une autre voie de transfert de matériel fin depuis l'embouchure du fleuve se fait par dispersion d'un panache turbide de surface. Cette voie de transfert est aperçue sur les images satellite et peut être de direction différente du transport de fond. Au niveau du prodelta de la Têt, alors que le transport de fond est dirigé vers le sud-est, le transport de surface (**hypopycnal**) se fait dans le sens de la circulation côtière le long du littoral principalement vers le sud. Dans les deux cas, transport de fond et de surface, l'issue finale du matériel fin se fait à l'extrémité sud

du golfe du Lion : les canyons du Lacaze-Duthiers et du Cap de Creus et la partie du plateau entre le promontoire du Cap de Creus et le canyon portant le même nom (**Figure 5-7**).

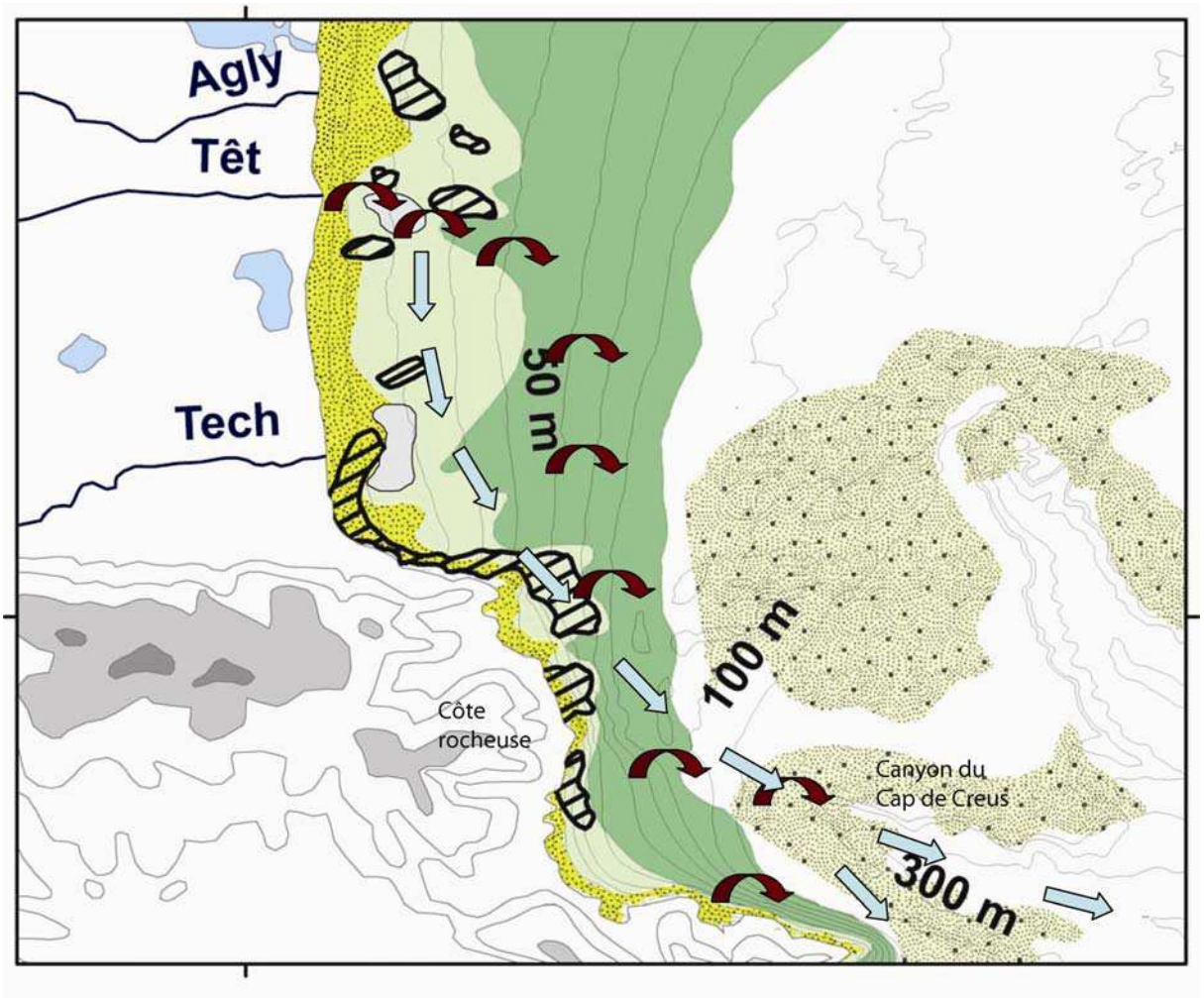

Figure 5-7 : Schéma de connexion de la zone prodeltaïque de la Têt avec les autres unités sédimentaires fonctionnelles de la zone côtière du golfe du Lion (redessinée d'après Aloïsi et al., 1973 ; Monaco et Aloïsi, 2000). Les flèches arrondies rouges correspondent au transport de matériel fin sur le fond et les flèches droites bleue-ciel représentent le transport du matériel par les panaches fluviaux de surface. La limite inférieure de la carte correspond à la frontière franco-espagnole au niveau du promontoire du Cap de Creus.

La carte morpho-sédimentaire du golfe du Lion représentée sur la **Figure 5-7** montre la continuité de la vasière médiane le long du littoral roussillonnais jusqu'au-delà de la frontière franco-espagnole et le promontoire du Cap de Creus. Les études récentes montrent que la zone située entre le début de la côte rocheuse et la tête du canyon du Cap de Creus correspond à une zone de contournement sédimentaire et donc de non-dépôt (**DeGeest et al., soumis**). En

effet, le plateau se rétrécie dans cette zone et les courants s'accélère limitant ainsi le dépôt de matériel dans cette zone.

5.1.3.2 Apports de la modélisation

La modélisation apporte une information importante concernant l'extension spatiale des mécanismes observés au niveau du prodelta de la Têt. Les sorties du modèle Symphonie calibré en partie avec les données acquises au cours de nos expériences de terrain confirment plusieurs choses.

1. Le transfert du matériel fluviatile observé le long du littoral sur les images satellites en période de crue (**Figure 5-8**), formant un long fleuve turbide s'écoulant vers le sud et le canyon du Cap de Creus est confirmé par les courants modélisés dans le golfe du Lion. Ceux-ci montrent la circulation générale sur le plateau d'est en ouest ainsi que l'intensification des courants à l'extrémité sud-ouest du golfe du Lion (**Figure 5-9**).

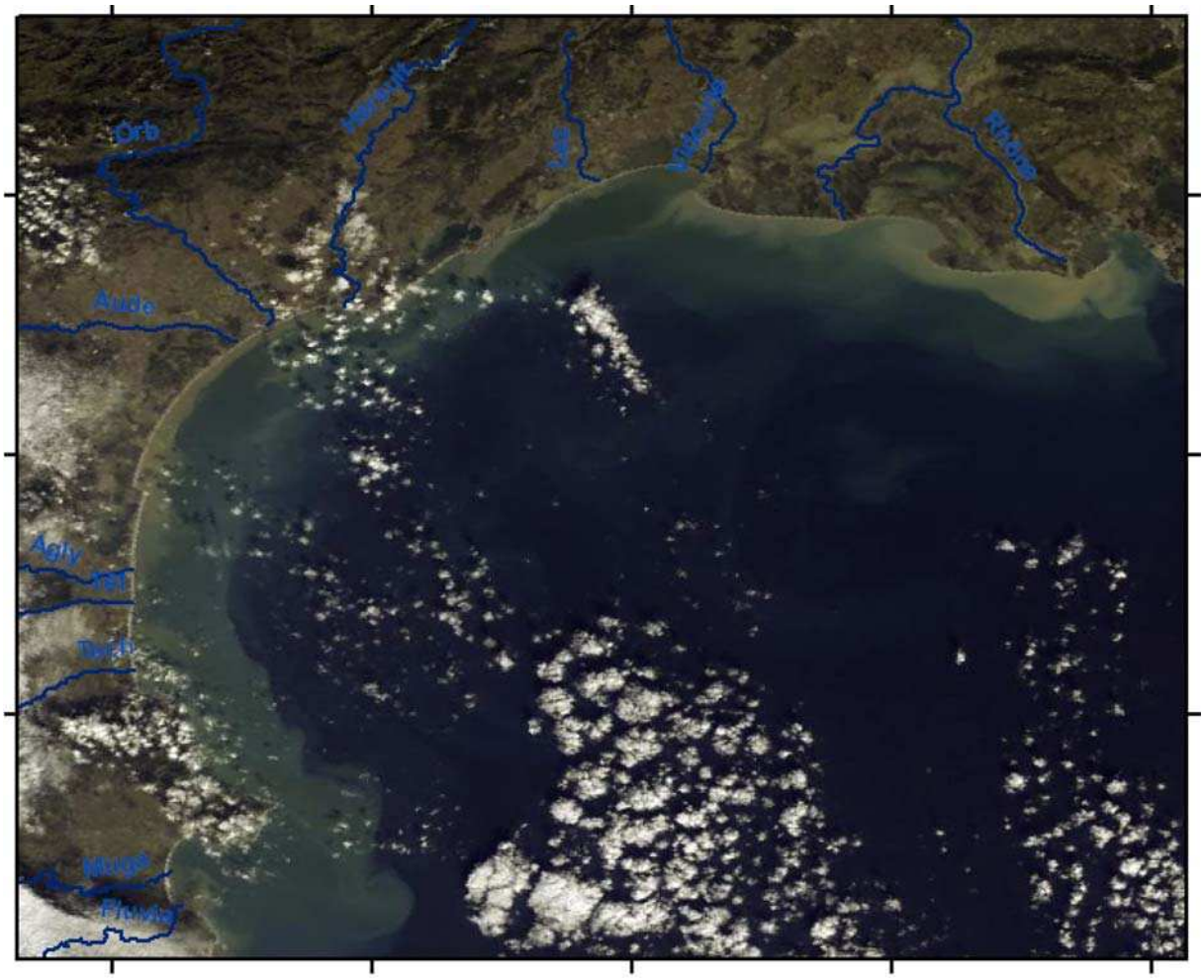

Figure 5-8 : Image satellite du 8 décembre 2003 après une crue généralisée montrant l'écoulement du fleuve côtier turbide vers le sud et le canyon du Cap de Creus.

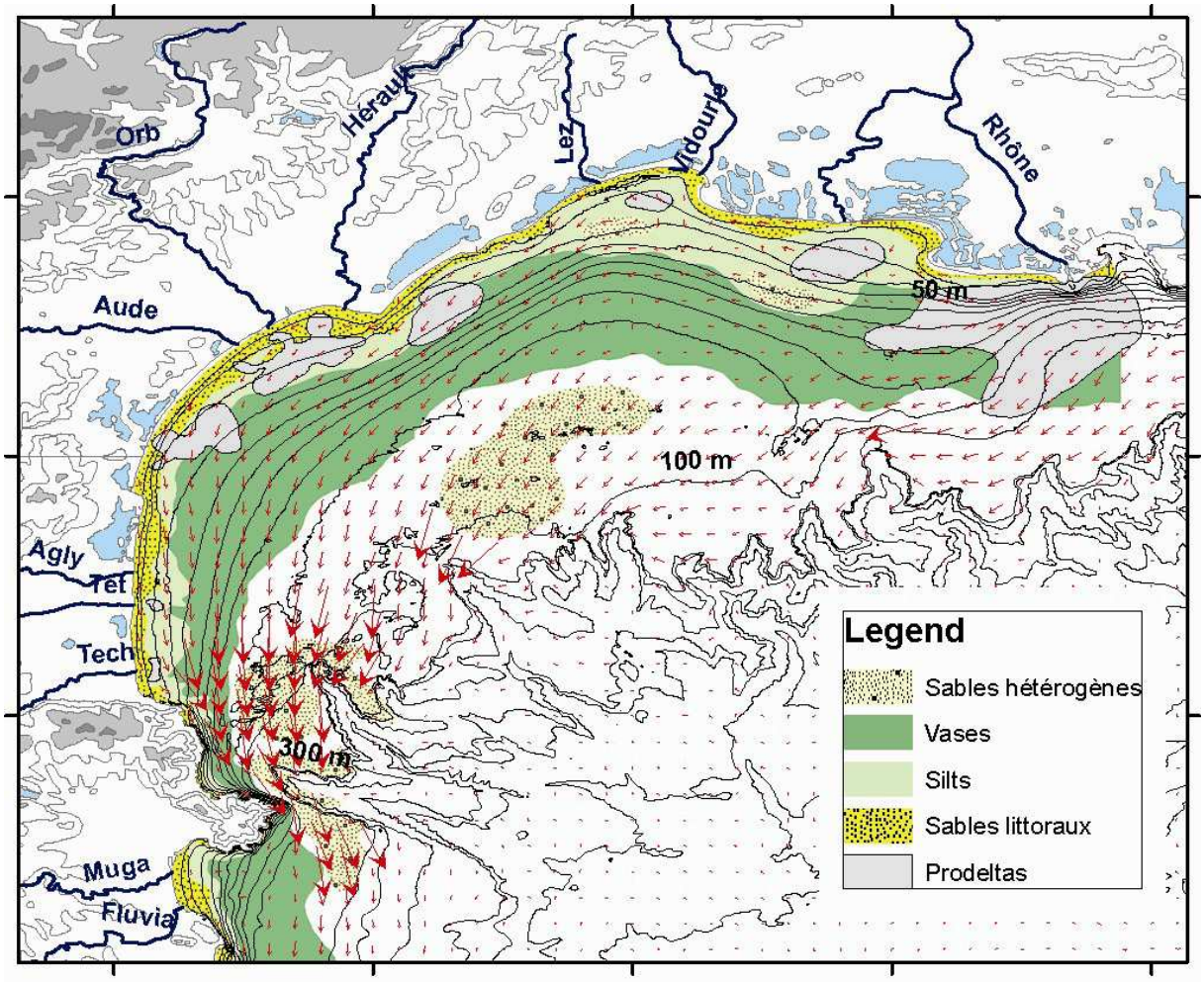

Figure 5-9 : Carte générale des fonds sédimentaires du golfe du Lion (Monaco et Aloïsi, 2000) et superposition des courants modélisés durant un épisode de tempête (Ulses, 2005).

2. Une simulation des épaisseurs de sédiment érodées et déposées durant la période novembre 2003-mai 2004 caractérisée par des évènements extrêmes de crues et tempêtes confirme : (i) que le prodelta du Rhône est une zone de dépôt préférentielle du matériel fluviatile, (ii) le rôle de stockage de la vasière médiane au détriment de la zone côtière et de l'ensemble des prodeltas associés aux fleuves côtiers qui apparaissent en érosion (**Figure 5-10**). Le plateau externe et l'extrémité sud-ouest du golfe du Lion sont également fortement érodés par les forts courants de tempêtes laissant affleurer des formations plus anciennes. Une zone de dépôt apparaît également au niveau du canyon du Cap de Creus montrant la zone de transfert préférentielle entre le plateau et le bassin profond.

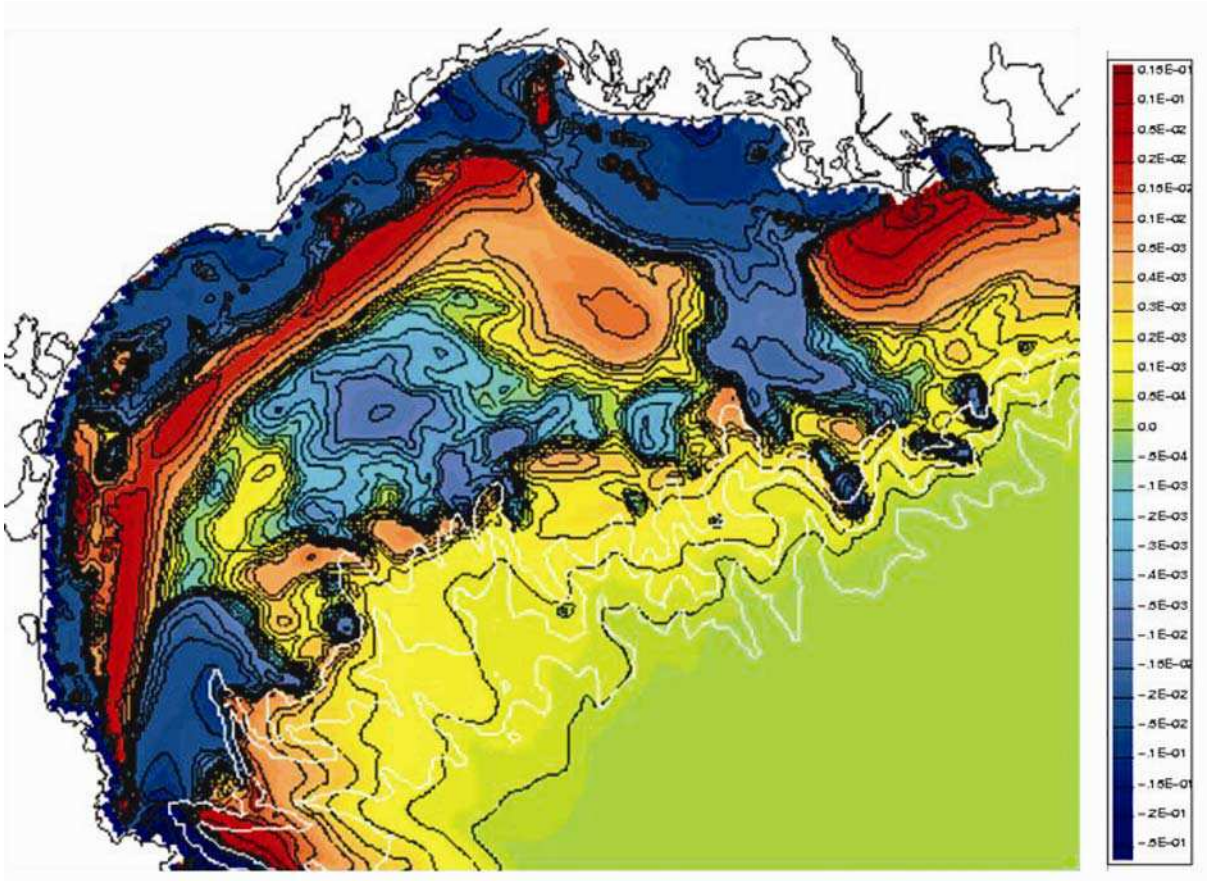

Figure 5-10 : Simulation des épaisseurs de sédiment érodées(en bleu) et déposées (en rouge) durant la période novembre 2003-2004 (Ulses, 2005 ; Ulses et al., soumis).

Les simulations n'ont été pas encore été faites pour l'année 2004-2005 caractérisée par la formation et l'écoulement d'eaux denses sur le plateau, mais on s'attend à obtenir la confirmation des données acquises au niveau du pro delta comme pour l'année 2003-2004.

5.1.4 Conclusions

Le prodelta de la Têt est un exemple de système côtier dans une mer sans marée, soumis aux apports d'un fleuve côtier à caractère torrentiel et aux agents hydrodynamiques intenses du domaine marin. Cette unité de la zone côtière est très dynamique et se caractérise par un taux de sédimentation très faible. Les apports des fleuves (crues extrêmes) arrivent à peine à équilibrer l'impact des agents hydrodynamiques (tempêtes extrêmes, circulation hivernale intense). Le bilan a été d'ailleurs négatif sur les deux années étudiées, mais les taux de sédimentation mesurés font penser que des mesures sur une année moins énergétique auraient montré un bilan sédimentaire positif. Il en résulte que le prodelta joue à la fois le rôle de puits

de matière de la zone côtière et de source pour les autres unités (vasière médiane et domaine du large).

Le signal sédimentaire du prodelta de la Têt montre deux aspects différents selon l'échelle à laquelle on se place. A l'échelle séculaire, ce signal montre l'importance des forçages hydrodynamiques sur les apports fluviatiles. La modification de la couche sédimentaire de surface est accentuée par l'impact anthropique (limitation des apports par effet barrage) et le changement climatique (recrudescence des tempêtes). A l'échelle pluriséculaire, des périodes d'apports plus intenses traduites par des unités prodeltaïques dans le signal sédimentaire, montrent que le prodelta a pleinement joué son rôle de stockage de matière dans la zone côtière au cours de la période fini-Holocène.

Les autres prodeltas du golfe du Lion (Tech, Aude, Vidourle) fonctionnent de la même manière. Ils sont de véritables réacteurs en jouant à la fois le rôle de stockage et d'échange de matière sédimentaire mais aussi de matière organique et de toutes sortes de polluants à l'interface Terre-Mer. La remise en suspension de ces éléments par les agents hydrodynamiques intervient donc dans la qualité des eaux de la zone côtière. Leur gestion doit faire partie intégrante du développement et de la gestion intégrée de la zone côtière.

5.2 Conclusion générale et perspectives

Le but de cette étude était de caractériser la dynamique sédimentaire d'une zone prodeltaïque soumise aux apports discontinus d'un fleuve côtier et sous l'influence des agents hydrodynamiques marins. La réalisation d'une plateforme instrumentée sur le prodelta de la Têt a constitué une première étape. Les deux années suivies ont été des années extrêmes et ont permis de caractériser l'impact des évènements hydro-climatiques intenses caractéristiques du climat méditerranéen. Dans ce sens, des évènements avec des périodes de retour importantes se sont produits sur notre site d'étude et leur mesure s'est parfaitement déroulée. La couverture sédimentaire du golfe du Lion s'est mise en place non pas progressivement mais à la suite d'évènements hydro-climatiques majeurs ; ce sont eux qui contrôle sa dynamique. Dans ce sens, les prodeltas sont les témoins à l'interface Terre-Mer de la dynamique fluviomarine et la compréhension des processus qui les régissent ne peut se faire qu'au travers de leur suivi haute-résolution et sur le long terme.

La stratégie employée lors de cette étude, suivi automatisé et à haute fréquence, s'est révélée adaptée à l'étude d'évènements brefs et intenses. Un petit système comme la Têt a été relativement facile à instrumenter alors que l'instrumentation d'un gros système comme le Rhône aurait été plus difficilement réalisable et le dispositif n'aurait sans doute pas résisté aux phénomènes hydrologiques violents du Rhône. Cependant, ces systèmes fonctionnent de la même façon et les résultats issus de l'étude du système Têt peuvent être extrapolés aux autres systèmes plus larges. Nous avons donc acquis un certain savoir-faire en termes de suivi et d'instrumentation qui pourrait très bien être appliqué sur d'autres environnements comme les autres prodeltas méditerranéens, les embouchures des fleuves, les graus des lagunes…
Dans cette étude, on a essayé de coupler des mesures hydrodynamiques haute-fréquence à l'échelle évènementielle avec des prélèvements sédimentaires qui intègrent les phénomènes hydro-sédimentaires sur une période plus longue. Cette étude multi-échelle a ainsi permis de faire le lien entre les travaux faits il y a quelques années sur l'enregistrement sédimentaire du golfe du Lion à l'échelle Holocène en utilisant des techniques de mesure géophysique avec des études de la dynamique évènementielle haute-fréquence. On a ainsi essayé de relier les échelles pluriséculaires, séculaires, interannuelles, saisonnières et évènementielles ; en faisant l'hypothèse que les phénomènes actuels se sont déroulés à l'identique dans le passé et traduisent les mêmes processus.

Les premiers bilans des quantités de matière stockées dans les prodeltas restent cependant à affiner. L'utilisation du ^{210}Pb et du modèle de taux d'apports constants atteint sans doute ces limites dans ces environnements très dynamiques où la résultante sédimentaire ne traduit pas des phénomènes constants dans le temps. De plus ces bilans ont été basés sur de trop rares prélèvements et une couverture sédimentaire plus fine (qui avait été prévue) permettrait d'affiner les bilans au niveau de ces prodeltas.
Les processus hydrosédimentaires se déroulant à l'interface eau-sédiment ont été relativement bien décrits à l'interface Terre-Mer. Des mesures de la dynamique des particules dans la colonne d'eau ont été menées avec succès dans le cadre de cette étude, mais les phénomènes complexes, comme par exemple l'agrégation/floculation au niveau du choc salin n'ont pas été entièrement approchés. Des mesures complémentaires de la dynamique des particules notamment à l'interface eau de mer/eau douce sont envisagées dans le futur. Ceci permettrait d'expliquer aussi mécanismes de complexassions des particules fines avec les contaminants qui sont concentrés au niveau des prodeltas.

Enfin, les prodeltas, unités fonctionnelles à l'interface Terre-Mer, sont des réacteurs d'échange dans la zone côtière et participent pleinement à la qualité des eaux littorales. Leur suivi haute-fréquence initié durant cette étude doit être continué sur le long terme. Il s'inscrit dans le cadre de la Zone Atelier ORME, soutenue par le CNRS-DEDD et le futur observatoire du littoral méditerranéen du Cépralmar et de la région Languedoc-Roussillon. Le long terme permettra de valider les scénarios climatiques et les changements de l'environnement sous l'impact de l'activité humaine.

Table des illustrations

Table des tableaux

Références bibliographiques (hors articles)

Agence de l'Eau Rhône-Méditerranée et Corse, 2007. L'eau dans le bassin Rhône-Méditerranée. Availble at: http://www.rhone-mediterranee.eaufrance.fr/.

Aloïsi, J.C., 1986. Sur un modèle de sédimentation deltaïque. Contribution à l'étude des marges passives. Thèse d'Etat, Univ. Perpignan, 162 pp.

Aloïsi, J.C., Got, H. and Monaco, A., 1973. Carte géologique du précontinent languedocien au 1/250000ième., International Institute for Aerial Survey and Earth Sciences (I.T.C.) (Eds.), Netherlands.

Aloïsi, J.-C. and Monaco, A., 1975. La sédimentation infralittorale. Les prodeltas nord-méditerranéens. C. R. Acad. Sci. D, 280: 2833-2836.

Aloïsi, J.-C., Monaco, A. and Pauc, H., 1975. Mécanisme de la formation des prodeltas dans le Golfe du Lion. Exemple de l'embouchure de l'Aude (Languedoc). Bull. Inst. Géol. Bassin Aquitaine, 18: 3-12.

Aloïsi, J.C., Monaco A., Planchais, N., Thommeret, J. and Thommeret, Y., 1978. The Holocene transgression in the golfe du Lion, southwestern France: paleogeographic and paleobotanical evolution. Géogr. Phys. Quat., XXXII(2) : 145-163.

Anguenot, F. and Monaco, A., 1967. Etude de transits sédimentaires, sur le littoral du Roussillon, par la méthode des traceurs radioactifs. Cah. Océanogr., 19(7) : 579-589.

Antonelli, C., 2002. Flux sédimentaires et morphogenèse récente dans le chenal du Rhône aval. PhD Thesis, Univ. Aix-Marseille I, 279 pp.

Antonelli, C. and Provansal, M., 2002. Vers une ré-évaluation des matières en suspension du Rhône aval par acquisition de mesures sur toute la colonne d'eau, Colloque "Geomorphology : from Expert Opinion to Modelling" Strasbourg.

Aunay, B., 2007. Apport de la connaissance géologique fine des aquifères côtiers à la fiabilité des modèles de simulations hydrodynamiques pour la gestion des ressources en eau de la frange littorale. PhD Thesis, Univ. Montpellier.

Balland, P., Martin, X., Monadier, P., Thibault, M., Portier, B., Laurain, C., Nassiet, Y. and Robert de-Saint-Vincent, E., 2004. La sécurité des digues du delta du Rhône - Politique de constructibilité derrière les digues, Ministère de l'écologie et du développement durable.

Banque Hydro, 2007. Banque nationale de données pour l'hydrométrie et l'hydrologie. Ministère de l'Environnement. Available at http://www.hydro.eaufrance.fr/.

Beaudouin, C., Suc, J.-P., Cambon, G., Touzani, A., Giresse, P., Pont, D., Alois, J.-C., Marsset, T., Cochonat, P., Duzer, D. and Ferrier, J., 2005. Present-Day Rhythmic Deposition in the Grand Rhone Prodelta (NW Mediterranean) According to High-Resolution Pollen Analyses. J. Coast. Res., 21(2) : 292-306.

BRGM, 1996. Carte géologique de Perpignan 1/50000e.

Butel, R., Dupuis, H. and Bonneton, P., 2002. Spatial variability of wave conditions on the French Atlantic Coast using In-Situ data. J. Coast. Res., SI 36: 96-108.

Canals, M., Puig, P., de Madron, X.D., Heussner, S., Palanques, A. and Fabres, J., 2006. Flushing submarine canyons. Nature, 444(7117): 354-357.

Carles Ibàñez, N.P.A.C., 1996. Changes in the hydrology and sediment transport produced by large dams on the lower Ebro River and its estuary. Regulated Rivers: Research & Management, 12(1): 51-62.

Cattaneo, A., Trincardi, F., Asioli, A. and Correggiari, A., 2007. The Western Adriatic shelf clinoform: energy-limited bottomset. Cont. Shelf Res., 27(3-4): 506-525.

Certain, R., 2002. Morphodynamique d'une côte sableuse microtidale à barres : le Golfe du Lion (Languedoc-Roussillon). PhD Thesis, Univ. Perpignan, 209 pp.

Coleman, J.M. and Wright, L.D., 1975. Modern river deltas: variability of processes and sand bodies. In: M.L. Broussard (Editor), Deltas Models for Exploration Houston Geological Society, Houston, pp. 99–149.

Compagnie Nationale du Rhône, 2006. Available at http://www.cnr.tm.fr/fr/index.htm.

Courtois, G., Monaco, A., 1969. Radioactive methods for the quantitative determination of coastal drift rate. Mar. Geol., 7 (3): 183-206.

DeGeest, A.L., Mullenbach, B.L., Puig, P., Nittrouer, C.A., Drexler, T.M., Durrieu de Madron, X. and Orange, D.L., soumis. Sediment accumulation in the western Gulf of Lions, France: The role of Cap de Creus Canyon in linking shelf and slope sediment dispersal systems. Cont. Shelf Res.

Delorme, A., 1980. Mémoire sur la protection de la ville de Perpignan contre les inondations.

Delrieu, G., Véronique Ducrocq, Eric Gaume, John Nicol, Olivier Payrastre, Eddy Yates, Pierre-Emmanuel Kirstetter, Hervé Andrieu, Pierre-Alain Ayral, Christophe Bouvier, Jean-Dominique Creutin, Marc Livet, Sandrine Anquetin, Michel Lang, Luc Neppel, Charles Obled, Jacques Parent du-Châtelet, Georges-Marie Saulnier, Andrea Walpersdorf and Wobrock, W., 2005. The Catastrophic Flash-Flood Event of 8–9 September 2002 in the Gard Region, France: A First Case Study for the Cévennes–Vivarais Mediterranean Hydrometeorological Observatory. J. Hydromet., 6(1) : 34-52.

Denamiel, C., 2006. Etude de la dynamique sédimentaire dans le Golfe d'Aigues-Mortes. PhD Thesis, Univ. Montpellier.

Desailly, B., 1990. Crues et inondations en Roussillon. Le risque et l'aménagement fin du XVIIe siècle - milieu du XXe siècle. PhD Thesis, Univ. Paris X - Nanterre, 352 pp.

Diaz, J., Palanques, A., Nelson, C.H. and Guillén, J., 1996. Morpho-structure and sedimentology of the Holocene Ebro prodelta mud belt (northwestern Mediterranean Sea). Cont. Shelf Res., 16(4): 435-456.

DRL Software Ltd, 2003. Sediview Procedure Manual.

Durand, P., 1999. L'évolution des plages de l'ouest du Golfe du Lion au XXème siècle. PhD Thesis, Univ. Lumière Lyon 2, 461 pp.

Durrieu de Madron, X., Abassi, A., Heussner, S., Monaco, A., Aloïsi, J.C., Radakovitch, O., Giresse, P., Buscail, R., and Kerhervé, P., 2000. Particulate matter and organic carbon budgets for the Gulf of Lion (NW Mediterranean). Oceanol. Acta, 23(6) : 717-730.

Estournel, C., Durrieu de Madron, X., Marsaleix, P., Auclair, F., Julliand, C. and Vehil, R., 2003. Observation and modeling of the winter coastal oceanic circulation in the Gulf of Lion under wind conditions influenced by the continental orography (FETCH experiment). J. Geophys. Res., 108(C3) : 8059, doi : 10.1029/2001JC000825.

Fan, S., Swift, D.J.P., Traykovski, P., Bentley, S., Borgeld, J.C., Reed, C.W. and Niedoroda, A.W., 2004. River flooding, storm resuspension, and event stratigraphy on the northern California shelf: observations compared with simulations. Mar. Geol., 210(1-4): 17-41.

Ferré, B., 2004. Comparaison de l'effet des tempêtes et du chalutage sur la resuspension et le transport de matières particulaires dans le Golfe du Lion. PhD Thesis, Univ. Perpignan, 256 pp.

Ferré, B., Durrieu de Madron, X., Estournel, C., Ulses, C., Le Corre, G., soumis. Impact of natural (waves and currents) and anthropogenic (trawl) resuspension on the export of particulate matter to the open ocean. Application to the Gulf of Lion (NW Mediterranean. Continental Shelf Research.

Galloway, W.E., 1975. Process framework for describing the morphologic and stratigraphic evolution of deltaic systems. In: M.L. Broussard (Editor), Deltas, Models for Exploration. Houston Geology Society, Houston, pp. 87-98.

Garcia-Estevez, J., 2005. Géochimie d'un fleuve côtier méditerranéen : la Têt en Roussillon. Origines et transferts de matières dissoutes et particulaires de la source jusqu'à la mer. PhD Thesis, Univ. Perpignan, 263 pp.

Gaume, E., Livet, M., Desbordes, M. and Villeneuve, J.-P., 2004. Hydrological analysis of the river Aude, France, flash flood on 12 and 13 November 1999. J. Hydrol., 286(1-4): 135-154.

Goldberg, E.D., 1963. Geochronology with 210-lead radioactive dating, I.A.E.A., Vienna.

Got, H., 1973. Etude des corrélations tectonique-sédimentation au cours de l'histoire quaternaire du précontinent Pyrénéo-catalan. PhD Thesis, Univ. Sci. Tech. Languedoc, 294 pp.

Grémare, A., Amouroux, J.M. and Vétion, G., 1998. Long-term comparison of macrobenthos within the soft bottoms of the Bay of Banyuls-sur-mer (northwestern Mediterranean Sea). J. Sea Res., 40: 281-302.

Guarracino, M., 2004. Contrôle hydrodynamique du transfert de la matière particulaire sur la marge continentale du Golfe du Lion. PhD Thesis, Univ. Perpignan.

Guizien, K., soumis. Mesures de l'état de mer au large de Banyuls S/ Mer (Sud Roussillon) de 2002 à 2005. Met Mar.

Hay, A.E., 1991. Sound Scattering from Particle-laden, Turbulent Jet. J. Acoust. Soc. Am., 20: 868.

Hovius, N., 1998. Controls on sediment supply by large rivers. In: K.W. Shanley, McCabe, P.J. (Editor), Relative Role of Eustasy, Climate and Tectonism in Continental Rocks. SEPM Special Publication, pp. 3-16.

Jestin, H., Bassoullet, P., Le Hir, P., L'Yavanc, J. and Degres, Y., 1998. Development of ALTUS, a high frequency acoustic submersible recording altimeter to accurately monitor bed elevation and quantify deposition or erosion of sediments., Oceans'98-IEEC/OES Conference, Nice (France), pp. 189-194.

Labaune, C., 2005. Architecture, genèse et évolution du littoral du Languedoc-Roussillon : Impact des facteurs physiques au cours du Quaternaire terminal. PhD Thesis, Univ. Perpignan, 327 pp.

Labrune, C., Grémare, A., Guizien, K. and Amouroux, J.M., sous presse. Long-term comparison of soft bottom macrobenthos in the Bay of Banyuls-sur-Mer (north-western Mediterranean Sea): A reappraisal. J. Sea Res.

Lansard, B., 2004. Distribution et remobilisation du plutonium dans les sédiments du prodelta du Rhône (Méditerranée nord-occidentale). PhD Thesis, Univ. Méditerranée Aix-Marseille II, 344 pp.

Maillet, G.M., Vella, C., Berne, S., Friend, P.L., Amos, C.L., Fleury, T.J. and Normand, A., 2006. Morphological changes and sedimentary processes induced by the December

2003 flood event at the present mouth of the Grand Rhone River (southern France). Mar. Geol., 234(1-4): 159-177.

McCave, I.N., 1972. Transport and escape of fine-grained sediment from shelf areas, In: Shelf Sediment Transport: Process and Pattern, Van Nostrand Reinhold, New York, pp. 225-248.

Milliman, J.D. and Syvitski, J.P.M., 1992. Geomorphic/Tectonic Control of Sediment Discharge to the Ocean: The Importance of Small Mountainous Rivers. J. Geol., 100, 5: 525-544.

Monaco, A., 1971. Contribution à l'étude géologique et sédimentologique de plateau continental du Roussillon (Golfe du Lion). Thèse d'Etat, Univ. Sci. Tech. Languedoc, Montpellier, 285 pp.

Monaco, A., 1975. Les facteurs de la sédimentation marine argileuse. Les phénomènes physico-chimiques à l'interface. Bull. B.R.G.M, IV(3) : 147-174.

Monaco, A., Aloïsi, J.-C., 2000. Carte de la nature des fonds du Golfe du Lion. CNRS - CEFREM, site ORME : http://medias.obs-mip.fr/orme/, Perpignan.

NKE Electronics, 2006. Notice d'utilisation S-ALTUS.

Ogston, A., Drexler, T.M., Puig, P., soumis. Sediment delivery, resuspension, and transport characterizing canyon environments in the southwest Gulf of Lions. Cont. Shelf Res.

ORME, 2007. Observatoire régional de la Méditerranée. Available at: http://medias.obs-mip.fr/orme/.

Palanques, A., Durrieu de Madron, X., Puig, P., Fabres, J., Guillén, J., Calafat, A., Canals, M., Heussner, S. and Bonnin, J., 2006. Suspended sediment fluxes and transport processes in the Gulf of Lions submarine canyons. The role of storms and dense water cascading. Mar. Geol., 234(1-4): 43-61.

Pardé, M., 1925. Le régime du Rhône. Etude hydrologique. PhD Thesis, Univ. Grenoble, 2 vol., 887 et 440 pp.

Pardé, M., 1941. La formidable crue d'octobre 1940 dans les Pyrénées-Orientales. Revue géographique des Pyrénées et du Sud-ouest : 237-279.

Pauc, H., 2005. Formation of the Aude, Orb and Hérault prodeltas and their characterisation using physicochemical and sedimentological parameters. Mar. Geol., 222-223: 335-343.

Po River Basin Authority, 2005. Available at http://www.adbpo.it/.

Puig, P., Palanques, A., Orange, D., Canals, M., soumis. Dense shelf water cascading and furrows formation in the Cap de Creus submarine canyon, northwestern Mediterranean margin. Cont. Shelf Res.

Radakovitch, O., 1995. Etude du dépôt et du transfert du matériel particulaire par le ^{210}Po et le ^{210}Pb. Application aux marges continentales du golfe de Gascogne (NE Atlantique) et du golfe du Lion (NW Méditerranée). PhD Thesis, Univ. Perpignan, 250 pp.

Radakovitch, O., Charmasson, S., Arnaud, M. and Bouisset, P., 1999. ^{210}Pb and caesium accumulation in the Rhône delta sediments. Estuar. Coast. S. Sci., 48: 77-92.

RD Instruments, 1996. Acoustic Doppler Current profilers - Principles of Operation: A Practical Primer, RD Instruments, San Diego, Ca., USA.

RD Instruments, 2001. Waves User's Guide.

Roussiez, V., 2006. Les éléments métalliques. Traceurs de la pression anthropique et du fonctionnement hydro-sédimentaire du golfe du Lion. PhD Thesis, Univ. Perpignan, 247 pp.

Roussiez, V., Aloïsi, J.-C., Monaco, A. and Ludwig, W., 2005. Early muddy deposits along the Gulf of Lions shoreline: A key for a better understanding of land-to-sea transfer of sediments and associated pollutant fluxes. Mar. Geol., 222-223: 345-358.

Safege-Cetiis, 2006. Etude de faisabilité d'un émissaire de rejet en mer des eaux usées des STEP de Perpignan, Pôle Gestion des Eaux Usées - Communauté d'agglo de la ville de Perpignan.

Serrat, P., 1999. Dynamique sédimentaire actuelle d'un système fluvial méditerranéen : l'Agly (France). C. R. Acad. Sci. D, 329: 189-196.

Serrat, P., Ludwig, W., Navarro, B. and Blazi, J.-L., 2001. Variabilité spatio-temporelle des flux de matières en suspension d'un fleuve côtier méditerranéen : la Têt (France). C. R. Acad. Sci. D, 333: 389-397.

Thorne, P.D. and Campbell, S.C., 1992. Backscattering by a Suspension of Spheres. J. Acoust. Soc. Am., 92(2): 1 978.

Traykovski, P., Geyer, W.R., Irish, J.D. and Lynch, J.F., 2000. The role of wave-induced density-driven fluid mud flows for cross-shelf transport on the Eel River continental shelf. Cont. Shelf Res., 20(16) : 2113-2140.

Ulses, C., 2005. Dynamique océanique et transport de la matière particulaire dans le Golfe du Lion : Crue, tempête et période hivernale. PhD Thesis, Univ. Paul Sabatier, Toulouse, 247 pp.

Ulses, C., Estournel, C., Durrieu de Madron, X., Palanques, A., soumis. Suspended Sediment Transport in the Gulf of Lion (NW Mediterranean): Impact of Extreme Storms and Floods. Continental Shelf Research.

Vörösmarty, C.J., Fekete, B. and Tucker, B.A., 1996. River discharge database, version 1.0 (RivDIS v1.0), Studies and Reports in Hydrology, UNESCO, Paris (1996).

Wheatcroft, R.A., 2000. Oceanic flood sedimentation: a new perspective. Cont. Shelf Res., 20(16): 2059-2066.

Wheatcroft, R.A. and Drake, D.E., 2003. Post-depositional alteration and preservation of sedimentary event layers on continental margins, I. The role of episodic sedimentation. Mar. Geol., 199: 123-137.

Annexes

1. Settling velocity, effective density, and mass composition of suspended sediment in a coastal bottom boundary layer, Gulf of Lions, France.

Curran, K.J., Hill, P.S., Milligan, T.G., Mikkelsen, O.A., Law, B.A., Durrieu de Madron, X., **Bourrin, F.**, 2007.

Continental Shelf Research, 27: 1408-1421.

2. Origin and distribution of terrestrial organic matter in the NW Mediterranean (Gulf of Lions): application of the newly developed BIT index.

Kim, J.-H., Schouten, S., Buscail, R., Ludwig, W., Bonnin, J., Sinninghe Damsté, J., **Bourrin, F.**, 2006.

Geochemistry, Geophysics, Geosystems, 7 (11).

Available online at www.sciencedirect.com
ScienceDirect
Continental Shelf Research 27 (2007) 1408–1421
CONTINENTAL SHELF RESEARCH
www.elsevier.com/locate/csr

Settling velocity, effective density, and mass composition of suspended sediment in a coastal bottom boundary layer, Gulf of Lions, France

K.J. Curran[a,*], P.S. Hill[a], T.G. Milligan[b], O.A. Mikkelsen[c], B.A. Law[b], X. Durrieu de Madron[d], F. Bourrin[d]

[a]*Department of Oceanography, Dalhousie University, Halifax, NS, Canada B3H 4J1*
[b]*Fisheries and Oceans Canada, Bedford Institute of Oceanography, 1 Challenger Dr., PO Box 1006, Dartmouth, NS, Canada B2Y 4A2*
[c]*School of Ocean Sciences, University of Wales at Bangor, Menai Bridge, Anglesey, Wales LL59 5AB, UK*
[d]*Centre de Formation et de Recherche sur l'Environnement Marin (CEFREM), CNRS—Université de Perpignan, Perpignan cedex 66860, France*

Received 26 July 2006; received in revised form 27 November 2006; accepted 8 January 2007
Available online 31 January 2007

Abstract

Particle size distribution and size-specific settling velocity are critical parameters for understanding the transport of fine sediment on continental margins. In this study, observed floc size versus settling velocity, volume distributions of particles 2 μm–1 cm in diameter, and calculated effective densities for all particle sizes provided estimates of the mass distribution in suspension, which is used to apportion mass among component particles, microflocs, and macroflocs. Measurements were made during relatively quiescent environmental conditions. Observations of size distributions based on mass demonstrate an increase in the component particle fraction through time. The increase in the percentage of component particles in suspension had implications on water column properties, as small changes in the component particle fraction affected water column optical transmission in a way that was not as easily detected by changes in the volume concentration distribution or total mass concentration. Flocs larger than 133 μm in diameter only comprised one quarter to one third of the mass in suspension. This finding may explain why suspension bulk clearance rates are often an order of magnitude lower than those predicted by other methods.

Keywords: Fine sediment; Flocs; Settling velocity; Effective density; Particle size distribution; Mass composition; Gulf of Lions; France

1. Introduction

In marine environments, the transport and deposition of fine sediment depend on the abundance and size of flocs. Floc size and abundance are controlled by sediment concentration and turbulence, which affect the suspended particle size distribution. The settling flux of fine sediment to

*Corresponding author. Tel.: 1 902 494 6717; fax: 1 902 494 3877.
E-mail addresses: kcurran@dal.ca (K.J. Curran), phill@phys.ocean.dal.ca (P.S. Hill), milligant@mar.dfo-mpo.gc.ca (T.G. Milligan), oss202@bangor.ac.uk (O.A. Mikkelsen), lawb@mar.dfo-mpo.gc.ca (B.A. Law), demadron@univ-perp.fr (X. Durrieu de Madron), fbourrin@univ-perp.fr (F. Bourrin).

0278-4343/$ - see front matter © 2007 Elsevier Ltd. All rights reserved.
doi:10.1016/j.csr.2007.01.014

the seabed is dependent upon size-specific particle settling velocities and on the distribution of mass among different-sized particles in suspension. Studies that have estimated settling velocity of fine sediment particles in various marine environments (e.g. estuaries, fjords, and coastal environments) demonstrate that particles ranging from 1 μm to several millimeters in diameter exhibit settling velocities ranging from 0.001 to $>10\,\mathrm{mm\,s^{-1}}$, with the settling velocity generally increasing with increased particle size (Dyer et al., 1996; Hill et al., 1998; Dyer and Manning, 1999; Sternberg et al., 1999; Mikkelsen and Pejrup, 2001; Fox et al., 2004; Xia et al., 2004). From a size versus settling velocity relationship a size-specific effective density can be estimated by re-arranging Stokes' Law. Particles ranging from 1 μm to several millimeters in diameter exhibit effective densities ranging from 1 to $>1000\,\mathrm{kg\,m^{-3}}$, with the effective density generally decreasing with increased particle size (Hill et al., 1998; Dyer and Manning, 1999; Sternberg et al., 1999; Fox et al., 2004; Xia et al., 2004).

To estimate the settling flux of mass to the seabed, temporal observations of the in situ particle size distribution are required (Agrawal and Pottsmith, 2000). Eisma (1986) provided a simplified characterization of floc dynamics in suspension, where the in situ particle size distribution is partitioned into 'microflocs' and 'macroflocs'. Microflocs are small, tightly packed flocs approximately less than 125 μm in diameter. They are composed of smaller grains bound by organic matter. Macroflocs are porous, loosely bound flocs approximately greater than 125 μm in diameter. They are primarily composed of microflocs. Eisma (1986) argued that macroflocs are fragile and easily broken into their microfloc constituents, and that microflocs are more robust and not as easily broken into their constituents. For simplicity, a similar characterization of the suspended particle size distribution is employed in this study to apportion mass in suspension, whereby constituent particle sizes less than microflocs are termed 'component particles'.

Floc fraction, f, is defined as the fraction of mass in suspension bound within flocs. Various methods have been used to quantify f (Syvitski et al., 1995; Mikkelsen and Pejrup, 2001; Curran et al., 2002, 2004a; Fox et al., 2004). The Stokes' Law method estimates the effective density of flocs from an observed size-versus-settling-velocity relationship (Syvitski et al., 1995; Curran et al., 2002, 2004a; Fox et al., 2004). Size-dependent effective densities are multiplied by floc volumes in a range of size classes to estimate the mass in suspension bound within flocs. That mass is divided by the total mass in suspension to obtain the floc fraction. Stokes' Law however applies to smooth, impermeable spheres under non-turbulent flow in which viscous forces dominate (Hawley, 1982). Such conditions are not typical for natural particles settling in marine environments. A second method uses the disaggregated inorganic grain size (DIGS) distribution of the seabed to estimate the relative proportion of suspended sediment deposited within single grains and flocs (Curran et al., 2004b; Fox et al., 2004). A third method estimates the bulk effective density of the suspension by dividing the total suspended solids concentration within a known volume of fluid by the total volume concentration of flocs observed within that fluid (Mikkelsen and Pejrup, 2001; Fox et al., 2004). The bulk effective density for the suspension and median floc diameter are used to estimate the bulk settling velocity of the suspension, which represents the settling velocity when the suspension is fully flocculated ($f=1$). The bulk settling velocity is compared to the clearance rate of the suspension estimated from an observed size versus settling velocity relationship. The ratio of the clearance rate to bulk settling velocity is proportional to the fraction of flocs in suspension.

Studies that have estimated f indicate that the majority of fine sediment in suspension is flocculated (Syvitski et al., 1995; Curran et al., 2002, 2004a; Fox et al., 2004). Syvitski et al. (1995) observed that more than 90% of the suspended mass below the surface layer in Halifax Harbour, Canada, was bound within flocs greater than 50 μm in diameter. Curran et al. (2002) observed floc fractions near 100% below the Eel River flood plume, northern California, for flocs greater than 125 μm in diameter. Highly flocculated suspensions of flocs greater than 125 μm in diameter were also observed below a glacial meltwater plume in Disenchantment Bay, Alaska, and below discharge plumes proximal to the Po River mouth, Italy (Curran et al., 2004a; Fox et al., 2004).

Methods for quantifying f provide insight into the fraction of mass in suspension bound within flocs, but do not describe the distribution of mass apportioned into component particles, microflocs, and macroflocs. A method to estimate the fraction of mass bound within different particle sizes would improve understanding of the behavior of fine

sediment in suspension and its affect on water column properties. This study estimates the fraction of mass in suspension bound within component particles, microflocs, and macroflocs, using the particle mass size distribution from 2 μm to 1 cm in diameter. Variations in the in situ size distributions of particle volume, particle projected area, particle mass, and particle settling mass flux in the bottom boundary layer offshore of the Têt River mouth, Gulf of Lions, France, were tracked through time.

2. Methods

2.1. Overview

The continental shelf in the Gulf of Lions, France, is narrow and crescent shaped with a heavily incised slope at the shelf break (water depth of 120 m), which descends to the adjacent Algero-Balearic Basin (Courp and Monaco, 1990). In the southern Gulf of Lions, strong Tramontane winds blow from the north-northwest between the Pyrenees and the Massif Central Mountains throughout the year and generally result in a southward flowing current associated with coastal downwelling (Estournel et al., 2003). Mean Tramontane wind speeds are 10–15 $m\,s^{-1}$, and the mean southward flowing current speed is 0.2 $m\,s^{-1}$. In rare instances Tramontane winds blow from the west-northwest and the coastal current flows northward. Strong winds blowing from the southeast, associated with lows passing over the basin, strongly influence sediment transport due to the generation of large wind waves and intense alongshore currents (Ferré et al., 2005). Tides are small on a regional scale and do not affect the circulation.

More than 10.5×10^6 t of sediment, mostly fine-grained, is discharged to the Gulf of Lions annually, with the Rhône River to the northeast being the source of up to 80% of the mass (Courp and Monaco, 1990). The shelf is characterized by low annual sediment inputs that vary between years, with the exception of the Rhône River submarine delta. In the southwest region of the Gulf of Lions, the Têt River mouth prodelta is characterized by a muddy bottom deposit that occupies the inner-shelf. The Têt River is flood dominated, and the sediment supply is limited by flow regulation.

In this study, the Têt River Buoy Site was the location of an IN situ Size and SEttling Column Tripod (INSSECT) deployment from April 18, 2005 at 1200 GMT to April 22, 2005, at 1200 GMT (Fig. 1). The Têt River Buoy Site is located in 28 m water depth and is approximately 2.5 km offshore of the Têt River mouth (LAT: 42°N 70.883, LON: 3°E 06.647). The INSSECT is a multi-instrumented tripod designed to measure fine sediment properties close to the seabed in coastal environments (Mikkelsen et al., 2004). It was equipped with a digital floc camera (DFC), a digital video camera (DVC) and settling column, a LISST-100 Type B laser particle size analyzer, a compass/tilt sensor, and a sediment trap system that rotates under the DVC settling column.

The LISST-100 Type B laser particle size analyzer measures the volume concentration distribution of particles 1.25–250 μm in diameter and the DFC the volume concentration distribution of particles 125 μm–1 cm in diameter. The DVC measures particles 226 μm–5 mm in diameter and is used to estimate the size versus settling velocity of particles in suspension. The compass/tilt sensor measures the orientation and tilt of the INSSECT. During the deployment, the DFC and LISST-100 were synchronized to take measurements every 15 min, while the DVC captured a 1 min video clip every 90 min. Compass/tilt was recorded every minute. The DFC was positioned 1.7 m above the bottom (mab), and the LISST-100 and the top of the DVC settling column system were positioned 1.5 mab. The sediment trap system provides measure of the sediment flux that can later be analyzed for settling mass flux and the DIGS distribution.

Surface wave height and wave period, and current velocity, current direction, and water temperature at 2.5 mab, were measured using a bottom-mounted, upward-looking RDI 600 kHz ADCP deployed on a buoy less than 500 m from the INSSECT. Estimates of combined wave-current bottom shear stress were made using the model of Grant and Madsen (1986). Salinity at 2.5 mab was not measured throughout the deployment, although conductivity, temperature, and depth (CTD) profiles were collected opportunistically. Wind data was acquired from Météo France at Torreilles (the French National Weather Data Centre Station 66212001), approximately 9 km northwest of the deployment site.

2.2. Particle size distributions

The raw LISST-100 data were inverted with manufacturer's software that outputs volume concentration distributions using a factory calibration

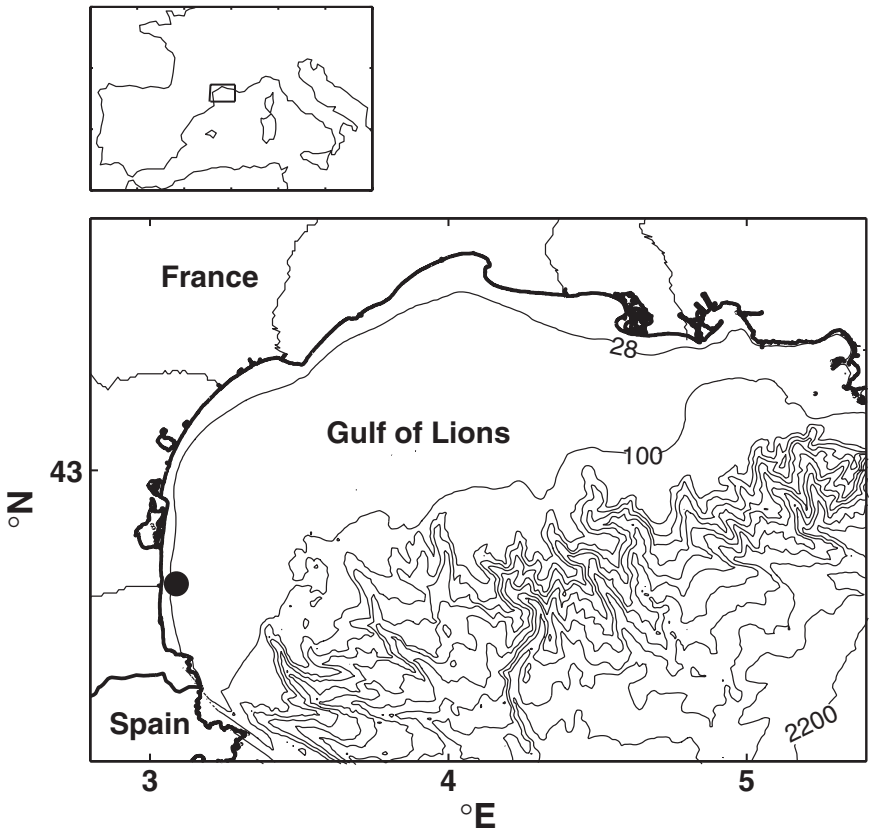

Fig. 1. Site map of the Gulf of Lions study area, France. The INSSECT deployment site was at 28 m water depth approximately 2.5 km offshore of the Têt River mouth, marked by the filled circle. Isobaths greater than 100 m increase at 200 m intervals from 200 to 2200 m. Wave height, wave period, current velocity, and water temperature were measured at an adjacent buoy less than 500 m from the INSSECT. Wind data was acquired from Météo France at Torreilles (Station 66212001), approximately 9 km northwest of the deployment site.

of the scattering pattern of particles of known size and volume concentration (Traykovski et al., 1999; Agrawal and Pottsmith, 2000; Mikkelsen et al., 2005). For each sample period, 6 volume concentration distributions were collected over 30 s. The mean volume concentration distribution was used to represent each sample time. The LISST-100 volume concentrations ($mm^3 L^{-1}$) were binned into size classes with logarithmically spaced diameter midpoints between 1.25 and 250 μm. The DFC images were analyzed using the same area of interest (AOI) for each image, and the threshold value (gray scale value that defines particle edges from the image background) for each image was user defined. Particle areas in the AOI of each image were converted to equivalent circular diameters. Particle volumes were estimated assuming spherical geometry. The volume concentrations ($mm^3 L^{-1}$) were binned into size classes with logarithmically spaced diameter midpoints between 125 μm and 1 cm.

Particles in suspension smaller than 1.25 μm in diameter result in an overestimate of volume by the LISST-100 in the smallest size classes, believed to be caused by scattering from such small, irregularly shaped particles (Agrawal, pers. comm.). Particles in suspension larger than 250 μm still scatter light and can also cause an overestimate of volume in the largest size classes (Agrawal and Pottsmith, 2000). In this study, there was an overestimate of volume by the LISST-100 in the smallest size classes so the smallest three bins were removed. In the largest three bins the LISST-100 under-estimated the volume concentration compared to the DFC by up to several orders of magnitude, so they were also removed. The result was LISST-100 volume concentration distributions ranging from 2 to 165 μm in diameter. After trimming the LISST-100 and DFC volume concentration distributions, only one size bin overlapped between the two instrument distributions. The LISST-100 volume concentrations

in each size bin were multiplied by the ratio of the DFC to LISST-100 volume concentrations in the overlapping size bin to reconcile the volume concentration difference between the two instruments. The mean adjustment factor ($\pm$standard deviation) for all merged distributions was 2 ± 0.8, and was similar to that observed by Mikkelsen et al. (2005). The particle projected area concentration distributions were estimated from the merged particle volume concentration distributions assuming spherical geometry.

2.3. Particle settling velocity (w_f) and effective density ($\rho_f - \rho_w$)

The DVC settling column was equipped with a baffled top to minimize flow disruptions of settling particles within the column. Particle settling velocities estimated from the DVC were combined into a floc size versus settling velocity and floc size versus effective density relationship for the entire deployment, following the procedure of Fox et al. (2004). Floc effective densities were estimated from the observed floc settling velocities using Stokes' Law. These were fit to the model of Khelifa and Hill (2006) to estimate the effective density of particles 2 μm−1 cm in diameter. Observations suggest that flocculated suspensions exhibit a range of particle sizes that cannot be characterized by a single fractal dimension, as the packing arrangement of component particles within flocs changes as a function of size (Li and Logan, 1995; Dyer and Manning, 1999). The Khelifa and Hill (2006) model accounts for a decrease in floc density with an increase in floc size in a way that is consistent with observations from 26 published data sets. In the model, particle effective density follows the form

$$\rho_f - \rho_w = (\rho_s - \rho_w)\left(\frac{D}{d_c}\right)^{F-3}, \quad (1)$$

where ρ_f is the floc effective density, ρ_w is the density of seawater, ρ_s is the average density of the floc component grains, D is the particle diameter in a given size class, d_c is the median component grain diameter in flocs, and F relates particle mass to particle diameter. It is akin to a size-specific fractal dimension. For particle sizes less than or equal to the median component grain diameter the effective density is equal to the average density of the floc component grains. The settling velocities for particles 2 μm–1 cm in diameter were estimated with

$$w_s = \frac{1}{18}\theta g \frac{\rho_s - \rho_w}{\mu} d_c^{3-F} \frac{D^{F-1}}{1 + 0.15\,\mathrm{Re}^{0.687}}, \quad (2)$$

where w_s is the particle settling velocity, θ is the particle shape factor (assumed to be spheres, where $\theta = 1$), g is the gravitational acceleration, μ is the dynamic viscosity of seawater, and Re is the particle Reynolds number (Khelifa and Hill, 2006). Particle mass concentration distributions were estimated from the particle volume concentration distributions using the size-specific particle effective densities estimated from Eq. (1). Particle settling mass flux distributions were estimated from the particle mass concentration distributions using the size-specific particle settling velocities estimated from Eq. (2).

3. Results

The INSSECT was deployed at 1200 GMT on April 18, 2005. Throughout the deployment, winds predominantly blew from the northwest at $<10\,\mathrm{m\,s^{-1}}$. In the late morning of April 19, the wind shifted and blew from the southeast at $<5\,\mathrm{m\,s^{-1}}$ until early afternoon, when it strengthened and shifted back to the northwest (Fig. 2). On April 22, the winds decreased to $<5\,\mathrm{m\,s^{-1}}$ for the remainder of the deployment period. The bottom current predominantly flowed northward at $<0.1\,\mathrm{m\,s^{-1}}$ early in the deployment. It increased to $0.18\,\mathrm{m\,s^{-1}}$ at 0745 GMT on April 20, then decreased and flowed southward at approximately $0.1\,\mathrm{m\,s^{-1}}$ on April 22, following the decrease in wind speeds at midday on April 21 (Fig. 2). The significant wave height was generally <0.3 m during the deployment, although significant wave heights >0.5 m were observed on April 20 due to a localized weather event that resulted in wind blowing from the southeast on April 19 (Fig. 2). The peak wave period ranged from 2 to 9 s during the deployment, with the shortest wave periods associated with the peak wind wave event on April 20.

The combined wave-current bottom shear stress was generally <0.04 Pa, although fluctuations in bottom shear stress occurred throughout the deployment (Fig. 2). The highest bottom shear stress of 0.039 Pa during the deployment was observed on April 20 at 0745 GMT, when the current velocity and significant wave height were at a maximum

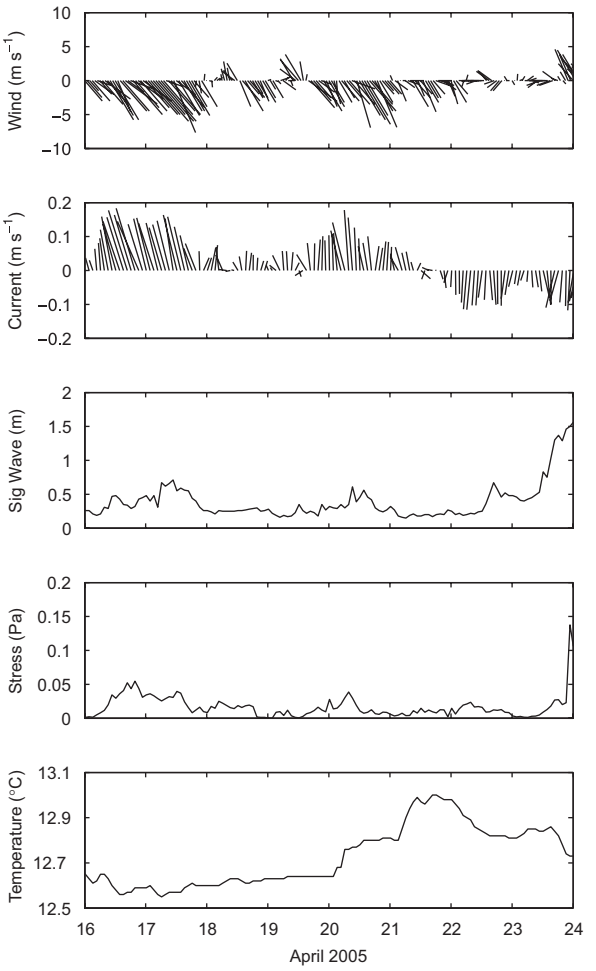

Fig. 2. Wind speed, current speed at 2.5 m above bottom (mab), significant wave height, combined wave-current bottom shear stress, and water temperature at 2.5 mab at the Têt River Buoy Site. INSSECT was deployed from April 18, 2005 at 1200 GMT to April 22, 2005, at 1200 GMT. Wind speed is indicated by stick length and wind direction is indicated by stick orientation. Positive wind speeds represent winds blowing from the south and negative wind speeds represent winds blowing from the north. Bottom current speed and current direction are similarly represented in the second panel. Positive bottom current speeds represent currents flowing from the south and negative bottom current speeds represent currents flowing from the north.

(Fig. 2). The elevated bottom shear stress was short-lived and returned to <0.02 Pa by 1045 GMT on April 20, where it remained for the remainder of the deployment period. The water temperature at 2.5 mab was relatively constant at 12.6 °C during the first 72 h of the deployment (Fig. 2). On April 20, the water temperature increased to 12.7 °C at 0315 GMT. The temperature slowly increased to a maximum of 12.8 °C by the end of the day and then again increased to 13 °C at 1045 GMT on April 21. The temperature then decreased to 12.9 °C prior to the INSSECT recovery on April 22.

Digital video of settling flocs resulted in 1044 independent estimates of in situ floc size and settling velocity at 1.5 mab. Observed settling velocities ranged from 0.2 to 32.3 mm s^{-1} for flocs 226.1 μm–1.7 mm in diameter (Fig. 3). The data were binned into logarithmically-spaced diameter size classes. Median settling velocity as a function of diameter followed the expression:

$$w_f = 0.004 d_f^{0.77} (r^2 = 0.96), \quad (3)$$

where w_f is the floc settling velocity (mm s^{-1}) and d_f is the binned floc equivalent spherical diameter (μm) (Fig. 3). Settling velocities estimated from Eq. (2) ranged from 0.3 to 1.2 mm s^{-1} for binned flocs sizes 263.1 μm–1.6 mm in diameter (Fig. 3).

Floc effective densities estimated using Stokes' Law ranged from 465.7 to 1.1 kg m^{-3} for flocs 226.1 μm–1.7 mm in diameter (Fig. 3). Median floc size versus effective density as a function of diameter followed the expression:

$$\rho_f - \rho_w = 7971 d_f^{-1.19} (r^2 = 0.98), \quad (4)$$

where $\rho_f - \rho_w$ is the floc effective density (kg m^{-3}). Floc effective densities estimated from Eq. (4) ranged from 10.5 to 1.2 kg m^{-3} for binned flocs 263.1 μm–1.6 mm in diameter (Fig. 3).

The density of seawater (ρ_w), estimated from a CTD profile taken at the time of the INSSECT deployment, was 1029 kg m^{-3}. The median component grain size diameter within flocs (d_c) and sediment density (ρ_s) were adjusted to fit the Khelifa and Hill (2006) model to the observed particle settling velocity and effective density data (Fig. 4). The values of d_c and ρ_s were 5 μm and 1600 kg m^{-3}, respectively. Settling velocities estimated from the Khelifa and Hill (2006) model ranged from 0.3 to 1.5 mm s^{-1} for particles 263.1 μm–1.6 mm in diameter. Effective densities estimated from the Khelifa and Hill (2006) model ranged from 11.4 to 1.4 kg m^{-3} for particles 263.1 μm–1.6 mm in diameter. At particle diameters $<\sim$5 μm the modeled effective densities were constant at 571 kg m^{-3}, which is the mean effective density for small component particles.

The particle volume concentration, particle projected area concentration, particle mass concentration, and particle settling mass flux distributions were apportioned into component particle (<36 μm

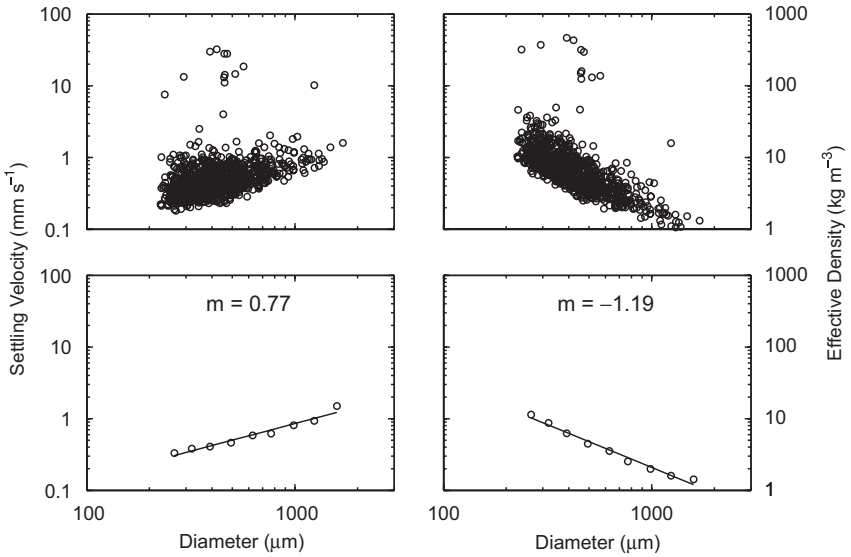

Fig. 3. Unbinned particle size versus settling velocity and particle size versus effective density during the deployment period (upper panels, $n = 1044$). The particle effective density was estimated by rearranging Stokes' Law. The lower panels exhibit the median particle size versus settling velocity and particle size versus effective density relationships for binned data, where 'm' is the slope.

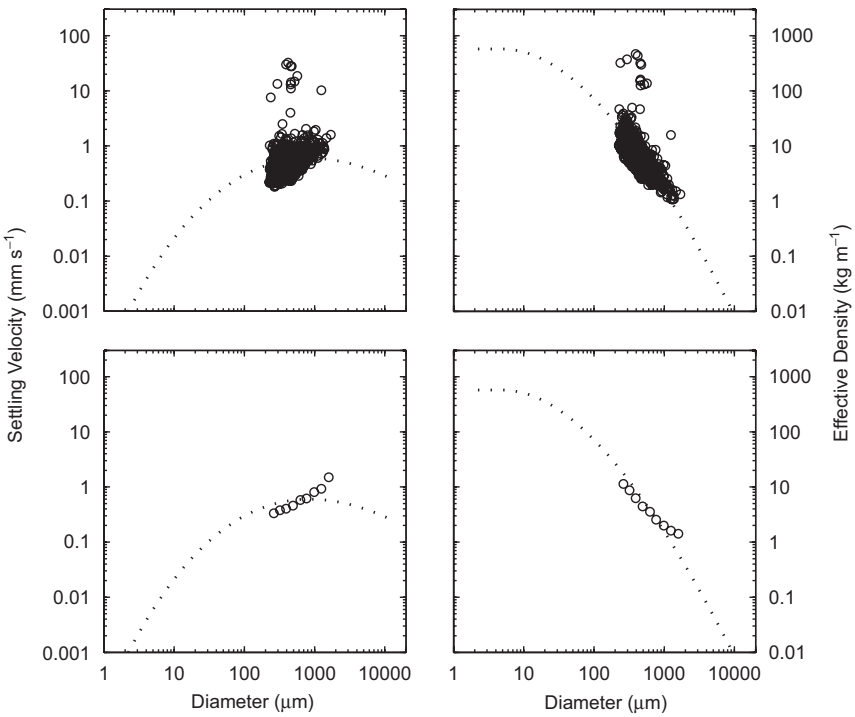

Fig. 4. Unbinned, observed particle size versus settling velocity and particle size versus effective density estimated using Stokes' Law during the deployment period (open circles, upper panels) versus estimates from the Khelifa and Hill (2006) model (dashed line, upper panels). Lower panels demonstrate the median of binned particle size versus settling velocity and particle size versus effective density data presented in the upper panels (open circles) versus estimates from the Khelifa and Hill (2006) model (dashed line).

in diameter), microfloc (36–133 μm in diameter), and macrofloc (>133 μm in diameter) fractions. These boundaries differ slightly from those of Eisma (1986) due to the logarithmically spaced diameter midpoints of the merged particle size distributions used in this study. The suspension composition

based on particle volume concentration was dominated by the macrofloc fraction throughout the deployment. On average, 85.4% of the volume concentration in suspension was accounted for by macroflocs, 7.2% by microflocs, and 7.4% by component particles (Fig. 5). Throughout the deployment the percentage of component particles and microflocs by volume increased slightly. Following the suspension event on April 19, the absolute volume concentration remained relatively constant, while the component particle and microfloc percentages slightly increased (Fig. 5).

The increase in the component particle fraction in suspension throughout the deployment was more obvious when the suspension was represented by particle projected area concentration and particle mass concentration. Based on the projected area concentration of particles, the suspension composition was dominated by the component particle fraction throughout the deployment. On average, 66.2% of the particle projected area concentration in suspension was accounted for by component particles, 7.8% by microflocs, and 26% by macroflocs (Fig. 5). The suspension composition based on particle mass concentration was also dominated by

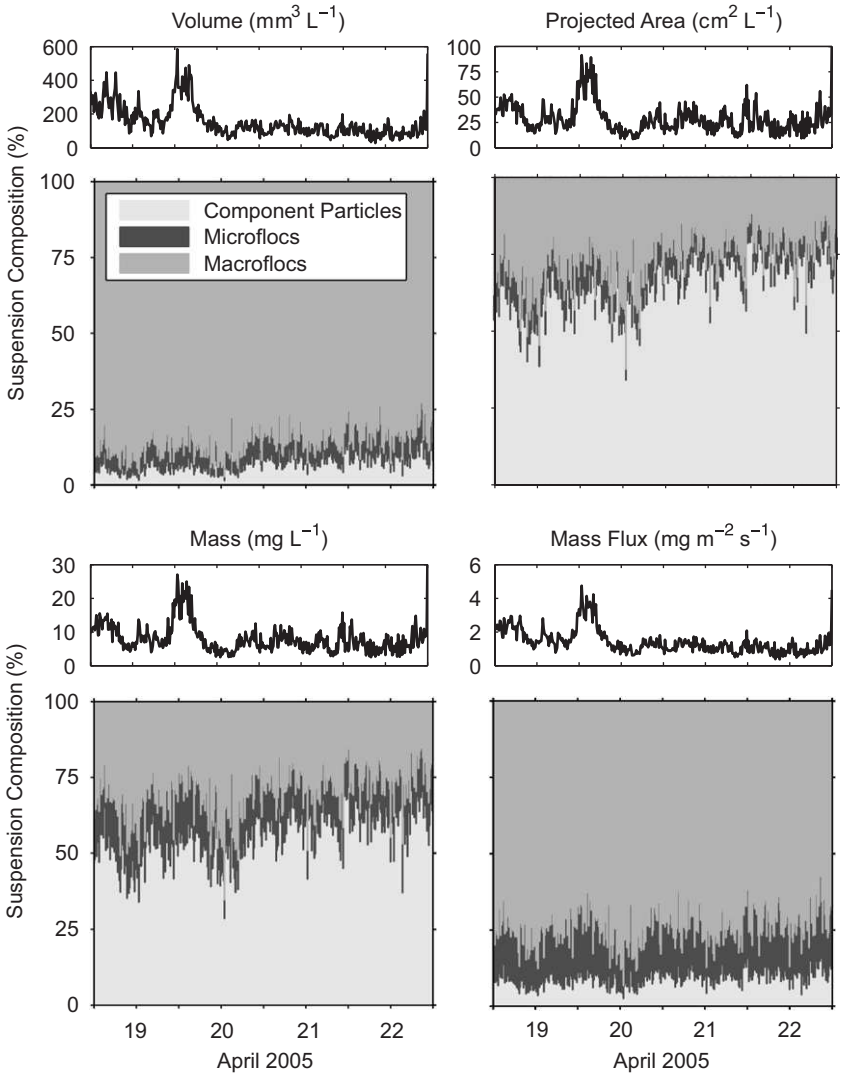

Fig. 5. Particle volume concentration, particle projected area concentration, particle mass concentration, and particle settling mass flux apportioned into component particle (<36 μm in diameter), microfloc (36–133 μm in diameter), and macrofloc (>133 μm in diameter) fractions.

the component particle fraction. On average, 56.4% of the particle mass concentration in suspension was accounted for by component particles, 14.3% by microflocs, and 29.3% by macroflocs (Fig. 5). The highest macrofloc fractions by particle projected area and particle mass were observed following the suspension events in the afternoons of April 18 and 19 (Fig. 5).

The particle suspension composition based on the settling mass flux was dominated by the macrofloc fraction throughout the deployment. On average, 73.5% of the particle settling mass flux was accounted for by macroflocs, 17.1% by microflocs, and 9.4% by component particles (Fig. 5). Elevated periods of particle settling mass flux of macroflocs followed the resuspension events in the afternoons of April 18 and 19. The absence of a subsequent resuspension event during the elevated bottom shear stress period of April 20 suggests that sediments resuspended prior to April 20 were advected from the field site rather than re-deposited on the seabed.

4. Discussion

Increase in the suspended sediment concentration late in the morning of April 19 was likely associated with resuspension of a loosely consolidated mud layer deposited prior to the survey, which was resuspended by the bottom shear stress in excess of 0.01 Pa in the afternoon of April 18 and morning of April 19 (Fig. 2). Bottom shear stress in the range of 0.01–0.02 Pa has been observed to resuspended aggregate 'fluff' layers off the seabed (Thomsen and Gust, 2000; Schaaff et al., 2002, 2006; El Ganaoui et al., 2004). The resuspended sediment was likely advected from the field site by the strong northward bottom current observed at this time, and subsequent increases in bottom shear stress were not sufficient to resuspend the more consolidated underlying sediments that mobilize at shear stresses in excess of 0.04–<0.1 Pa (Thomsen and Gust, 2000; El Ganaoui et al., 2004; Schaaff et al., 2006). Following the resuspension event on April 19 there was a small increase in the component particle fraction in suspension throughout the remainder of the deployment period.

Increase in the component particle fraction in suspension was associated with an increase in water temperature. The increase in bottom water temperature may be considered a proxy for physical change in the bottom water mass. The cause of change in the bottom temperature may have been advection or the downward mixing of surface water. It is believed that the increase in the component particle fraction was associated with a transient population of small particles that entered the field site within the warm water mass. Advection or downward mixing as the source of the small particles was supported by CTD profiles collected around the deployment site, which demonstrated an increase in bottom water temperature and conductivity between April 18 and 22, indicating the intrusion of warmer and saltier water during this period.

The observed size versus settling velocity and size versus effective density relationships were similar to those observed in other estuaries and fjords, and on continental shelves (Kranck et al., 1993; Fennessy et al., 1994; Hill et al., 1998; Dyer and Manning, 1999; Sternberg et al., 1999; Fox et al., 2004). Particles exhibited significant differences in settling velocity and effective density between particles sizes, and particles of similar size also exhibited differences in settling velocity and effective density by up to an order of magnitude (Fig. 3). The volume distributions 2 μm–1 cm in diameter and particle effective densities provided for the first time estimates of the particle mass concentration in suspension bound within component particles, microflocs, and macroflocs, as well as the settling mass flux to the seabed of these size fractions (Fig. 5).

Suspension composition by particle volume concentration and particle settling mass flux varied similarly through time, as did suspension composition by particle projected area concentration and particle mass concentration (Fig. 5). This is explained by similar scaling with diameter for particle volume and particle settling mass flux, and for particle projected area and particle mass. Particle volume scales with particle diameter cubed (d^3) and particle projected area scales with particle diameter squared (d^2). Particle mass is the product of particle volume and particle density and in this study scaled with particle diameter raised to the power 1.81. Particle settling mass flux is the product of particle mass and particle settling velocity and in this study scaled with particle diameter raised to the power 2.56. These relationships are dependent on the floc packing arrangement and are not necessarily true for all environments.

Previous methods that estimate the floc fraction (f) in suspension only characterize the abundance of large flocs, not the abundance of all particle sizes (Syvitski et al., 1995; Mikkelsen and Pejrup, 2001;

Curran et al., 2002, 2004a; Fox et al., 2004). Each method exhibits limitations. In the method that uses seabed size distributions, estimates of the fraction of mass deposited within flocs does not distinguish between the macrofloc and microfloc populations, and also assumes that all floc sizes can be characterized by a single floc settling velocity. This results in inaccurate estimates of f since flocs do not exhibit a single settling velocity. In the method that uses the bulk density approximation, it is assumed that flocs in suspension can be represented by a single floc diameter and that observed suspension clearance rates for all particle sizes can be estimated from an observed size versus settling velocity relationship. This results in inaccurate estimates of f since the settling velocities of small particles are not accurately estimated from an observed size versus settling velocity relationship, and again, flocs do not exhibit a single settling velocity.

The method for approximation of f that relies on Stokes' Law is a comparable approach to that presented in this study, as it makes use of an observed size versus settling velocity relationship to estimate particle effective density. Fox et al. (2004) argued that f was a factor of 2–3 times higher than it should be when estimated using the Stokes' approximation. In a study by Li and Logan (1997) it was observed that Stokes' Law underestimated the settling velocity of flocs by a factor of 2–3. The underestimate was attributed to reduced drag forces on sinking flocs caused by water passing through their porous and permeable interiors. If it is assumed that Stokes' Law underestimates the settling velocity of flocs by a factor of 2–3, then the estimate of floc density may be overestimated by this factor (Fox et al., 2004). The result is an overestimate of mass bound within individual flocs. In this study, floc effective densities were estimated from Stokes' Law and used to estimate particle effective densities with the Khelifa and Hill (2006) model. If particle effective densities estimated using Stokes' Law were overestimated by a factor of 2–3 the absolute mass within flocs presented in this study would also be overestimated by this factor (Fig. 5). The relative proportion of mass among different particle size classes, however, would remain the same, since the overestimate of particle mass would apply to all size classes uniformly. Only the absolute mass and absolute settling mass flux would be overestimated by a factor of 2–3.

The Khelifa and Hill (2006) model makes use of suspended sediment characteristics to estimate particle effective density. Upon recovery of INSSECT the flux cup sediment samples were lost, preventing estimate of the density of the floc component grains and the median component grain size diameter that act as input variables to the Khelifa and Hill (2006) model. As a result, particle effective densities estimated from Stokes' Law were used to fit the Khelifa and Hill (2006) model. Subsequent studies should quantify the density of the floc component grains and the median component grain size diameter from bulk sediment samples. This would prevent potential error in the estimate of particle effective densities due to the use of Stokes' Law. Measurement of the suspended mass concentration in situ would also permit comparison with the total particle mass concentration estimated from the particle size distributions.

Few studies have tracked changes in the entire suspended particle size distribution through time (Bale and Morris, 1987; Gibbs et al., 1989; Eisma et al., 1990; Mikkelsen et al., 2006). This is difficult as it often requires use of multiple instruments that analyze different particle sizes in suspension. Bale and Morris (1987) used a Malvern Instruments particle sizer to estimate changes in the in situ volume concentration distribution of particles 1.9–188 μm in diameter, in the Tamar Estuary, England. Gibbs et al. (1989) used an in situ holographic microscopic system and a ship board inverted microscope to estimate changes in the in situ volume concentration distribution of particles <200 μm in diameter, in the Gironde Estuary, France. Eisma et al. (1990) used an in situ camera system to estimate changes in the in situ volume concentration distribution of particles 3.6–644 μm in diameter, in the Scheldt Estuary, Netherlands. The studies demonstrated that changes in the volume concentration within different particle size classes can only be used to constrain relative changes in the floc fraction by volume in suspension, since flocs are porous and changes in volume concentration due to floc formation and floc breakup are non-conservative.

Mikkelsen et al. (2006) used an in situ digital floc camera and LISST-100 Type C to estimate changes in the in situ volume concentration distribution of particles 2.5 μm–1 cm in diameter, proximal to rivers discharging into the western Adriatic Sea, Italy. Results of the study indicated that when stress in the water column increased there was a decrease in the volume concentration of macroflocs in suspension accompanied by an increase in the volume concen-

tration of microflocs in suspension, presumably due to floc breakup and microfloc resuspension. As the stress decreased the volume concentration of macroflocs again increased and then rapidly decreased under calm conditions, presumably as macroflocs settled out of suspension. Mikkelsen et al. (2006) were unable to determine the absolute relationship between floc size and stress based on changes in the volume concentration distribution alone, due to other factors that contribute to changes in the volume concentration distribution such as sediment deposition, resuspension, advection, and microbial mediation.

Caution must be taken when characterizing suspension composition by the particle volume distribution, because a few large particles in suspension can represent a significant fraction of the total volume (Droppo et al., 2005), but not necessarily a significant fraction of the total mass. In this study it was difficult to detect temporal increases in the percentage of component particles in suspension by changes in the particle volume concentration distribution. The increase was more easily detected by changes in the distribution of particle mass. Particle mass concentration better reveals the behavior of the component particle fraction because small particles have more mass per unit volume than large porous flocs, due to their higher densities.

The increase in the component particle mass fraction in suspension observed between April 20 and the end of the deployment affected the optical properties of the water column. The beam attenuation coefficient, C, represents the fraction of light absorbed and scattered by particles in suspension as the light traverses a meter-thick parcel of water. Changes in C typically are attributed to changes in the suspended sediment concentration. The increase in C observed towards the end of the study period however was associated with an increase in the percentage of component particles in suspension and not an increase in the absolute suspended mass concentration (Fig. 6). The suspended mass concentration was relatively constant while the area-to-mass ratio increased due to the greater relative abundance of component particles (Fig. 6). Similar results for optical backscatter were observed by Gibbs and Wolanski (1992) and Hatcher et al. (2001) who detected changes in the projected-area of suspended particles due to changes in the suspension composition and not due to an increase in suspended concentration. These observations serve as a reminder that changes in suspension optical properties may reflect changes in the projected-area in suspension due to floc formation and floc breakup rather than absolute changes in the suspended mass concentration.

The mean bulk effective settling velocity estimated from the suspension composition by mass concentration was $0.18\,\mathrm{mm\,s^{-1}}$. The suspension clearance rate (or bulk effective settling velocity) decreased throughout the deployment as the fraction of mass bound within component particles increased (Fig. 7). Suspension composition by mass concentration may provide an explanation of observed clearance rates of fine sediment suspensions. In a study by Curran et al. (2002) on fine sediment dynamics in the Eel River flood plume,

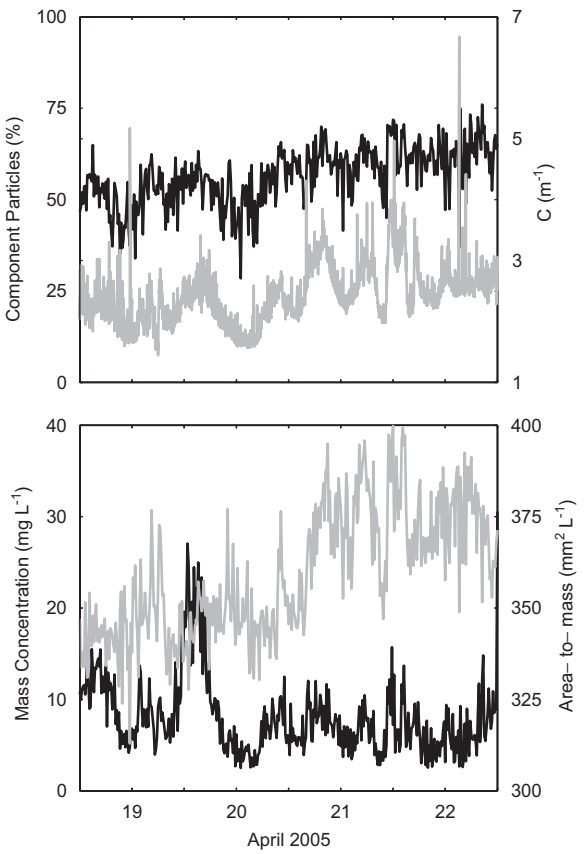

Fig. 6. Increase through time in the percentage of component particles in suspension by mass (black line, upper panel) has implications on water clarity as demonstrated by an increase in the beam attenuation coefficient, C, through time (gray line, upper panel). The mass concentration in suspension remains relatively constant from April 20 to the end of the deployment period (black line, lower panel), while the area-to-mass ratio in suspension increases due to the increased presence of component particles (gray line, lower panel).

it was observed that suspended sediments were primarily bound within large flocs that deposited on the order of 1 mm s^{-1}, although the estimated plume clearance rate was on the order of 0.1 mm s^{-1}. Curran et al. (2002) reconciled this difference by invoking advection of flocculated sediment from the nearshore that resupplied large flocs as they deposited in the offshore region of the plume. Similarly, in an unpublished study on dynamics in a glacial meltwater plume within an Alaskan fjord, plume clearance rates were estimated to be on the order of 0.1 mm s^{-1} despite the presence of a highly flocculated suspension and floc settling velocities on the order of 1 mm s^{-1}. Previous estimates of the floc fraction in suspension were often greater than 100% (Curran et al., 2002, 2004a; Fox et al, 2004), although this is not physically possible and likely arose from the overestimate of floc density due to Stokes' Law. Contradiction between predicted and observed bulk clearance rates of fine sediment suspensions thus may be explained by the overestimate of mass bound within large flocs due to the use of Stokes' Law to estimate f.

Due to the relatively quiescent environmental conditions observed during this study, results did not provide significant insight into the dynamics that control floc formation, breakup, deposition, and resuspension. This study did demonstrate that under calm conditions the majority of mass in suspension was bound within small component particles and not large flocs. As well, by observing the particle mass distribution in suspension, small changes in the component particle fraction could be observed that were not easily detected by changes in the distribution of particle volume. This finding demonstrates that suspensions may be dynamic even in the absence of significant changes in forcing variables that control floc formation and breakup, and that a small change in suspension composition may affect water column properties (e.g. optical transmission). Last, estimates of the fraction of mass bound within component particles, microflocs, and macroflocs provide insight into the particle settling mass flux to the seabed, which may reconcile differences between predicted and observed bulk clearance rates of fine sediment suspensions.

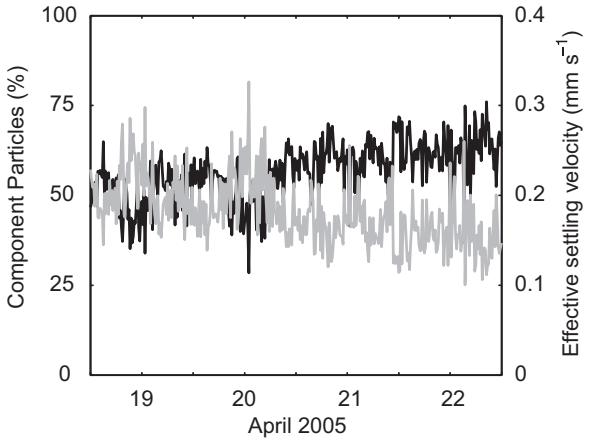

Fig. 7. Percentage of component particles in suspension by mass concentration (black line) and suspension bulk effective settling velocity (gray line). The bulk effective settling velocity decreases with an increase in the fraction of component particles in suspension. The mean bulk effective settling velocity for the deployment period was 0.18 mm s^{-1}.

5. Conclusion

In this study, measurements of floc size versus settling velocity and particle volume distributions 2 μm–1 cm in diameter were made during relatively quiescent environmental conditions in a coastal bottom boundary layer. Particle effective density was estimated using Stokes' Law and the model of Khelifa and Hill (2006). The model relates particle mass to particle diameter with an exponent that varies as a function of particle size. The effective densities for all particle sizes were combined with the volume distributions to construct particle size distributions based on mass.

Results demonstrated that macroflocs only composed one quarter to one third of the suspension by mass throughout the deployment. The size versus settling velocity and size versus effective density observations were similar to those from other marine environments. Settling velocity scaled as diameter raised to a power just less than one, demonstrating that floc density decreased with increasing floc diameter. In addition, the binned settling velocities were tightly correlated with particle diameter, although variation in settling velocity within the size bins was large.

The abundance of component particles increased throughout the deployment. This was linked to an increase in water temperature and believed to be associated with advection or downward mixing of a different water mass at the field site. The total mass in suspension remained relatively constant between April 20 and the end of the deployment period. The increase in component particles reduced the optical transmission within the water column due to an increase in particle projected area per unit of mass.

Changes in the projected area of suspended particles due to floc formation and floc breakup, and not due to changes in the suspended mass concentration, underline the effect of fine sediment dynamics on water column properties (Gibbs and Wolanski, 1992; Hatcher et al., 2001).

The mean bulk effective settling velocity estimated from the mass distributions was $0.18\,\mathrm{mm\,s^{-1}}$. This value was an order of magnitude lower than settling velocities observed for large flocs in suspension. Previous studies observed fine sediments to be bound within large flocs that settled out of suspension on the order of $1\,\mathrm{mm\,s^{-1}}$, while estimated suspension clearance rates were of the order $0.1\,\mathrm{mm\,s^{-1}}$ (Curran et al., 2002). This study suggests that the difference between observed and predicted clearance rates may be explained by the overestimate of mass bound within flocs, due to the use of Stokes' Law to estimate particle effective density. The results of this study suggest that fine sediment suspensions may not be as highly flocculated as previously believed. Future studies should pursue similar observations within more energetic environments and at higher suspended sediment concentrations.

Acknowledgments

Sincere appreciation is given to the captain and crew of R/V *Endeavor* for their assistance in deploying field equipment. Thanks also to Jerome Bonnin for his logistical support in France in preparing for this cruise. This research was supported by the US Office of Naval Research (ONR), as part of the EuroSTRATAFORM program (contract N00014-04-1-0165 awarded to P.S. Hill and contract N00014-04-1-0182 awarded to T.G. Milligan).

References

Agrawal, Y.C., Pottsmith, H.C., 2000. Instruments for particle size and settling velocity observations in sediment transport. Marine Geology 168, 89–114.

Bale, A.J., Morris, A.W., 1987. In situ measurements of particle size in estuarine waters. Estuarine, Coastal and Shelf Science 24, 253–263.

Courp, T., Monaco, A., 1990. Sediment dispersal and accumulation on the continental margin of the Gulf of Lions: sedimentary budget. Continental Shelf Research 10, 1063–1087.

Curran, K.J., Hill, P.S., Milligan, T.G., 2002. Fine-grained suspended sediment dynamics in the Eel River flood plume. Continental Shelf Research 22, 2537–2550.

Curran, K.J., Hill, P.S., Milligan, T.G., Cowan, E.A., Syvitski, J.P.M., Konings, S.M., 2004a. Fine-grained sediment flocculation below the Hubbard Glacier meltwater plume, Disenchantment Bay, Alaska. Marine Geology 203, 83–94.

Curran, K.J., Hill, P.S., Schell, T.M., Milligan, T.G., Piper, D.J.W., 2004b. Inferring the mass fraction of floc-deposited mud: application to fine-grained turbidites. Sedimentology 51, 927–944.

Droppo, I.G., Leppard, G.G., Liss, S.N., Milligan, T.G., 2005. Opportunities, needs, and strategic direction for research on flocculation in natural and engineered systems. In: Droppo, I.G., Leppard, G.G., Liss, S.N., Milligan, T.G. (Eds.), Flocculation in Natural and Engineered Environmental Systems. CRC Press, New York, pp. 407–421.

Dyer, K.R., Manning, A.J., 1999. Observation of the size, settling velocity, and effective density of flocs, and their fractal dimension. Journal of Sea Research 41, 87–95.

Dyer, K.R., Cornelisse, J., Dearnaley, M.P., Fennessy, M.J., Jones, S.E., Kappenberg, J., McCave, I.N., Pejrup, M., Puls, W., van Leussen, W., Wolfstein, K., 1996. A comparison of in situ techniques for estuarine floc settling velocity measurements. Journal of Sea Research 36, 15–29.

Eisma, D., 1986. Flocculation and de-flocculation of suspended matter in estuaries. Netherlands Journal of Sea Research 20, 183–199.

Eisma, D., Schuhmacher, T., Boekel, H., van Heerwaarden, J., Franken, H., Laan, M., Vaars, A., Eijgenraam, F., Kalf, J., 1990. A camera and image-analysis system for in situ observation of flocs in natural waters. Netherlands Journal of Sea Research 27, 43–56.

El Ganaoui, O., Schaaff, E., Boyer, P., Amielh, M., Anselmet, F., Grenz, C., 2004. The deposition and erosion of cohesive sediments determined by a multi-class model. Estuarine, Coastal and Shelf Science 60, 457–475.

Estournel, C., Durrieu de Madron, X., Marsaleix, P., Auclair, F., Julliand, C., Vehil, R., 2003. Observation and modeling of the winter coastal oceanic circulation in the Gulf of Lion under wind conditions influenced by the continental orography (FETCH experiment). Journal of Geophysical Research 108, 8059, doi:10.1029/2001JCO00825.

Fennessy, M.J., Dyer, K.R., Huntley, D.A., 1994. INSSEV: an instrument to measure the size and settling velocity of flocs in situ. Marine Geology 117, 107–117.

Ferré, B., Guizien, K., Durrieu de Madron, X., Palanques, A., Guillién, J., Grémare, A., 2005. Fine-grained sediment dynamics during a storm event in the inner-shelf of the Gulf of Lion (NW Mediterranean). Continental Shelf Research 25, 2410–2427.

Fox, J.M., Hill, P.S., Milligan, T.G., Ogston, A.S., Boldrin, A., 2004. Floc fraction in the waters of the Po River prodelta. Continental Shelf Research 24, 1699–1715.

Gibbs, R.J., Wolanski, E., 1992. The effect of flocs on optical backscattering measurements of suspended material concentration. Marine Geology 107, 289–291.

Gibbs, R.J., Tshudy, D.M., Konwar, L., Martin, J.M., 1989. Coagulation and transport of sediments in the Gironde Estuary. Sedimentology 36, 987–999.

Grant, W.D., Madsen, O.S., 1986. The continental shelf bottom boundary layer. Annual Review of Fluid Mechanics 18, 265–305.

Hatcher, A., Hill, P.S., Grant, J., 2001. Optical backscatter of marine flocs. Journal of Sea Research 46, 1–12.

Hawley, N., 1982. Settling velocity distribution of natural aggregates. Journal of Geophysical Research 87, 9489–9498.

Hill, P.S., Syvitski, J.P.M., Cowan, E.A., Powell, R.D., 1998. In situ observations of floc settling velocities in Glacier Bay, Alaska. Marine Geology 145, 85–94.

Khelifa, A., Hill, P.S., 2006. Models for effective density and settling velocity of flocs. Journal of Hydraulic Research 44, 390–401.

Kranck, K., Petticrew, E., Milligan, T.G., Droppo, I., 1993. In situ particle size distributions resulting from flocculation of suspended sediment. In: Mehta, A.J. (Ed.), Nearshore and Cohesive Sediment Transport. Coastal and Estuarine Studies, vol. 42. Springer, New York, pp. 60–75.

Li, X., Logan, B.E., 1995. Size distributions and fractal properties of particles during a simulated phytoplankton bloom in a mesocosm. Deep Research II 42, 125–138.

Li, X., Logan, B.E., 1997. Collision frequencies of fractal aggregates with small particles by differential settling. Environmental Science and Technology 31, 1229–1236.

Mikkelsen, O.A., Pejrup, M., 2001. The use of a LISST-100 laser particle sizer for in-situ estimates of floc size, density and settling velocity. Geo-Marine Letters 20, 187–195.

Mikkelsen, O.A., Hill, P.S., Milligan, T.G., Moffatt, D., 2004. INSSECT—an instrumented platform for investigating floc properties close to the seabed. Limnology and Oceanography: Methods 2, 226–236.

Mikkelsen, O.A., Hill, P.S., Milligan, T.G., Chant, R.J., 2005. In situ particle size distributions and volume concentrations from a LISST-100 laser particle sizer and a digital floc camera. Continental Shelf Research 25, 1959–1978.

Mikkelsen, O.A., Hill, P.S., Milligan, T.G., 2006. Single-grain, microfloc and macrofloc volume variations observed with a LISST-100 and digital floc camera. Journal of Sea Research 55, 87–102.

Schaaff, E., Grenz, C., Pinazo, C., 2002. Erosion of particulate inorganic and organic matter in the Gulf of Lion. Comptes Rendus Geoscience 334, 1071–1077.

Schaaff, E., Grenz, C., Pinazo, C., Lansard, B., 2006. Field and laboratory measurements of sediment erodibility. Journal of Sea Research 55, 30–42.

Sternberg, R.W., Berhane, I., Ogston, A.S., 1999. Measurement of the size and settling velocity of suspended aggregates on the northern California continental shelf. Marine Geology 154, 227–242.

Syvitski, J.P.M., Asprey, K.W., Le Blanc, K.W.G., 1995. In situ characteristics of particles settling within a deep-water estuary. Deep Sea Research II 42, 223–256.

Thomsen, L., Gust, G., 2000. Sediment erosion thresholds and characteristics of resuspended aggregates on the western European continental margin. Deep-Sea Research I 47, 1881–1897.

Traykovski, P., Latter, R.J., Irish, J.D., 1999. A laboratory evaluation of the laser in situ scattering and transmissometery instrument using natural sediment. Marine Geology 159, 355–367.

Xia, X.M., Li, Y., Yang, H., Wu, C.Y., Sing, T.H., Pong, H.K., 2004. Observations on the size and settling velocity distributions of suspended sediments in the Pearl River Estuary, China. Continental Shelf Research 24, 1809–1826.

Geochemistry Geophysics Geosystems G3
AN ELECTRONIC JOURNAL OF THE EARTH SCIENCES
Published by AGU and the Geochemical Society

Article
Volume 7, Number 11
22 November 2006
Q11017, doi:10.1029/2006GC001306
ISSN: 1525-2027

Origin and distribution of terrestrial organic matter in the NW Mediterranean (Gulf of Lions): Exploring the newly developed BIT index

Jung-Hyun Kim
CEFREM-CNRS UMR 5110, Université de Perpignan, 52 Avenue Paul Alduy, F-66860 Perpignan Cedex, France

Department of Marine Biogeochemistry and Toxicology, Royal Netherlands Institute for Sea Research (NIOZ), P.O. Box 59, 1790 AB Den Burg, Texel, Netherlands (jhkim@nioz.nl)

Stefan Schouten
Department of Marine Biogeochemistry and Toxicology, Royal Netherlands Institute for Sea Research (NIOZ), P.O. Box 59, 1790 AB Den Burg, Texel, Netherlands

Roselyne Buscail, Wolfgang Ludwig, and Jérôme Bonnin
CEFREM-CNRS UMR 5110, Université de Perpignan, 52 Avenue Paul Alduy, F-66860 Perpignan Cedex, France

Jaap S. Sinninghe Damsté
Department of Marine Biogeochemistry and Toxicology, Royal Netherlands Institute for Sea Research (NIOZ), P.O. Box 59, 1790 AB Den Burg, Texel, Netherlands

François Bourrin
CEFREM-CNRS UMR 5110, Université de Perpignan, 52 Avenue Paul Alduy, F-66860 Perpignan Cedex, France

[1] The Branched and Isoprenoid Tetraether (BIT) index is based on the relative abundance of nonisoprenoidal glycerol dialkyl glycerol tetraethers (GDGTs) derived from organisms living in terrestrial environments versus a structurally related isoprenoid GDGT "crenarchaeol" produced by marine Crenarchaeota. The BIT index varies between 0 and 1, representing marine and terrestrial organic matter (OM) end-members, respectively (Hopmans et al., *Earth Planet. Sci. Lett.*, *224*, 107–116, 2004). In this study, the applicability of the BIT index to trace terrestrial OM is tested in combination with other organic parameters (TOC, C/N ratio, $\delta^{13}C_{org}$, total lipid, and *n*-alkane) in the Gulf of Lions, a river-dominated continental margin of the western Mediterranean. We analyzed a variety of soils and riverbed sediments from the continent as well as surface sediments from the shelf and canyons. The BIT index in soils and riverbed sediments shows high values (>0.9), while it varies between 0.02 and 0.83 in marine sediments, decreasing seaward from the inner shelf to the slope. For marine surface sediments, high BIT values are associated with lower $\delta^{13}C_{org}$ values as well as higher TOC contents and higher *n*-alkane concentrations. Our results confirm that the BIT index can be applied in coastal marine environments in order to characterize terrestrial OM as proposed by Hopmans et al. (2004). Therefore the BIT index is a useful addition to the proxies presently available for studying the origin and distribution of OM in continental margins and especially valuable in multiproxy studies.

Components: 11,102 words, 5 figures, 2 tables.

Keywords: BIT index; GDGT; terrestrial organic matter; Gulf of Lions.

Index Terms: 1055 Geochemistry: Organic and biogenic geochemistry; 3022 Marine Geology and Geophysics: Marine sediments: processes and transport.

Received 15 March 2006; **Revised** 30 August 2006; **Accepted** 11 September 2006; **Published** 22 November 2006.

Kim, J.-H., S. Schouten, R. Buscail, W. Ludwig, J. Bonnin, J. S. Sinninghe Damsté, and F. Bourrin (2006), Origin and distribution of terrestrial organic matter in the NW Mediterranean (Gulf of Lions): Exploring the newly developed BIT index, *Geochem. Geophys. Geosyst.*, *7*, Q11017, doi:10.1029/2006GC001306.

1. Introduction

[2] One of the major issues in studying sedimentary organic matter (OM) on continental margins is to make accurate estimates of the relative contributions of terrestrial and marine OM. Detailed information of the origin of OM will considerably improve our knowledge on the sedimentary processes ruling the transport of sediments from the continent to the deep-sea and therefore improve the estimate of the global carbon budgets. Furthermore, as the natural particulate OM fraction has the potential to adsorb organic micropollutants and heavy metals, the understanding of the fate of the terrestrial OM in the coastal environment is of utmost importance to determine the impact of anthropogenic activities and to establish efficient strategies to protect the coastal zones.

[3] The stable carbon isotope composition ($\delta^{13}C_{org}$) and the C/N ratio have been widely used to trace sources of particulate OM [e.g., *Meyers*, 1994; *Middelburg and Nieuwenhuize*, 1998; *Kerhervé et al.*, 2001]. However, interpretation of these proxies is often complicated by the fact that bulk material represents mixtures from several sources, and thus their isotope ratios are weighted averages. Furthermore, selective degradation of OM components during early diagenesis can substantially alter C/N ratios. Organic compounds in sediments that have a demonstrable origin from certain living organisms are termed biological markers or biomarkers [e.g., *Brassell*, 1993]. Many organic compounds, particularly lipid biomarkers, are relatively resistant to degradation, and can be well preserved in sediments. Identification and quantification of major lipid biomarkers as well as measuring the isotopic compositions of individual lipid biomarkers showed great potential of providing less equivocal proxies for the sources of OM. A large range of marine and terrestrial lipid biomarkers (e.g., alkenones, taraxerol, long-chain *n*-alkanes, *n*-alcohols, and fatty acids) is available [e.g., *Brassell*, 1993; *Meyers*, 1997]. However, quantification of the relative input of terrestrial OM is still complicated due to large variations in concentrations of compounds in the different plant materials and different degradation rates of terrestrial and marine organic compounds [e.g., *Sinninghe Damsté et al.*, 2002a].

[4] An alternative approach to reconstruct the relative amounts of terrestrial and marine OM is to use the newly developed proxy, the Branched and Isoprenoid Tetraether (BIT) index [*Hopmans et al.*, 2004]. This index is based on a group of nonisoprenoidal glycerol dialkyl glycerol tetraethers (GDGTs) derived from anaerobic bacteria thriving in terrestrial environments [*Weijers et al.*, 2006a] and a structurally related isoprenoid GDGT "crenarchaeol" predominantly produced by marine planktonic Crenarchaeota [*Sinninghe Damsté et al.*, 2002b]. The BIT index varies between 0 and 1, representing marine and terrestrial OM endmembers, respectively [*Hopmans et al.*, 2004]. There are several advantages to the use of the BIT index compared to other molecular and bulk proxies. First, the terrestrial and marine GDGTs have a similar chemical structure and are therefore likely to be degraded at similar rates during sediment diagenesis. As a result, the BIT index is less sensitive to diagenetic effects compared to individual lipid compounds and other conventional organic carbon tracers. Second, the branched GDGTs are derived from seemingly ubiquitous anaerobic bacteria living in terrestrial environments, mostly soils and peats [*Schouten et al.*, 2000; *Hopmans et al.*, 2004; *Weijers et al.*, 2006a]. Therefore they are not specific for particular vegetation types but for terrestrial vegetation in general. Third, the BIT index is easily measured in a single GDGT analysis of lipid extracts and

does not require specific chemical degradation procedures. Fourth, the BIT index is fully related to fluvial input of terrestrial OM and not to eolian transport [*Hopmans et al.*, 2004; *Weijers et al.*, 2006b]. Therefore the BIT index has a great potential to estimate the relative amount of fluvial terrestrial OM input. However, the BIT index has not been widely tested yet and its use as a robust proxy for terrestrial OM input still has to be validated in various coastal settings.

[5] The main goals of this study are thus (1) to test the general applicability of the newly developed BIT index in combination with other organic parameters and (2) to better understand the origin and distribution of OM in coastal zones. We choose the Gulf of Lions to conduct this study as it is a river dominated continental margin where during flood events large amounts of terrestrial matter are delivered to the coastal zone via rivers. Furthermore, physical, biological as well as sedimentological processes have been widely studied in the Gulf of Lions [e.g., *Buscail and Germain*, 1997; *Durrieu de Madron et al.*, 1999; *Monaco et al.*, 1999; *Liquete et al.*, 2004]. This area combines therefore the necessary conditions to study and validate the newly developed BIT index as a proxy for continental versus marine OM input.

2. Study Area

[6] The Gulf of Lions is located in the northwestern Mediterranean basin between 42N-3E and 43N-6E. Its continental shelf is crescent shaped and fairly broad (up to 20 miles) and its continental slope is incised by numerous submarine canyons (Figure 1a). From a hydrodynamic point of view, the Gulf of Lions is a complex region where several intense and highly variable phenomena such as the energetic general circulation along the continental slope (the "courant liguro-provençal"), the cascading of dense water both on the shelf and offshore, the mesoscale circulation (eddies, filaments, etc.), the internal waves (mainly in the near-inertial band), the seasonal variation of stratification, and the extreme meteorological events interact. The major physical forcings in the Gulf of Lions are the strong winds (both from land and sea), the general circulation and the fresh water discharge from rivers. The Northern Current flowing along the continental slope is part of the cyclonic circulation of the western Mediterranean basin (Figure 1a). The core of this geostrophic current is about several hundreds meters thick and primarily composed of Modified Atlantic Water (upper 150 m) and Levantine Intermediate Water (deeper down) [*Millot*, 1990, 1991]. It constraints the shelf circulation and influences the shelf-slope exchanges. Furthermore, it forms a density front that separates the continental influenced fresh shelf water and the more saline open ocean water.

[7] Several sources of particulate matter feed the continental shelf in the Gulf of Lions: fluvial and atmospheric (primarily Saharan dust deposition) input of continental material, biological production, and resuspended coastal sediment. Riverine inputs of water and sediments in the Gulf of Lions originate mainly from the Rhône River, which is, since the damming of the Nile at Aswan, the largest Mediterranean river in terms of its freshwater discharge [*Ludwig et al.*, 2003]. Also the smaller coastal rivers (e.g., the Têt, Orb, Aude, and Hérault Rivers) can significantly contribute to the sediment budgets in this environment. Although on average much lower than the Rhône discharges, the particulate inputs by these rivers arrive almost exclusively via the occurrence of short and violent flash-floods [*Serrat*, 1999; *Serrat et al.*, 2001], thereby providing important pulses of terrestrial matter injections into the marine environment.

[8] The Rhône River has a catchment's area of 97,800 km^2 [*Pont et al.*, 2002] and discharges on average about 1,700 m^3/s [*Thill et al.*, 2001] of freshwater into the Gulf of Lions. Its discharge regime is rather constant, but during floods peak discharges greater than 10,000 m^3/s can be measured (e.g., in December 2003 [*Arnau et al.*, 2004]). The Rhône River has high mean sediment discharge of about 7–10 10^6 tons/yr [*Sempéré et al.*, 2000; *Pont et al.*, 2002], accounting for ~80% of the riverine inputs to the Gulf of Lions [*Durrieu de Madron et al.*, 2000]. The formation of the Rhône prodelta is centered at ~30 m water depth with high sediment accumulation rates of >20 cm/yr [*Radakovitch et al.*, 1999].

[9] The Têt River has a catchment's area of about 1,400 km^2 [*Ludwig et al.*, 2004]. It delivers water and suspended materials into the southwestern part of the Gulf of Lions where these sediments built a prodeltaic deposit on the inner shelf [*Buscail et al.*, 1990, 1995; *Courp and Monaco*, 1990; *Guidi-Guilvard and Buscail*, 1995]. The average water discharge of the river is close to 10 m^3/s, but it can increase by more than two orders of magnitude during major floods [*Ludwig et al.*, 2004]. *Serrat et al.* [2001] estimated the annual mean sediment discharge to 53,000 ± 16,000 tons/yr for the reference period of 1980–1999. Also here, this

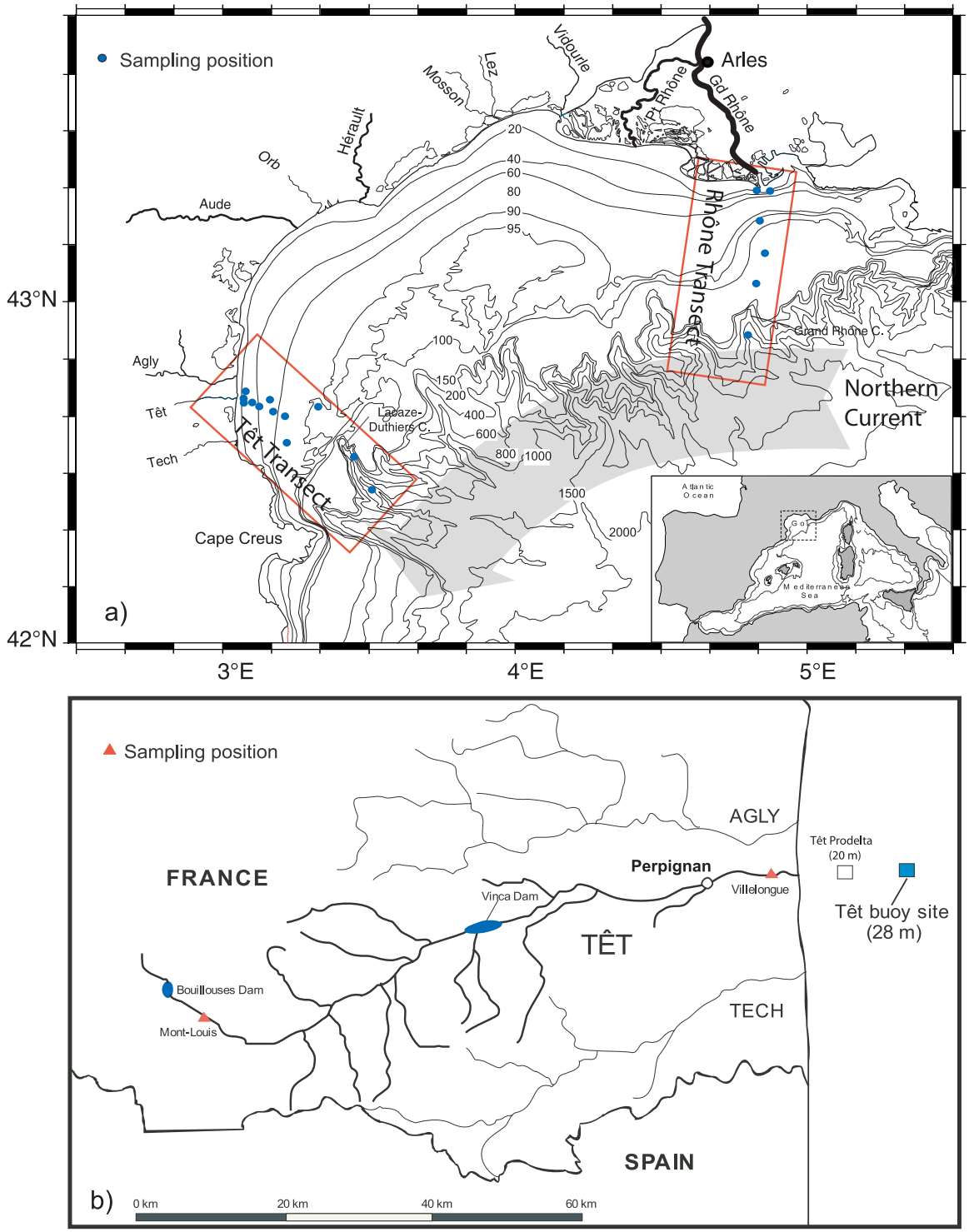

Figure 1. Map of the study area showing (a) the Gulf of Lions with main rivers and submarine canyons and (b) the detailed catchment area of the Têt River and sampling stations. Blue dots in Figure 1a indicate the sampling positions of Rhône and Têt transects. Red triangles in Figure 1b show the sampling positions along the Têt River. The Têt buoy site is located off Têt River mouth in 28 m water depth.

value is accompanied by a very high interannual and seasonal variability, since in some years, about 2–3 times of this amount was discharged during only three days (e.g., 1996 [see *Serrat et al.*, 2001]).

3. Material and Methods

3.1. Soil and Sediment Sampling

[10] In this study, soils and riverbed sediments from the land as well as surface sediments from the shelf and canyons were investigated (Table 1 and Figure 1b). Detailed sample information is summarized in Table 1. Four soil samples were taken near the Bouillouses dam situated at an altitude of 2000 m. Soil samples SO-LB1 were taken a few meters from the shore of the Bouillouses dam, representing a histosoil with the vegetation essentially composed of pasture grass. Soil samples SO-LB2 were collected downstream a few hundred meters from the dam and a few meters from the Têt River shore in a wetland (peat-like) where the vegetation is essentially made of furze and carex. The surrounding forest is mainly composed of beech trees, Douglas and Laricio pine trees. One Têt riverbed sediment sample was taken in Mont-Louis (RBS-ST1). This muddy-sand sediment was dry-sieved (<63 μm) for chemical analyses.

[11] The core tops of fifteen sediment cores recovered from October 2003 to July 2005 from the Têt buoy site (42.7041N, 3.0668E) were analyzed, giving a time series of about 21 months. This site is located 2 km off the Têt River mouth at 28 m water depth and is part of the POEM-L2R (Observation Platform of the Mediterranean Environment of the Littoral of Languedoc-Roussillon) station maintained by the CEFREM since 2003. One additional core top of the sediment core recovered closer to the Têt River mouth (20 m water depth, 42.7092N, 3.0541E) on the 28 April 2004 was also analyzed. Sediment cores were sliced at 1 cm interval, frozen and freeze-dried in the laboratory a few hours after core sub-sampling. Additionally, to provide a picture of the offshore extent of terrestrial OM inputs, surface sediments were collected along two transects located off the Rhône and Têt river mouths. The two transects span from the prodelta to depths of almost one thousand meter (Table 1) into the submarine canyons incising the slope (Figure 1a). The sediment cores were recovered using a box corer during the REMORA 3 cruise in November 2002 [*Roussiez et al.*, 2005]. The cores were sliced and immediately deep-frozen on board. Soils and sediment samples were freeze-dried and homogenized prior to analysis.

3.2. Chemical Analyses

3.2.1. Bulk Sediment Analyses

[12] Bulk chemical parameters were analyzed using milled, freeze-dried sediment sub-samples. Total nitrogen, total and organic carbon concentrations (TN, TC and TOC, respectively) were measured on homogenized, precisely weighed samples in an automatic CN-analyzer LECO 2000 at CEFREM. TOC values were obtained after acidification with 2N HCl (overnight, at 50°C) in order to remove carbonates prior to the analyses. The analyses are performed by dry combustion in a furnace and the CO_2 and N_2 formed are quantitatively measured by infra-red adsorption for TC and TOC, and thermal conduction for TN [*Cauwet et al.*, 1990]. Extensive testing and application at CEFREM showed long-term precisions for TOC and TN of about 2% and for TC of 0.3%. To calculate C/N ratio, we used TOC and organic nitrogen that corresponds to the difference between TN and mineral nitrogen ($NH_4^+ + NO_2^- + NO_3^-$). *Delille et al.* [1990] found that mineral nitrogen corresponds to about 10% of TN in the surface sediments of 3 stations located on the NW Mediterranean continental shelf and slope and sampled monthly during 2 years (March 1984 to April 1986, 78 samples). We therefore corrected TN to obtain organic nitrogen according to *Delille et al.* [1990].

[13] After acidification of the samples with 2 M HCl, the stable carbon isotopic composition of TOC ($\delta^{13}C_{org}$) was determined using a Flash EA 1112 Elemental Analyser interfaced with a ThermoFinnigan Delta^{Plus} mass spectrometer at NIOZ. Isotope values were calibrated to a benzoic acid standard ($\delta^{13}C_{org} = -27.8‰$ with respect to Vienna Pee Dee Belemnite (VPDB) calibrated on NBS-22 and corrected for blank contribution. The $\delta^{13}C_{org}$ values are reported in the standard delta notation relative to VPDB standard. The analyses were done at least in duplicate. The analytical error was usually smaller than ±0.2‰.

3.2.2. Lipid Analyses

3.2.2.1. Total Lipid Analysis

[14] Total lipid contents of sediments were measured at CEFREM using a colorimetric method

Table 1. Detailed Information on Samples, Including Sampling Dates and Sample Positions

Sample Type	Sample Code	Geological Setting	Cruise	Station	Core Type	Date, dd/mm/yy	Core Depth, cm	Longitude, E	Latitude, N	Water Depth, m	Distance From the River Mouth, km
Soils	SO-LB1-T	Meadow				22/06/2005	5–15				
	SO-LB1-B	Meadow				22/06/2005	25–30				
	SO-LB2-T	Wetland				22/06/2005	5–10				
	SO-LB2-B	Wetland				22/06/2005	15–25				
Têt riverbed sediment	RBS-ST1	Têt River		Mont-Louis		22/06/2005					
Marine surface sediment											
Têt buoy site (28 m)	TB-10/10/2003	Têt Prodelta		POEM-L2R	Scuba Diving Hand Core	10/10/2003	0–1	3.0668	42.7041	28	2.5
	TB-26/11/2003	Têt Prodelta		POEM-L2R	Scuba Diving Hand Core	26/11/2003	0–1	3.0668	42.7041	28	2.5
	TB-12/12/2003	Têt Prodelta		POEM-L2R	Scuba Diving Hand Core	12/12/2003	0–1	3.0668	42.7041	28	2.5
	TB-11/02/2004	Têt Prodelta		POEM-L2R	Scuba Diving Hand Core	11/02/2004	0–1	3.0668	42.7041	28	2.5
	TB-15/03/2004	Têt Prodelta		POEM-L2R	Scuba Diving Hand Core	15/03/2004	0–1	3.0668	42.7041	28	2.5
	TB-18/04/2004	Têt Prodelta		POEM-L2R	Scuba Diving Hand Core	18/04/2004	0–1	3.0668	42.7041	28	2.5
	TB-28/04/2004	Têt Prodelta		POEM-L2R	Scuba Diving Hand Core	28/04/2004	0–1	3.0668	42.7041	28	2.5
	TB-26/05/2004	Têt Prodelta		POEM-L2R	Scuba Diving Hand Core	26/05/2004	0–1	3.0668	42.7041	28	2.5
	TB-23/06/2004	Têt Prodelta		POEM-L2R	Scuba Diving Hand Core	23/06/2004	0–1	3.0668	42.7041	28	2.5
	TB-28/07/2004	Têt Prodelta		POEM-L2R	Scuba Diving Hand Core	28/07/2004	0–1	3.0668	42.7041	28	2.5
	TB-30/09/2004	Têt Prodelta		POEM-L2R	Scuba Diving Hand Core	30/09/2004	0–1	3.0668	42.7041	28	2.5
	TB-13/12/2004	Têt Prodelta		POEM-L2R	Scuba Diving Hand Core	13/12/2004	0–1	3.0668	42.7041	28	2.5
	TB-15/03/2005	Têt Prodelta		POEM-L2R	Scuba Diving Hand Core	15/03/2005	0–1	3.0668	42.7041	28	2.5
	TB-20/05/2005	Têt Prodelta		POEM-L2R	Scuba Diving Hand Core	20/05/2005	0–1	3.0668	42.7041	28	2.5
	TB-06/07/2005	Têt Prodelta		POEM-L2R	Scuba Diving Hand Core	06/07/2005	0–1	3.0668	42.7041	28	2.5
Têt prodelta (20 m)	TP-28/04/2004	Têt Prodelta			Scuba Diving Hand Core	28/04/2004	0–1	3.0541	42.7092	20	1.4
Têt transect	SS-35	Têt Prodelta	REMORA 3	35	Multitube	22/10/2002	1–2	3.0652	42.7155	27	2.2
	SS-352	Têt Prodelta	REMORA 3	352	Multitube	22/10/2002	1–2	3.0639	42.7282	27	2.3
	SS-351bis	Shelf	REMORA 3	351bis	Multitube	22/10/2002	1–2	3.0900	42.6988	33	5.0
	SS-353	Shelf	REMORA 3	353	Multitube	22/10/2002	1–2	3.1524	42.7121	51	9.4
	SS-37bis	Shelf	REMORA 3	37bis	Multitube	23/10/2002	1–2	3.2062	42.5825	81	20.5
	SS-34bis	Shelf	REMORA 3	34bis	Multitube	23/10/2002	1–2	3.3256	42.6920	91	23.7
	SS-38bis	Lacaze-Duthiers Canyon	REMORA 3	38bis	Multitube	24/10/2002	1–2	3.4395	42.5418	603	38.4
	SS-39bis	Lacaze-Duthiers Canyon	REMORA 3	39bis	Multitube	23/10/2002	1–2	3.5112	42.4489	783	49.0

Table 1. (continued)

Sample Type	Sample Code	Geological Setting	Cruise	Station	Core Type	Date, dd/mm/yy	Core Depth, cm	Longitude, E	Latitude, N	Water Depth, m	Distance From the River Mouth, km
Rhône transect	SS-KB16	Rhône Prodelta	REMORA 3	KB16	Multitube	03/11/2002	1–2	4.8239	43.3203	15	1.5
	SS-KB4	Rhône Prodelta	REMORA 3	KB4	Multitube	03/11/2002	1–2	4.8678	43.3181	26.6	2.3
	SS-9X	Shelf	REMORA 3	9X	Multitube	02/11/2002	1–2	4.8324	43.2328	95	10.4
	SS-2	Shelf	REMORA 3	2	Multitube	14/10/2002	1–2	4.8547	43.1393	105	21.3
	SS-3	Shelf	REMORA 3	3	Multitube	14/10/2003	1–2	4.8217	43.0481	112	31.4
	SS-4	Grand Rhône Canyon	REMORA 3	4	Multitube	02/11/2002	1–2	4.7969	42.9007	781	48.0

[*Barnes and Blackstock*, 1973] after extraction with a mixture of chloroform:methanol (MeOH) (2:1 v/v). Absorption of the products was measured at 520 nm with a Beckman spectrophotometer.

3.2.2.2. Lipid Extraction and Purification Procedure

[15] Hydrocarbon and GDGT analyses were conducted at NIOZ. Soil and sediment samples (1–12 g) for hydrocarbon and GDGT analyses were either ultrasonically extracted with MeOH (3×), MeOH:dichloromethane (DCM) (1:1 v/v; 3×), and DCM (3×) or extracted with an Accelerated Solvent Extractor (DIONEX ASE 200) using a mixture of DCM:MeOH (9:1 v/v) at a temperature of 100°C and a pressure of 7.6×10^6 Pa. The supernatants were combined, the solvents were removed by rotary evaporation, and the extracts were taken up in DCM and dried over anhydrous Na_2SO_4. Afterward, activated copper was added and stirred overnight for removal of elemental sulfur. The extracts were cleaned over $MgSO_4$ column with DCM and separated into three fractions over an Al_2O_3 column (activated for 2 h at 150°C) using hexane:DCM (9:1 v/v), hexane:DCM (1:1 v/v), and DCM:MeOH (1:1 v/v), respectively.

3.2.2.3. Aliphatic Hydrocarbon Analysis

[16] For aliphatic hydrocarbon (*n*-alkane) analysis, the hexane:DCM, 9:1 v/v fractions of the total lipid extract were further purified over a $AgNO_3$ impregnated silica gel column using hexane. A known amount of standard, perdeutero-*n*-C_{24} alkane was added and used as reference for quantification of each compound. Analyses were performed on a Hewlett Packard 5890 series II gas chromatograph equipped with an on-column injector and fitted with a fused-silica capillary column (25 m × 0.32 mm) coated with CP Sil 5 (film thickness 0.12 μm). Helium was used as carrier gas. The GC oven was heated from 70°C to 130°C at 20°C/min, followed by 4°C/min to 320°C (10 min holding time). Effluents were detected using flame ionization (FID). To identify compounds in selected samples, GC-MS analyses were performed with a Thermofinnigan TRACE gas chromatograph using the GC conditions described above. The column was directly inserted into the electron impact ion source of a Thermofinnigan DSQ quadrupole mass spectrometer, scanning a mass range of *m*/*z* 50–800 at 3 scans per second and an ionization energy of 70 eV. Compound identifications are based on comparison of relative GC retention times and mass spectra published in the literature. Quantification of com-

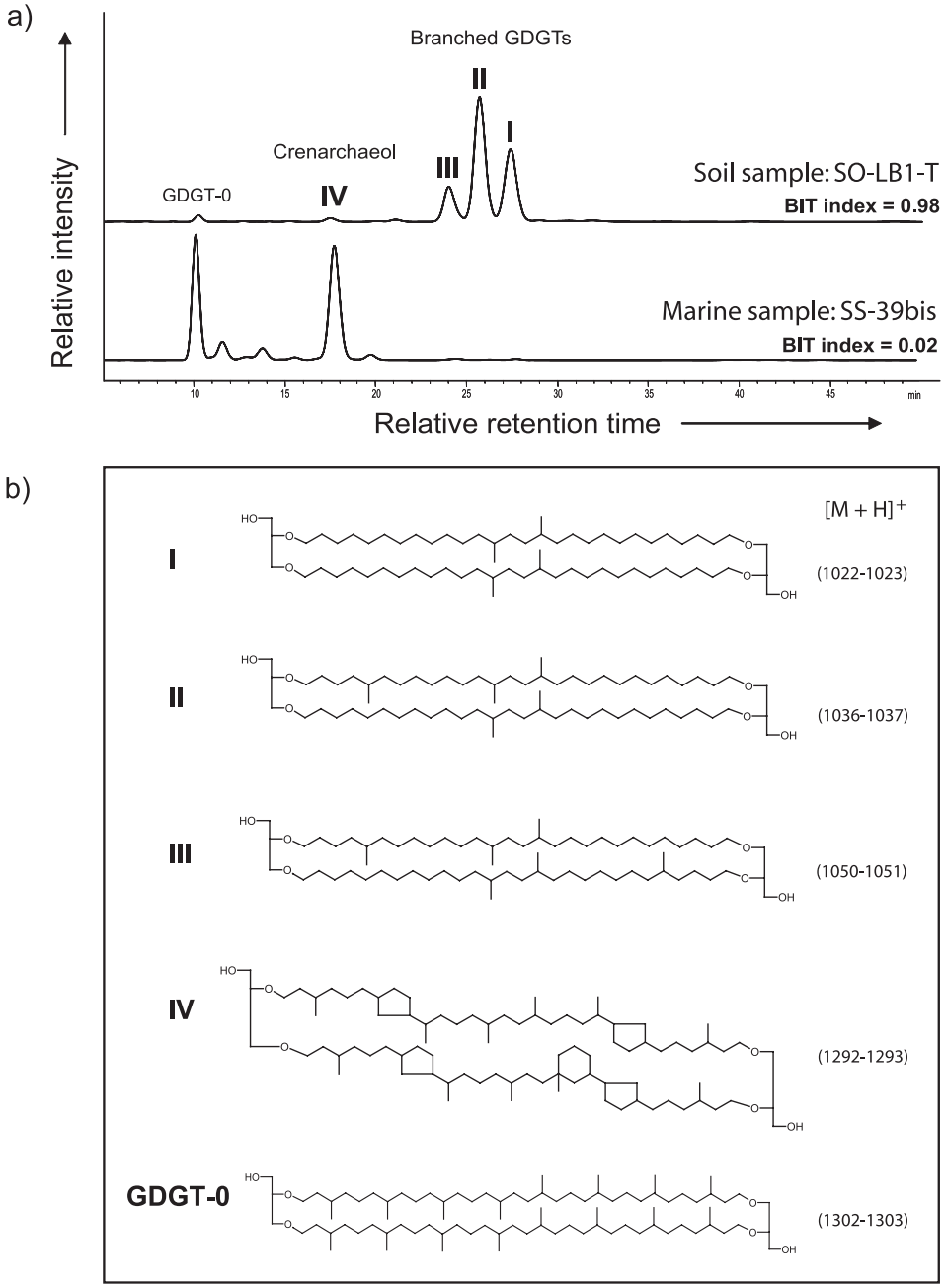

Figure 2. (a) HPLC/APCI-MS base peak chromatograms of GDGT lipids in a soil (SO-LB1-T) and a marine sediment (SS-39bis) and (b) GDGT structures: I, II, and III indicate the branched GDGTs, and IV is crenarchaeol.

pounds was performed by peak area integration in FID chromatograms. Data were acquired and integrated using ATLAS analytical software.

3.2.2.4. GDGT Analysis

[17] The polar fractions (DCM:MeOH, 1:1; v/v) were analyzed for GDGTs according to the procedure described by *Hopmans et al.* [2000, 2004]. Aliquots of polar fractions were blown down under a stream of nitrogen, redissolved by sonication (5 min) in hexane:propanol (99:1 v/v), and filtered through 0.45 μm PTFE filters. The samples were analyzed with a high performance liquid chromatography/atmospheric pressure positive ion chemical ionization mass spectrometry (HPLC/APCI-MS). Analyses were performed on an HP (Palo Alto, CA, USA) 1100 series LC-MS, equipped with auto-injector and Chemstation chro-

Table 2. Results of Bulk OM, Total Lipid, *n*-Alkane, and GDGT Analyses[a]

Sample Type	Sample Code	TOC, wt.%	C/N Ratio	$\delta^{13}C_{org}$, ‰ VPDB	Terr. TOC,[b] %	Total Lipids, mg/g_{sed}	CPI_{27-31}	C_{max}	31/(29+31)	ACL_{27-31}	ΣALK_{27-31}, $\mu g/g_{TOC}$	BIT Index	Branched GDGTs, $\mu g/g_{TOC}$	Crenarchaeol, $\mu g/g_{TOC}$	Terr. TOC,[b] %
Soils	SO-LB1-T	7.8	12.8	−25.8	n.d.	n.d.	8.6	31	0.6	29.9	410	0.98	27.3	0.5	n.d.
	SO-LB1-B	6.2	13.7	−25.7	n.d.	n.d.	16.2	31	0.6	29.8	200	0.99	21.5	0.2	n.d.
	SO-LB2-T	16.1	56.2	−28.7	n.d.	n.d.	15.9	31	0.5	29.7	3200	1.00	183.8	0.2	n.d.
	SO-LB2-B	4.4	15.8	−27.2	n.d.	n.d.	8.9	31	0.6	29.9	760	0.98	36.0	0.7	n.d.
Têt riverbed sediment	RBS-ST1	4.2	10.5	−27.0	n.d.	n.d.	9.2	29	0.4	28.9	670	0.99	105.7	1.4	n.d.
Marine surface sediment															
Têt buoy site (28 m)	TB-10/10/2003	0.6	12.4	−23.9	56	0.2	7.2	29	0.4	29.2	130	0.21	1.8	7.2	20
	TB-26/11/2003	0.3	13.2	−23.3	46	0.1	5.5	29	0.5	29.1	120	0.19	2.4	10.3	18
	TB-12/12/2003	1.7	5.9	−26.0	86	1.6	7.9	29	0.4	28.9	660	0.52	9.1	9.8	52
	TB-11/02/2004	1.5	11.9	−25.1	73	0.9	10.0	29	0.4	28.9	410	0.37	10.0	16.9	36
	TB-15/03/2004	0.4	17.7	−23.4	48	0.1	6.3	31	0.5	29.4	170	0.13	0.9	5.9	11
	TB-18/04/2004	0.2	12.4	−22.8	40	0.1	4.2	29	0.5	29.2	120	0.15	0.6	3.8	13
	TB-28/04/2004	0.3	13.8	−23.1	45	0.1	6.2	29	0.5	29.4	150	0.19	1.6	7.4	17
	TB-26/05/2004	0.4	14.5	−23.4	49	0.1	7.8	29	0.5	29.3	170	0.22	1.8	6.8	21
	TB-23/06/2004	0.5	9.9	−23.1	44	0.1	7.9	31	0.5	29.5	270	0.13	1.4	9.6	11
	TB-28/07/2004	0.5	20.6	−23.3	48	0.2	6.6	29	0.5	29.2	90	0.15	0.5	3.0	13
	TB-30/09/2004	0.4	16.5	−22.8	40	0.1	3.0	29	0.4	29.1	110	0.18	1.6	7.3	17
	TB-13/12/2004	0.5	21.6	−23.7	53	0.2	7.0	29	0.4	29.1	110	0.19	2.6	12.4	17
	TB-15/03/2005	0.5	12.3	−24.3	61	0.1	5.2	29	0.4	29.1	50	0.20	0.03	0.1	18
	TB-20/05/2005	0.5	12.5	−23.5	49	0.1	3.8	29	0.4	29.1	60	0.17	0.04	0.2	16
	TB-06/07/2005	0.5	16.2	−23.4	48	0.1	8.4	29	0.4	29.0	70	0.12	0.02	0.1	10
Têt prodelta (20 m)	TP-28/04/2004	1.4	18.4	−25.7	82	1.1-	8.1	29	0.4	28.9	470	0.55	6.1	7.4	55
Têt transect	SS-35	0.7	24.8	−24.4	63	n.d.	5.9	29	0.4	29.1	70	0.26	5.2	14.6	25
	SS-352	0.6	19.8	−23.9	56	n.d.	7.9	29	0.4	29.2	90	0.27	7.6	20.6	26
	SS-351bis	0.6	13.4	−23.7	53	n.d.	9.3	29	0.4	29.1	70	0.20	7.6	29.8	19
	SS-353	1.0	12.2	−23.4	49	n.d.	5.0	29	0.5	29.3	60	0.12	10.9	83.5	10
	SS-37bis	0.9	12.7	−23.3	48	n.d.	6.1	29	0.5	29.4	60	0.09	7.5	74.5	7
	SS-34bis	0.3	10.5	−22.5	35	n.d.	4.7	29	0.5	29.4	60	0.05	1.7	36.6	3
	SS-38bis	0.9	11.9	−22.4	35	n.d.	5.2	31	0.5	29.5	50	0.02	1.6	94.5	0
	SS-39bis	0.7	10.4	−22.4	34	n.d.	3.1	31	0.5	29.6	70	0.02	1.4	62.4	0

Table 2. (continued)

Sample Type	Sample Code	TOC, wt.%	C/N Ratio	$\delta^{13}C_{org}$, ‰ VPDB	Terr. TOC,[b] %	Total Lipids, mg/g_{sed}	CPI_{27-31}	C_{max}	31/(29+31)	ACL_{27-31}	ΣALK_{27-31}, $\mu g/g_{TOC}$	BIT Index	Branched GDGTs, $\mu g/g_{TOC}$	Crenarchaeol, $\mu g/g_{TOC}$	Terr. TOC,[b] %
Rhône	SS-KB16	1.8	13.0	−25.9	84	n.d.	8.2	29	0.4	29.0	270	0.83	15.0	3.1	83
Transect	SS-KB4	1.7	14.8	−25.5	79	n.d.	8.8	29	0.4	29.0	270	0.80	9.8	2.5	80
	SS-9X	1.0	12.1	−24.4	63	n.d.	4.2	29	0.5	29.3	110	0.12	3.4	26.6	10
	SS-2	0.8	11.3	−23.3	47	n.d.	3.8	31	0.5	29.4	120	0.06	3.1	54.2	4
	SS-3	0.3	7.8	−22.7	39	n.d.	3.4	31	0.5	29.4	110	0.05	2.5	53.3	3
	SS-4	0.7	10.1	−22.5	36	n.d.	3.5	31	0.5	29.6	110	0.02	0.6	25.8	0

[a] Notes: n.d., not determined; C_{max}, carbon number of the homologue with highest abundance; 31/(29+31), ratio of the n-C_{31} to the sum of the n-C_{29} and n-C_{31} alkane; ACL (average chain length), $ACL_{27-31} = (\Sigma[C_i] \times i)/\Sigma[C_i]$, where i is the range of carbon numbers and C_i is the relative concentration of the alkane containing i carbon atoms; CPI (Carbon Preference Index), $CPI_{27-31} = {}^1/_2 \times (\Sigma\text{odd } C_{27}\text{-to-}C_{31}/\Sigma\text{even } C_{26}\text{-to-}C_{30}) + {}^1/_2 \times (\Sigma\text{odd } C_{27}\text{-to-}C_{31}/\Sigma\text{even } C_{28}\text{-to-}C_{32})$.

[b] Terr. TOC indicates the calculated terrestrial TOC content based on $\delta^{13}C_{org}$ and BIT index, respectively (see text).

matography manager software. Separation was achieved on a Prevail Cyano column (2.1 × 150 mm, 3 μm; Alltech, Deerfield, IL, USA), maintained at 30°C. Flow rate of the hexane:propanol (99:1 v/v) eluent was 0.2 ml/min, isocratically for the first 5 min, thereafter with a linear gradient to 1.8% propanol in 45 min. After each analysis, the column was cleaned by back-flushing hexane/propanol (90:10, v/v) at 0.2 ml/min for 10 min. Detection was achieved using APCI-MS of the eluent. Conditions for APCI-MS were as follows: nebulizer pressure 60 psi, vaporizer temperature 400°C, drying gas (N_2) flow 6 l/min and temperature 200°C, capillary voltage −3 kV, corona 5 μA (~3.2 kV). GDGTs were detected by single ion monitoring of their $[M + H]^+$ ions and quantification of the GDGT compounds was achieved by integrating the peak areas and comparing these to a standard curve prepared with known amounts of GDGT-0 which contains no cyclopentane ring (see Figure 2 for the structure).

[18] Values of BIT index were calculated according to *Hopmans et al.* [2004]:

$$\text{BIT index} = [\text{I} + \text{II} + \text{III}]/[\text{I} + \text{II} + \text{III} + \text{IV}]$$

The roman numerals refer to the GDGTs indicated in Figure 2. I, II, and III are branched GDGTs and are tracers for terrestrial OM and IV the isoprenoid GDGT, "crenarchaeol", a tracer for marine OM [*Hopmans et al.*, 2004]. The analyses were done at least in duplicate and mean concentrations and BIT values are reported.

4. Results

4.1. Soils and Riverbed Sediments

[19] The TOC contents of the soils were relatively high (4.4 to 16.1 wt.%; see Table 2). The C/N ratios varied between 12.8 and 56.2 and the $\delta^{13}C_{org}$ values ranged from −25.7 to −28.7‰. For the Têt River bed sediment, the TOC content was lower than in the soils but remained relatively high (4.2 wt.%; see Table 2). The C/N ratio was 10.5 and the $\delta^{13}C_{org}$ value −27‰.

[20] In all soils and sediments a homologous series of n-alkanes (n-C_{21} to n-C_{35}) was detected. The distributions of n-alkanes showed a strong odd-over-even carbon number predominance in the range of C_{27}–C_{31} n-alkanes with the carbon preference index (CPI_{27-31} [*Kolattukudy*, 1976]) varying between 8 and 16 (Table 2). n-C_{31} was the major n-alkane in the soils, while the Têt River bed

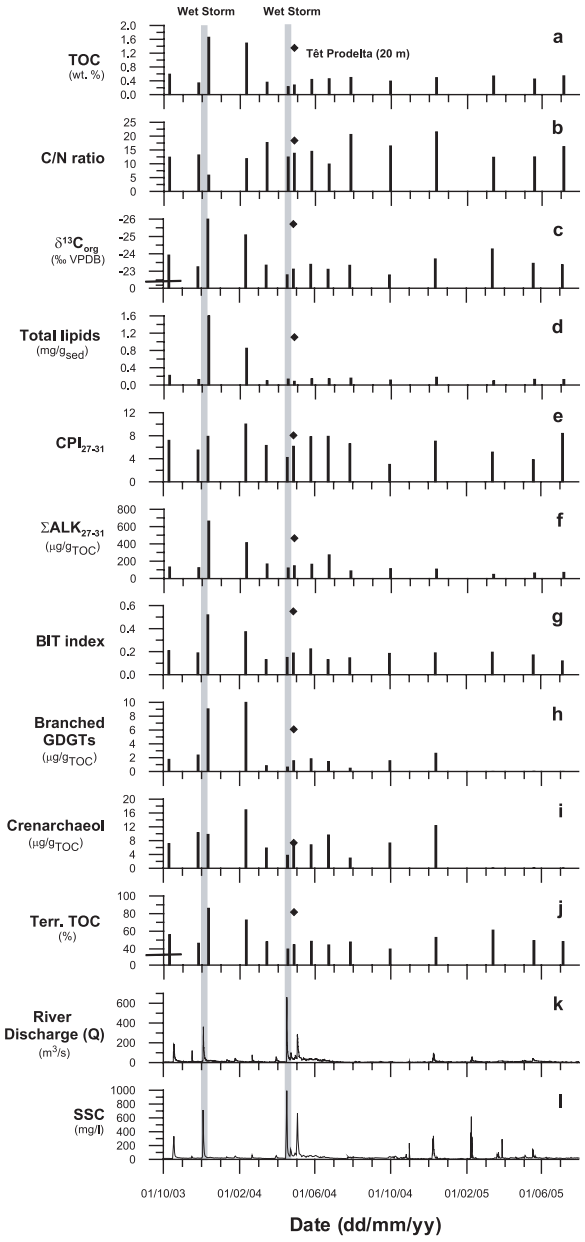

Figure 3. Results of bulk sediment and lipid analyses from Têt buoy site surface sediments: (a) TOC contents in wt.%, (b) C/N ratio, (c) $\delta^{13}C_{org}$ in ‰, (d) total lipids in mg/g_{sed}, (e) CPI_{27-31}, (f) ΣALK_{27-31} in mg/g_{TOC}, (g) BIT index, (h) sum of branched GDGTs concentration in $\mu g/g_{TOC}$, (i) crenarchaeol concentration in $\mu g/g_{TOC}$, (j) calculated terrestrial TOC (terr. TOC) based on $\delta^{13}C_{org}$ in%, (k) river discharge (Q) in m^3/s, and (l) suspended sediment concentration (SSC) in mg/l. The hourly data of Têt River discharge are the sum of the water discharge at the "Joffre" hydrologic station (code Y047030) and the Basse River, a small affluent (code Y0475610) obtained from the "HYDRO" data bank hosted at the French Ministry of Environment. Filled diamonds indicate the data for the core top sample taken in the Têt prodelta at 20 m water depth on 28 April 2004. Note that the *y* axis of $\delta^{13}C_{org}$ is inverted.

sediment was dominated by *n*-C_{29}. The average chain-length of the range of C_{27}–C_{31} *n*-alkanes (ACL_{27-31}) showed quite stable values of around 29. The summed C_{27} to C_{31} *n*-alkane concentrations (ΣALK_{27-31}) varied between 200 and 3200 $\mu g/g_{TOC}$.

[21] As expected, the BIT index from these soils and the riverbed sediment were close to 1 (Table 2 and Figure 2a). The concentrations of branched GDGTs ranged between 22 and 184 $\mu g/g_{TOC}$, while the concentrations of crenarchaeol varied between 0.2 and 1.4 $\mu g/g_{TOC}$.

4.2. Time Series of Têt Prodelta Surface Sediments

[22] The TOC contents of the surface sediments at the Têt buoy site were relatively low between 0.2 and 0.6 wt.% (Figure 3a). However, substantially higher TOC contents were observed in the sediments sampled in December 2003 and February 2004, containing 1.7 and 1.5 wt.% of TOC, respectively. In contrast to TOC, the C/N ratios of surface sediments strongly fluctuated between 5.9 and 21.6 (Figure 3b). Interestingly, the sediments with enhanced TOC had lower C/N ratios compared to those from other periods. The $\delta^{13}C_{org}$ values ranged from −26.0 to −22.8‰, with the ^{13}C depleted values in the TOC-rich sediments (Figure 3c).

[23] The total lipid concentrations of the surface sediments varied between 0.1 and 1.6 mg/g_{sed}, with the highest concentration in the TOC-rich sediment taken in December 2003 (Figure 3d). The CPI_{27-31} of the *n*-alkanes ranged from 3 and 10 (Figure 3e). Two sediments sampled in March and June 2004 had the *n*-C_{31} as the most dominant *n*-alkane, whereas distributions in all other samples were dominated by the *n*-C_{29} (Table 2). However, the differences in the abundances of *n*-C_{31} and *n*-C_{29} in the surface sediments where *n*-C_{31} was dominating were very small. This was reflected in the ratio of the *n*-C_{31} to the *n*-C_{29} alkane (31/(29+31)), which showed no substantial changes over time (Table 2). The ACL_{27-31} showed quite stable values of around 29 (Table 2). The ΣALK_{27-31} varied between 50 and 660 $\mu g/g_{TOC}$ (Figure 3f).

[24] The BIT index for the surface sediments from the Têt buoy site varied between 0.12 and 0.52, showing higher values in the TOC-rich sediments obtained in December 2003 and February 2004 (Figure 3g). The concentration of branched GDGTs ranged between 0.02 and 10 $\mu g/g_{TOC}$ (Figure 3h),

while that of crenarchaeol varied between 0.1 and 17 $\mu g/g_{TOC}$ (Figure 3i). Branched GDGTs were strongly enhanced in the TOC-rich sediments sampled in December 2003 and February 2004. Clear systematic seasonal patterns were not observed in the BIT index as well as in the concentrations of crenarchaeol and branched GDGTs.

4.3. Têt and Rhône Transects

4.3.1. Têt Transect

[25] The TOC contents of the surface sediments from the Têt transect generally varied between 0.3 and 1.0 wt.% (Figure 4a), with higher values offshore than around the prodelta (except at station 34bis). The C/N ratios fluctuated between 10.4 and 24.8, with the highest value in the Têt prodelta (Figure 4b). The $\delta^{13}C_{org}$ values generally increased seaward from −24.4 to −22.4‰ (Figure 4c).

[26] The CPI_{27-31} ranged from 3.1 to 9.3 and decreased substantially with increasing distance from the coast (Figure 4d). *n*-C_{29} was the most abundant sedimentary *n*-alkanes in the prodelta and shelf sediments, whereas in the canyon samples *n*-C_{31} was slightly more abundant (Table 2). This was reflected in the 31/(29+31) ratio, showing slightly increased values with increasing distances from the coast. The ACL_{27-31} showed quite stable values between 29 and 30 with perhaps a slight seaward increase. The ΣALK_{27-31} in the Têt transect remained fairly constant between 50 and 90 $\mu g/g_{TOC}$ (Figure 4e).

[27] The BIT index varied between 0.02 and 0.27, showing a decreasing trend from the Têt prodelta to the Lacaze–Duthiers Canyon (Figure 4f). The concentrations of branched GDGTs ranged between 1.4 and 11 $\mu g/g_{TOC}$ and, in contrast to the BIT index, showed a less clear trend (Figure 4g). The concentrations of crenarchaeol varied more widely between 15 and 95 $\mu g/g_{TOC}$ but again with no particular trend (Figure 4h).

4.3.2. Rhône Transect

[28] The TOC contents of the surface sediments of the Rhône transect abruptly decreased seaward, ranging from 1.8 wt.% in the Rhône prodelta to 0.7 wt.% in the Grand Rhône Canyon (Figure 4j). The C/N ratios showed the same pattern, decreasing from 14.8 to 10.1 toward the Grand Rhône Canyon (Figure 4k) as well as the $\delta^{13}C_{org}$ values which increased from −25.9 to −22.5‰ (Figure 4l).

[29] The CPI_{27-31} sharply decreased from 8.8 to 3.4 with increasing water depths (Figure 4m). The 31/(29+31) ratio and the ACL_{27-31} increased slightly seaward similar to what was observed for the Têt transect (Table 2). The ΣALK_{27-31} in the Rhône transect showed an abrupt shift from the prodelta area (270 $\mu g/g_{TOC}$) to the Grand Rhône Canyon (110 $\mu g/g_{TOC}$) (Figure 4n).

[30] The BIT index ranged from 0.83 to 0.02, with a substantial decrease from the Rhône prodelta to the Grand Rhône Canyon (Figure 4o). The concentrations of branched GDGTs ranged between 0.6 and 15 $\mu g/g_{TOC}$, with the highest concentration in the prodelta (Figure 4p). The concentrations of crenarchaeol showed an opposite pattern compared to that of branched GDGTs, i.e., with low concentrations in the sediments of the prodelta (~2.8 $\mu g/g_{TOC}$) and higher concentrations offshore (54 $\mu g/g_{TOC}$; Figure 4q).

5. Discussion

5.1. Bulk Proxies for Transport of Terrestrial OM to the Marine Environment

[31] Higher plant-derived OM is characterized by a higher C/N ratio (e.g., >20 [*Meyers and Ishiwatari*, 1993]) than that of OM derived from marine organisms (6 to 9 [*Müller*, 1977]) as terrestrial OM contains a higher percentage of nonprotein materials. Due to humification and mineralization of plant litter in soils, C/N ratios of soil OM are typically lower compared to vascular plants, varying between 8 and 20 [e.g., *Hedges and Oades*, 1997]. The C/N ratios of the investigated soils are well within the range cited above except the sample SO-LB2-T. The relatively high C/N ratio (56.2) of the sample SO-LB2-T can be attributed to the high abundance of nondegraded plant roots. The $\delta^{13}C_{org}$ of higher plants that use the Calvin-Benson cycle of carbon fixation (i.e., so-called C_3 plants) ranges from −29.3 to −25.5‰, with an average value of about −27‰ [e.g., *Fry and Sherr*, 1984; *Tyson*, 1995; *Meyers*, 1997]. The $\delta^{13}C_{org}$ values (−28.7 to −25.7‰) of the investigated soils near the Têt River are typical of C_3 vegetation. Consequently, our data indicate that soil OM was primarily derived from C_3 plants, and it is thus likely that C_3-derived soil OM is the dominant OM contribution to fine fractions (<63 μm) of riverbed sediments. Indeed, the riverbed sample RBS-ST1 showed low C/N ratio (10.5) and low $\delta^{13}C_{org}$ (−27‰).

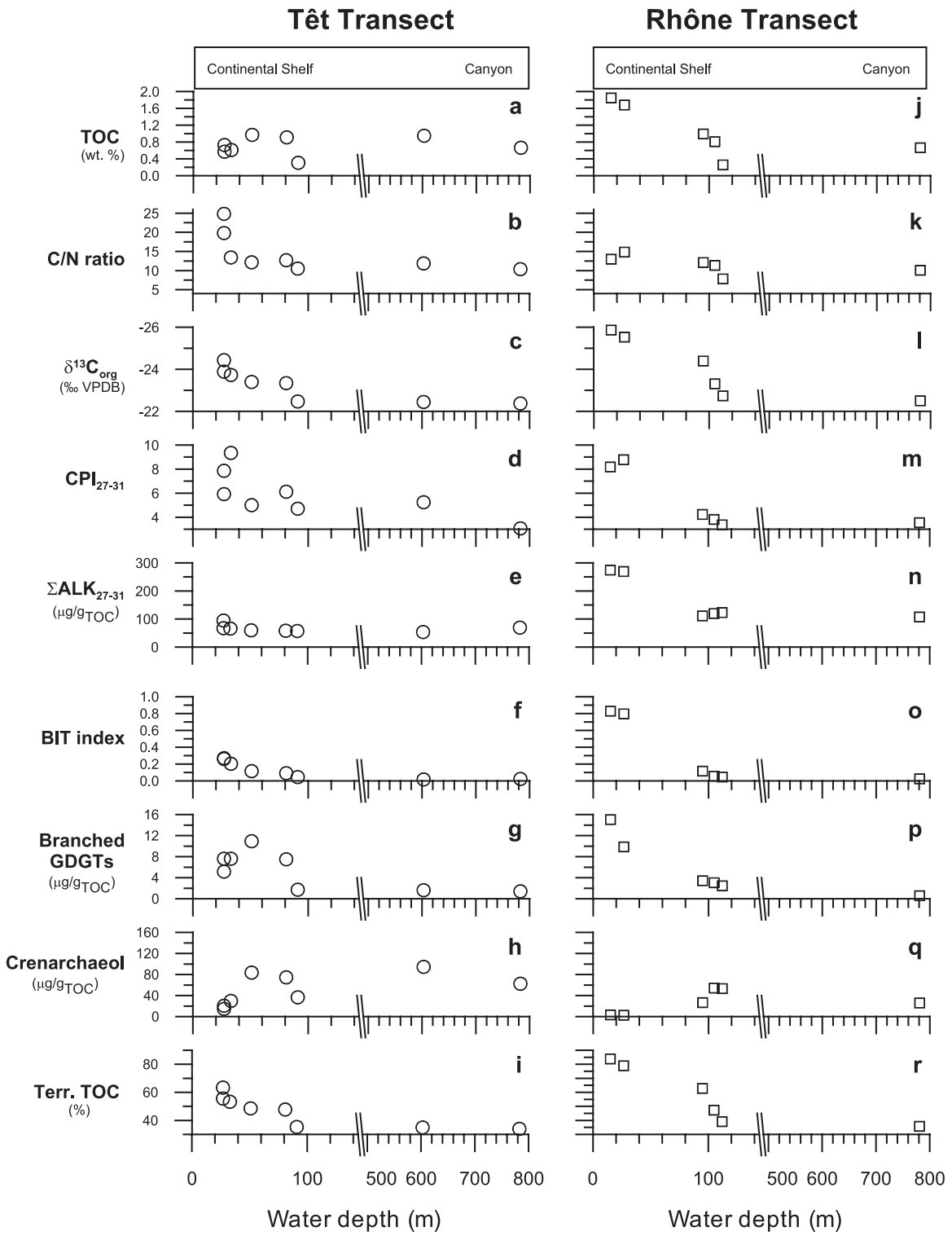

Figure 4. Results of bulk sediment and lipid analyses from transect surface sediments: (a) TOC contents in wt.%, (b) C/N ratio, (c) $\delta^{13}C_{org}$ in ‰, (d) CPI_{27-31}, (e) ΣALK_{27-31} in mg/g_{TOC}, (f) BIT index, (g) sum of branched GDGTs concentration in $\mu g/g_{TOC}$, (h) crenarchaeol concentration in $\mu g/g_{TOC}$, and (i) calculated terrestrial TOC (terr. TOC) based on $\delta^{13}C_{org}$ in % are for the Têt transect, while (j) TOC contents in wt.%, (k) C/N ratio, (l) $\delta^{13}C_{org}$ in ‰, (m) CPI_{27-31}, (n) ΣALK_{27-31} in mg/g_{TOC}, (o) BIT index, (p) sum of branched GDGTs concentration in $\mu g/g_{TOC}$, (q) crenarchaeol concentration in $\mu g/g_{TOC}$, and (r) calculated terrestrial TOC based on $\delta^{13}C_{org}$ in % are for the Rhône transect. Note that the y axis of $\delta^{13}C_{org}$ is inverted.

[32] At the Têt buoy site, the significant enhancements of TOC content and total lipid concentration in the sediments sampled in December 2003 and February 2004 (Figure 3) corresponds to lower C/N ratios (5.9 and 11.9) as well as lower $\delta^{13}C_{org}$ values (−26.0 and −25.1‰). The C/N ratio is closer to a marine value than most other samples from this time series, suggesting an increased marine OM input. However, the $\delta^{13}C_{org}$ value indicates the opposite. Considering that soil OM can have similar a C/N ratio as marine OM and C/N ratios around 10–12 are commonly found in total suspended solids of the Têt River during floods (Ludwig, unpublished results), our data suggest that terrestrial OM input was enhanced and soil OM was dominant rather than vascular plant detritus. On the basis of the $\delta^{13}C_{org}$ values (Table 2), the TOC contents of surface sediments were separated into a marine and terrestrial portion. We estimated the portions of marine and terrestrial OM with a simple binary mixing model, assuming terrestrial ($\delta^{13}C_{terr} = -27‰$) and marine ($\delta^{13}C_{mar} = -20‰$) OM end-members [e.g., *Meyers*, 1994, 1997]:

$$TOC = OM_{mar} + OM_{terr}$$

$$\delta^{13}C_{org} * TOC = \delta^{13}C_{mar} * OM_{mar} + \delta^{13}C_{terr} * OM_{terr}$$

where OM_{mar} and OM_{terr} are the contents of marine and terrestrial OM, and $\delta^{13}C_{mar}$ and $\delta^{13}C_{terr}$ are the isotopic compositions of marine and terrestrial OM, respectively. The estimated contribution of terrestrial OM was much higher for the TOC-rich sediments sampled in December 2003 and February 2004, corresponding to 86% and 73% of TOC, respectively (Figure 3j), while TOC was estimated to contain 50% terrestrial OM on average during the other periods.

[33] The prodelta sediments from the Têt transect (Figure 4) showed similar TOC contents, C/N ratios, and $\delta^{13}C_{org}$ values as those from the Têt prodelta time series during "low TOC" periods (i.e., all samples except those taken in December 2003 and February 2004; Figure 3). Interestingly, the TOC contents were slightly higher in the mid shelf than in the prodelta across the Têt transect, while the estimated terrestrial OM, based on $\delta^{13}C_{org}$, remained more or less at the same level (Figure 4i). The canyon sediments showed similar TOC contents, and C/N ratios, compared to those from the prodelta, but lower $\delta^{13}C_{org}$ values and thus lower estimated terrestrial OM portions. This suggests that contribution of marine OM is enhanced in the mid shelf and the canyon.

[34] All bulk parameters from the Rhône transect showed a distinctive difference between the prodelta and the mid shelf as well as the canyon (Figure 4). OM in the Rhône prodelta sediments showed C/N ratios >13 and $\delta^{13}C_{org}$ values of approximately −26.0‰. This indicates a substantial contribution of soil OM originating from C_3 plants as illustrated in a scatterplot for the C/N ratio and the $\delta^{13}C_{org}$ (Figure 5a). The calculated contribution of terrestrial OM based on the two end-member isotopic mixing model corresponds to 79–84% (Figure 4r). The estimated terrestrial TOC portions of the mid shelf and canyon sediments were much lower than those in the prodelta, decreasing from 63% to 36% offshore. This suggests that terrestrial OM in the mid shelf and the canyon is substantially diluted by increased marine OM contributions or that less soil OM reaches the mid shelf to the canyon.

5.2. Molecular Proxies for Transport of Terrestrial OM to the Marine Environment

[35] The presence of C_{27}, C_{29}, and C_{31} *n*-alkanes is evidence for an origin of predominantly epicuticular waxes of higher plants [*Eglinton and Hamilton*, 1967], whereas aquatic algal and photosynthetic bacterial contributions are indicated by the presence of *n*-C_{17} alkane [e.g., *Cranwell et al.*, 1987]. Epicuticular waxes derived from higher plants generally have high (>5) CPI values [e.g., *Eglinton and Hamilton*, 1963; *Mazurek and Simoneit*, 1984], while marine- and petroleum-derived *n*-alkanes have a CPI of 1 [*Simoneit*, 1984]. Therefore the predominance of C_{27}, C_{29}, and C_{31} *n*-alkanes and the high CPI values in the terrestrial samples (CPI > 8) as well as in the marine sediments of the Gulf of Lions (CPI > 3) indicate that *n*-alkanes are predominantly derived from terrestrial sources, i.e., land-plant epicuticular waxes. This is consistent with previous results by *Bouloubassi et al.* [1997]. Small variations in 31/(29+31) and ACL_{27-31} through the whole sample series investigated imply no significant changes in terrestrial OM sources. Terrestrial *n*-alkanes in marine sediments can be derived from either contemporary vascular plant leaves or *n*-alkanes from soils [e.g., *Eglinton et al.*, 1997; *Pearson and Eglinton*, 2000]. In our data set, the enhanced *n*-alkane concentrations in the Rhône prodelta were accompanied by depleted $\delta^{13}C_{org}$ values and low

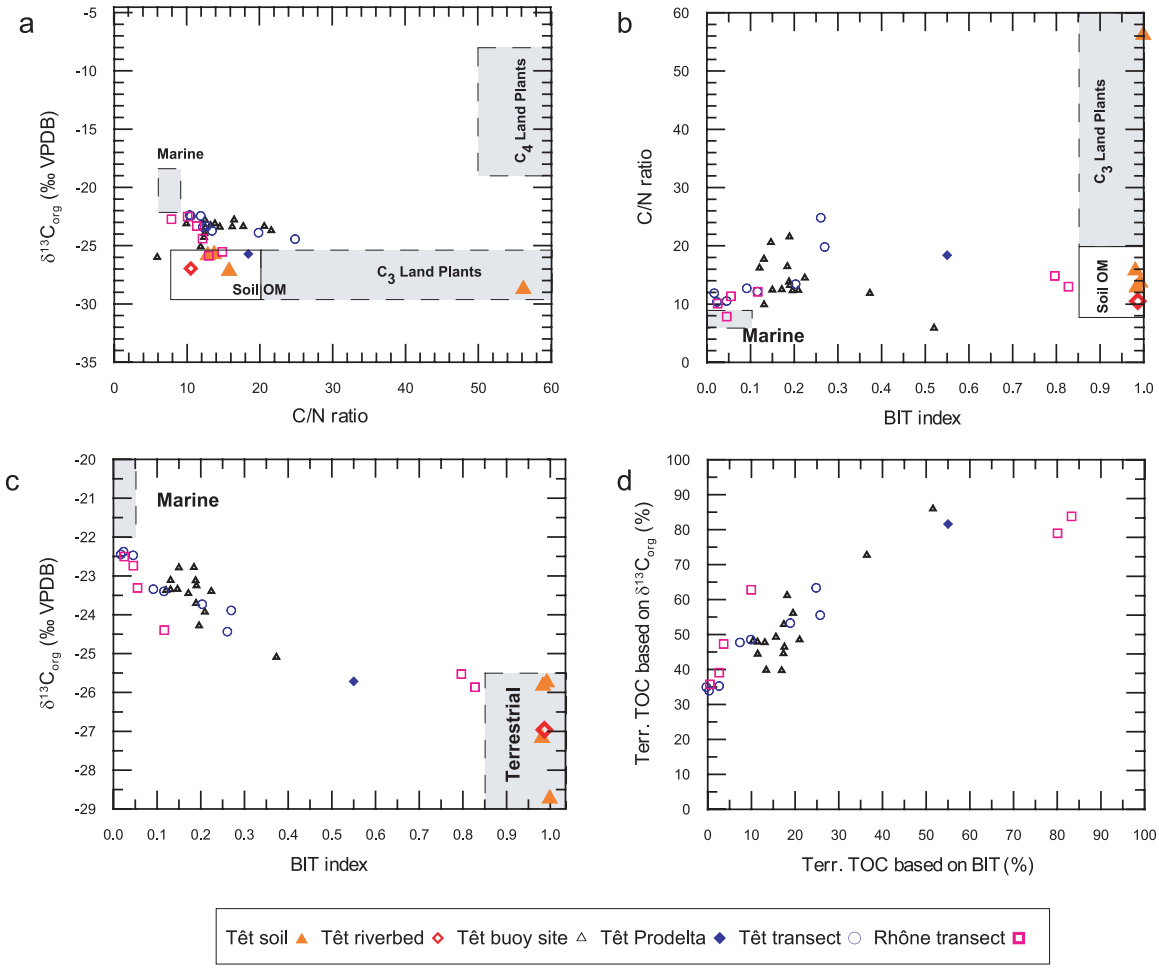

Figure 5. Scatterplots for (a) $\delta^{13}C_{org}$ and C/N ratio (boundaries of major OM sources are according to *Müller* [1977], *Sackett* [1989], *Meyers and Ishiwatari* [1993], *Meyers* [1994], *Tyson* [1995], and *Hedges and Oades* [1997]), (b) BIT index and C/N ratio, (c) BIT index and $\delta^{13}C_{org}$, and (d) calculated terrestrial TOC percentages based on $\delta^{13}C_{org}$ and BIT index.

C/N ratios (<20). This suggests that the contribution of *n*-alkanes derived from soils is more important than from contemporary vascular plant leaves in the Gulf of Lions, which could be dispersed by wind over much larger distances [e.g., *Pancost and Boot*, 2004].

[36] As expected [cf. *Hopmans et al.*, 2004], high abundances of branched GDGTs were measured in the soils and the riverbed sediment and thus the BIT indices showed values close to 1 (Table 2). Interestingly, crenarchaeol was also found in those samples, although its concentration was much lower than that of branched GDGTs (Table 2). Crenarchaeol was initially considered to be exclusively produced by nonthermophilic marine planktonic Crenarchaeota [*Sinninghe Damsté et al.*, 2002b], but it was also recently found in lake sediments [*Powers et al.*, 2004], peats [*Weijers et al.*, 2004], soils [*Weijers et al.*, 2006b], and river water [*Herfort et al.*, 2006] albeit in relatively low concentrations. Crenarchaeol was also identified in Nevada hot springs having pHs between 6.0 and 9.2 and temperatures between 40 and 84°C [*Pearson et al.*, 2004]. Accordingly, our results along with the previous observations imply that crenarchaeol is not a biomarker exclusively produced in marine environments. The identification of crenarchaeol in terrestrial environments is consistent with molecular ecological work showing that nonthermophilic crenarchaeota are present in soils [e.g., *Buckley et al.*, 1998], lake systems [e.g., *Keough et al.*, 2003], and rivers [e.g., *Abreu et al.*, 2001; *Wells et al.*, 2006]. However, compared to marine environments [e.g., *Karner et al.*, 2001], the amounts of Crenarchaeota found on land are relatively low [e.g., *Buckley et al.*, 1998]. Therefore we may

expect the amount of crenarchaeol produced by terrestrial Crenarchaeota to be much lower than that by marine Crenarchaeota. However, the concentrations of crenarchaeol from the terrestrial samples (0.2 to 1.4 $\mu g/g_{TOC}$) investigated in this study were in some cases higher than those from marine samples (0.1 to 95 $\mu g/g_{TOC}$). In contrast, the concentrations of branched GDGTs in the soils from the Têt River catchments were much higher (22 to 184 $\mu g/g_{TOC}$) than that from marine environments (0.16 to 15 $\mu g/g_{TOC}$). Consequently, the BIT values were well below 1 in marine environments and usually much lower than in terrestrial environments. One concern related to the lower concentrations of crenarchaeol in the time series of Têt prodelta surface sediments compared to the terrestrial samples (only in some cases) is that possible selective degradations of branched GDGTs after entering into marine environments may bias the BIT index, causing lower values and thus misleading as higher marine OM input. A recent study by *Schouten et al.* [2004] showed that the different isoprenoidal GDGT isomers degraded at similar rates. Therefore we expect that crenarchaeol and branched GDGTs which have a similarly functionalized chemical structure are likely to be degraded at similar rates during sediment diagenesis [*Hopmans et al.*, 2004]. Nevertheless, degradation impacts on the BIT index should be tested in near future to better assess the robustness of this index.

[37] The BIT index was compared with the C/N ratio and the $\delta^{13}C_{org}$, widely used bulk proxies to trace sources of OM in marine sediments (Figures 5b and 5c). The C/N ratios and the BIT values do not show a linear relationship (Figure 5b). This may be attributed to the fact that the C/N ratio can be strongly affected by diagenesis and that it characterizes not just two end-members (marine versus terrestrial) in our study area. Indeed, different terrestrial OM sources (e.g., higher land plant detritus and soils) complicate the interpretation of this proxy as C/N ratios from soils can be similar to those from marine sources (see Figure 5a). When all the BIT values generated in this study are compared with $\delta^{13}C_{org}$ values, a strong correlation is visible (Figure 5c). $\delta^{13}C_{org}$ values of soil OM depend on the soil sources of C_3 or C_4 plants and are generally higher compared to those of vascular plants due to humification and mineralization of plant litter in soils [e.g., *Mariotti and Peterschmitt*, 1994]. The $\delta^{13}C_{org}$ values of the investigated soils lie well within the range representative of C_3 vegetation (Figure 5a). The $\delta^{13}C$ values of the *n*-alkanes in the soils and the marine sediments varied between −30 and −35‰ (unpublished data), supporting a predominant origin from C_3 plants for the terrestrial OM. Accordingly, $\delta^{13}C_{org}$ in marine sediments in the Gulf of Lions is affected by mixing of marine OM with C_3-plant derived terrestrial OM originating from or higher land plants or soil OM. The good correlation between $\delta^{13}C_{org}$ and BIT index, a proxy of soil-derived terrestrial OM input, is probably due to the high proportion of soil OM in marine sediments.

[38] Similar to the calculation of terrestrial OM based on the $\delta^{13}C_{org}$ values, we estimated the portions of marine and terrestrial OM, assuming terrestrial (BIT_{terr} = 0.99) and marine (BIT_{mar} = 0.02) OM end-members (Table 2). The estimated contributions of terrestrial OM based on the BIT indices ranged from 0 to 83%, showing generally lower percentages compared to those based on the $\delta^{13}C_{org}$ values (Figure 5d). Part of this discrepancy may lie in the assumed end-member values for $\delta^{13}C_{org}$. For example, if we assume that the marine end-member is −21‰ instead of −20‰ then this will substantially lower the terrestrial OC estimates. Nevertheless, both methods showed the same trends and a strong positive correlation to each other. This strongly suggests that the $\delta^{13}C_{org}$ and the BIT index are overall better proxies than the C/N ratio to assess terrestrial OM input into the Gulf of Lions. Furthermore, this study shows that the BIT index, in combination with other proxies, provides a good constraint for the relative estimation of soil-derived terrestrial OM amount in marine surface sediments.

[39] The elevated *n*-alkane concentrations in our data set were positively correlated with higher BIT values. In general, *n*-alkanes are transported by river runoff or by wind to marine environments and are therefore less specific for fluvial OM inputs [e.g., *Pancost and Boot*, 2004]. Nevertheless, the sharp increase of ΣALK_{27-31} in the Têt prodelta time series (Figure 3) and an abrupt shift of ΣALK_{27-31} in the Rhône transect (Figure 4) indicate that in this coastal setting fluvial transports of *n*-alkanes seem to be much more important than aeolian *n*-alkane inputs. A positive relationship between the *n*-alkane concentrations and the BIT values further supports the fluvial input of *n*-alkanes to TOC in marine sediments in the Gulf of Lions. Moreover, the rather stable 31/(29+31) ratio and ACL values suggest a similar constant terrestrial OM sources. Saharan dust is a major source of atmospheric particulate input in the

Mediterranean Sea [*Löye-Pilot and Martin*, 1996]. In the sparse vegetation of the Sahara, C_4 plants (e.g., halophytes and other herbs) are dominant [e.g., *Ehleringer et al.*, 1977]. Therefore C_4 plant signals (*n*-alkane $\delta^{13}C$: −17 to −24‰ [e.g., *Schefuß et al.*, 2003; *Bendle et al.*, 2006]) are representative as atmospheric terrestrial OM inputs from the African continent. Our preliminary *n*-alkane $\delta^{13}C$ results (−30 to −35‰) suggest that terrestrial OMs were predominantly transported by rivers into the Gulf of Lions.

5.3. Origin and Distribution of OM in the Gulf of Lions

[40] River floods and storm waves are major processes for the deposition and dispersal of terrestrial OM in modern, river-dominated coastal oceans. A "wet storm" is connected to a flood with a high river discharge, while a "dry storm" is without significant river runoff [*Ogston et al.*, 2000]. During wet storms, enhanced riverine suspended materials can form a fine-grained flood deposit on continental shelves [*Mullenbach and Nittrouer*, 2000].

[41] In the Têt prodelta surface sediment time series, the highest BIT values were obtained in the TOC-rich sediments sampled in December 2003 and February 2004. This was accompanied by lower $\delta^{13}C_{org}$ and by higher *n*-alkane and branched GDGT concentrations. Therefore all bulk and molecular proxies (Figure 3) suggest that terrestrial OM proportions were enhanced in the sediments sampled in December 2003 and February 2004. The increased terrestrial OM signals in the Têt prodelta surface sediment time series correspond well to the high Têt River discharge (Q = ~400 m^3/s, Figure 3k) and high suspended sediment concentration (SSC = ~700 mg/l; Figure 3l) during the December wet storm in 2003 [*Guillen et al.*, 2006]. It is likely that this event resulted in significant soil erosion, transporting soil OM including soil-derived branched GDGTs via the Têt River to the Têt prodelta.

[42] The wet storm in April 2004 was accompanied by the highest Têt River discharge (660 m^3/s) and the highest SSC (1000 mg/l) within the time frame of this study (Figure 3). Interestingly, the surface sediments recovered after this wet storm did not show enhanced terrestrial OM signal. In contrast, the core collected at 20 m water depth on the 28 April 2004 near to the Têt buoy site did show an increased TOC content (1.4 wt%), lower $\delta^{13}C_{org}$ value (−25.7‰), and higher ΣALK_{27-31} (470 $\mu g/g_{TOC}$) and BIT (0.55) values, all suggesting an increased terrestrial OM deposit (Table 2 and Figure 3). This suggests that the Têt River flood plume in April 2004 did not reach the Têt buoy site (28 m water depth) but was limited to the nearshore (at least up to 20 m water depth) and further propagated along the coast. This further implies that, besides river discharge amounts, hydrodynamics processes are foremost important for the transport and deposition of river-derived OM in the coastal zones.

[43] In the sediments of the cross-shelf transects, higher BIT values were recorded in the Rhône prodelta, accompanied by higher TOC contents, lower $\delta^{13}C_{org}$, and higher *n*-alkane concentration. Accordingly, higher BIT values in marine sediments are in accordance with other bulk parameters, suggesting enhanced terrestrial OM inputs to marine environments. The BIT values from the Rhône prodelta are higher compared to those from the Têt prodelta. This is probably due to much larger water discharge, resulting from its much larger drainage basin and thus high mean sediment input from the Rhône River to the shelf. This is in agreement with the particularly high sediment accumulation rates (>20 cm/yr) in the Rhône prodelta [*Radakovitch et al.*, 1999]. The low BIT values of the surface sediments in the canyons, along with enhanced $\delta^{13}C_{org}$, indicate that terrestrial OM was not deposited there or only temporarily. This supports the idea that upper canyons (300–800 m water depth) are by-pass conduits rather than terrestrial OM accumulation zones [e.g., *Monaco et al.*, 1990; *Durrieu de Madron*, 1994; *Buscail and Germain*, 1997].

[44] This study thus suggests that the BIT index is a useful proxy to trace floods and storm events in river dominated continental margins. Further work is necessary to better constrain different origins of terrestrial OM deposited in the Gulf of Lions and thus to better understand sediment depositional and transport processes from the rivers across canyons to open oceans.

6. Conclusions

[45] Branched GDGTs as well as crenarchaeol were detected in all soil samples surveyed in this study. The BIT index from terrestrial samples shows high values (>0.9), while it varies between 0.02 and 0.83 in marine environments, decreasing seaward from the inner shelf to the slope. For marine surface sediments, higher BIT values are

associated with lower $\delta^{13}C_{org}$ values as well as higher TOC contents and higher *n*-alkane concentrations, suggesting higher portion of terrestrial OM in sediments. These results support the idea that the BIT index can be applied in marine environments in order to characterize terrestrial OM as proposed by *Hopmans et al.* [2004] and hence to estimate the relative terrestrial OM amount in marine sediments. Furthermore, our study shows that soil OM along with contemporary vascular land plant detritus has an important contribution to TOC in marine sediments in the Gulf of Lions. The BIT index along with the concentration of branched GDGTs can serve as indicators for soil-derived terrestrial OM input to continental margins.

Acknowledgments

[46] We would like to thank G. Jeanty, J. Carbonne, and N. Delsaut at CEFREM and M. Woltering and J. Ossebaar at NIOZ for sample preparation and analytical support and E. Hopmans for assistance with the HPLC/APCI-MS. We are also grateful to V. Roussiez for kindly supplying shelf sediments collected during the REMORA 3 cruise organized by M. Arnaud from IRSN (La Seyne-sur-mer, France) as well as to L. Herfort, J. W. H. Weijers, S. Heussner, and X. Durrieu de Madron for fruitful discussions.

References

Abreu, C., G. Jurgens, P. De Marco, A. Saano, and A. A. Bordalo (2001), Crenarchaeota and Euryarchaeota in temperate estuarine sediments, *J. Appl. Microbiol.*, *90*, 713–718.

Arnau, P., C. Liquete, and M. Canals (2004), River mouth plume events and their dispersal in the northwestern Mediterranean Sea, *Oceanography*, *17*, 22–31.

Barnes, H., and J. Blackstock (1973), Estimation of lipids in marine animals and tissue: Detailed investigations of the sulfovanilin method for total lipids, *J. Exp. Mar. Biol. Ecol.*, *12*, 103–118.

Bendle, J. A., K. Kawamura, and K. Yamazaki (2006), Seasonal changes in stable carbon isotopic composition of n-alkanes in the marine aerosols from the western North Pacific: Implications for the source and atmospheric transport, *Geochim. Cosmochim. Acta*, *70*, 13–26.

Bouloubassi, I., E. Lipiatou, A. Saliot, I. Tolosa, J. M. Mayona, and J. Albaigés (1997), Carbon sources and cycle in the western Mediterranean: The use of molecular markers to determine the origin of organic matter, *Deep Sea Res., Part II*, *44*, 781–799.

Brassell, S. C. (1993), Applications of biomarkers for delineating marine paleoclimatic fluctuations during the Pleistocene, in *Organic Geochemistry: Principles and Applications*, edited by M. H. Engel and S. A. Macko, pp. 699–783, Springer, New York.

Buckley, D. H., J. R. Graber, and T. M. Schmidt (1998), Phylogenetic analysis of non-thermophilic members of the kingdom Crenarchaeota and their diversity and abundance in soils, *Appl. Environ. Microbiol.*, *64*, 4333–4339.

Buscail, R., and C. Germain (1997), Present-day organic matter sedimentation on the Northwestern Mediterranean margin: Importance of off-shelf export, *Limnol. Oceanogr.*, *42*, 217–229.

Buscail, R., R. Pocklington, R. Daumas, and L. Guidi (1990), Fluxes and budget of organic matter in the benthic boundary layer over the northwestern Mediterranean margin, *Cont. Shelf Res.*, *10*, 1089–1122.

Buscail, R., R. Pocklington, and C. Germain (1995), Seasonal variability of the organic matter in a sedimentary coastal environment: Sources, degradation and accumulation (continental shelf of the Gulf of Lions-Northwestern Mediterranean Sea), *Cont. Shelf Res.*, *15*, 843–869.

Cauwet, G., F. Gadel, M. M. De Souza Sierra, O. Donard, and M. Ewald (1990), Contribution of the Rhône river to organic carbon inputs to the northwestern Mediterranean Sea, *Cont. Shelf Res.*, *10*, 1025–1037.

Courp, T., and A. Monaco (1990), Sediment dispersal and accumulation on the continental margin of the Gulf of Lions: Sedimentary budget, *Cont. Shelf Res.*, *10*, 1063–1087.

Cranwell, P. A., G. Eglinton, and N. Robinson (1987), Lipids of aquatic organisms as potential contributors to lacustrine sediments, *Org. Geochem.*, *11*, 513–527.

Delille, D., L. Guidi, and G. Cahet (1990), Temporal variations of benthic bacterial microflora on the Northwestern Mediterranean continental shelf and slope, *Mar. Ecol.*, *11*, 105–115.

Durrieu de Madron, X. (1994), Hydrography and nepheloid structures in the Grand Rhone canyon, *Cont. Shelf Res.*, *14*, 457–477.

Durrieu de Madron, X., O. Radkovitch, S. Heussner, M. D. Loye-Pilot, and A. Monaco (1999), Role of the climatological and current variability on shelf-slope exchanges of particulate matter: Evidence from the Rhône continental margin (NW Mediterranean), *Deep Sea Res., Part I*, *46*, 1513–1538.

Durrieu de Madron, X., A. Abassi, S. Heussner, A. Monaco, J. C. Aloisi, O. Radakovitch, P. Giresse, R. Buscail, and P. Kerherve (2000), Particulate matter and organic carbon budgets for the Gulf of Lions (NW Mediterranean), *Oceanol. Acta*, *23*, 717–730.

Eglinton, G., and R. J. Hamilton (1963), The distribution of alkanes, in *Chemical Plant Taxonomy*, edited by T. Swain, pp. 187–208, Elsevier, New York.

Eglinton, G., and R. J. Hamilton (1967), Leaf epicuticular waxes, *Science*, *156*, 1322–1335.

Eglinton, T. I., B. C. Benitez-Nelson, A. Pearson, A. P. McNichol, J. E. Bauer, and E. R. M. Druffel (1997), Variability in radiocarbon ages of individual organic compounds from marine sediments, *Science*, *277*, 796–799.

Ehleringer, J. R., T. E. Cerling, and B. R. Helliker (1977), C_4 photosynthesis, atmospheric CO_2, and climate, *Oecologia*, *112*, 285–299.

Fry, B., and E. B. Sherr (1984), $\delta^{13}C$ measurements as indicators of carbon flow in marine and freshwater ecosystems-*Contrib. Mar. Sci.*, *27*, 13–47.

Guidi-Guilvard, L. D., and R. Buscail (1995), Seasonal survey of metazoan meiofauna and surface sediment organics in a non-tidal turbulent sublittoral prodelta (NW Mediterranean), *Cont. Shelf Res.*, *15*, 633–653.

Guillen, J., F. Bourrin, A. Palanques, X. Durrieu DeMadron, P. Puig, and R. Buscail (2006), Sediment dynamics during "wet" and "dry" storm events on the Têt inner shelf (SW Gulf of Lions), *Mar. Geol.*, in press.

Hedges, J. I., and J. M. Oades (1997), Comparative organic geochemistries of soils and marine sediments, *Org. Geochem.*, *27*, 319–361.

Herfort, L., S. Schouten, J. P. Boon, M. Woltering, M. Baas, J. W. H. Weijers, and J. S. Sinninghe Damsté (2006), Characterization of transport and deposition of terrestrial organic matter in the southern North Sea using the BIT index, *Limnol. Oceanogr.*, *51*, 2196–2205.

Hopmans, E. C., S. Schouten, R. D. Pancost, M. T. J. van der Meer, and J. S. Sinninghe Damsté (2000), Analysis of intact tetraether lipids in archaeal cell material and sediments by high performance liquid chromatography/atmospheric pressure chemical ionization mass spectrometry, *Rapid Commun. Mass Spectrom.*, *14*, 585–589.

Hopmans, E. C., J. W. H. Weijers, E. Schefuß, L. Herfort, J. S. Sinninghe Damsté, and S. Schouten (2004), A novel proxy for terrestrial organic matter in sediments based on branched and isoprenoidtetraether lipids, *Earth Planet. Sci. Lett.*, *224*, 107–116.

Karner, M. B., E. F. DeLong, and D. F. Karl (2001), Archaeal dominance in the mesopelagic zone of the Pacific Ocean, *Nature*, *409*, 507–510.

Keough, B. P., T. M. Schmidt, and R. E. Hicks (2003), Archaeal nucleic acids in picoplankton from Great Lakes on three continents, *Microbiol. Ecol.*, *46*, 238–248.

Kerhervé, P., S. Minagawa, S. Heussner, and A. Monaco (2001), Stable isotopic (δ^{13}C and δ^{15}N) in settling organic matter of the Northwestern Mediterranean Sea: Biogeochemical implications, *Oceanol. Acta*, *24*, 77–85.

Kolattukudy, P. E. (1976), *The Chemistry and Biochemistry of Natural Waxes*, Elsevier, New York.

Liquete, C., M. Canals, P. Arnau, R. Urgeles, and X. Durrieu de Madron (2004), The impact of humans on strata formation along Mediterranean margins, *Oceanography*, *17*, 42–51.

Loÿe-Pilot, M. D., and J. M. Martin (1996), Saharan dust input to the Western Mediterranean sea: An eleven year record in Corsica, in *The Impact of Desert Dust Across the Mediterranean*, edited by S. Guerzoni and R. Chester, pp. 191–199, Springer, New York.

Ludwig, W., M. Meybeck, and F. Abousamra (2003), Riverine transport of water, sediments, and pollutants to the Mediterranean Sea, *UNEP MAP Tech. Rep. Ser. 141*, 111 pp., United Nations Environ. Programme/Mediter. Action Plan, Athens.

Ludwig, W., P. Serrat, L. Cesmat, and J. Garcia-Esteves (2004), Evaluating the impact of the recent temperature increase on the hydrology of the Têt River (Southern France), *J. Hydrol.*, *289*, 204–221.

Mariotti, A., and E. Peterschmitt (1994), Forest savanna ecotone dynamics in India as revealed by carbon isotope ratios of soil organic matter, *Oecologia*, *97*, 475–480.

Mazurek, M. A., and B. R. T. Simoneit (1984), Characterization of biogenic and petroleum-derived organic matter in aerosols over remote, rural and urban areas, in *Identification and Analysis of Organic Pollutants in Air*, edited by L. H. Keith, pp. 353–370, Elsevier, New York.

Meyers, P. A. (1994), Preservation of source identification of sedimentary organic matter during and after deposition, *Chem. Geol.*, *144*, 289–302.

Meyers, P. A. (1997), Organic geochemical proxies of paleoceanographic, paleolimnologic and paleoclimatic processes, *Org. Geochem.*, *27*, 213–250.

Meyers, P. A., and R. Ishiwatari (1993), Lacustrine organic geochemistry: An overview of indicators of organic matter sources and diagenesis in lake sediments, *Org. Geochem.*, *20*, 867–900.

Middelburg, J. J., and J. Nieuwenhuize (1998), Carbon and nitrogen stable isotopes in suspended matter and sediments from the Schelde Estuary, *Mar. Chem.*, *60*, 217–225.

Millot, C. (1990), The Gulf of Lions' hydrodynamics, *Cont. Shelf Res.*, *10*, 885–894.

Millot, C. (1991), Mesoscale and seasonal variabilities of the circulation in the western Mediterranean, *Dyn. Atmos. Oceans*, *15*, 179–214.

Monaco, A., P. E. Biscaye, J. Soyer, R. Pocklington, and S. Heussner (1990), Particle fluxes and ecosystem response on a continental margin, *Cont. Shelf Res.*, *10*, 809–839.

Monaco, A., X. Durrieu de Madron, O. Radakovitch, S. Heussner, and J. Carbonne (1999), Origin and variability of downward biogeochemical fluxes on the Rhône continental margin (NW Mediterranean), *Deep Sea Res., Part I*, *46*, 1483–1511.

Mullenbach, B. L., and C. A. Nittrouer (2000), Rapid deposition of fluvial sediment in the Eel Canyon, northern California, *Cont. Shelf Res.*, *20*, 2191–2212.

Müller, P. J. (1977), C/N ratios in Pacific deep-sea sediments: Effect of inorganic ammonium and organic nitrogen compounds sorbed by clays, *Geochim. Cosmochim. Acta*, *41*, 765–776.

Ogston, A. S., D. A. Cacchione, R. W. Sternberg, and G. C. Kineke (2000), Observations of storm and river flood-driven sediment transport on the northern California continental shelf, *Cont. Shelf Res.*, *20*, 2141–2161.

Pancost, R. D., and C. S. Boot (2004), The palaeoclimatic utility of terrestrial biomarkers in marine sediments, *Mar. Chem.*, *92*, 239–261.

Pearson, A., and T. I. Eglinton (2000), The origin of n-alkanes in Santa Monica Basin surface sediment: A model based on compound-specific Δ^{14}C and δ^{13}C data, *Org. Geochem.*, *31*, 1103–1116.

Pearson, A., Z. Huang, A. E. Ingalls, C. S. Romanek, J. Wiegel, K. H. Freeman, R. H. Smittenberg, and C. L. Zhang (2004), Nonmarine Crenarchaeol in Nevada hot springs, *Appl. Environ. Microbiol.*, *70*, 5229–5237.

Pont, D., J. P. Simonnet, and A. V. Walter (2002), Medium-term changes in suspended sediment delivery to the ocean: Consequences of catchment heterogeneity and river management (Rhône river, France), *Estuarine Coastal Shelf Sci.*, *54*, 1–18.

Powers, L. A., J. P. Werne, T. C. Johnson, E. C. Hopmans, J. S. Sinninghe Damsté, and S. Schouten (2004), Crenarchaeotal membrane lipids in lake sediments: A new paleotemperture proxy for continental paleoclimate reconstruction, *Geology*, *32*, 613–616.

Radakovitch, O., S. Charmasson, M. Arnaud, and P. Bouisset (1999), ^{210}Pb and caesium accumulation in the Rhone delta sediment, *Estuarine Coastal Shelf Sci.*, *48*, 77–92.

Roussiez, V., W. Ludwig, J. L. Probst, and A. Monaco (2005), Background levels of heavy metals in surficial sediments of the Gulf of Lions (NW Mediterranean): An approach based on ^{133}Cs normalization and lead isotope measurements, *Environ. Pollut.*, *138*, 167–177.

Sackett, W. M. (1989), Stable carbon isotope studies on organic matter in the marine environment, in *Handbook of Environmental Isotope Geochemistry*, edited by P. Fritz and J. C. Fontes, pp. 139–169, Elsevier, New York.

Schefuß, E., V. Ratmeyer, J.-B. W. Stuut, J. H. F. Jansen, and J. S. Sinninghe Damsté (2003), Carbon isotope analyses of *n*-alkanes in dust from the lower atmosphere over the central eastern Atlantic, *Geochim. Cosmochim. Acta*, *67*, 1757–1767.

Schouten, S., E. C. Hopmans, R. D. Pancost, and J. S. Sinninghe Damsté (2000), Widespread occurrence of structurally diverse tetraether membrane lipids: Evidence for the ubiquitous presence of low-temperature relatives of

hyperthermophiles, *Proc. Natl. Acad. Sci. U. S. A.*, *97*, 14,421–14,426.

Schouten, S., E. C. Hopmans, and J. S. Sinninghe Damsté (2004), The effect of maturity and depositional redox conditions on archaeal tetraether lipid palaeothermometry, *Org. Geochem.*, *35*, 567–571.

Sempéré, R., B. Charriere, F. Van Wambeke, and G. Cauwet (2000), Carbon inputs of the Rhone River to the Mediterranean Sea: Biogeochemical implications, *Global Biogeochem. Cycles*, *14*, 669–681.

Serrat, P. (1999), Dynamique sédimentaire actuelle d'un système fluvial méditerranéen: L'Agly (France), *C. R. Acad. Sci., Ser. IIa Sci. Terre Planetes*, *329*, 189–196.

Serrat, P., W. Ludwig, B. Navarro, and J.-L. Blazi (2001), Variation spatio-temporelles des flux de matières en suspension d'un fleuve côtier méditerranéen: La Têt (France), *C. R. Acad. Sci., Ser IIa Sci. Terre Planetes*, *333*, 389–397.

Sinninghe Damsté, J. S., W. I. C. Rijpstra, and G. J. Reichart (2002a), The influence of oxic degradation on the sedimentary biomarker record II: Evidence from Arabian Sea sediments, *Geochim. Cosmochim. Acta*, *66*, 2737–2754.

Sinninghe Damsté, J. S., E. C. Hopmans, S. Schouten, A. C. T. van Duin, and J. A. J. Geenevasen (2002b), Grenarchaeol: The characteristic core glycerol dibiphytanyl glycerol tetraether membrane lipid of cosmopolitan pelagic crenarchaeota, *J. Lipid Res.*, *43*, 1641–1651.

Simoneit, B. R. T. (1984), Organic matter of the troposphere: III. Characterization and sources of petroleum and pyrogenic residues in aerosols over the western United States, *Atmos. Environ.*, *18*, 51–67.

Thill, A., S. Moustier, J.-M. Garnier, C. Estournel, J.-J. Naudin, and J.-Y. Bottero (2001), Evolution of particle size and concentration in the Rhône river mixing zone: Influence of salt flocculation, *Cont. Shelf Res.*, *21*, 2127–2140.

Tyson, R. V. (1995), *Sedimentary Organic Matter: Organic Facies and Palynofacies*, CRC Press, Boca Raton, Fla.

Weijers, J. W. H., S. Schouten, M. Van der Linden, B. Van Geel, and J. S. Sinninghe Damsté (2004), Water table related variations in the abundance of intact archaeal membrane lipids in a Swedish peat bog, *FEMS Microbiol. Lett.*, *239*, 51–56.

Weijers, J. W. H., S. Schouten, E. C. Hopmans, J. A. J. Geenevasen, O. R. P. David, J. M. Coleman, R. D. Pancost, and J. S. Sinninghe Damsté (2006a), Membrane lipids of mesophilic anaerobic bacteria thriving in peats have typical archaeal traits, *Environ. Microbiol.*, *8*, 648–657.

Weijers, J. W. H., S. Schouten, O. Spaargaren, and J. S. Sinninghe Damsté (2006b), Occurrence and distribution of tetraether membrane lipids in soils: Implications for the use of the TEX_{86} proxy and the BIT index, *Org. Geochem.*, in press.

Wells, L. E., M. Cordray, S. Bowerman, L. A. Miller, W. F. Vincent, and J. W. Deming (2006), Archaea in particles-rich waters of the Beaufort Shelf and Franklin Bay, Canadian Arctic: Clues to an allochthonous origin?, *Limnol. Oceanogr.*, *51*, 47–59.

Résumé

Le golfe du Lion est une marge continentale à construction deltaïque soumise à l'impact des apports sédimentaires (1) du Rhône, un des plus gros fleuves méditerranéens, à caractère saisonnier ; (2) ainsi que d'une série de fleuves côtiers à caractère torrentiel. Des zones de dépôts temporaires du matériel fin se développent en face de ces fleuves vers 30 m de profondeur à la limite d'action des houles de tempête. La dynamique de ces zones soumise à l'impact des évènements extrêmes joue un rôle important dans (1) la dissémination des sédiments fins et des contaminants associés depuis les sources (bassins versants) jusque vers le large, et (2) la qualité des eaux dans la zone littorale. Une station de suivi automatique haute fréquence et à long terme a été installée sur le fleuve Têt, exemple de fleuve côtier méditerranéen à caractère torrentiel et sur son prodelta afin de suivre la variabilité, l'impact des évènements hydro-climatiques sur le devenir des sédiments fins dans la zone littorale. Les crues engendrées par les entrées maritimes sont les principales sources de sédiments fins à la zone littorale. Les tempêtes qui accompagnent ces crues créent une redistribution de ce matériel vers la vasière circa-littorale vers 50 m de profondeur et la limite du plateau où se situent les canyons sous-marins. La succession de ces évènements extrêmes au cours de l'année détermine la conservation du matériel fin dans la zone littorale ou son exportation vers le large. Une forte variabilité interannuelle existe également dans le golfe du Lion entre des années humides avec de fortes crues et tempêtes apportant et redistribuant de grandes quantités de matériel sédimentaire sur le plateau et des années sèches caractérisées par des courants intenses à l'origine de plongées d'eaux denses dévalant et érodant le plateau jusqu'au canyons sous-marins. Les évènements hydro-climatiques extrêmes (crues, tempêtes, plongées d'eaux denses) sont les acteurs principaux qui façonnent les fonds sédimentaires du golfe du Lion. L'impact des activités humaines et du changement climatique sur la fréquence de ces évènements extrêmes semble jouer un rôle important sur la variabilité de la qualité du milieu littoral et du devenir des sédiments fins et contaminants.

Abstract

The Gulf of Lions is a continental margin with deltaic construction subjected to the impact of the sedimentary contributions (1) of the Rhone, one of the largest Mediterranean rivers, with seasonal hydrological cycle; (2) as well as series of torrential coastal rivers. Temporary deposit areas of the fine-grained sediment develop directly front of these rivers around 30 m water depth corresponding to the storm wave base. The dynamic of these zones subjected to the impact of the extreme events plays an important role in (1) the dissemination of the fine sediments and the associated contaminants from sources (catchment) to the sea, and (2) the water quality of the littoral zone. An automatic high frequency and long-term monitoring station was installed on the Têt River, example of mediterranean torrential coastal rivers and on its prodelta in order to estimate the variability, the impact of the hydro-climatic events on the behaviour of fine sediments in the littoral zone. Flash-floods generated by marine winds are the principal sources of fine sediments at the littoral zone. Storms associated to floods create redistribution of this material towards the circa-littoral mud belt around 50 m of water depth and the shelf edge where are located the underwater canyons. The succession of these extreme events during the year determines the preservation of the fine material in the littoral zone or its export towards the shelf. A strong interannual variability also exists in the Gulf of Lions between wet years with strong floods and storms supplying and redistributing great quantities of sedimentary material on the shelf and, dry years characterized by intense currents originating from dense water cascading descending and eroding the shelf to the underwater canyons. The extreme hydro-climatic events (flash-floods, storms, dense water cascading) are the principal actors who shape the bottom sediments of the Gulf of Lions. The impact of the human activities and climatic change plays an important role on the frequency of these extreme events and on the variability of littoral water quality and the fine-grained sediments and contaminants dispersal.